

**Regulation of mitotic progression:
Focus on Plk1 function and
the novel Ska complex
at kinetochores**

Dissertation zur Erlangung des
naturwissenschaftlichen Doktorgrades
der Bayerischen Julius-Maximilians-Universität Würzburg

vorgelegt von
Anja Hanisch

Flensburg

Martinsried / Würzburg 2006

Eingereicht am:

Mitglieder der Promotionskommission:

Vorsitzender:

Gutachter: Prof. Dr. Erich A. Nigg

Gutachter: Prof. Dr. Georg Krohne

Tag des Promotionskolloquiums:

Doktorurkunde ausgehändigt am:

Hiermit erkläre ich ehrenwörtlich, dass ich die vorliegende Dissertation selbständig angefertigt habe und keine anderen als die von mir angegebenen Quellen und Hilfsmittel benutzt habe. Sämtliche Experimente wurden von mir selbst durchgeführt, soweit nicht explizit auf Dritte verwiesen wird. Diese Dissertation hat weder in gleicher noch in ähnlicher Form einem anderen Prüfungsverfahren vorgelegen. Ich habe weder bereits früher akademische Grade erworben noch versucht zu erwerben.

Anja Hanisch

Martinsried, den 24.10.2006

TABLE OF CONTENTS

SUMMARY	1
ZUSAMMENFASSUNG	2
INTRODUCTION	3
1 General overview of the cell cycle and M phase	3
2 The different stages of M phase and onset of mitosis	4
3 Polo-like kinase 1	6
3.1 Structure, regulation and targeting of Plk 1	6
3.2 Functions of Plk 1	8
4 Structure and function of kinetochores	12
4.1 Structure and components of human kinetochores	12
4.2 The spindle assembly checkpoint	13
4.2.1 Attachment versus tension	14
4.2.2 Models of Mad1-assisted Mad2 activation	15
4.3 Spindle assembly dynamics and kinetochore-fibre formation	16
4.4 K-fibre dynamics in chromosome congression	19
4.5 Molecular basis of KT-MT attachment and stabilisation	19
AIM OF THE WORK	23
PART I - Search for Plk1 PBD interaction partners and functional analysis of Plk1 PBD expressing cells	25
RESULTS I	26
1 Unbiased search for Plk1 PBD interacting proteins by pull downs and immunoprecipitations	26
1.1 Bacterial expression and purification of GST-PBD ^{WT} and GST-PBD ^{HK538/540AA}	26
1.2 PBD ^{WT} but not PBD ^{AA} recognises specifically phosphorylated peptides and proteins	27
1.2.1 The PBD ^{WT} but not PBD ^{AA} recognises the PBDtide	27
1.2.2 Far Western binding of PBD ^{WT} but not PBD ^{AA} to phosphorylated Mklp2	27
1.3 Large scale pull down from a mitotic lysate with GST-PBD ^{WT} and GST-PBD ^{AA} lacks sufficient specificity	28
1.4 Generation of inducible myc-PBD ^{WT} and myc-PBD ^{AA} HeLa S3 cell lines	29
1.5 Immunoprecipitations of myc-PBD ^{WT} and myc-PBD ^{AA} expressed in stable cell lines increase the specificity	30

TABLE OF CONTENTS

2	Biased search for Plk1 PBD interacting proteins by immunoprecipitations followed by Western blot analysis	33
2.1	Among the tested proteins only Cdc20, Cdc27, Bub1 and Ect2 co-immunoprecipitated specifically with myc-PBD ^{WT}	33
2.2	Endogenous Plk1 does not co-immunoprecipitate any of the myc-PBD ^{WT} interacting candidates	34
2.3	Analysis of the interaction between Plk1 and Cdc20	35
2.3.1	Endogenous Cdc20 interacts with both full length Plk1 ^{WT} and Plk1 ^{AA} in a mitosis specific manner	36
2.3.2	Endogenous Cdc20 interacts specifically with myc-Plk1 but not with the other members of the Polo-like kinase family	37
2.3.3	Tagging of Cdc20 interferes with the Plk1 interaction	38
2.4	Analysis of the interaction between Plk1 and MST2	39
2.4.1	The interaction of myc-Plk1 with FLAG-MST2 depends on an intact PBD and is specific for both the MST2 and the Plk1 kinase family member	40
2.4.2	Myc-Plk1 co-immunoprecipitates endogenous MST2 in a cell cycle dependent way and their interaction is direct	40
2.4.3	Interaction between MST2 and Plk1 is independent of their respective kinase activities and of Cdk1/Cyclin B phosphorylation	42
2.4.4	GST-Plk1 and FLAG-MST2 do not phosphorylate each other <i>in vitro</i>	43
2.5	Initial analysis of the relationship between Plk1 and BubR1	44
2.5.1	The spindle assembly checkpoint induced phosphorylated form of BubR1 is reduced in Plk1 RNAi cells	44
2.5.2	BubR1 KT localisation is not dependent on the presence of Plk1	46
3	Plk1 PBD expression reveals distinct dependencies on proper targeting for different Plk1 functions and implicates Plk1 in chromosome congression	47
3.1	An intact phosphopeptide binding motif is required for localisation of the Plk1 PBD	47
3.2	Overexpression of PBD ^{WT} results in displacement of endogenous Plk1 and causes mitotic arrest	48
3.3	PBD ^{WT} expression allows bipolar spindle formation but causes chromosome congression defects	50
3.4	PBD overexpression does not interfere with centrosome maturation	52
3.5	Chromatid arm separation occurs in PBD expressing cells but not in Plk1-depleted cells	54
3.6	The PBD is essential for mitotic progression	54
3.7	The PBD is dispensable for centrosome maturation and separation but not for chromosome congression	55

DISCUSSION I	58
1 Plk1 PBD pull downs and immunoprecipitations revealed many PBD interacting proteins	58
2 The significance of the specific Cdc20-Plk1 and MST2-Plk1 interactions remains to be elucidated	60
3 PBD expression shows distinct requirements of different Plk1 functions for PBD-mediated targeting and reveals a novel role of Plk1 in chromosome congression	61
SUMMARY I	66
PART II - Characterisation of two novel spindle and kinetochore associated proteins, termed Ska1 and Ska2	69
RESULTS II	70
1 Localisation analysis of uncharacterised proteins from a proteomic spindle inventory	70
2 Ska1, identified in the spindle inventory, in complex with Ska2 is required for timely anaphase onset	72
2.1 Identification of Ska1 at spindle MTs and outer KTs	72
2.2 Requirements for Ska1 localisation to KTs	73
2.3 Ska1 interacts with Ska2 (FAM33A)	80
2.4 Ska1 and Ska2 levels are constant throughout the cell cycle	81
2.5 Influence of Ska complex formation on protein stability and localisation	82
2.6 Ska1 and Ska2 are required for proper mitotic progression	84
2.7 Role of Ska complex in stabilisation of KT-MT interaction and checkpoint silencing	86
DISCUSSION II	88
SUMMARY II	92
MATERIALS AND METHODS	93
1 Cloning procedures	93
2 Expression and purification of recombinant protein	94
3 Antibody Production	95
4 Cell culture, synchronisation, drug concentrations and cold treatment on living cells	95
5 Generation of myc-PBD stable inducible HeLa S3 cell lines	96
6 Transient transfections and RNAi	96
7 Immunofluorescence microscopy	97
8 Live-cell imaging	98
9 Cell extracts, Immunoprecipitation, Western Blot and Far Western analysis	98

TABLE OF CONTENTS

10 Mitotic chromosome spreads	99
11 <i>In vitro</i> phosphopeptide binding	101
12 <i>In vitro</i> kinase assays	102
13 Phosphatase assays	102
14 Yeast-two hybrid analysis	102
15 <i>In vitro</i> coupled transcription translation	103
APPENDIX	104
1 List of abbreviations	104
2 Table of created plasmids	106
3 Table of proteins identified by mass spectrometry in GST-PBD pull down	109
ACKNOWLEDGEMENTS	118
REFERENCES	119
PUBLICATIONS	133
LEBENS LAUF	134

SUMMARY

During mitosis the duplicated chromosomes have to be faithfully segregated into the nascent daughter cells in order to maintain genomic stability. This critical process is dependent on the rearrangement of the interphase microtubule (MT) network, resulting in the formation of a bipolar mitotic spindle. For proper chromosome segregation all chromosomes have to become connected to MTs emanating from opposite spindle poles. The MT attachment sites on the chromosomes are the kinetochores (KTs), which are also required to monitor the integrity of KT-MT interactions via the spindle assembly checkpoint (SAC).

The first part of this work concerns the action of Polo-like kinase 1 (Plk1). Plk1 is one of the most prominent mitotic kinases and is involved in the regulation of multiple essential steps during mitosis consistent with its dynamic localisation to spindle poles, KTs and the central spindle. Despite a nice model of Plk1 targeting to different mitotic structures via its phosphopeptide binding Polo-box domain (PBD), the exact molecular details of Plk1 functioning, in particular at the KT, remain obscure. By two different approaches we obtained cells with an unlocalised Plk1 kinase activity: first by generating stable HeLa S3 cell lines, which upon induction expressed the PBD and thus displaced endogenous Plk1 from its sites of action. Secondly, by rescuing cells RNAi-depleted of Plk1 with the catalytic Plk1 domain only. Centrosome maturation, bipolar spindle assembly and loss of cohesion between the chromatid arms proceeded normally in either cells, in contrast to Plk1-depleted cells, arguing that PBD-mediated targeting of Plk1 is less critical for the tested functions. Remarkably, however, both the PBD expressing as well as the Plk1-depleted cells rescued with the catalytic domain of Plk1 arrested in early mitosis in a SAC-dependent manner with uncongressed chromosomes. These data disclose a so far unrecognised role of Plk1 in proper chromosome congression and point at a particular requirement for PBD-mediated localised Plk1 activity at the KT.

In the second part of the thesis, we characterised a novel spindle and KT associated protein, termed Ska1, which was originally identified in a spindle inventory. Ska1 associated with KT following MT attachment during prometaphase and formed a complex with at least another novel protein of identical localisation, called Ska2. Ska1 was required for Ska2 stability *in vivo* and depletion of either Ska1 or Ska2 resulted in the loss of both proteins from the KT. The absence of Ska proteins did not disrupt overall KT structure but most strikingly induced cells to undergo a prolonged SAC-dependent delay in a metaphase-like state. The delay was characterised by weakened kinetochore-fibre stability, recruitment of Mad2 protein to a few KT and the occasional loss of individual chromosomes from the metaphase plate. These data indicate that the Ska1/2 complex plays a critical role in the maintenance of a KT-MT attachments and/or SAC silencing.

ZUSAMMENFASSUNG

Während der Mitose müssen die replizierten Chromosomen präzise auf die neu entstehenden Tochterzellen verteilt werden, um genomische Stabilität zu garantieren. Dieser Prozeß hängt von dem Umbau des Mikrotubuli (MT)-Netzwerkes der Interphase zu einer mitotischen bipolaren Spindel ab. Für eine fehlerfreie Trennung aller Chromosomen müssen diese jeweils mit MT der entgegengesetzten Spindelpole verknüpft werden. Kinetochore bilden die Anheftungspunkte der MT an den Chromosomen und überwachen mittels des Spindel-Kontrollpunktes (SAC) auch die korrekte Ausbildung der Kinetochor-MT Interaktionen.

Der erste Teil dieser Arbeit befasst sich mit der Polo-like Kinase 1 (Plk1). Plk1 gehört zu den wichtigsten mitotischen Kinasen und ist an der Regulation vieler essentieller Schritte im Verlauf der M-Phase beteiligt, was sich auch in ihrer dynamischen Lokalisation widerspiegelt (Spindelpole, Kinetochore, Zentralspindel). Obwohl wir schon eine Vorstellung davon haben, wie Plk1 mittels ihrer Phosphopeptid-bindenden Polo-box Domäne (PBD) an die mitotischen Zielstrukturen bindet, ist dennoch weiterhin unklar, wie Plk1 auf molekularer Ebene ihre Funktionen, besonders hinsichtlich der Kinetochore, ausübt. Auf zwei Arten generierten wir Zellen mit ungebundener Plk1 Aktivität: zum einen, indem wir stabile HeLa S3 Zelllinien herstellten, die induzierbar die PBD exprimierten, welche wiederum endogene Plk1 von ihren Zielstrukturen verdrängte, und zum anderen, indem wir in Plk1 depletierten Zellen nur die Kinase-Domäne von Plk1 exprimierten. Zentrosomreifung, Ausbildung bipolarer Spindeln und Abbau der Chromosomenchäson verliefen im Gegensatz zu Plk1-RNAi behandelten Zellen normal, was darauf schließen lässt, dass für diese Funktionen PBD-vermitteltes Binden von Plk1 an die jeweiligen Zielstrukturen nicht essentiell ist. Stattdessen arretierten diese Zellen SAC-abhängig mit unzulänglich an der Metaphase-Platte ausgerichteten Chromosomen. Unsere Daten offenbaren eine neue Rolle von Plk1 bei der Bildung der Metaphase-Platte und deuten darauf hin, dass diese spezielle Funktion eine PBD-vermittelte Lokalisation der Plk1 Aktivität am Kinetochor benötigt.

Der zweite Teil dieser Arbeit ist der Charakterisierung eines neuen Spindel- und Kinetochor-assoziierten Proteins namens Ska1 gewidmet, das wir im Zuge eines Spindelkomponenten-Screens identifizierten. Wir fanden heraus, dass Ska1 in einem Komplex mit mindestens einem weiteren uncharakterisierten Protein identischer Lokalisation, Ska2 genannt, existiert. Ska1 wird für Ska2 Stabilität benötigt und die Lokalisationen dieser Ska Proteine hängen voneinander ab. Obwohl sie für den richtigen Aufbau des Kinetochores verzichtbar sind, führt ihre Depletion zu einem überlangen Verbleib der Zellen in einem Metaphase-ähnlichen Zustand, der durch destabilisierte Kinetochor-Fasern, Ansammlung von Mad2 an einzelnen Kinetochoren und den gelegentlichen Verlust einzelner Chromosomen von der Metaphase-Platte charakterisiert ist. Dies weist auf eine Rolle des Ska-Komplexes bei der Stabilisierung gebildeter Kinetochor-MT-Anheftungen hin und/oder auf eine Beteiligung an der Inaktivierung des SAC.

INTRODUCTION

1 General overview of the cell cycle and M phase

The principle “*omnis cellula e cellula*” (every cell originates from a pre-existing cell), phrased by the German pathologist Rudolf Virchow in 1858, forms the basis of the cell theory. A new cell is not formed *de novo* by progressive growth of material in the environment but by division of a pre-existing cell. The process of cell division is part of the cell cycle machinery whose major tasks are to precisely replicate the DNA and to equally segregate the duplicated chromosomes into the nascent daughter cells.

These fundamental tasks are accomplished at two distinct stages of the cell cycle, at interphase and M phase, respectively. Their proper timing and faithfulness is guaranteed by an elaborate order of (ir)reversible steps within each round of the cycle. The driving force of the cell cycle is the coordinated, oscillating activity of special heterodimeric protein complexes consisting of a catalytic and a regulatory subunit. The latter is formed of a so called Cyclin whose protein levels raise and fall in a defined manner in the course of the cell cycle. The catalytic subunit is a serine/threonine kinase, which is only active if bound to its specific Cyclin. These kinases are therefore called Cyclin-dependent kinases (Cdks).

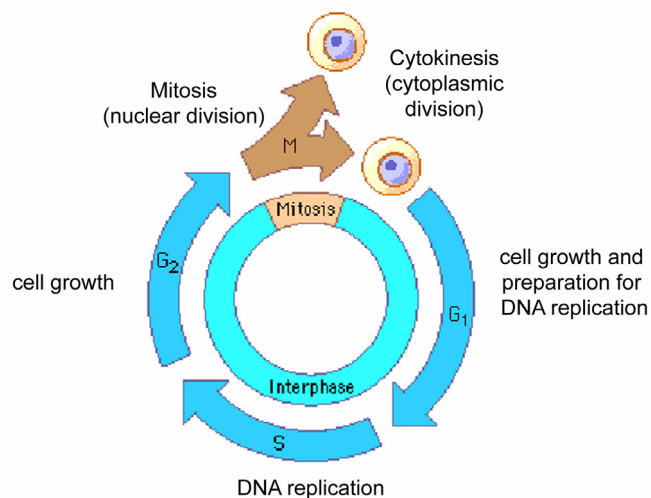


Figure 1 Overview of the different cell cycle stages in eukaryotic cells. Interphase is divided into G₁, S and G₂ phase. In M phase, mitosis is followed by cytokinesis. Illustration adapted and modified from Murray and Hunt, Cell Cycle – an introduction, 1993.

Interphase, the period between chromosome segregation and cell division, is subdivided into G₁, S and G₂ phase (G stands for gap, S for synthesis). Based on the state of nutrients and growth factors, typical somatic cells have to decide in G₁ phase whether they enter into a quiescence state (G₀ phase) or whether they commit themselves to proliferation. Mitogenic stimuli in animal cells induce the synthesis of the D-type Cyclins (G₁ Cyclins), which in complex with Cdk4 and Cdk6 enable the expression of Cyclin E and Cyclin A (S Cyclins) from late G₁ phase on. Cdk2-

INTRODUCTION

Cyclin E and Cdk2-Cyclin A activities are not only required for DNA replication but also for centrosome duplication during S phase. After S phase, the cell enters G2 phase. Here the cells have to control the integrity of their replicated chromosomes, since any DNA defects which are not detected and repaired during G2 will persist and be transferred to the daughter cells during the following M phase. The G2-M phase transition is therefore tightly controlled (see Introduction, chapter 2) with Cdk1-Cyclin B being the key regulator of both mitotic entry and progression (Murray, 2004).

2 The different stages of M phase and onset of mitosis

M phase is divided into mitosis, the time period during which the sister chromatids are faithfully segregated so that each daughter inherits a complete set of chromosomes, and cytokinesis, the cleavage of the cytoplasm. The distinction between mitosis and cytokinesis was merely made on morphological changes observed by light microscopy. Nowadays it is clear that at the molecular level these processes are strongly intertwined, and when using the term mitosis, also often cytokinesis is included.

Mitosis comprises several morphologically different stages. During prophase the interphase chromatin condenses into defined chromosomes, each of them consisting of two sister chromatids. In somatic animal cells the duplicated and during G2 phase matured centrosomes start nucleating highly dynamic microtubules (MTs) in all directions forming the so called asters. These asters move away from each other around the nuclear envelope and will form the future spindle poles. At the onset of the next stage, termed prometaphase, the nuclear envelope breaks down allowing the MTs to capture chromosomes at their kinetochores (KTs). KTs are specialised proteinaceous structures, which are formed at either sides of the centromer, a heterochromatic DNA region at which the sister chromatids are held together (initially described as primary constriction of the chromosome). Chromosomes, which have attached to MTs emanating from opposite spindle poles are moved to the equator of the cell in a process called congression. Metaphase is the state when all chromosomes have aligned at the corresponding metaphase plate. The former two halves of the MT arrays now form the typical bipolar spindle with their minus-ends proximal to the poles. Within the spindle we distinguish different sets of MTs: the astral MTs, which link the spindle poles to the cell cortex, the KT-MTs, which are attached to the KTs and the interpolar MTs that overlap in an anti-parallel fashion at the cell equator and hence connect the two spindle poles. Once the chromosomes are all aligned, cohesion between sister chromatids is lost at the onset of anaphase and subsequently they are pulled apart to the opposite poles. Whereas chromosome movement is driven by shortening of the KT-MTs in anaphase A, the separation in anaphase B is further enhanced by increased pole-pole spacing. During anaphase the division plane is determined by mechanisms involving spindle-cortex interactions, followed by accumulation of actin and myosin II, the components of the contractile ring, in the region of the furrow. In telophase, the nuclear envelope reforms around the decondensing segregated sister chromatids.

Simultaneously, the actin-myosin ring contracts thereby also deforming the attached cell membrane, leading to furrow ingression and cytokinesis. In the course of cytokinesis, the anti-parallel MT array at the cell equator, the central spindle, is compressed into a compact midbody, the remnant of the midzone. Finally, abscission takes place resulting in the two new daughter cells.

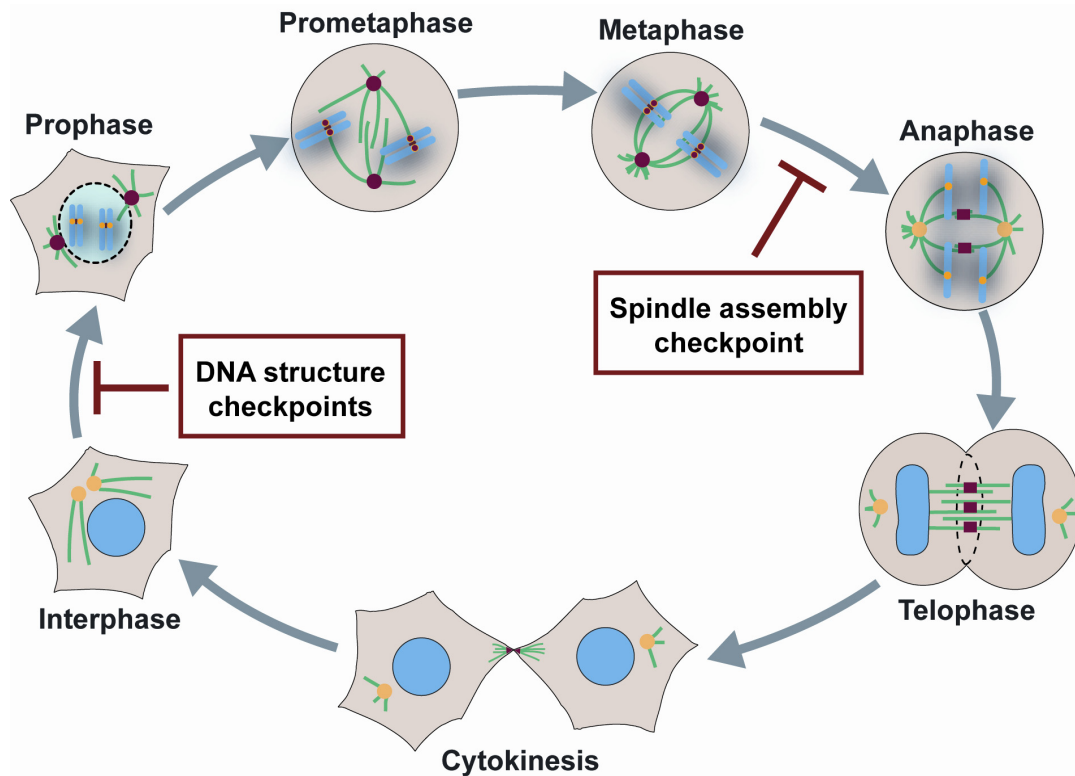


Figure 2 The classical stages of M phase and the checkpoints that can delay either entry into mitosis (DNA structure checkpoints) or anaphase onset (Spindle assembly checkpoint). Illustration adapted from Nigg EA, *Nature Reviews*, 2001

At the molecular level mitotic progression is driven by two post-translational mechanisms: reversible protein phosphorylation and irreversible proteolysis. These processes are intimately linked and exert control on each other.

The key mitotic regulator is Cdk1. Cdk1 protein levels are constant throughout the cell cycle, but its activity is strictly regulated by protein-protein interactions and reversible phosphorylation. Its regulatory subunits are Cyclin A and Cyclin B. Whereas Cyclin A accumulates during S phase, Cyclin B synthesis shows a steep increase just before the G2-M transition and Cyclin B is the main activating Cdk1 partner for mitotic entry. However, only a conformational change of Cdk1 upon Cyclin binding is not sufficient for Cdk1 activity. Cdk1 requires phosphorylation by Cdk-activating kinase (Cak) and dephosphorylation at two residues (Thr14 and Tyr15) in the ATP binding site, by the dual-specificity phosphatase Cdc25C. Only at the G2-M transition when all the conditions are adequate for mitotic commitment the activity of Cdc25C exceeds the one of the opposing kinases Wee1 and Myt1, which create the inhibitory phosphorylations (Nigg, 2001; Ferrari, 2006). Once activated, Cdk1-Cyclin B can promote its own full and rapid activation in a positive feedback loop: both by phosphorylating and thereby further

INTRODUCTION

activating Cdc25C (Hoffmann *et al.*, 1993) and by phosphorylating its inhibitory kinase Wee1, which leads to Wee1 degradation (Watanabe *et al.*, 2004). Also Polo-like kinase 1 (Plk1) has been implicated in the Cdk1 amplification loop (see Introduction, chapter 3).

Cdk1 promotes entry and progression through mitosis by phosphorylation of various substrates. It is involved in chromosome condensation by the phosphorylation of condensins (Kimura *et al.*, 1998), in golgi fragmentation (Lowe *et al.*, 1998), its phosphorylating lamins leads to their depolymerisation (Peter *et al.*, 1991) and finally to nuclear envelope breakdown. Other substrates are MT-associated proteins and kinesin-related motor proteins which play a role in centrosome separation and spindle assembly (Blangy *et al.*, 1995). Cdk1 also has regulatory functions in the control of the anaphase-promoting complex/cyclosome (APC/C), an E3 ubiquitin ligase, which targets critical mitotic substrates for degradation and thereby promotes exit from mitosis (see Introduction, chapter 3 and 4).

3 Polo-like kinase 1

Cdk1 collaborates with other mitotic kinases in the regulation of mitosis. One of the most prominent ones is Polo-like kinase (Plk). The founding member of the Plk family is *Drosophila* Polo. Polo mutants show abnormal spindle poles (Sunkel and Glover, 1988). Whereas budding yeast and fission yeast contain only a single Plk family member (Cdc5 and Plo1, respectively), mammals and *Xenopus* have four, called Plk1, Plk2, Plk3 and Plk4 (Sak) in humans, and flies possess Plk4 besides Polo.

3.1 Structure, regulation and targeting of Plk 1

Common among all Polo kinases is their highly conserved serine/threonine kinase domain in the N-terminus and two (or one in the case of Plk4) conserved so called Polo-boxes in the C-terminus, which so far have not been found in other proteins. The whole non-catalytic region (326-630aa in Plk1) including the linker region and the structurally homologous Polo-boxes themselves is called the Polo-box domain (PBD) since it functions as a single unit. For Plk1, the PBD has been shown to be required for its targeting to substrates and subcellular localisations (Lee *et al.*, 1999; Seong *et al.*, 2002; Reynolds and Ohkura, 2003). Using a phosphopeptide based proteomic screen, Yaffe and coworkers discovered that the PBD of Plk1 constitutes a phosphopeptide-binding domain, which binds with maximal affinity to phosphopeptides containing the consensus sequence S-pS/pT-P/X (Elia *et al.*, 2003a). Similar preferences were also shown for the PBDs of Plk2 and Plk3 (Elia *et al.*, 2003b).

Crystallography studies have confirmed specific binding of phosphopeptides to a cleft at the interface of the two Polo-box repeats (Cheng *et al.*, 2003; Elia *et al.*, 2003b). The phosphate group of the ligand is engaged in eight hydrogen-bonding interactions with the PBD surface but only two aminoacid residues in human Plk1, His538 and Lys540 of the Polo-box 2, interact directly

with the phosphate moiety via their side chains and are essential for phosphopeptide binding (Elia *et al.*, 2003b). The serine -1 side chain of the phospholigand is directed towards the PBD binding surfaces and participates in three hydrogen-bonds giving an explanation for the strong selection of phosphopeptides with serine in -1 position.

In addition to its purported targeting function, the PBD was also shown to interact with the catalytic domain of Plk1, resulting in a mutual inhibition of function, at least *in vitro* (Jang *et al.*, 2002a). Interestingly, mutations of the His538 and Lys540 that disrupted phosphodependent interactions did not affect the PBD-kinase domain interactions, indicating that the kinase domain binds the PBD at a site distinct from the phosphopeptide binding pocket (Elia *et al.*, 2003b). This notwithstanding, phosphopeptide binding to the PBD results in kinase activation, suggesting that the induction of a structural change liberates the catalytic domain from its inhibitory interaction with the PBD (Elia *et al.*, 2003b).

Since the PBD of Plk1 interacted with a number of proteins only after they had been phosphorylated at specific sites, a model for Plk1 targeting and action has emerged, according to which a so called priming kinase phosphorylates a particular docking protein thereby creating an optimal PBD binding site. Binding of the PBD to this docking protein functions as a structural switch that stabilises a PBD conformation, which is no longer able to interact with the kinase domain. The liberated active Plk1 kinase domain is now positioned to phosphorylate either the docking protein itself (processive phosphorylation model) or other downstream targets (distributive phosphorylation model), which are present in the proximity of the specific subcellular structure Plk1 had been targeted to (Elia *et al.*, 2003a; Elia *et al.*, 2003b; Lowery *et al.*, 2005).

The motif recognised by the PBD can be created by proline-directed serine/threonine kinases and in fact Cdk1-Cyclin B has been shown to prephosphorylate Plk1 docking proteins (Elia *et al.*, 2003b). But also Plk1 itself can act as its own 'priming' kinase (Neef *et al.*, 2003; Zhou *et al.*, 2003).

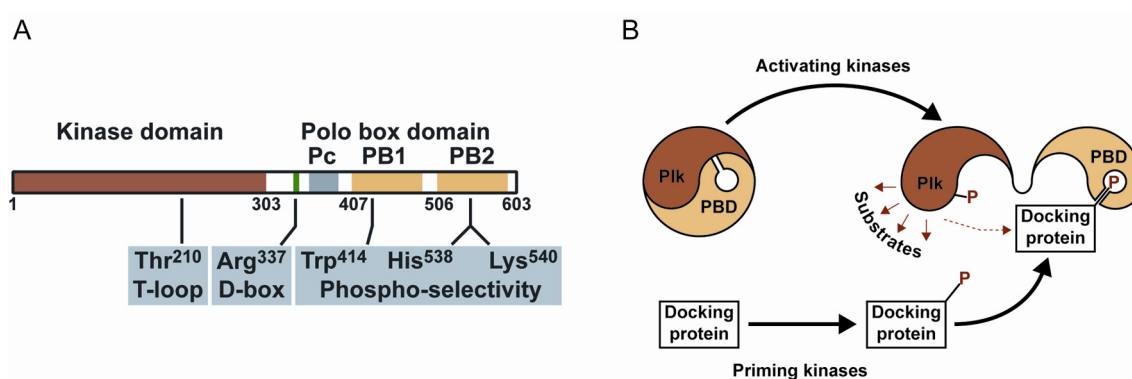


Figure 3 A) Plk1 domain structure. The N-terminal half harbours the catalytic activity whereas the C-terminal PBD is essential for targeting. Residues essential for activation, destruction and phosphopeptide binding, respectively, are indicated. B) Model of Plk1 targeting to prephosphorylated docking proteins thereby inducing its kinase activity. Illustrations adapted from Barr *et al.*, Nature Reviews, 2004

INTRODUCTION

Similar to structurally related kinases, Plk1 activity is also regulated by phosphorylation of a residue (Thr210) within the so-called activation loop (Jang *et al.*, 2002b). This phosphorylation event correlates with mitotic entry, and on the molecular level presumably stabilises the activation loop in an open conformation and, in addition, prevents the binding of the PBD (Jang *et al.*, 2002a). This may explain why the overexpression of PBD did not interfere with endogenous Plk1 kinase activity *in vivo* (Seong *et al.*, 2002). The *in vivo* upstream activating kinase of Plk1 has not been identified yet, although Ste20-like kinase (SLK) in humans (Ellinger-Ziegelbauer *et al.*, 2000) and its homologue Plkk1 in *Xenopus* (Qian *et al.*, 1998) have been suggested to phosphorylate Plk1 and Plx1 *in vitro*, respectively.

Plk1 expression levels increase from late S phase to mitosis. Accordingly, Plk1 subcellular localisation becomes most evident during mitosis and shows a very dynamic pattern. Plk1 localises to the centrosomes and spindle poles from prophase to metaphase, to the KTs from prometaphase onwards (although some centromere staining might already be present in prophase, unpublished data) and redistributes to the central spindle and midbody during anaphase and cytokinesis (Golsteyn *et al.*, 1995; Lee *et al.*, 1995; Arnaud *et al.*, 1998; Barr *et al.*, 2004).

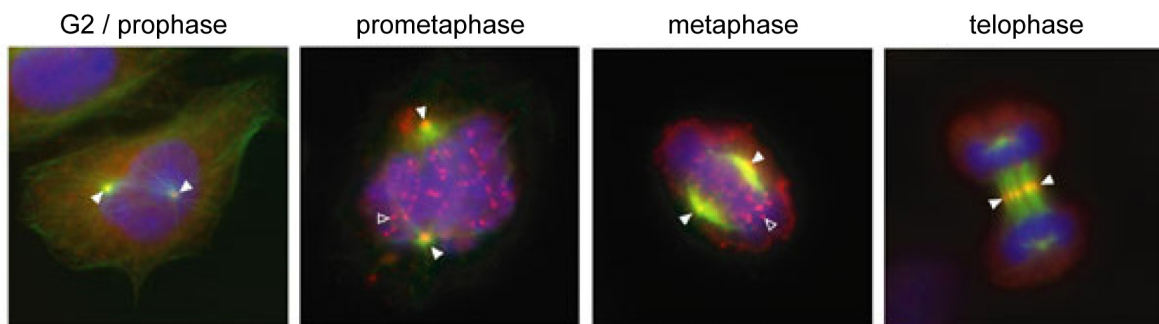


Figure 4 Dynamic Plk1 localisation in the course of mitotic progression. Plk1 (in red, arrows) localises to the centrosomes and spindle poles from late G2 phase until metaphase and from prometaphase until anaphase. Plk1 is also found at the KTs. Upon anaphase it relocates to the central spindle and midbody. Images adapted from Barr *et al.*, *Nature Reviews*, 2004.

3.2 Functions of Plk 1

In line with its dynamic localisation to different mitotic substructures, Plk1 has been shown to be required for several steps during mitotic progression.

Several lines of evidence suggest that Plk1 is involved in the regulation of mitotic entry. *Xenopus* Plx1 was shown to phosphorylate and activate Cdc25C *in vitro* (Kumagai and Dunphy, 1996) and Plk1 phosphorylation in the nuclear export signal of human Cdc25C during prophase has been shown to promote the nuclear localisation of Cdc25C, which is important for its action on the nuclear Cdk1-Cyclin B complex (Toyoshima-Morimoto *et al.*, 2002). Also the Cdk1 inhibitory kinases Wee1 and Myt1 are Plk1 *in vitro* substrates (Nakajima *et al.*, 2003; Watanabe *et al.*, 2004), but only for Wee1 an *in vivo* inactivation upon Plk1 phosphorylation could be demonstrated so far. Instead of being the trigger kinase for Cdk1 activation, Plk1 might rather be part of the Cdk1

amplification loop (Abrieu *et al.*, 1998), especially since interfering with Plk1 functions by different means results in a mitotic and not a G2 arrest (Lane and Nigg, 1996; Seong *et al.*, 2002; Sumara *et al.*, 2004; van Vugt *et al.*, 2004).

In accordance with Plk1 localisation to the centrosomes and spindle poles in mitosis, Plk1 is involved in centrosome maturation and separation. Centrosome maturation takes place in G2/early prophase and leads to an increase in the MT nucleation activity of the duplicated centrosomes by recruiting additional γ -tubulin and γ -tubulin ring complexes (γ -TuRC). *Drosophila* Polo was the first Plk family member to be identified whose mutants had defective, immature spindle poles (Sunkel *et al.*, 1988). But also in human cells centrosome maturation and consequently bipolar spindle formation requires Plk1 as shown by antibody microinjection or small interfering RNAs (RNAi). In both cases γ -tubulin recruitment is impaired and cells fail to form bipolar spindles. Instead, they arrest with monopolar spindles and a rosette-like DNA arrangement (Lane *et al.*, 1996; Sumara *et al.*, 2004; van Vugt *et al.*, 2004). One substrate of Plk1 at the centrosomes has been shown to be the Ninein-like protein (Nlp), which is displaced from the centrosomes upon mitotic entry most likely in order to allow the recruitment of mitotic MT nucleation promoting proteins. The removal of Nlp is promoted by Plk1 phosphorylation (Casenghi *et al.*, 2003). A role in centrosome maturation and separation has also been postulated for the Aurora-A kinase (Hannak *et al.*, 2001; Berdnik and Knoblich, 2002), which localises to the centrosomes from late S phase on and after nuclear envelope breakdown to the spindle poles until anaphase (Marumoto *et al.*, 2005). But if and how Plk1 and Aurora-A function together has not been elucidated.

Sister chromatid segregation and mitotic exit are coordinated by the action of the APC/C. This E3 ubiquitin ligase is activated by association with Cdc20, its substrate-specificity factor, and targets key mitotic regulators for degradation by the 26S proteasome. APC/C-mediated degradation of Cyclin A and Cyclin B is required for Cdk1 inactivation to allow exit from mitosis, whereas the proteolysis of securin releases the protease separase, which cleaves sister chromatid cohesion, the prerequisite for chromosome segregation. Plk1 has been implicated in promoting the metaphase-anaphase transition at different levels, including the modulation of APC/C activity and sister chromatid cohesion.

APC/C activity is regulated by different mechanisms. The degradation of its inhibitor Emi1 in prometaphase is required for APC/C activation in late mitosis. Emi1 is targeted for SCF ^{β -TrCP}-mediated degradation after Plk1 phosphorylating its degron motif (Moshe *et al.*, 2004). An Emi1 homologue, XErp1, was identified in *Xenopus* and found to be regulated in a similar Plx1-dependent manner (Schmidt *et al.*, 2005). Whereas Cyclin A proteolysis is initiated in prometaphase, the degradation of the APC/C substrates Cyclin B and securin is inhibited by the spindle assembly checkpoint (SAC) until all chromosomes are properly attached in a bipolar manner. APC/C activation at anaphase onset is not only regulated by the presence or absence of inhibitors but also by phosphorylation of several subunits (Apc1, Cdc27, Cdc16, Cdc23) (Kraft *et al.*, 2003). In vertebrates, Cdk1 and Plk1 seem to be the main kinases to perform these activating phosphorylations (Kotani *et al.*, 1998; Shirayama *et al.*, 1998; Patra and Dunphy, 1998; Kotani *et al.*, 1999; Golan *et al.*, 2002), but how they exactly contribute to APC/C activation and whether they are

INTRODUCTION

essential is still a matter of debate (Kraft *et al.*, 2003). Although Plx1 activity is required for exit from meiosis II (Descombes and Nigg, 1998) and to prevent premature inactivation of the APC/C in *Xenopus* egg extracts (Brassac *et al.*, 2000), in human somatic cells Plk1 seems not to be essential for APC/C activation since even in Plk1-depleted cells Cyclin B and securin degradation proceeds normally once the SAC has been simultaneously overridden (Sumara *et al.*, 2004;van Vugt *et al.*, 2004). Therefore, Plk1 phosphorylation had been suggested to have a more stimulatory rather than essential role in mitotic APC/C activation by supporting the essential Cdk1 phosphorylation of the APC/C (Kraft *et al.*, 2003).

Plk1 facilitates anaphase onset also by promoting the dissociation of chromosome cohesion. The protein complex, which holds the two sister chromatids together is called cohesin. The cohesin complex, comprising Smc1, Smc3, Scc3 (SA1 and SA2) and the kleisin subunit Scc1, is supposed to form a ring-like structure which encircles the duplicated chromosomes so that they remain associated with each other. In order to allow segregation of the chromosomes, this cohesion has to be dissolved. In vertebrates, this occurs in two steps. The bulk of cohesin is removed from the chromosome arms during prophase and early prometaphase in a cleavage independent way requiring Plk1 phosphorylation of the SA2 subunit (Sumara *et al.*, 2002;Hauf *et al.*, 2005), whereas residual cohesin at the centromeric region is maintained until anaphase onset by Shugosin, which protects this area from Plk1 phosphorylation (Clarke *et al.*, 2005;McGuinness *et al.*, 2005). Upon APC/C and concomitant separase activation the Scc1 subunit of the residual centromeric cohesin is cleaved, promoted by previous Plk1 phosphorylation of Scc1 (Alexandru *et al.*, 2001;Hauf *et al.*, 2005). Although Plk1 assists sister chromatid resolution, it seems not to be essential, since even in Plk1-depleted cells chromosomes are still able to separate by cleavage when forced to enter anaphase (Gimenez-Abian *et al.*, 2004).

The function of Plk1 at the KTs is the most obscure. Plk1-depleted cells do form KT-MT attachments but KTs are most likely not occupied by a full set of MTs and/or the attachments are not stable (Sumara *et al.*, 2004;van Vugt *et al.*, 2004). This might result indirectly from the failure of Plk1-depleted cells to form bipolar spindles, as KT-MTs are less stable in the absence of tension across the spindle. Moreover, sister KTs which are not under tension are specifically phosphorylated at certain epitopes recognised by the 3F3/2 antibody (Gorbsky and Ricketts, 1993;Nicklas *et al.*, 1995;Nicklas *et al.*, 1998). Plk1 kinase activity has been shown to be required to create these phosphoepitopes and might therefore constitute one component of the tension sensing branch of the SAC (see Introduction, chapter 4) (Wong and Fang, 2005;Ahonen *et al.*, 2005). However, the exact role of Plk1 at the KTs has still to be established.

Finally, Plk1 has also been implicated in cytokinesis consistent with its localisation at the midzone and midbody from anaphase on. Overexpression of Plk1 leads to multinucleation (Mundt *et al.*, 1997). In line with this, either overexpression of the C-terminal half of Plk1 or RNAi of Plk1 both followed by forced inactivation of the SAC gave rise to a failure in completion of cytokinesis, whereas the initial cleavage furrow ingression was unaffected (Seong *et al.*, 2002;van Vugt *et al.*, 2004). Targets of Plk1, which are required for proper cytokinesis involve the dynactin component NudC (Zhou *et al.*, 2003) and the kinesin Mklp2 (Neef *et al.*, 2003). Mklp2 is required for cleavage

furrow ingression and cytokinesis. It has been demonstrated that Plk1 phosphorylates Mklp2 at the central spindle thereby creating its own PBD binding site on Mklp2 and that this phosphorylation is essential for cytokinesis. The targeted Plk1 can then phosphorylate other targets at the central spindle and the cortex to further mediate cytokinesis (Neef *et al.*, 2003).

Not only Plk1 presence and activity are needed for mitotic exit and cytokinesis. At a certain point during anaphase it is also essential to get rid of the kinase in order to properly complete these processes. Plk1 degradation in late mitosis is mediated by APC/C-Cdh1 and requires the D-box motif within the Plk1 linker region (Lindon and Pines, 2004).

Altogether, Plk1 has been involved at multiple steps during mitotic progression. But how at the molecular level it exactly exerts its effects on all these different processes and how this leads to mechanistic changes remains obscure, not least because only a few Plk1 interaction partners have been identified so far. This lack of mechanistic understanding is perhaps illustrated best by our ignorance about the role of Plk1 at KTs.

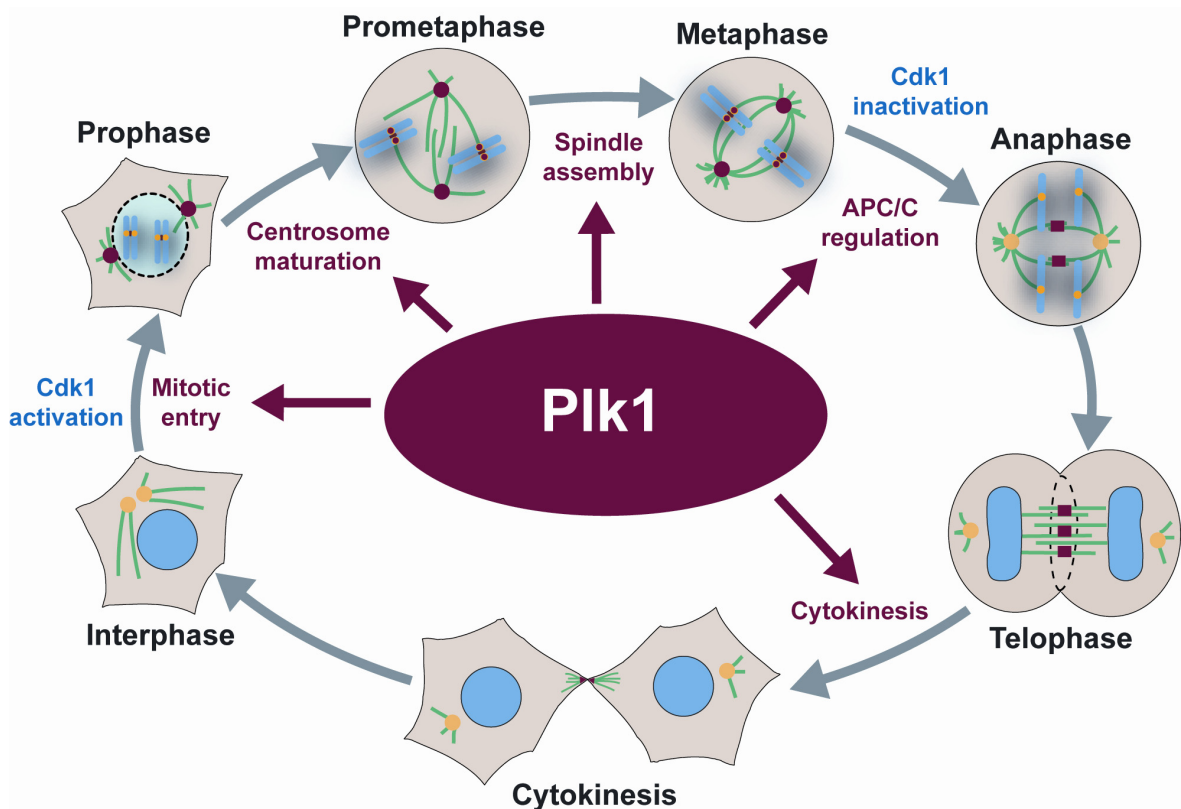


Figure 5 Plk1 is required at multiple steps during M phase progression. Illustration adapted from Barr *et al.*, *Nature Reviews*, 2004.

4 Structure and function of kinetochores

KTs are specialised structures, which form the attachment sites for spindle MTs on the chromosomes. They monitor the integrity of the KT-MT attachments and if they detect errors they respond by activating the SAC, which delays the metaphase-anaphase transition until all chromosomes have achieved proper, bipolar attachments. Furthermore, KT's mediate the MT-dependent chromosome movements during congression in prometaphase and segregation in anaphase.

4.1 Structure and components of human kinetochores

By electron tomography, two distinct regions of a KT can be distinguished called the inner and the outer KT plate (McEwen *et al.*, 1998). The inner plate is a special chromatin structure, which is formed on and inclusive of highly repetitive α -satellite sequences and characterised by the incorporation of the centromere specific histone H3 variant CENP-A (Palmer *et al.*, 1991; Sullivan *et al.*, 1994). CENP-A is essential for the recruitment of many KT components including proteins of the inner KT like CENP-C, CENP-H and CENP-I (Carroll and Straight, 2006).

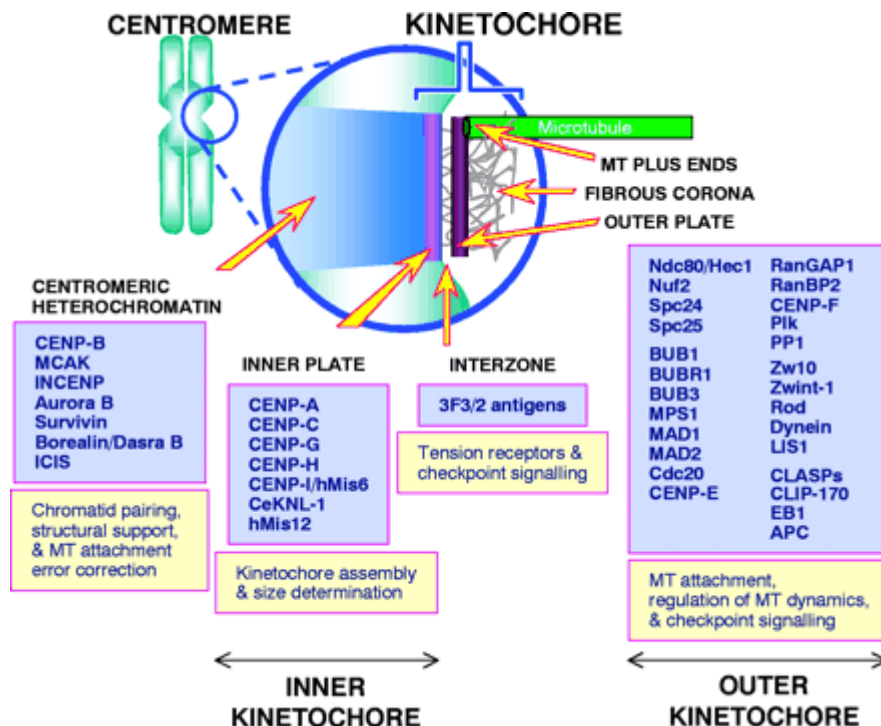


Figure 6 Structure and protein composition of the centromeric region with its attached KT. The KT is composed of an inner and an outer KT plate, which is associated with the fibrous corona. Illustration adapted from Maiato *et al.*, *Journal of Cell Science*, 2004.

Whereas the inner plate exists as a discrete heterochromatin domain throughout the cell cycle, the outer plate is a proteinaceous layer not formed before nuclear envelope breakdown. The outer plate and its associated fibrous corona contain structural components (e.g. the Hec1/Ndc80 complex) (Ciferri *et al.*, 2005; DeLuca *et al.*, 2005) and CENP-F (Rattner *et al.*, 1993), protein kinases e.g. Plk1 (Arnaud *et al.*, 1998; Ahonen *et al.*, 2005), MT-dependent motor proteins (e.g. CENP-E and dynein) (Pfarr *et al.*, 1990; Steuer *et al.*, 1990; Yen *et al.*, 1991; Yao *et al.*, 1997), MT (+) tips (e.g. CLASPs, CLIP-170, EB1, APC) (Maiato *et al.*, 2003; Green *et al.*, 2005; Maiato *et al.*, 2005; Tanenbaum *et al.*, 2006) and components of the SAC (e.g. Mad2 and BubR1) (Musacchio and Hardwick, 2002). The outer plate harbours about 20-30 end-on attachment sites for the MT tips (Rieder, 1982) and is essential for proper MT binding. The centromeric heterochromatin, the region between two sister KTs, is involved in the correction of inappropriate attachments of MTs and comprises the proteins of the chromosomal passenger complex (CPC) (Vagnarelli and Earnshaw, 2004) and the depolymerase MCAK (Kline-Smith *et al.*, 2004).

4.2 The spindle assembly checkpoint

The SAC is a surveillance mechanism, which in its active state monitors the proper bipolar attachments of MTs to KTs and prevents anaphase onset until both sister KTs of each duplicated chromosome form correct MT interactions. Rieder and coworkers observed that anaphase in vertebrate somatic cells did not start until about 20 min after the last KT had attached to the spindle (Rieder *et al.*, 1994). This delay in mitotic progression in response to a “wait anaphase” signal ensures synchronous and faithful chromosome segregation. What is the site of production of this inhibitory signal? By laser irradiation it was possible to selectively destroy the unattached KT on the last monooriented chromosome in Ptk1 cells. Since these cells were able to enter anaphase 20 min after the surgery despite the uncongressed irradiated chromosome, it became evident that the source of the “wait anaphase” signal is the unattached KT (Rieder *et al.*, 1995). This conclusion was supported by yeast genetics that revealed a number of KT localised proteins, namely the Mad and Bub proteins, to be involved in SAC signalling (Li and Murray, 1991; Hoyt *et al.*, 1991). Except for Bub2, homologues of all these proteins have been found in vertebrates, called Mad1 (Chen *et al.*, 1998), Mad2 (Li and Benezra, 1996), Bub1 (Taylor and McKeon, 1997), BubR1 (yeast Mad3) (Chan *et al.*, 1999) and Bub3 (Taylor *et al.*, 1998)). The downstream target of this signal turned out to be Cdc20, the APC/C activating and specificity conferring cofactor, after the identification of yeast Mad2 binding deficient Cdc20 mutants, which were no longer sensitive to the SAC (Visintin *et al.*, 1997; Hwang *et al.*, 1998; Kim *et al.*, 1998). Like all the other SAC proteins, also Cdc20 localises to the outer KTs in pre-anaphase cells. The precise *in vivo* form of the Cdc20-APC/C inhibitor is still an issue of debate but the prevailing models hold that the SAC proteins Mad2 (Hoyt, 2001; Chan and Yen, 2003) and/or BubR1 (Tang *et al.*, 2001) sequester Cdc20 either as separate complexes (Fang, 2002) or in a complex that contains stoichiometric amounts of BubR1, Bub3, Mad2 and

INTRODUCTION

Cdc20 (mitotic checkpoint complex, MCC) (Sudakin *et al.*, 2001), thereby blocking Cdc20 activation of the APC/C for its substrates like securin and Cyclin B.

Taken together KTs integrate all functions of the SAC: they monitor the spindle-KT interactions and emit a signal if errors are detected, transmit the inhibitory signal throughout the cytoplasm and are finally the effector sites that prevent sister-chromatid separation (Musacchio *et al.*, 2002).

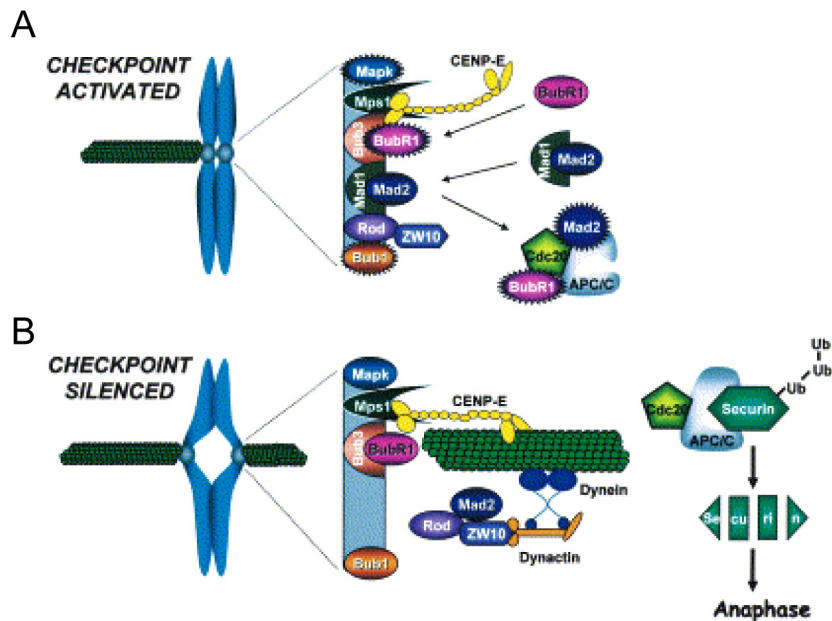


Figure 7 The SAC and its downstream targets. A) Active SAC. As long as KTs are not properly attached, checkpoint proteins are recruited to the unattached KT and Mad2 and BubR1 inhibit the APC/C activator Cdc20. B) Silenced SAC. Once all KTs are properly attached, checkpoint proteins are removed from the KT or become inactive. Consequently, Cdc20 is no longer inhibited, thus leading to anaphase onset. Illustrations adapted from Cleveland *et al.*, *Cell*, 2003.

4.2.1 Attachment versus tension

Until now it could not be satisfyingly determined how an improperly attached chromosome is detected by the SAC. Does the SAC respond to a lack of attachment of MTs to the KTs or to the absence of tension across the sister KTs (Pinsky and Biggins, 2005)? For identification of the primarily sensed defect, attachment and tension had to be dissected from each other. This is a challenging task, since they are intimately linked: on the one hand unattached KTs are not under tension and on the other hand application of tension stabilises and thus increases the number of KT-MT attachments (Nicklas and Ward, 1994; King and Nicklas, 2000).

Initial evidence for tension being the feature sensed by the SAC came from micromanipulation experiments on the sex-chromosomes of praying mantids spermatocytes (Li and Nicklas, 1997). The presence of an improperly attached chromosome delayed the metaphase-anaphase transition by 5-6 hours unless tension was applied to this chromosome by a microneedle, a condition that enabled the cells to continue to anaphase already within 1 hour. This

finding was supported by experiments in budding yeast whose KT's attach to one MT only, a situation that excludes the possibility of partial MT occupancy. Tension defects were created in meiotic yeast cells by suppressing recombination in meiosis I (Shonn *et al.*, 2000) or similarly in mitosis by preventing prior replication (Stern and Murray, 2001). Anaphase onset was delayed in both meiotic and mitotic cells although attachment occurred. On the other hand, in Rieders experiment, the destruction of the last unattached KT was sufficient to silence the SAC despite the lack of tension across the sister KT of the irradiated chromosome (Rieder *et al.*, 1995).

It has been tried to assign the two potential conditions of SAC silencing, full MT occupancy and exerted tension, to activities of subsets of SAC components (Skoufias *et al.*, 2001; Zhou *et al.*, 2002). In an oversimplified view, which neglects the intimate relationship between attachment and tension, Mad2 has been suggested to be a selective marker for unattached KT's, since it disappears from KT's upon attachment (Li *et al.*, 1996; Chen *et al.*, 1996) and is able to rebind previously attached KT's upon addition of the MT depolymerising drug nocodazole (Waters *et al.*, 1998), whereas BubR1 whose KT localisation is not affected by attachment has been implicated in sensing tension (Taylor *et al.*, 2001). But since Mad2 has been found later also at syntelically attached, tension-defective KT's of monastrol treated cells (Mayer *et al.*, 1999; Kapoor *et al.*, 2000), and BubR1 has been shown to be required for SAC activation in response to lack of attachment (Pinsky *et al.*, 2005), it emerges that the attachment and the tension sensing pathway are rather interrelated (Cleveland *et al.*, 2003).

4.2.2 Models of Mad1-assisted Mad2 activation

How defective KT-MT attachments are detected, remains an open question but detailed models have evolved to describe how the checkpoint protein Mad2 binds Cdc20 and inhibits the APC/C. Structural studies have revealed that recombinant Mad2 exists in a monomeric open conformation, O-Mad2 (also known as N1) and a closed conformation, C-Mad2 (also known as N2), which most likely forms a dimer (Luo *et al.*, 2004). Since C-Mad2 has a higher affinity for Cdc20 than O-Mad2, the closed form is more potent in inhibiting the APC/C *in vitro* (Fang *et al.*, 1998; Luo *et al.*, 2004). These common observations lead to different models of Mad2 action (Chan *et al.*, 2005b; Yu, 2006).

Luo and coworkers observed similar conformational changes of Mad2 upon binding to either Mad1 or Cdc20 and found out that the Mad2 binding sites of both Mad1 and Cdc20 have a common motif. From that they concluded that KT-associated Mad1 might recruit Mad2 to unattached KT's in order to promote the conformational switch from O-Mad2 to C-Mad2, thereby facilitating subsequent Mad2-Cdc20 interactions (Luo *et al.*, 2002). By the use of different Mad2 mutants it was shown that a preformed Mad1-C-Mad2 complex can recruit another cytoplasmic O-Mad2 molecule to the KT via Mad2 dimerisation (DeAntoni *et al.*, 2005; De *et al.*, 2005). According to the two-state Mad2 model, Mad1 subsequently induces the conversion of the C-Mad2-O-Mad2 dimer to a C-Mad2-C-Mad2 dimer and eventually it is a C-Mad2 that is released from this complex

INTRODUCTION

and transferred to Cdc20 (Luo *et al.*, 2004), whereas the Mad2 template model suggests the active conformation of Mad2 to be an unconverted O-Mad2 dimerised with C-Mad2 at the KT. Only upon release from the unattached KT and binding to Cdc20 the O-Mad2 molecule adopts the closed conformation resulting in a C-Mad2-Cdc20 complex (DeAntoni *et al.*, 2005; De *et al.*, 2005). It has been proposed that the C-Mad2-Cdc20 complex might act in a catalytic manner by binding and further converting the cytosolic pool of O-Mad2 into the inhibitory C-Mad2. Such a mechanism of exponential amplification could be suited to explain how the “wait anaphase” signal produced from only a single unattached KT is able to activate the SAC over all KTs (De *et al.*, 2005).

Silencing of the SAC might be in part attributed to p31^{comet} (CMT2), a protein that by selective binding to C-Mad2 and concomitant release of Cdc20 is able to promote mitotic exit (Habu *et al.*, 2002; Xia *et al.*, 2004).

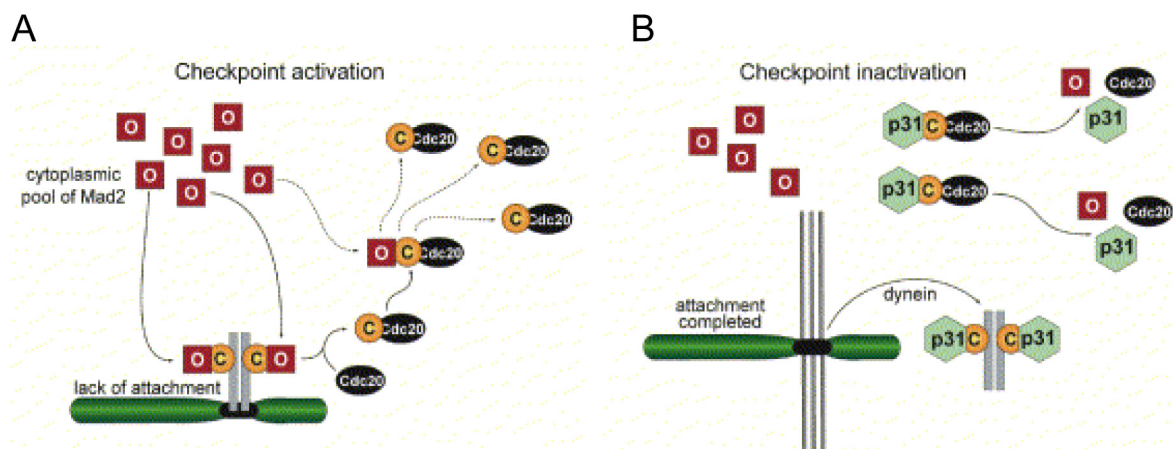


Figure 8 Mad2 template model. A) O-Mad2 is recruited to the unattached KT via dimerisation with C-Mad2. The released C-Mad2-Cdc20 complex can bind to cytoplasmic O-Mad2s and catalyse their interaction with Cdc20 molecules, thus propagating the “wait-anaphase” signal throughout the cytoplasm. B) The checkpoint silencing protein p31 acts by binding to C-Mad2 and thereby blocking the interaction of C-Mad2 with Cdc20. Illustrations adapted from DeAntoni *et al.*, *Current Biology*, 2005.

4.3 Spindle assembly dynamics and kinetochore-fibre formation

In all eukaryotic cells, a bipolar spindle apparatus has to be formed in order to faithfully segregate the chromosomes. The mitotic spindle starts forming during prophase when the two highly dynamic centrosome-nucleated MT arrays, the asters, migrate apart, a movement which involves the plus-end directed, antiparallel MT cross-linking motor protein Eg5 (Blangy *et al.*, 1995). These MT arrays will finally form the two halves of the bipolar spindle with their minus-ends at the poles and their plus-ends extending away from the poles. Upon nuclear envelope breakdown in prometaphase the MTs continuously probe the three-dimensional cytoplasmic space with their plus-ends in a random manner to search for and capture the chromosomes at their KTs (Kirschner and Mitchison, 1986). The prerequisite for this “search and capture” model of how KTs acquire MTs during mitosis lies in an intrinsic property of MTs, the dynamic instability (Mitchison and Kirschner, 1984). This describes the *in vitro* and *in vivo* behaviour of MTs wherein MT ends undergo sudden,

stochastic changes from a polymerising to a depolymerising state (catastrophe) and the other way around (rescue). Once the searching MTs make contact with KT, they are stabilised, whereas those that fail to capture KTs depolymerise (Hayden *et al.*, 1990). At their first encounter, the KT interacts only laterally with the MT surface. This initial, unstable interaction is followed by a rapid poleward movement of the captured chromosome along the MT lattice (Rieder and Alexander, 1990), which is most likely accomplished by the minus-end directed motor activity of KT-associated cytoplasmic dynein (Sharp *et al.*, 2000). Since MT density is highest near the spindle poles, the attached KT can now capture the sides or plus-ends of additional MTs. The plus-ends of the initially laterally attached MTs are unstable and shorten until they reach into the outer KT and the fibrous corona where they will be transformed into stable end-on attachments. Like this, a bundle of KT-MTs, which all terminate in a single KT, the so called kinetochore-fibre (K-fibre), is formed. The monooriented chromosome at the spindle pole experiences strong “polar ejection forces” that push it towards the cell equator, thereby increasing the chances of its still unattached sister KT to encounter MTs emanating from the opposite spindle pole. The molecular basis of these forces are chromosome arm associated plus-end motor proteins (chromokinesins) like Kid (Mazumdar and Misteli, 2005). When chromokinesins capture MTs they can move their chromosome toward the plus-end, away from the pole. Once both sister KTs of a chromosome are attached to MTs from opposite poles (bipolar attachment), the newly bioriented chromosome will progressively move, i.e. congress, to the spindle equator. But recently it has been shown that chromosomes near the poles can congress to the metaphase plate even before bipolar attachment has occurred by attaching to and sliding along the K-fibre of another already aligned chromosome (Kapoor *et al.*, 2006).

Although the “search and capture” model has been widely accepted to describe how K-fibres and spindles form, it emerged that this mechanism failed to accomplish the experimentally observed rates of chromosome capture as long as unbiased, random MT dynamics were assumed (Wollman *et al.*, 2005). Furthermore, since the model is based on centrosome-nucleated MTs it does not explain how functional spindles are assembled in cells that naturally lack centrosomes, like higher plants and many animal oocytes (Szollosi *et al.*, 1972; Karsenti *et al.*, 1984), or in animal somatic cells, which have been deprived of their centrosomes and associated astral MTs (Debec *et al.*, 1995; Khodjakov *et al.*, 2000). In these cells, an additional mechanism must exist for KT-MT formation.

Spindle assembly experiments in *Xenopus* oocyte extracts have shown that MTs are organised into bipolar spindles around plasmid DNA coated beads (Heald *et al.*, 1996) in the absence of centrosomes. This is a consequence of a Ran-GTP gradient which is highest around the chromosomes because it is created by the chromatin-bound Ran-GTP exchange factor RCC1 (Carazo-Salas *et al.*, 1999). RCC1 association with the chromosomes provides also the driving force for the nuclear import machinery in interphase. Since high Ran-GTP concentrations are generated within the nucleus as compared to the cytoplasm, nuclear Ran-GTP is able to bind to importin, a carrier which mediates nuclear transport by binding to the nuclear localisation sequence of its cargo protein. This binding releases the cargo protein. Similarly, Ran-GTP binds to importin in mitosis and thus frees and enriches spindle assembly factors like the MT nucleation factor Tpx2 in

INTRODUCTION

the vicinity of chromosomes (Kufer *et al.*, 2003;Gruss and Vernos, 2004). Tpx2 promotes the formation of short MT “stubs” on the KT corona, which elongate by addition of tubulin subunits to their KT-associated plus-ends pushing the minus-ends more and more away from the KT. Motor proteins have been shown to be able to sort the elongating, randomly oriented MTs into a bipolar array by both focusing minus-ends and pushing apart plus-ends (Gaglio *et al.*, 1996;Walczak *et al.*, 1998). This KT-driven pathway of spindle and K-fibre formation has been named the “self-assembly” model.

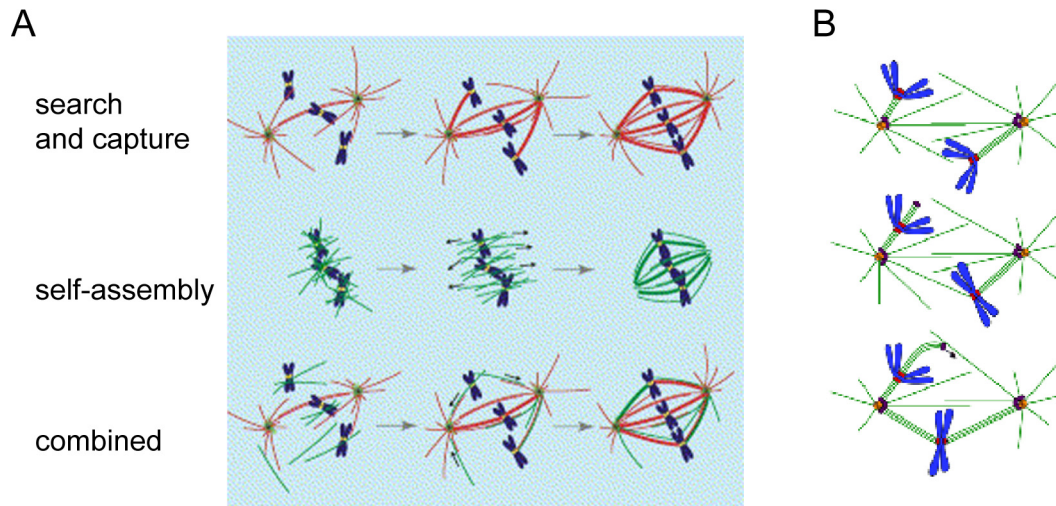


*Figure 9 Bipolar spindle assembly pathways. A) The three prevailing models explaining spindle assembly and K-fibre formation. The third one combines the “search and capture” and the “self-assembly” model. Illustration adapted from Gadde and Heald, Current Biology, 2004. B) The combined spindle assembly model. Detailed illustration of how astral MTs capture and integrate KT-derived K-fibres into a bipolar spindle with proper MT polarity. Illustration adapted from Khodjakov *et al.*, Journal of Cell Biology, 2003.*

Since it was demonstrated that the “self-assembly” route was active in animal somatic cells when the centrosomes were removed (Khodjakov *et al.*, 2000), the next obvious question arose whether this pathway worked simultaneously along with the centrosome-mediated pathway in unperturbed cells or whether the latter one usually suppressed the former in the presence of functional centrosomes. Imaging of centrosome containing, untreated either PtK1 or *Drosophila* S2 cells expressing GFP-tagged tubulin revealed that K-fibres often formed and grew from unattached KTs independent of whether centrosomes were close by. The minus-ends of these elongating K-fibres were then captured by astral MTs, transported poleward through a dynein-dependent mechanism and finally incorporated in the bipolar centrosome-nucleated MT array (Khodjakov *et al.*, 2003;Maiato *et al.*, 2004). Therefore, these observations combine the “search and capture” and the “self-assembly” model and show that both pathways contribute to K-fibre formation concurrently in the same cell, a conclusion that also accounts for the experimental kinetics of spindle formation (Gadde and Heald, 2004;Rieder, 2005).

4.4 K-fibre dynamics in chromosome congression

Chromosome congression to the spindle equator, or alignment, defines the metaphase stage and is required for accurate chromosome segregation in anaphase. Still the exact mechanism and molecular basis of congression are rather obscure. Two dynamic features of K-fibres critical for the movements of congressing chromosomes in prometaphase are described: stably attached MTs within a K-fibre display unidirectional poleward MT flux, i.e. tubulin dimers are continuously incorporated into the MT plus-ends at the KT, while they are disassembled at the same rate from the MT minus-ends at the poles (Mitchison, 1989; Maddox *et al.*, 2003). Apart from fluxing KT-MTs, KTs switch abruptly between phases of poleward and away from the pole movements, a property called KT directional instability (Skibbens *et al.*, 1993). For these oscillations to occur, polymerisation of the K-fibre at one KT must be highly coordinated with simultaneous depolymerisation of the corresponding K-fibre at the sister KT. Surprisingly, although K-fibres act as units, the dynamics of their individual MTs are not coordinated at any time point (VandenBeldt *et al.*, 2006). The poleward movement involves pulling forces driven to varying degrees by both MT flux and depolymerisation of MT plus-ends at the leading KT ("Pac-Man" KT activity) (Maddox *et al.*, 2003). High tension at the leading KT is believed to trigger the transition to away from the pole movement, which is fuelled not only by the pulling forces of the sister KT but also by the polar ejection forces from the proximal pole. Based on observations of MT dynamics in *Xenopus* egg extracts using fluorescence speckle microscopy of tubulin, it was proposed that at high tension KTs act according to a "slip-clutch" mechanism, switching to polymerisation in order to prevent detachment of depolymerising ends (Maddox *et al.*, 2003). Whatever the precise mechanism underlying the chromosome movements might be, repeated iterations of switches finally lead to congression at the metaphase plate. Gradients of the polar ejection forces and the poleward MT flux are speculated to form positional cues for the biased chromosome movement to the equator (Kapoor and Compton, 2002; Maiato and Sunkel, 2004).

4.5 Molecular basis of KT-MT attachment and stabilisation

As mentioned above attachment of MTs to KTs is intimately linked to their stabilisation. Compared to spindle MTs with unattached plus-ends, MTs within K-fibres are less sensitive to depolymerisation induced by cold treatment or calcium exposure (Rieder, 1981). The turn over of the latter ones is also slowed down (Mitchison *et al.*, 1986). Consequently, if K-fibres are detached from their KT *in vivo* by microsurgery, they will rapidly depolymerise. Also *in vitro*, plus-ends of purified MTs can be stabilised by KTs from isolated chromosomes. The region of the KT that initially encounters MTs is the outer KT together with its associated corona, the former one harbouring the MT plus-end attachment sites. KT proteins involved in proper MT attachment are usually characterised by two phenotypes: their inactivation will result in chromosome congression defects or in segregation defects with one or more lagging chromosomes (Biggins and Walczak,

INTRODUCTION

2003). As a caveat, also impairment of many in particular inner KT proteins might indirectly result in similar phenotypes due to an overall disruption of the KT structure.

Obvious candidates for linking a MT to its KT and for subsequent chromosome movement are the KT-associated motor proteins cytoplasmic dynein and CENP-E. Both accumulate particularly at unattached KTs and are released when KTs acquire a full set of MTs. The dynein-dynactin complex has been shown to be required for SAC inactivation by transporting Mad2 away from its sites of action, the KTs, to the spindle poles (Howell *et al.*, 2001). But although it might contribute to chromosome congression (Sharp *et al.*, 2000; Maiato *et al.*, 2004), it seems not to be essential for this process because inhibition of dynein activity by expression of the dynactin subunit p50 dynamitin did neither affect the number of MTs attached to a KT nor the alignment of chromosomes (Howell *et al.*, 2001). KTs in cells with disrupted CENP-E function or depleted of CENP-E show reduced MT-binding efficiency and reduced tension (Yao *et al.*, 2000; McEwen *et al.*, 2001). Moreover, a few chromosomes remain monooriented very close to the spindle poles (Schaar *et al.*, 1997). However, the observation that the majority of the chromosomes still aligns nicely at the metaphase plate and exhibits normal oscillations argues that the plus-end directed motor CENP-E is not essential for attachment *per se* and for congression (Yao *et al.*, 2000; McEwen *et al.*, 2001). As discovered recently, it rather assists congression of monooriented chromosomes by transporting them from the spindle pole to the equator along preformed K-fibres (Kapoor *et al.*, 2006).

Yeast genetics revealed the importance of the Ndc80 complex for KT-MT attachments. The Ndc80 complex is highly conserved from yeast to humans and comprises apart from the human homologue of Ndc80, Hec1 (for highly enhanced in cancer 1), the proteins Nuf2, Spc24 and Spc25. The components of the Ndc80 complex are stably bound to KTs from prophase until late anaphase irrespectively of the attachment status (DeLuca *et al.*, 2002; Hori *et al.*, 2003; Bharadwaj *et al.*, 2004). Cells with impaired Ndc80 complex function (by RNAi or antibody microinjection) have elongated spindles due to a lack of pulling forces from the KT, display reduced tension across sister KTs, have cold-sensitive K-fibres and finally fail to congress their chromosomes all indicative of a requirement of the Ndc80 complex for formation of stable KT-MT attachments (Martin-Lluesma *et al.*, 2002; DeLuca *et al.*, 2002; McClelland *et al.*, 2003; McClelland *et al.*, 2004; Bharadwaj *et al.*, 2004; DeLuca *et al.*, 2005). RNAi-depleted cells arrest in prometaphase in a SAC-dependent manner but at the same time have been shown to be required for the recruitment of a subset of outer KT proteins including checkpoint proteins like Mad1, Mad2, Mps1, Zw10 and Rod (Martin-Lluesma *et al.*, 2002; McClelland *et al.*, 2003; Hori *et al.*, 2003). Although the Ndc80 complex plays a clear role in attachment and congression, there is no evidence so far that it is able to directly bind to MT plus-ends. In yeasts this is mediated by an adaptor between the KTs and the MTs, termed the Dam1-DASH complex, which is required for KT-MT attachments (Cheeseman *et al.*, 2001; Miranda *et al.*, 2005) but so far lacks homologues in higher eukaryotes. This complex comprises 10 small subunits which assemble into a ring structure around MTs (Miranda *et al.*, 2005; Westermann *et al.*, 2005) and requires both MTs and the Ndc80 complex for KT localisation (Janke *et al.*, 2002).

The complex of RanGAP1-RanBP2 was originally identified at the cytoplasmic filaments of the nuclear pore complexes during interphase and suggested to increase the efficiency of hydrolysis of exported Ran-GTP at this site. Surprisingly, this complex was subsequently also found to localise to the spindle and KTs during mitosis. This targeting was dependent on SUMO-1 modification of RanGAP1 and more importantly on the attachment of MTs to KTs as depolymerisation of MTs or weakening of the attachments by Hec1 RNAi lead to the loss of RanGAP1-RanBP2 from the KTs (Joseph *et al.*, 2002; Joseph *et al.*, 2004). Also the production of Ran-GTP around the chromosomes and the complex formation of Ran-GTP with its mitotic effector Crm1 were shown to be essential for targeting this complex to KTs (Arnaoutov *et al.*, 2005). Perturbation of this localisation in cells by inhibition of Ran-GTP production or by RNAi-depletion of RanBP2 resulted in prolonged periods in a prometaphase state with elongated bipolar spindles, uncongressed chromosomes and cold-sensitive and therefore unstable K-fibres that did not terminate discretely at KTs (Salina *et al.*, 2003; Joseph *et al.*, 2004; Arnaoutov *et al.*, 2005). Altogether, apart from its regulation of spindle assembly factors another mitotic function of Ran emerges to be the proper targeting of RanGAP1-RanBP2 whose KT localisation is required for stabilising KT-MT attachments (Arnaoutov and Dasso, 2005).

There is yet another group of proteins, which only recently has been implicated in both KT-MT interactions and regulation of KT-MT dynamics: the MT plus-end tracking proteins (+TIPs). The first class of +TIPs requires attached MTs for their KT localisation and comprises EB1 and its interaction partner, the adenomatous polyposis coli protein (APC) (Nakamura *et al.*, 2001; Green *et al.*, 2005). Since EB1 binds selectively to KTs that are attached to polymerising MTs, EB1 and APC might assist in capturing KTs by the dynamic MT plus-ends (Tirnauer *et al.*, 2002a) consistent with chromosome alignment defects in cells with impaired EB1/APC function (Green *et al.*, 2005). Furthermore, EB1 at the KTs promoted MT polymerisation and acted as an anti-pausing factor (Rogers *et al.*, 2002; Tirnauer *et al.*, 2002b). The KT localisation of the second class of +TIPs is independent of MTs. Out of dynein/dynactin, Lis1, cytoplasmic linker protein 170 (CLIP-170) and the CLIP-associated protein (CLASP), the latter two have attracted most attention. CLIP-170 localises selectively to both unattached outer KTs and growing MT plus-ends positioning it at a perfect site for linking MTs to KTs, i.e. for initial MT capture. In line with this, RNAi depletion of CLIP-170 resulted in defective chromosome alignment due to a problem in efficiently forming KT-MT attachments rather than impaired MT dynamics (Dujardin *et al.*, 1998; Perez *et al.*, 1999; Tanenbaum *et al.*, 2006). CLASP1 preferentially localises to growing MT plus-ends and to the outer corona but in contrast to its interaction partner CLIP-170 it remains at the KTs even if they are fully attached. CLASP1 is apparently not required for the attachment process *per se* but instead is essential for regulating MT dynamics, especially the promotion of MT growth by incorporating MT subunits in fluxing K-fibres in *Drosophila* S2 cells (Maiato *et al.*, 2003; Maiato *et al.*, 2005).

Proper KT-MT attachments are characterised by sister KTs, which are each attached to MTs emanating from opposite poles. These bipolar attachments result in tension across the sister KTs whereas monotelic attachments (only one sister KT attached to MTs from one pole) and syntelic attachments (both sister KTs are attached to MTs from the same pole) do not. The CPC

INTRODUCTION

(consisting of Aurora-B kinase, its targeting and activation subunit INCENP, Survivin and Borealin, all components localising to the centromeric region (Vagnarelli *et al.*, 2004)) has been implicated in correcting improper attachments and promoting bi-orientation by selectively detaching and increasing the turnover of KT-MT attachments that do not generate tension in budding yeast (Tanaka *et al.*, 2002; Dewar *et al.*, 2004) or by selectively disassembling syntelically and merotelically attached K-fibres in vertebrates (Lampson *et al.*, 2004; Cimini *et al.*, 2006; Knowlton *et al.*, 2006). Impairing Aurora-B function does not only accumulate cells with stabilised defective attachments (Adams *et al.*, 2001; Kallio *et al.*, 2002; Ditchfield *et al.*, 2003; Lampson and Kapoor, 2005) but also renders the SAC insensitive to the lack of tension (Biggins and Murray, 2001; Ditchfield *et al.*, 2003; Carvalho *et al.*, 2003). In vertebrates, the Kin-I kinesin MCAK might be the downstream target of Aurora-B in correcting aberrant attachments. Both its depolymerising activity and its respective outer KT and centromere localisation have been shown to be regulated by Aurora-B wherein tension from bipolar attachment may influence the access of MCAK to Aurora-B (Kline-Smith *et al.*, 2004; Lan *et al.*, 2004; Andrews *et al.*, 2004).

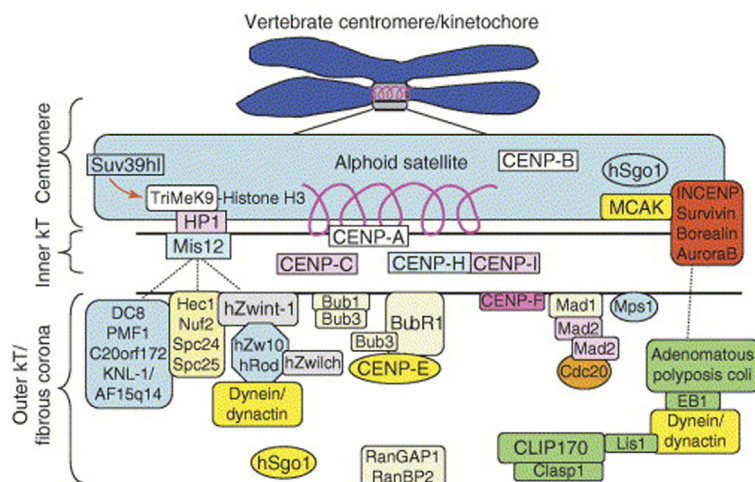


Figure 10 Current view of the molecular organisation of the vertebrate KT/centromere region based on observed interactions and localisation dependencies of the known KT components. Illustration adapted from Chan *et al.*, *Trends in Cell Biology*, 2005.

AIM OF THE WORK

Plk1 is one of the key regulating mitotic kinases. Still its mechanism of action is rather unknown. To elucidate how Plk1 is contributing to proper mitotic progression we wanted to search for novel mitotic and phosphorylated Plk1 interaction partners, which primarily interact with Plk1 via its C-terminal targeting domain, the so called PBD. Furthermore, we wanted to find out to which extent the multiple proposed mitotic Plk1 functions depend on the recruitment of Plk1 activity to the different subcellular structures via the PBD and whether it was possible to specifically interfere with only a subset of Plk1 functions by disrupting PBD-dependent targeting. In this context, in particular the so far unknown function of Plk1 at the KTs caught our interest (Part I).

Knowing the protein composition of the mitotic spindle would provide useful information for understanding the essential mechanisms of spindle assembly and chromosome movements during prometaphase and anaphase. In order to identify novel spindle associated proteins a mass spectrometry (MS) based inventory of the human mitotic spindle was performed identifying amongst others a so far uncharacterised spindle and KT associated protein, termed Ska1. We aimed to understand the requirements for KT localisation of Ska1 and its interaction partner Ska2 and to reveal the function of this novel KT complex in proper progression through mitosis (Part II).

PART I

**Search for Plk1 PBD interaction partners and
functional analysis of Plk1 PBD expressing cells**

RESULTS I

1 Unbiased search for Plk1 PBD interacting proteins by pull downs and immunoprecipitations

The C-terminal PBD of Plk1 has been shown to act as a phosphopeptide binding domain, to target Plk1 to its different subcellular structures and to exhibit an even higher affinity to the optimal PBD binding phosphopeptide (PBDtide) than full length Plk1 (Elia *et al.*, 2003a). These features prompted us to choose the PBD as a bait to search for novel, mitotic Plk1 PBD interacting phosphoproteins. A PBD mutant form, in which His538 and Lys540, two residues critical for phosphopeptide binding, were changed into alanine residues served as a negative control.

1.1 Bacterial expression and purification of GST-PBD^{WT} and GST-PBD^{HK538/540AA}

Expression of GST-tagged constructs encoding either the PBD wildtype (PBD^{WT}, 326-603aa) or the phosphopeptide binding mutant PBD^{HK538/540AA} (PBD^{AA}, 326-603aa) was performed in the *E. coli* strain JM 109-RIL, and the GST-tagged proteins were purified using glutathione sepharose. High amounts of both the GST-PBD^{WT} and the mutant PBD^{AA} could be isolated from the soluble fraction (Figure 11). In contrast to other tested PBD mutants (PBD deletion of 410-437aa or PBD^{YQL425-427AAA}, data not shown) (Lee *et al.*, 1998; Reynolds *et al.*, 2003), the PBD^{AA} was soluble suggesting that its overall domain structure was not impaired.

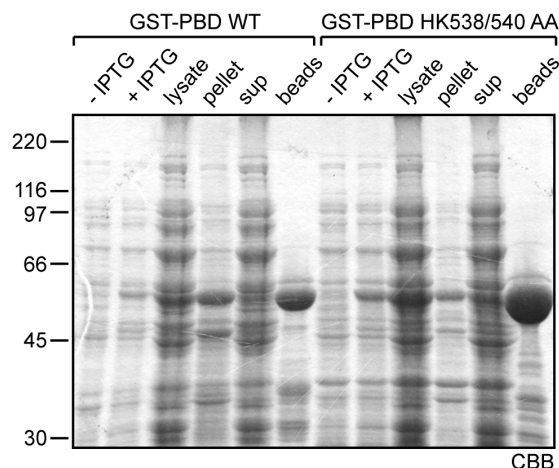


Figure 11 Induction, expression and purification of GST-PBD^{WT} and GST-PBD^{AA} from *E. coli* by immobilisation on glutathione beads. An SDS-PAGE gel was loaded with bacteria before (-IPTG) and after (+IPTG) induction, followed by samples of the crude bacterial lysate before spinning (lysate), the pellet fraction after spinning (pellet) and its corresponding cleared lysate (sup) and finally glutathione beads, which were used to isolate the expressed protein (beads). After electrophoresis the gel was stained with Coomassie Brilliant Blue (CBB).

1.2 PBD^{WT} but not PBD^{AA} recognises specifically phosphorylated peptides and proteins

1.2.1 The PBD^{WT} but not PBD^{AA} recognises the PBDtide

To verify the inability of the PBD^{AA} mutant to bind to phosphorylated residues, the immobilised GST-PBD^{WT} and PBD^{AA} proteins were used for an *in vitro* phosphopeptide binding assay with the PBDtide. As analysed by MS, the PBD^{WT} but not PBD^{AA} readily interacted with the optimal PBDtide (Figure 12A), confirming a previous study (Elia *et al.*, 2003a).

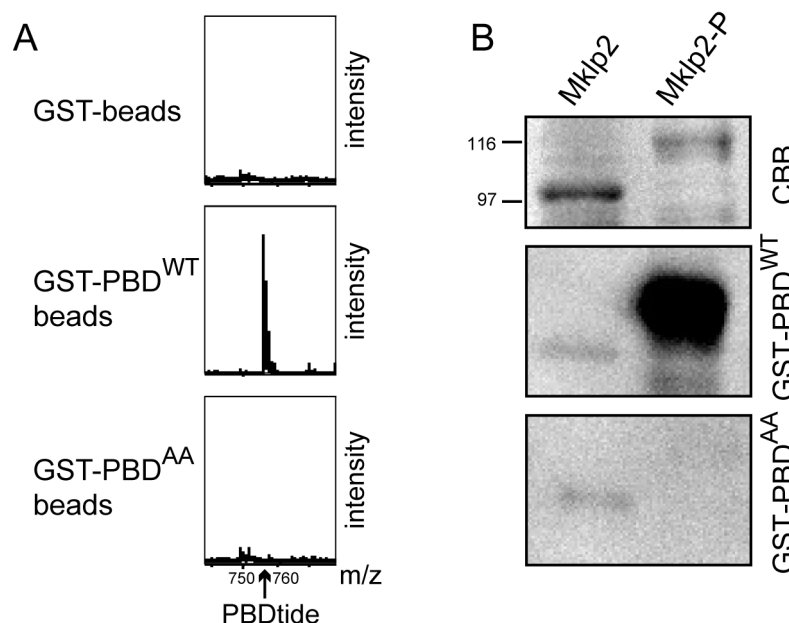


Figure 12 GST-PBD^{AA} has lost its ability to bind to phosphorylated peptides and proteins A) *In vitro* analysis of phosphopeptide binding to GST-PBD^{WT}, GST-PBD^{AA} and control (GST) coated glutathione-Sepharose beads. Phosphopeptide binding was determined by MS. Only with GST-PBD^{WT}, a phosphopeptide (PBDtide) of the correct m/z ratio was detected. B) Recombinant Mklp2, was either phosphorylated by Plk1 (Mklp2-P) in an *in vitro* kinase assay, or left untreated (Mklp2), separated by SDS-PAGE and transferred on membranes by Western blotting. Subsequently these membranes were incubated with either GST-PBD^{WT} or GST-PBD^{AA} for Far Western analysis. The CBB stained gel shows equal loading of the recombinant Mklp2 as well as the phosphorylation induced upshift of Mklp2-P.

1.2.2 Far Western binding of PBD^{WT} but not PBD^{AA} to phosphorylated Mklp2

In order to further demonstrate the different binding properties of the PBD^{WT} and the PBD^{AA}, we performed a Far Western analysis on unphosphorylated and Plk1 phosphorylated recombinant Mklp2 protein (obtained from Rüdiger Neef). Plk1-phosphorylated Mklp2 had been shown to be specifically recognised by the Plk1 PBD (Neef *et al.*, 2003). In line, only the GST-PBD^{WT} but not GST-PBD^{AA} was able to directly and specifically bind to the phosphorylated Mklp2 form (Figure

RESULTS I

12B). This further demonstrates that only the PBD^{WT} is able to interact with full length phosphorylated proteins, whereas the phosphopeptide binding mutant has lost this ability.

1.3 Large scale pull down from a mitotic lysate with GST-PBD^{WT} and GST-PBD^{AA} lacks sufficient specificity

HeLa S3 cells were grown in spinner cultures and synchronised in mitosis by a sequential thymidine/nocodazole block and release protocol. Since we were especially interested in proteins, which bind to the PBD only after prephosphorylation by a priming kinase we tried to increase the predominance of these proteins by two means: first we preincubated the obtained mitotic dounced lysate with the GST-PBD^{AA} immobilised on Affi-Gel beads in order to absorb all the proteins, which bind either unspecifically to the GST-tag or in a phosphorylation independent manner to the PBD surface. Only this precleared supernatant was then transferred to the GST-PBD^{WT} beads. Secondly, we did not analyse all the proteins which had bound to the PBD beads but only those, which were eluted from the beads upon incubation with an excess of the competing PBDtide. The eluate of the PBD^{WT} beads should therefore exclusively contain mitotic phosphorylated proteins, which interact with the PBD via its phosphopeptide binding cleft in a phosphorylation dependent manner.

The lysate itself, the PBDtide eluates, the beads after elution and the supernatant after incubation with the GST-PBD^{AA} (sup AA) and PBD^{WT} (sup WT) beads, respectively, were loaded on a NuPAGE gradient gel and CBB stained (Figure 13). Clearly much more protein was eluted from the immobilised PBD^{WT}, as compared to PBD^{AA}. The PBD^{WT} and the PBD^{AA} eluate lanes were cut into twelve corresponding slices each, in-gel digested with trypsin and analysed by MS (carried out by Roman Körner). About two thirds of the pulled down proteins were specific for the PBD^{WT} eluate. However, the specificity of this approach was still not sufficiently high, as altogether 375 proteins were eluted from the PBD^{WT} (Table 6), an amount which is unlikely to reflect physiological *in vivo* interactions only. Among the proteins, which had a good Mascot score, i. e. more than 100, many proteins of the minichromosomal maintenance complex (MCM) required for licensing of replication origins (Blow and Dutta, 2005; Maiorano *et al.*, 2006) were found along with dynein heavy chain, kinesin heavy chain, vimentin and lamins. Other groups of proteins with a good score include components of the intracellular membrane trafficking system (e. g. Adapter-related protein complex 3, SH3-containing GRB2-like protein 1, ABP130 and Ras-related protein Rab1B), proteins with an ubiquitin ligase activity (e. g. LASU1, Retinoblastoma-associated factor 600) and ubiquitin itself, metabolic enzymes (e. g. ATP citrate synthase, S-adenosylhomocysteine hydrolase-like protein, D-3-phosphoglycerate dehydrogenase, Adenosine monophosphate deaminase 2), chaperones (e. g. Hsp90, Hsp70, Hsp27), DNA binding proteins (e. g. alpha-complex protein 1, transcription factors), proteins involved in DNA synthesis (e. g. helicases, DNA primase chain p58, DNA polymerase alpha) and nucleoporins (e. g. RanBP7, Nup43, Nup160, Nup98, Nup133, Nup75). Most of the above mentioned proteins seemed to function in processes, which are not

apparently linked to spindle formation and chromosome segregation, the mitotic processes we were most interested in. Apart from dynein and kinesin heavy chains, the few proteins with a direct link to mitotic processes displayed a score below 100. These potentially interesting interacting partners include NuMA (score 87), Condensin subunit 2 (score 82), Hurp (score 73), Mad2A (score 59, but also pulled down by PBD^{AA}) and Bub3 (43).

Taken together, the *in vitro* PBD pull down experiment delivered more than 350 different proteins involved in many diverse cellular processes. Two thirds were specifically eluted from the PBD^{WT} so that we ended up with more than 200 potential Plk1 PBD^{WT} interacting partners demonstrating that this approach lacked sufficient specificity. Furthermore, the majority of the proteins with a reliable Mascot score above 100 was not apparently appealing for us since we were in particular interested in Plk1 PBD interacting partners, which play a role in mitosis.

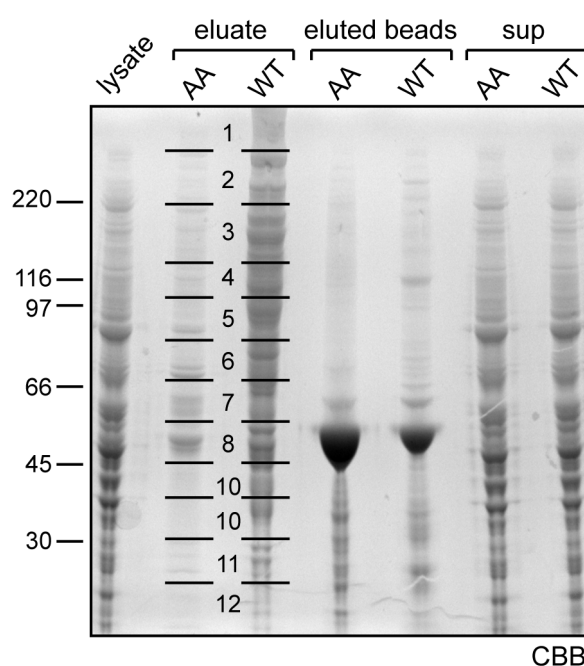


Figure 13 GST-PBD^{WT} pull down from mitotic HeLa S3 lysate lacks sufficient specificity despite PBD^{AA} preclearance and PBDtide elution. HeLa S3 cells were nocodazole blocked for 14 hours and released into fresh medium until the majority had reached metaphase. After douncing, the lysate was first transferred onto GST-PBD^{AA} coupled glutathione beads and after 4 hours incubation the supernatant was combined with GST-PBD^{WT} beads for overnight incubation. Proteins bound to both PBD^{WT} and PBD^{AA} were eluted with PBDtide, respectively, and subsequently the input lysate, PBDtide eluates, eluted beads and supernatants of either the GST-PBD^{AA} (AA) or the GST-PBD^{WT} (WT) were loaded on a NuPAGE gradient gel, which was stained with CBB and cut into the indicated slices for MS analysis.

RESULTS I

1.4 Generation of inducible myc-PBD^{WT} and myc-PBD^{AA} HeLa S3 cell lines

We hoped to increase the specificity of our search for PIK1 PBD interacting proteins by creating stable, inducible myc-PBD^{WT} and myc-PBD^{AA} HeLa S3 cell lines suitable for immunoprecipitations (IPs). The advantage of this approach is that the myc-PBDs are expressed within the cell and not exogenously added to an extract like the bacterially expressed GST-PBDs. Therefore, we no longer employ excessive amounts but rather moderately overexpressed PBDs and, importantly, the interactions with the potential PBD binding partners can occur *in vivo* at the physiological locations.

We created the myc-PBD^{WT} and PBD^{AA} stable inducible cell lines in HeLa S3 T-Rex cells with the Tet ON system (made by Herman Silljé and Anja Wehner). Hence the cells should only express the respective domains upon addition of tetracycline. Positive cell clones were screened by immunofluorescence (IF) microscopy after tetracycline induction for 24 hours (with kind help of Anja Wehner). Figure 14A shows the obtained positive clones for the myc-PBD^{WT} (# 15.5) and for the myc-PBD^{AA} (# 24.1), which were used for all the following experiments.

In order to test whether the cell lines, which were positive for myc-staining by IF, indeed expressed the PBD we performed Western blot analysis using an anti-PIK1 antibody that recognises also the PBD alone. The myc-PBD^{WT} and PBD^{AA} cell lines were incubated with tetracycline for either 8 or 24 hours or left untreated as a control. Western blot analysis of the respective cell extracts revealed that after 24 hours the exogenous proteins reached about 10 times the level of endogenous PIK1. But even after 8 hours the expression of the myc-PBDs was already clearly induced (Figure 14B).

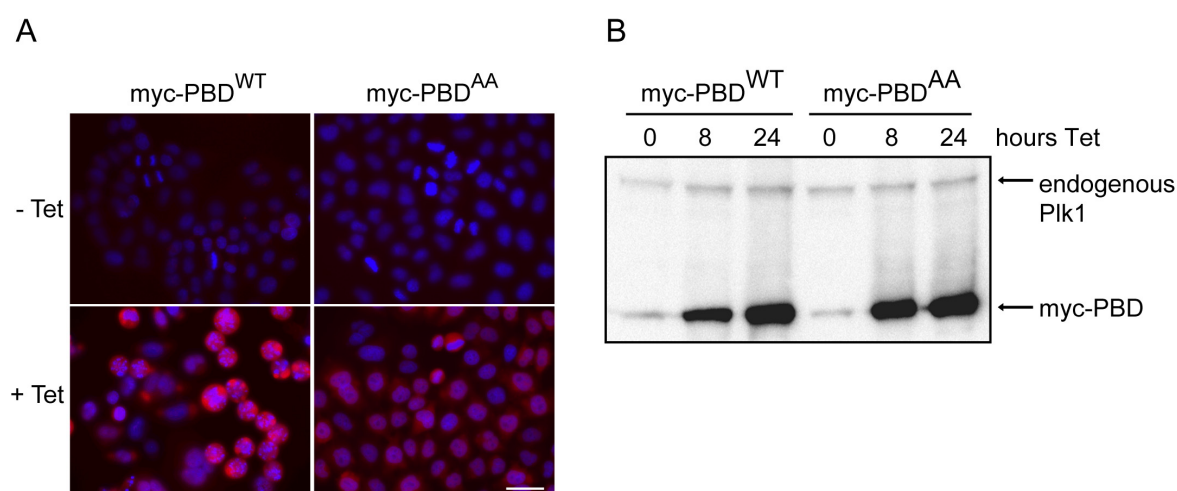


Figure 14 myc-PBD^{WT} clone 15.5 and myc-PBD^{AA} clone 24.1 express the respective domains to similar levels upon tetracycline (Tet) induction. A) The respective stable HeLa S3 cell lines were either left untreated (-Tet) or incubated with tetracycline (+Tet). After 24 hours of induction cells were fixed and permeabilised with PTEMF and stained with anti-myc 9E10 antibody (red) and with DAPI (DNA, blue). Scale bar indicates 20 μ m. B) Equal amounts of cell extract, prepared from the respective stable HeLa S3 cell lines after induction for the indicated hours with tetracycline, were separated by SDS-PAGE and probed after Western blotting with an anti-PIK1 antibody that also recognises the PBD.

1.5 Immunoprecipitations of myc-PBD^{WT} and myc-PBD^{AA} expressed in stable cell lines increase the specificity

The stable myc-PBD^{WT} and PBD^{AA} cell lines were each grown in several triple flask, arrested with aphidicolin at the G1/S transition for 14 hours and released into fresh medium before both nocodazole and tetracycline were added for another 14 hours. Mitotic cells were obtained by mitotic shake off and released in fresh medium without nocodazole in order to allow spindle formation and lysed with a cell cracker. The expressed PBDs were immunoprecipitated (IPed) from the extracts by anti-myc antibody (9E10) immobilised on protein G beads and the co-IPed potential PBD interactors were eluted from the PBDs by the PBDtide. Eluates and the beads after elution were loaded on a gradient NuPAGE gel. Distinct bands specific for the PBD^{WT} eluate were cut from the gel, in-gel digested with trypsin and analysed by MS (performed by Roman Körner) (Figure 15).

Importantly, the amount of proteins, which was eluted from the beads upon competition with the PBDtide, was strongly decreased compared to the GST-PBD pulldown. In fact we obtained distinct bands, which appeared only in the PBD^{WT} but not the PBD^{AA} eluate lane (Figure 15). Together this indicates that by expressing the myc-PBD in and IPing it from HeLa S3 cells we could strongly increase the specificity of the approach.

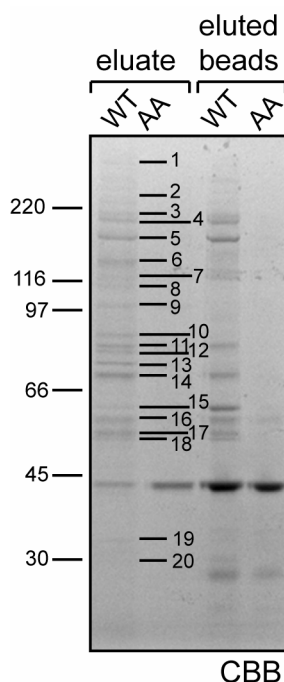


Figure 15 IPs of myc-PBD^{WT} and myc-PBD^{AA} expressed in the stable HeLa S3 cell lines increase the specificity for the PBD interaction but does not reveal any apparently relevant mitotic Plk1 PBD interaction partners. The respective synchronised stable cell lines were induced with tetracycline for 14 hours in the presence of nocodazole. Cells were released from nocodazole for 40 min until the majority had reached metaphase before being lysed in a cell cracker. The PBDs were isolated from the respective cell extracts by myc-antibodies coupled to protein G beads and their phosphorylation specific interaction partners were eluted by excess of PBDtide. The PBDtide eluates and the eluted beads of either the myc-PBD^{WT} (WT) or the myc-PBD^{AA} (AA) were loaded on a NuPAGE gradient gel, which was stained with CBB, and indicated distinct protein bands were cut out, followed by MS analysis.

RESULTS I

Unfortunately, however, none of the identified proteins seemed to be an apparently relevant Plk1 PBD interaction partner with respect to Plk1 functions in mitosis at the first glance (Table 1). Still it is important to mention that by both approaches, the GST-PBD pulldown and the myc-PBD IP, lamins, nucleoporins (albeit different ones), Hsp90/70 and, most interestingly, MCM components and vimentin were found as interactors. The latter two, MCMs and vimentin, have been proved later to be real Plk1 interaction partners (Yamaguchi *et al.*, 2005; Tsvetkov and Stern, 2005). Therefore, these screens did function, but from our perspective on mitotic spindle functioning and chromosome segregation these proteins were of less obvious interest.

Gel band #	Identified peptides from protein:	Gel band #	Identified peptides from protein:
1	desmoplakin, nucleoprotein TPR, ubiquitin protein ligase EDD	11	Hsp70, lamin A/C
2	KIF1B, APC subunit 1, RhoGEF12	12	Hsp70, lamin A/C, H4 protein
3	Nup188, 190 RhoGAP	13	lamin A/C, H4 protein
4	JNK-associated leucine zipper protein (JLP), dead box helicase, tensin3	14	NAC1 protein, NIPA
5	Nup155, anillin	15	vimentin
6	ATP citrate lyase, MCM2, exportin 1	16	tubulin α/β
7	MCM4, Mklp1	17	actin
8	MCM6, hsp90, MCM3, doc2, APC2	18	tubulin β , keratin, EEF1A
9	hsp90, Nup93, lamin A/C	19	monooxygenase, 14-3-3
10	lamin A/C, adaptor-related protein complex, dystrophin	20	14-3-3 ϵ , tropomyosin, tubulin

Table 1 Summary of the most prominent proteins identified by MS in the distinct gel bands of the PBDtide eluate from the myc-PBD^{WT} IP (see Figure 15).

2 Biased search for Plk1 PBD interacting proteins by immunoprecipitations followed by Western blot analysis

The above described unbiased screens for Plk1 PBD interacting phosphoproteins by pulldowns and IPs with the PBD, followed by MS analysis did not result in any apparently interesting candidates from our mitotic perspective. This could result from the insufficient specificity of these approaches and/or reflect that most regulatory mitotic proteins are present at relatively low levels and hence remained undetected by our MS approach. We therefore employed the myc-PBD^{WT} and myc-PBD^{AA} stable cell lines for IPs, which were no longer followed by an unbiased MS analysis but by Western blotting using many different available antibodies against spindle, KT and centrosome associated proteins.

2.1 Among the tested proteins only Cdc20, Cdc27, Bub1 and Ect2 co-immunoprecipitated specifically with myc-PBD^{WT}

Both the myc-PBD^{WT} and the myc-PBD^{AA} stable cell line were induced by tetracycline addition for 24 hours. But since only the PBD^{WT} overexpression resulted in an increased mitotic index (see Results, chapter A 3), we additionally treated the myc-PBD^{AA} cells with nocodazole for the last 14 hours in order to obtain equal amounts of mitotic cells from both cell lines. The mitotic cells were obtained by shake off and the PBD^{AA} cells were released to allow reformation of the spindle, before cell lysis and incubation with anti-myc 9E10 antibody covalently coupled to protein G sepharose beads. Inputs and myc-IPs (~30x input) were separated on SDS gels, blotted and probed with different available antibodies against known spindle proteins, all of them potential Plk1 PBD interaction candidates (Figure 16).

By far the majority of the tested proteins bound to neither the myc-PBD^{WT} nor the myc-PBD^{AA} (Figure 16A) confirming the specificity of the PBD interaction in this experiment. γ -tubulin was co-IPed by the PBD in a phosphorylation independent manner since it was detected in the IPs of both, the PBD^{WT} and the phosphobinding mutant (Figure 16A). The most interesting group of proteins was obviously the one that bound specifically to the PBD^{WT} only. This was observed for Cdc20, Cdc27, Bub1 and Ect2 (Figure 16B). All these proteins are known to be phosphorylated during mitosis and co-localise in part with the different structures, to which Plk1 is targeted in the course of mitosis like KTs (Cdc20, Bub1, Cdc27) (Weinstein, 1997; Taylor *et al.*, 1997; Topper *et al.*, 2002), central spindle and midzone / midbody (Ect2) (Chalamalasetty *et al.*, 2006). Therefore, these four proteins are good candidates for being real Plk1 PBD interactors and they were hence further investigated.

RESULTS I

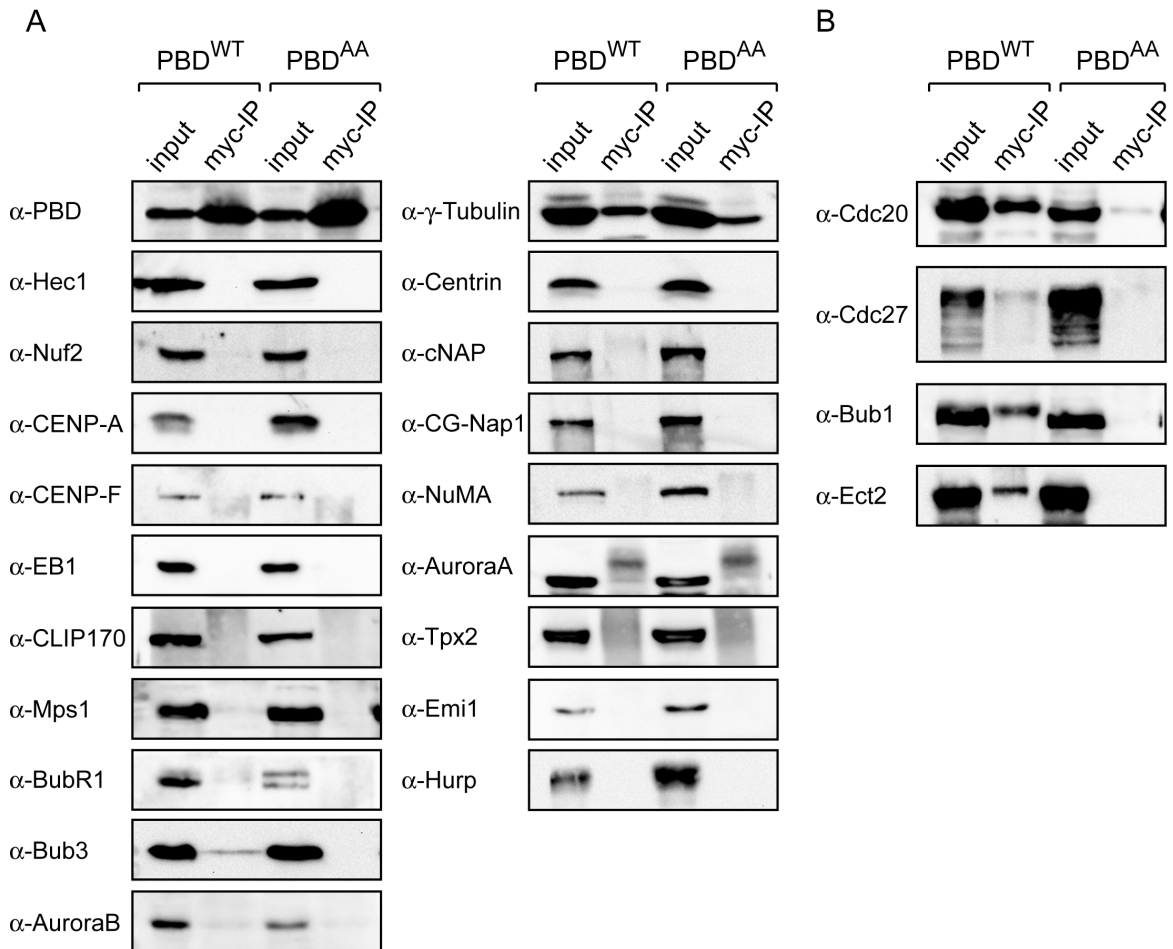


Figure 16 Cdc20, Cdc27, Bub1 and Ect2 bind specifically to the myc-PBD^{WT}. The stable cell lines were induced with tetracycline for 24 hours and the myc-PBD^{AA} was additionally treated with nocodazole for the last 14 hours and then released for 40 min (to allow spindle formation). IPs with the anti-myc antibody were performed from the respective mitotic lysates and inputs and immune complexes loaded on a SDS gel followed by Western blot analysis using the indicated antibodies A) The majority of the tested KT, centrosome and spindle associated proteins did neither bind to the myc-PBD^{WT} nor the PBD^{AA} beads. B) Only Cdc20, Cdc27, Bub1 and Ect 2 were specifically co-IPed by the myc-PBD^{WT}.

2.2 Endogenous Plk1 does not co-immunoprecipitate any of the myc-PBD^{WT} interacting candidates

In order to examine first whether the proteins, which co-IPed with the myc-PBD^{WT}, namely Cdc20, Cdc27, Bub1 and Ect2, also bind to the full length Plk1, secondly whether they interacted with Plk1 at endogenous levels and third whether this potential interaction was mitosis specific, we performed an endogenous Plk1-IP (control IP 9E10 antibodies) from both nocodazole and aphidicolin arrested HeLa S3 cells. Nocodazole arrested cells were always released into fresh medium to allow spindle reformation before lysis was performed.

In conformity with its expression levels, more Plk1 was IPed from the mitotic extract (Figure 17A). Neither Cdc20 and Cdc27 nor Bub1 could, however, be co-IPed (Figure 17A). In an independent experiment, Ect2 could not be co-IPed with endogenous Plk1 from mitotic extracts either (control IP GFP antibodies) (Figure 17B). Thus, we were not able to confirm the observed

interactions between Plk1 PBD and Cdc20, Cdc27, Bub1 and Ect2, respectively, on endogenous levels with the full length Plk1 protein.

These negative results, however, do not immediately exclude potential interactions since the Plk1 antibody, which binds to the linker region of the PBD could well have interfered with Plk1 binding to further proteins. This problem could have been overcome by reciprocal IPs of the respective endogenous candidates and analysis of the presence of Plk1 in the co-IPs. Unfortunately, obtained data were neither clear nor reproducible. This could be due to buffer conditions, which were not appropriate for the different interactions, or to antibodies not suitable for IPs. Therefore, IPs with overexpressed proteins were the only possible approach to further analyse these interactions.

Among the candidate Plk1 PBD interaction partners Bub1, Cdc27, Ect2 and Cdc20, it was only the latter one, which gave reliable and reproducible positive results in the overexpression analysis (Figure 18). Hence, the Plk1-Cdc20 interaction was chosen for more detailed examination.

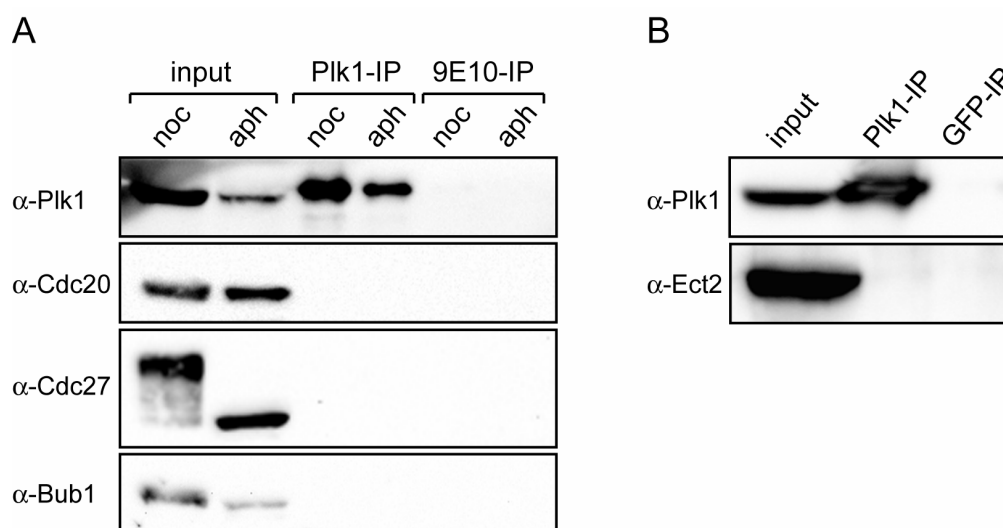


Figure 17 Non of the myc-PBD^{WT} interacting proteins, Cdc20, Cdc27, Bub1 and Ect2, could be co-IPed with full length endogenous Plk1. A) Lysates were prepared from mitotic HeLa S3 cells released for 40 min from a nocodazole block (to allow spindle formation) and from aphidicolin arrested cells. These lysates were then used for IPs with anti-Plk1 antibody and mouse 9E10 antibody (negative control), respectively. Lysates and immune complexes (~10x input) were separated by SDS-PAGE and probed by Western blotting with anti-Plk1, anti-Cdc20, anti-Cdc27 and anti-Bub1 antibodies, respectively. B) Lysates were prepared from mitotic HeLa S3 cells released for 40 min from a nocodazole block. These mitotic lysates were then used for IPs with anti-Plk1 antibody and mouse anti-GFP antibody (negative control), respectively. Lysate and immune complexes were separated by SDS-PAGE and probed after Western blotting with anti-Plk1 and anti-Ect2 antibodies.

2.3 Analysis of the interaction between Plk1 and Cdc20

Plk1 localises not only to the centrosomes and the central spindle in the course of mitosis, it is also detected at the outer KT from prometaphase to anaphase. However, nothing is known about Plk1 function at the KTs so far. Cdc20 also localises to the outer KT during mitosis and, importantly, is

RESULTS I

the target of the SAC (Musacchio *et al.*, 2002). The above described observation that Cdc20 was among the proteins that interacted specifically with the myc-PBD^{WT}, but not the myc-PBD^{AA}, encouraged us to further analyse this potential interaction, hoping to gain insights into Plk1 KT function.

2.3.1 Endogenous Cdc20 interacts with both full length Plk1^{WT} and Plk1^{AA} in a mitosis specific manner

IPs of the endogenous Plk1 protein did not co-IP endogenous Cdc20. Since the Plk1 antibody itself recognises the linker region of the PBD, it is, as mentioned above, possible that the antibody-Plk1 interaction sterically prevented the interaction of the PBD with its docking partner Cdc20. Overexpression of a myc-tagged Plk1 full length version followed by an IP using the anti-myc antibody (9E10) should, however, bypass this possible hindrance.

For this purpose, 293 cells were transfected with either myc-Plk1^{WT} or the full length Plk1 construct carrying the corresponding HK538/540AA mutations within its PBD (myc-Plk1^{AA}) and grown for 24 hours either asynchronously (asy) or in the presence of nocodazole (noc) for the last 14 hours. The latter were released from nocodazole for 45 min before preparation of the cell extract. The different lysates were used for IPs with the 9E10 antibody and inputs and IPs loaded on a SDS gel followed by Western blot analysis. Both myc-Plk1^{WT} and Plk1^{AA} were IPed to comparable levels in nocodazole treated and asynchronous cells (Figure 18A). Surprisingly, the full length Plk1^{AA} was found to interact with Cdc20 as strongly as the Plk1^{WT} (Figure 18A), although in the screen only the PBD^{WT}, and not the PBD^{AA}, was able to bind to Cdc20 (Figure 16B). Yet the interaction was mitosis specific as no Cdc20 could be recovered from Plk1^{WT} and Plk1^{AA} IPs in the asynchronous extracts (Figure 18A).

Of course, these contradictory findings might be reduced to the fact that we were dealing with overexpressed Plk1 protein, which might not reflect the physiological situation. Still it is tempting to assume a novel binding mode of Cdc20 to Plk1: the isolated PBDWT itself is sufficient to bind Cdc20 but in the physiological situation of a full length Plk1 the Cdc20 interaction requires also partly the N-terminus. Hence, only if both PBD and kinase domain are accessible for Cdc20, the binding is strong. It is believed that only mitotic Plk1, thanks to its phosphorylation at threonine residue 210, exhibits an open confirmation. Therefore, the conditions for Cdc20-Plk1 interactions are adequate only during mitosis and are then independent of the PBD phosphate moiety binding residues, as Cdc20 is “clamped” between both, the kinase domain and the PBD.

For this binding mode to be proven correct, Cdc20 should show an additional affinity to the Plk1 N-terminus and/or should even in asynchronous extracts be able to bind to the Plk1^{T210D} mutant, which is supposed to be constitutively in the open conformation (Jang *et al.*, 2002b). Therefore, we conducted an experiment under the same conditions as in Figure 18A, but overexpressed this time the myc-Plk1 kinase domain (myc-Plk1^{1-330aa}), the myc-Plk1^{T210D} mutant and myc-Plk1^{WT} as a control. The Plk1 kinase domain alone turned out to be unable to interact with endogenous Cdc20 (Figure 18B). Moreover, the myc-Plk1^{T210D} was already less efficient in co-

IPing Cdc20 from nocodazole treated extracts and failed to bind Cdc20 in the asynchronous extract (Figure 18B).

Since these results did not support our explanation for the intuitively contradictory situations, the exact mechanism of the Cdc20-Plk1 interaction, be it only partly PBD-dependent but still mitosis specific *in vivo* could not be elucidated.

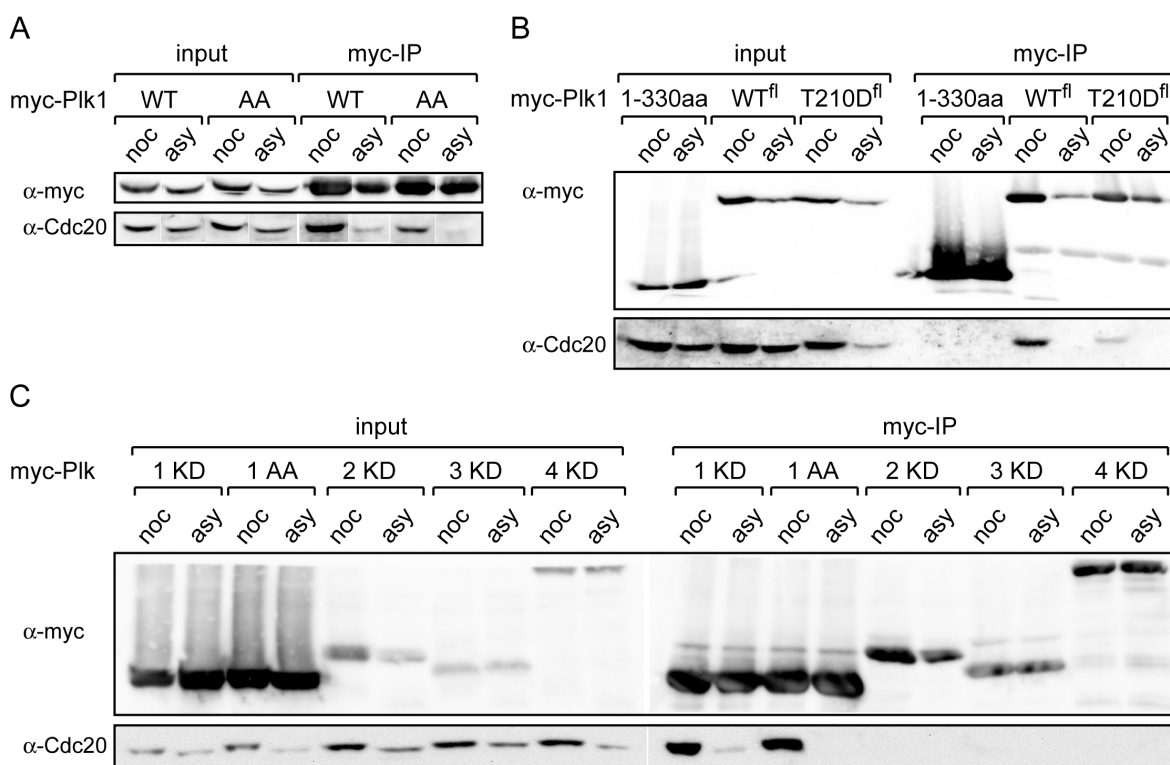


Figure 18 Both myc-Plk1^{WT} and Plk1-AA interact with endogenous Cdc20 in a mitosis specific manner and none of the other Plk family members can bind Cdc20. A) 293 cells were transfected with myc-tagged Plk1^{WT} and myc-Plk1^{AA} constructs for 24 hours and were either left untreated (asy) or treated with nocodazole (noc) for the last 14 hours and released for 45 min (to allow spindle formation). Lysates were used for IPs with the 9E10 antibody (myc) and inputs and IPs (~23x input) were separated by SDS-PAGE and followed by Western blotting using either 9E10 (myc) or anti-Cdc20 antibodies. B) Same as in A but transfected constructs encoded myc-Plk1 1-330aa, myc-Plk1^{WT} and myc-Plk1^{T210D}. C) Same as in A but transfected constructs encoded myc-Plk1^{K82R} (1KD), myc-Plk1^{AA} (1AA), myc-Plk2^{D233A} (2KD), myc-Plk3^{D164A} (3KD) and myc-Plk4^{D154A} (4KD), respectively.

2.3.2 Endogenous Cdc20 interacts specifically with myc-Plk1 but not with the other members of the Polo-like kinase family

The Plk family comprises up to date four members, Plk1, Plk2, Plk3 and Plk4 (Sak), which show high sequence similarity especially within the kinase domain but also within the C-terminus (Barr *et al.*, 2004). Still only Plk1 has so far been described to localise to KTs. We were interested in whether the observed interaction between Plk1 and the KT protein Cdc20 was specific for this member despite the sequence similarities within the Polo family.

RESULTS I

Since the wildtype Plk2, Plk3 and Plk4 expression levels were much lower than the one of Plk1^{WT}, we decided to overexpress the kinase dead (KD) versions of Plk1 to Plk4 (Plk1^{K82R}, Plk2^{D233A}, Plk3^{D164A}, Plk4^{D154A}). We had seen before that myc-Plk1^{K82R} is equally potent to interact with endogenous Cdc20 as Plk1^{WT} (data not shown). The cells were transiently transfected and the myc-IPs performed as described for Figure 18A,B. Comparable amounts of the respective myc-Plk members were IPed from the extracts (Figure 18C). Cdc20, however, only interacted with myc-Plk1^{WT} and Plk1^{AA} (Figure 18C). This high specificity of endogenous Cdc20 for only the overexpressed myc-Plk1 argues for a functional relevance of this interaction *in vivo*, most likely at the KT.

2.3.3 Tagging of Cdc20 interferes with the Plk1 interaction

During our studies Tang and coworkers demonstrated a link between the checkpoint kinase Bub1 and Cdc20 (Tang *et al.*, 2004), two proteins, which we found to interact specifically with the myc-PBD^{WT}. They showed that Bub1, stimulated by an active SAC, could phosphorylate Cdc20, which leads to an inhibition of the APC/C-Cdc20 in a catalytic manner. In line, nocodazole treated cells expressing Cdc20 proteins mutated at the Bub1 phosphorylation sites did override the SAC. Among the six Bub1 phosphorylation sites, all within the N-terminus of Cdc20, was one phosphoserine residue (S161), which was preceded by another serine (-1), together representing the minimally required PBD docking motif (SpS) (Elia *et al.*, 2003a; Elia *et al.*, 2003b).

Encouraged by our observation that Plk1 PBD interacts specifically with both Bub1 and Cdc20 (Figure 16B), we wanted to test whether Bub1 could be the priming kinase for the Plk1-Cdc20 interaction by creating an optimal PBD binding site on Cdc20. Therefore, we mutated the phosphorylated serine residue 161 of the potential PBD docking site in Cdc20 to an alanine (S161A) and checked whether co-overexpressed and IPed myc-Plk1^{WT} would still co-IP the Cdc20 PBD mutant S161A.

When performing the experiment we had to learn that a FLAG-tag, no matter whether it was positioned N-terminally (data not shown) or C-terminally of the Cdc20 wildtype sequence, interfered with the otherwise strong binding to the myc-Plk1 (Figure 19A). Since not even overexpressed FLAG-tagged wildtype Cdc20 interacted with Plk1, we were not able to test the behaviour of our Cdc20 S161A mutant.

As none of the FLAG-tagged Cdc20 constructs ever interacted with myc-Plk1, neither when myc-Plk1 was IPed nor when FLAG-Cdc20/Cdc20-FLAG was IPed, we wondered whether the detected interacting 55kD protein was indeed Cdc20 and not an unknown 55kD protein, which cross-reacted with the used Cdc20 antibody. To rule out the latter possibility, we depleted endogenous Cdc20 with specific siRNA oligos and tested whether the band that co-IPed with the myc-PBD^{WT} at the size of Cdc20 (55kD) disappeared. In the control (GL2 RNAi), myc-PBD^{WT} expressed from the stable HeLa S3 cell line interacted with a 55kD protein detected by the Cdc20 antibody. In the Cdc20 RNAi, however, this band was no longer detectable confirming that the

antibody was indeed specific for Cdc20 and did not cross-react with another unknown protein of the same size like Cdc20 (Figure 19B).

The fact that the Plk1-Cdc20 interaction was only analysable with endogenous Cdc20 on the one hand and overexpressed Plk1 on the other hand strongly limited the range of feasible experiments and would have made it impossible to continue this project in the long run. Therefore, the analysis of the Plk1 PBD interaction with Cdc20 ceased at this point.

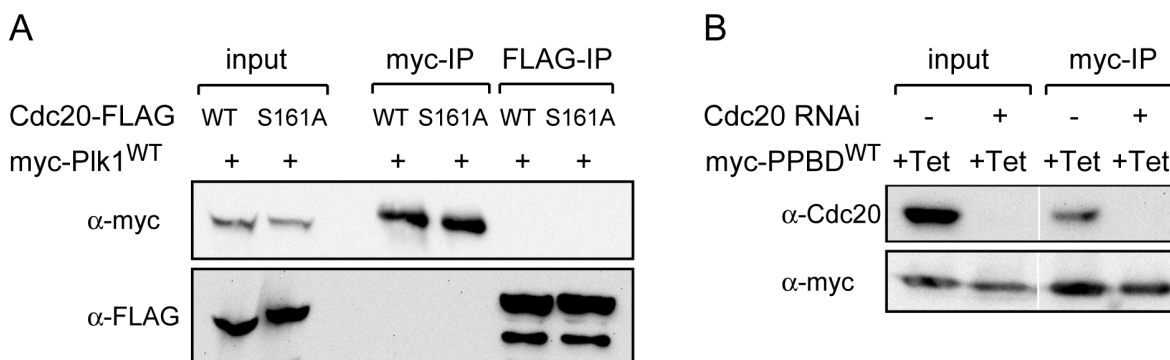


Figure 19 The FLAG-tag of Cdc20 interferes with the myc-Plk1 interaction. A) 293 cells were co-transfected with Cdc20-FLAG WT and Cdc20-FLAG S161A, respectively, and with myc-Plk1^{WT} for 24 hours. Cells were treated with nocodazole for the last 14 hours and released for 40 min before lysis. Extracts were split in two and used either for a myc-IP or a FLAG-IP. Inputs and IPs were separated by SDS-PAGE, followed by Western blotting using 9E10 antibody and anti-FLAG antibody, respectively. B) Cdc20 RNAi was performed for 48 hours in the myc-PPBD^{WT} stable cell line. PPBD^{WT} expression was induced by tetracycline (+Tet) for the last 24 hours before cells were lysed and used for an IP with the 9E10 antibody. Inputs and IPs were separated by SDS-PAGE followed by Western blotting using 9E10 antibody and anti-Cdc20 antibody, respectively.

2.4 Analysis of the interaction between Plk1 and MST2

MST2 is a member of the mammalian Ste20 kinases. Its closest homologue is MST1. Both have been implicated in promoting apoptosis (Lee *et al.*, 2001; Harvey *et al.*, 2003) and MST2 has been shown to phosphorylate and activate Lats1 kinase (Chan *et al.*, 2005a).

So far no role in mitosis has been assigned to MST2 but it has been found in a phage display screen for Plk1 PBD interactors by Lionel Arnaud in our department. GST-HA-Plk1 (300-603 aa) coupled to beads were, however, not able to bind myc-tagged MST2 protein produced by *in vitro* transcription/translation. Originally intended to serve as a negative control in a myc-Plk1 IP, we found MST2 as a strong interaction partner of Plk1 PBD. Since no Plk1 activating kinase has so far been established, the idea of MST2, interacting with and being upstream of Plk1, seemed interesting. Therefore, we analysed the accidentally observed interaction of Plk1 with MST2 in more detail.

RESULTS I

2.4.1 The interaction of myc-Plk1 with FLAG-MST2 depends on an intact PBD and is specific for both the MST2 and the Plk1 kinase family member

MST2 has high sequence similarity to MST1 and to a lesser extent to MST4. Since we were especially interested in Plk1 PBD interaction partners we started the analysis of the MST2-Plk1 interaction by inducing the expression of both the myc-PBD^{WT} and the myc-PBD^{AA} in the stable HeLa S3 cell lines and by simultaneously co-transfecting myc-MST constructs coding for the closely related family members MST2, MST1 and MST4. Nocodazole was added the last 14 hours before cells were released for 40 min into fresh medium and lysed. Myc-IPs out of the obtained extracts revealed that only MST2 but not MST1 or MST4 was able to interact with the PBD (Figure 20A). Moreover, the interaction took only place when the intact wildtype PBD was expressed, indicating that the interaction is phosphorylation dependent (Figure 20A).

As we learned from the Cdc20-Plk1 studies, the phosphopeptide binding capability of the PBD alone might differ from the one of full length Plk1. Therefore, we conducted an experiment with full length myc-Plk1^{WT} and myc-Plk1^{AA}, instead of the PBD alone, and co-transfected FLAG-MST2, MST1 and MST4 in 293T cells. In contrast to the results obtained with Cdc20, also the full length Plk1 still required the wildtype PBD for binding to MST2 (Figure 20B). Again, this interaction was very specific for MST2 since MST1 and MST4 were not co-IPed by myc-Plk1 (Figure 20B).

Since so far only Plk1 and none of the other Plk family members have been shown to be required for mitosis, we wanted to check whether the observed interaction is not only specific among the MST kinases but also among the Plks. In an experiment similar to the latter we co-transfected 293T cells with constructs encoding FLAG-MST2 and the KD versions of myc-Plk1, Plk2, Plk3 and Plk4, respectively. Western blot analysis of the different myc-Plk IPs showed that only Plk1 was able to bind to MST2 rendering the interaction very specific from the perspective of both kinases (Figure 20C).

Together, this demonstrates that the interaction between Plk1 and MST2 is specific for these respective kinase family members, is mediated via the PBD and, importantly, is clearly dependent on the PBD integrity, i.e. the PBD capability to act as a phosphopeptide binding domain. The latter fact strongly argues for a phosphorylation dependent relationship.

2.4.2 Myc-Plk1 co-immunoprecipitates endogenous MST2 in a cell cycle dependent way and their interaction is direct

Since many mitosis relevant proteins are phosphorylated during M-phase, we wanted to examine whether the observed phosphorylation dependency of the Plk1-MST2 interaction is specific for mitosis.

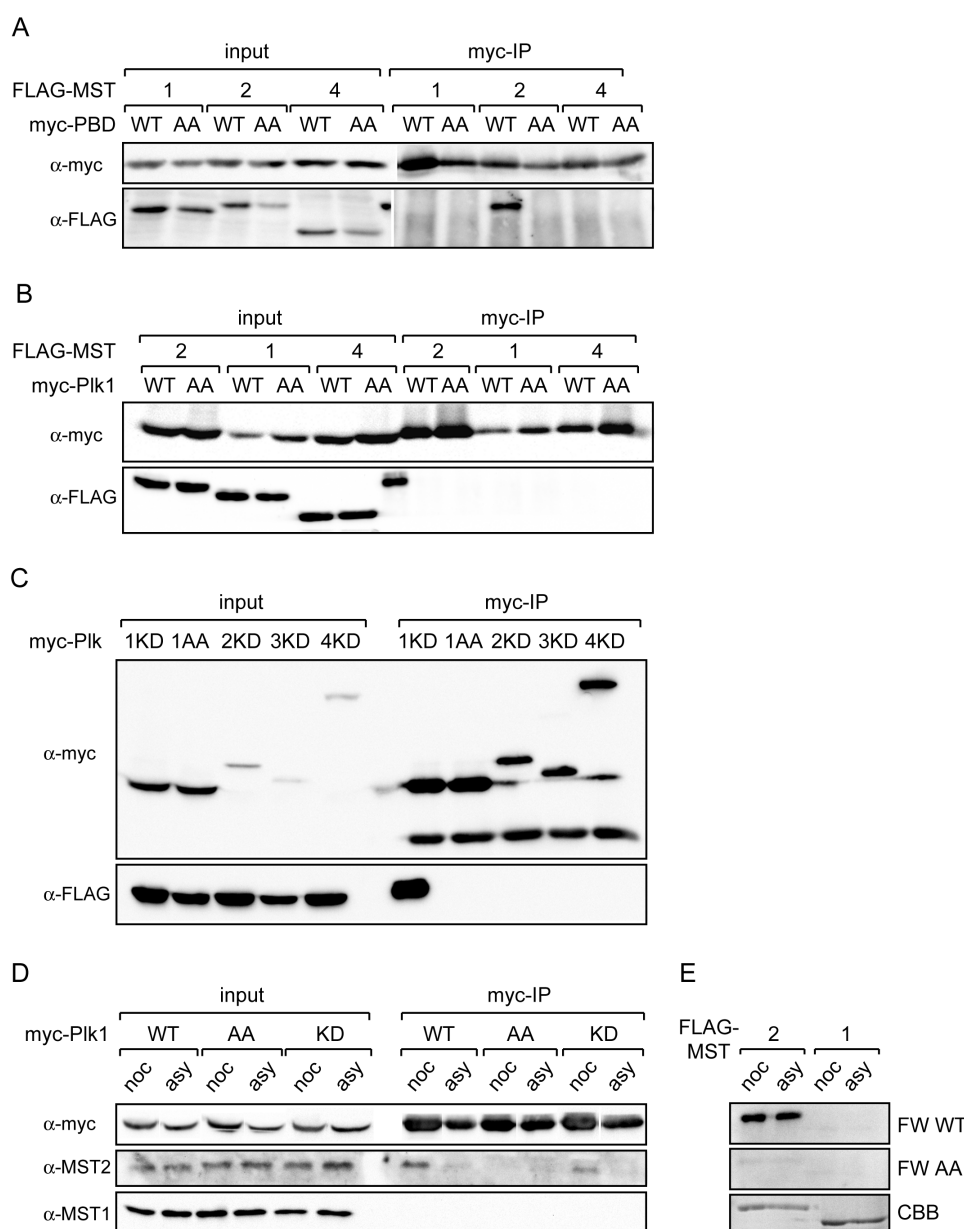


Figure 20 The interaction between myc-Plk1 and FLAG-MST2 is PBD and phosphorylation dependent, specific for the respective kinase family members and mitosis specific *in vivo*. A) The myc-PBD^{WT} and myc-PBD^{AA} stable HeLa S3 cell lines were induced with tetracycline and simultaneously co-transfected with FLAG-MST1, MST2 and MST4 for 24 hours, respectively. Cells were treated with nocodazole for the last 14 hours and released for 40 min before lysis. Extracts were then used for IPs with the 9E10 antibody and inputs and immune complexes were separated by SDS-PAGE and probed after Western blotting with 9E10 antibody and anti-FLAG antibody, respectively. B) 293T cells were co-transfected with myc-Plk1^{WT} and myc-Plk1^{AA}, respectively, and either FLAG-MST2, FLAG-MST1 or FLAG-MST4 for 24 hours. Further treatments as in A. C) 293T cells were transfected with myc-Plk1^{KD}, Plk1^{AA}, Plk2^{KD}, Plk3^{KD} and Plk4^{KD}, respectively, for 24 hours. Further treatments as in A. D) 293 cells were transfected with myc-Plk1^{WT}, Plk1^{AA} and Plk1^{KD}, respectively, for 24 hours. Cells were either left untreated (asy) or treated with nocodazole (noc) for the last 14 hours and released for 45 min before lysis. The respective extracts were then used for IPs with the 9E10 antibody and inputs and immune complexes were separated by SDS-PAGE and probed after Western blotting with 9E10 antibody, MST2 antibody and MST1 antibody, respectively. E) FLAG-MST2 and MST1 were each expressed in 293T cells for 24 hours, which were either grown asynchronously (asy) or nocodazole blocked (noc) and released for 45 min before preparation of the extracts. Far Western analysis was performed after separation of these extracts by SDS-PAGE using the bacterially expressed recombinant GST-PBD^{WT} and GST-PBD^{AA} proteins. CBB stained gel shows equal loading of the MST expressing lysates.

RESULTS I

We prepared extracts for myc-IPs from 293 cells which were transiently transfected with myc-Plk1^{WT}, Plk1^{AA} and Plk1^{KD}, respectively, and were either left untreated (asy) or blocked with nocodazole (noc) followed by a 45 min release to allow spindle formation. MST2 was only detected in nocodazole treated myc-Plk1^{WT} and myc-Plk1^{KD} IPs and was absent in IPs from asynchronously grown cells (Figure 20D).

When we performed Far Western analysis on FLAG-tagged MST2 and MST1 expressed in either nocodazole treated or asynchronous 293T cells with the recombinant GST-PBD^{WT} and GST-PBD^{AA} proteins, the dependency on the mitotic state of the MST proteins was lost (Figure 20E), possibly due to the excess amount of the recombinant GST-PBDs. But again only GST-PBD^{WT} and not the PBD^{AA} mutant was able to bind specifically to FLAG-MST2 (Figure 20E). Furthermore, we learned from this Far Western experiment that the binding of Plk1 to MST2 is direct.

Altogether, we conclude that the Plk1-MST2 interaction does not require a linker protein, is PBD-dependent and mitosis specific *in vivo*. This renders a scenario very likely, in which the required phosphorylation is created by a mitotic kinase.

2.4.3 Interaction between MST2 and Plk1 is independent of their respective kinase activities and of Cdk1/Cyclin B phosphorylation

Since the Plk1-MST2 interaction required mitosis specific phosphorylation it was an obvious question whether the phosphorylation of MST2, which as a consequence creates the binding site for Plk1 PBD is created by one of the interacting serine-threonine kinases themselves. In order to test this idea we performed IPs from 293T cells, which were co-transfected with the respective KD versions of myc-Plk1 (Plk1^{K82R}) and FLAG-MST2 (MST2^{D164A}), blocked with nocodazole and shortly released before lysis. It turned out that the interactions between Plk1 and MST2 were independent of their respective kinase activities, as combinations of KD mutants interacted with each other as strongly as the wildtype kinases (Figure 21A).

According to the Yaffe model on Plk1 targeting (Elia *et al.*, 2003a; Elia *et al.*, 2003b) the most prominent priming kinase for Plk1 PBD binding to a phosphorylated docking protein is the key mitotic kinase Cdk1/Cyclin B. We examined whether FLAG-MST2 isolated from transiently transfected asynchronous 293T cells could act as a substrate of Cdk1/Cyclin B in an *in vitro* kinase assay using the exogenous substrate Histone H1 (H1) as a positive control for Cdk1/Cyclin B activity. To attest to the specificity we included not only MST2^{WT} and MST2^{KD} (MST2^{D164A}) but also MST1^{WT} and MST1^{KD} (MST1^{D167A}). The presence of Cdk1/Cyclin B isolated from Sf9 insect cells (a gift from Rüdiger Neef) did not increase the ³²P incorporation into either autophosphorylated FLAG-MST2^{WT} or unphosphorylated FLAG-MST2^{KD} (Figure 21B).

Thus, we could not show that the most likely candidates for MST2 mitotic phosphorylation, Plk1, MST2 itself and Cdk1/CyclinB, were the kinases creating the PBD binding site on MST2.

2.4.4 GST-Plk1 and FLAG-MST2 do not phosphorylate each other *in vitro*

After having established that MST2 and Plk1 interact specifically with each other in mitosis via the PBD, the key question is, of course, the physiological relevance of this relationship. Since both Plk1 and MST2 are strong kinases, one obvious answer would be that one phosphorylates the other, resulting in e. g. activation or inactivation of the respective phosphorylated kinase.

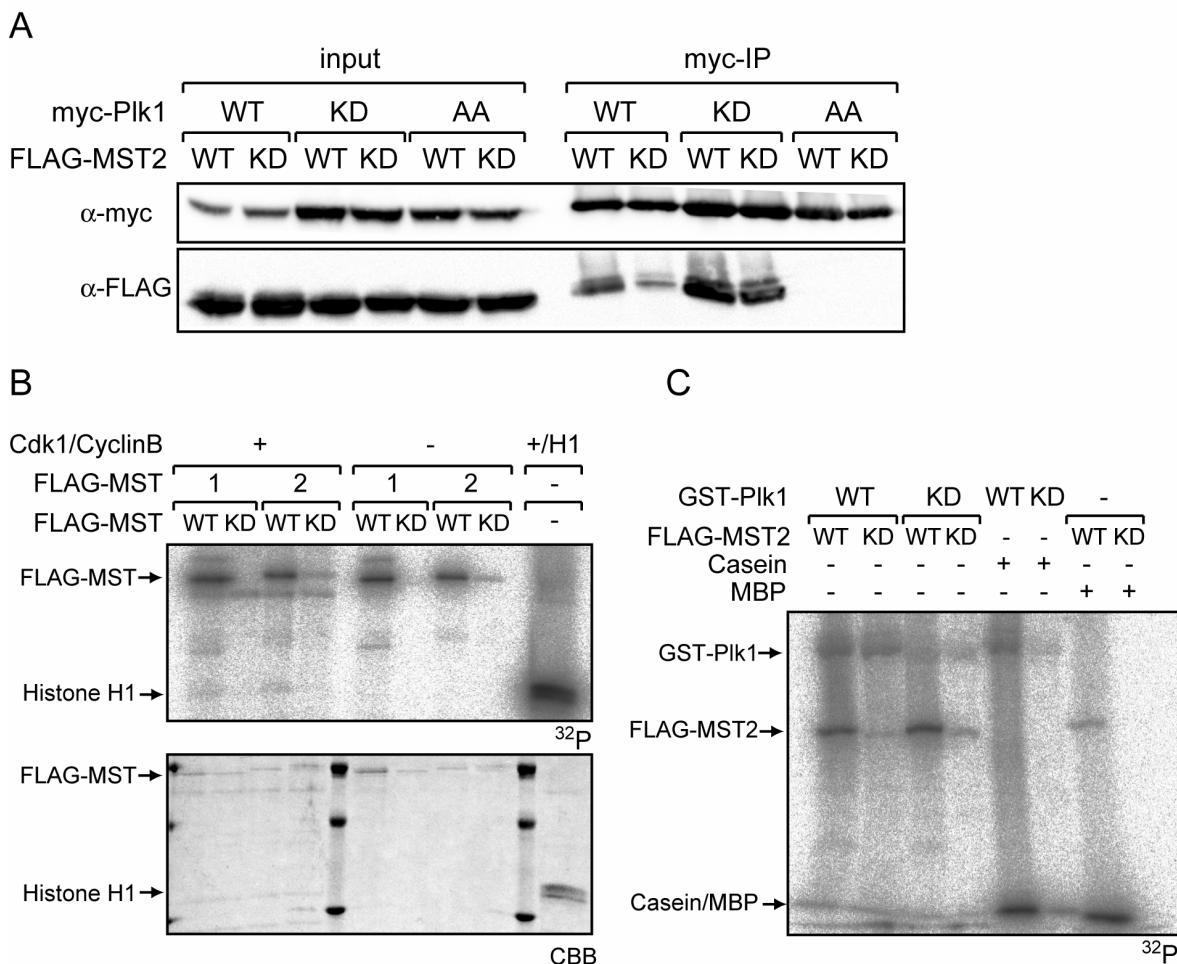


Figure 21 Neither Plk1, MST2 nor Cdk1/Cyclin B activities seem to be required for the Plk1-MST2 interaction and Plk1 and MST2 do not phosphorylate each other. **A)** 293T cells were co-transfected with myc-Plk1^{WT} and Plk1^{KD}, respectively, and FLAG-MST2^{WT} and MST2^{KD} for 24 hours. Cells were treated with nocodazole for the last 14 hours and released for 45 min before lysis. The respective extracts were then used for IPs with the 9E10 antibody and inputs and immune complexes were separated by SDS-PAGE and probed after Western blotting with 9E10 antibody and anti-FLAG antibody, respectively. **B)** In vitro kinase assay either in the presence (+) or absence (-) of insect cell derived Cdk1/Cyclin B on FLAG-MST1 and FLAG-MST2, WT and KD, respectively, which were isolated from transiently transfected asynchronous 293T cells. Histone H1 (H1) was used as a positive control for Cdk1 activity. Panels show the autoradiogram (³²P) and the corresponding CBB stained gel as a loading control. **C)** In vitro kinase assay with insect cell derived GST-Plk1^{WT} and GST-Plk1^{KD} combined with either FLAG-MST2^{WT} or FLAG-MST2^{KD}, respectively, which were isolated from transiently transfected asynchronous 293T cells. Casein and MBP were used as positive controls for Plk1 and MST2 activity, respectively. Panel shows the autoradiogram (³²P). Equal amounts of the respective recombinant Plk1 and MST2 proteins were used.

RESULTS I

In an *in vitro* kinase assay we combined GST-Plk1^{WT} and GST-Plk1^{KD} purified from asynchronous (not okadaic acid treated) Sf9 cells with FLAG-MST2^{WT} and MST2^{KD} isolated from asynchronous transiently transfected 293T cells. Casein was used as an exogenous substrate of Plk1 and MBP was used as a positive control for MST2 activity. Although both kinases were active, as proven by their autophosphorylation and the ³²P incorporation into their respective exogenous substrates, none of them was able to phosphorylate the other kinase (Figure 21C).

Since we were not able to assign any physiologically relevant function to the specific interaction between Plk1 and MST2, neither with respect to their cellular localisation (data not shown) nor to their phosphorylation status, we decided not to follow up this project any further.

2.5 Initial analysis of the relationship between Plk1 and BubR1

When we screened several spindle proteins for interaction with the PBD in the stable HeLa S3 cell lines, we observed that the input lane from the myc-PBD^{WT} expressing cells showed only one BubR1 band, whereas in the lysate from the nocodazole treated myc-PBD^{AA} expressing cells an additional BubR1 band of lower electrophoretic mobility was detected (Figure 16A), which had been shown to be created by phosphorylation (Li *et al.*, 1999). Hence, the mitotically arrested PBD^{WT} expressing cells (see Results, chapter A 3) do not create the same phosphorylated BubR1 form as cells arrested in mitosis by nocodazole do.

2.5.1 The spindle assembly checkpoint induced phosphorylated form of BubR1 is reduced in Plk1 RNAi cells

We were interested to find out, which upstream kinase might cause the BubR1 upshift upon SAC activation by nocodazole and obviously chose Plk1, which also co-localises with BubR1 at the outer KT. It had been suggested mainly by *in vitro* studies (Weaver *et al.*, 2003; Tanudji *et al.*, 2004) that the presence of CENP-E is required for this SAC-dependent BubR1 phosphorylation to occur. Therefore, we performed RNAi of Plk1, CENP-E and simultaneous RNAis of Plk1 and CENP-E in HeLa S3 cells, respectively. GL2 siRNA oligos were used as a negative control. Cells were either treated with nocodazole for the last 14 hours or left untreated before lysis and Western blot analysis.

In the control RNAi, BubR1 displayed one band in asynchronous cells. This band was reduced and accompanied by a very strong higher migrating band when treated with nocodazole. Remarkably, the reduction of Plk1 by RNAi in the nocodazole arrested cells was accompanied by a strong decrease of this upshifted BubR1 form (Figure 22A). The simultaneous RNAi of Plk1 and CENP-E, however, did not further promote the loss of the higher migrating band. If cells were depleted of CENP-E alone the upshifted BubR1 form persisted in the nocodazole treated cells (Figure 22A). The efficiency of the CENP-E RNAi could not be checked by Western blot due to

antibody problems, but treated cells showed a clear increase in the mitotic index when checked by light microscopy.

If Plk1 was the upstream kinase that created the higher migrating phosphorylated BubR1 form, then this upshifted form could possibly be generated in asynchronous cells by overexpressing hyperactive Plk1 or be reduced in nocodazole treated cells by overexpressing the KD Plk1 mutant. 293T extracts transfected with the different myc-Plk1 constructs or untransfected as a control either in the presence or absence of nocodazole were analysed by Western blotting using anti-Plk1 antibody to check the expression levels of the myc-constructs, anti-Bub1 antibody as a control for a related checkpoint kinase and anti- α -tubulin as a loading control. Although the BubR1 signal on the Western blot was very weak, it is obvious that no upshift could be induced by myc-Plk1^{T210D} overexpression in the absence of a drug and that the upshifted band in nocodazole treated cells did not disappear in myc-Plk1^{K82R} expressing cells (Figure 22B). This negative result, however, does not exclude a role of the endogenous Plk1 in phosphorylating BubR1.

Thus, the strong reduction of the higher migrating phosphorylated BubR1 form upon incomplete RNAi of Plk1 strongly suggests that Plk1 is involved in creating the SAC-dependent BubR1 upshift *in vivo*.

2.5.2 BubR1 KT localisation is not dependent on the presence of Plk1

Since the BubR1 phosphorylation in SAC active cells depends on the Plk1 presence we wanted to examine whether BubR1 was still able to localise to the KTs upon Plk1 RNAi. Plk1-depleted cells were chosen by the monopolar spindle phenotype (see also Results, chapter 3). Both control and Plk1-depleted cells retained BubR1 at the KTs. Plk1-mediated phosphorylation of BubR1 seems, therefore, not to be essential for proper BubR1 KT targeting.

The data showing that Plk1 is required for the formation of the SAC-dependent higher migrating form of BubR1 are crucial and encouraging for a further study of the mechanisms underlying the BubR1-Plk1 relationship. Sabine Elowe continued developing this project.

RESULTS I

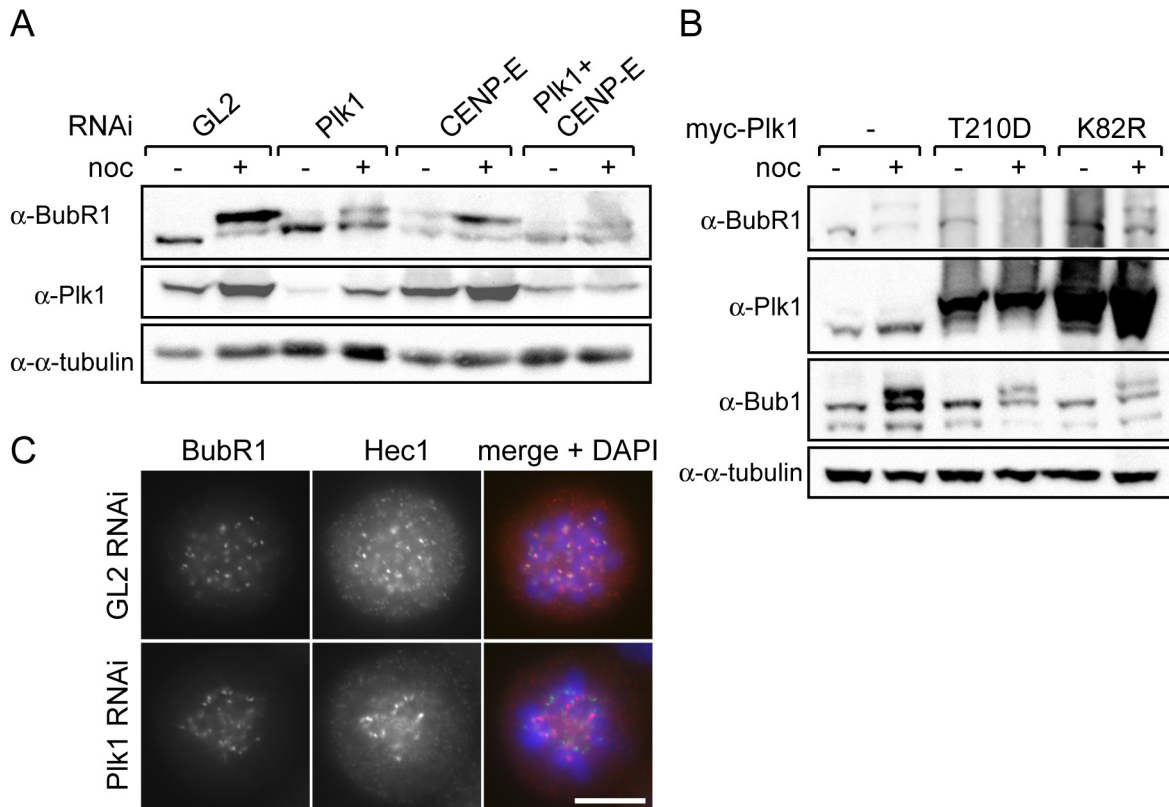


Figure 22 *Plk1* is required for the creation of the higher migrating, phosphorylated form of BubR1 in SAC active cells *in vivo* but *Plk1* presence is not essential for proper BubR1 KT targeting A) HeLa S3 cells were targeted by siRNAi oligos against either *Plk1*, *CENP-E* or simultaneously against both proteins for 36 hours. GL2 oligos were used as negative control. For the last 14 hours cell were arrested with nocodazole or left untreated, before scraping them off for the preparation of extracts. Equal amounts of extracts were separated by SDS-PAGE, followed by Western blotting using anti-BubR1, anti-*Plk1* and anti- α -tubulin antibody as a loading control, respectively. B) 293T cells were transfected with myc-*Plk1*^{T210D} and *Plk1*^{K82R}, respectively, for 24 hours. Untransfected cells were used as negative control. For the last 14 hours cells were arrested with nocodazole or left untreated, before scraping them off for the preparation of extracts. Equal amounts of extracts were separated by SDS-PAGE, followed by Western blotting using anti-BubR1, anti-*Plk1*, anti-Bub1 and anti- α -tubulin antibody as a loading control, respectively. C) HeLa S3 cells were treated with siRNA oligos against either *Plk1* or GL2 as control for 36 hours, then PTEMF fixed and stained with anti-BubR1 antibody (green), anti-Hec1 antibody (red) as a KT marker and DAPI (DNA, blue). Scale bar indicates 10 μ m.

3 Plk1 PBD expression reveals distinct dependencies on proper targeting for different Plk1 functions and implicates Plk1 in chromosome congression

The reason why we initially generated the myc-PBD^{WT} and PBD^{AA} stable inducible HeLa S3 cell lines was to create a tool for a specific search for novel, phosphorylation dependent Plk1 PBD interacting proteins. However, during the course of the analysis of potential candidates it became apparent that the expression of the PBD^{WT} but not the PBD^{AA} caused some interesting cellular phenotypes not obviously recognised before by other studies on Plk1 function.

3.1 An intact phosphopeptide binding motif is required for localisation of the Plk1 PBD

To analyse the role of the Plk1 PBD in mitotic progression, we first wanted to know whether the myc-PBD^{WT}, expressed from the stable tetracycline inducible HeLa S3 cell lines, localised to the same subcellular structures during mitosis as endogenous Plk1 does and to which degree this localisation is dependent on the phosphopeptide binding ability of the PBD.

As described above (Figure 14B), addition of tetracycline to the stable cell lines for 24 hours induced the expression of both myc-PBD^{WT} and myc-PBD^{AA} to about 10 times the level of endogenous Plk1. Shorter induction times (8 hours) produced more moderate expression levels, which turned out to be better suited for the analysis of subcellular localisation. The myc-tagged PBD proteins were visualised by staining with anti-myc antibodies and, simultaneously, the induced cells were co-stained with antibodies against γ -tubulin, α -tubulin and ANA autoimmune serum, markers for centrosomes, MTs and KT, respectively. The PBD^{WT} co-localised with KT from pro- to metaphase, with centrosomes from pro- to anaphase, and with the central spindle and the midbody during ana- and telophase (Figure 23A). This localisation is virtually identical to that of endogenous Plk1 (Barr *et al.*, 2004), confirming a critical role of the PBD in the subcellular distribution of Plk1 (Seong *et al.*, 2002). In case of the PBD^{AA} mutant, no clear staining of either KT or the central spindle could be observed in mitotic cells, and centrosome and midbody staining was clearly reduced (Figure 23B).

These results suggest that Plk1 localisation to the described structures is mediated largely via PBD-dependent docking to phosphorylated target proteins.

RESULTS I

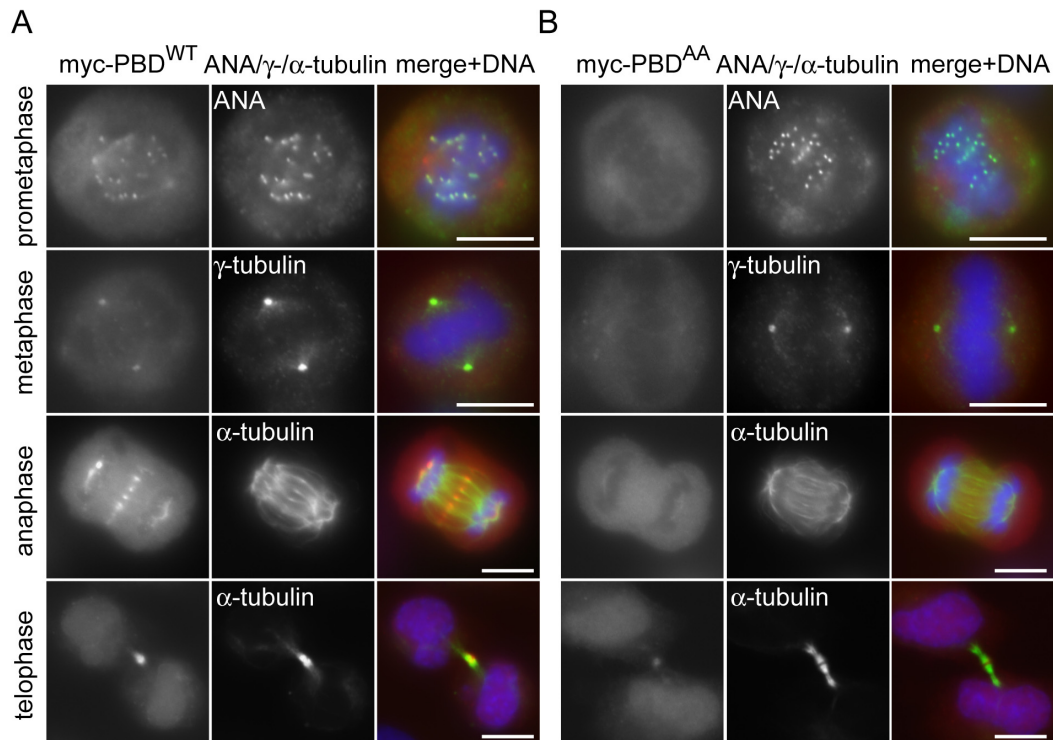


Figure 23 Localisation of the Plk1 PBD to diverse spindle structures requires an intact phosphopeptide binding motif. A) PBD^{WT} and B) PBD^{AA} stable cell lines were induced for 8 hours with tetracycline and then fixed and permeabilised with PTEMF or -20°C methanol for γ -tubulin staining. Cells were analysed by indirect IF microscopy using anti-myc antibody (9E10-TRITC, red), DAPI (DNA, blue) and either ANA autoimmune serum (green), anti- γ -tubulin (green) or anti- α -tubulin (green) antibodies to reveal co-localisation with KTs, centrosomes and spindle MTs, respectively. Scale bars indicate 10 μm .

3.2 Overexpression of PBD^{WT} results in displacement of endogenous Plk1 and causes mitotic arrest

The short term induction (8 hours) of PBD expression described above did not significantly change the cell cycle profile but longer induction times (24 hours) resulted in a marked increase in the mitotic index in cell populations expressing PBD^{WT}, but not PBD^{AA} (Figure 24A, left panel). This increase in mitotic index was quantitatively similar to that observed after Plk1 depletion by appropriate siRNAs (Figure 24A, right panel), whereas treatment of cells with control (GL2) siRNA oligos produced no effect (Figure 24A). In transient transfection studies, PBD^{WT} also caused a mitotic arrest, whereas PBD^{AA} was without effect, confirming the results obtained with the inducible cell lines (Figure 24B). Transient transfection was also used to explore the consequences of overexpressing the PBDs of Plk2 or Plk3. Neither one of these PBDs produced a significant mitotic arrest (Figure 24B), despite similar levels of expression, as judged by IF staining of the individual transfected cells (Figure 24C). This indicates that only the Plk1 PBD^{WT} is able to compete effectively with endogenous Plk1 protein for the binding to phosphorylated docking proteins, despite similar phosphopeptide binding specificities of these PBDs *in vitro* (Elia *et al.*, 2003b). Therefore, additional sequences or structural motifs within the docking proteins might further define PBD-binding specificity *in vivo*.

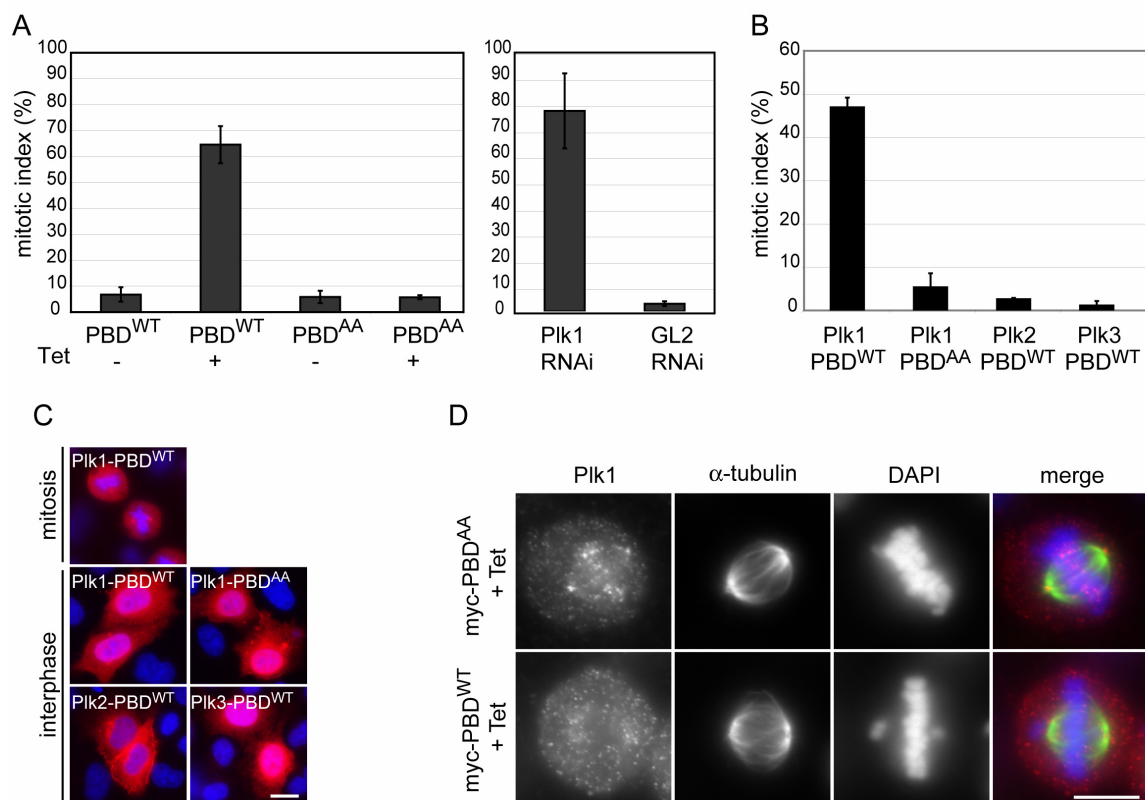


Figure 24 Overexpression of the Plk1 PBD^{WT} results in endogenous Plk1 displacement and mitotic arrest. **A)** Mitotic indexes of PBD^{WT} and PBD^{AA} stable cell lines after treatment for 24 hours with (+Tet) or without (-Tet) tetracycline (left graph). The mitotic indexes of cells treated for 36 hours with Plk1 and control (GL2) siRNA duplexes are also shown (right graph). The mitotic indexes were determined by IF microscopic analysis of the stained DNA. Histograms show results of three independent experiments (300 - 500 cells each) and bars indicate standard deviations. **B)** Mitotic indexes of cells transiently transfected with myc-tagged PBD^{WT} and the PBD^{AA} mutant form of Plk1 as well as the wildtype PBDs of Plk2 and Plk3, respectively. After 48 hours of transient transfection, cells were fixed and permeabilised with PTEMF and stained with anti-myc antibody (9E10-TRITC) and DAPI. The mitotic indexes of the transfected (myc-positive) cells were then determined by IF microscopic analysis of the stained DNA. Histograms show results of three independent experiments (more than 200 cells each) and bars indicate standard deviations. **C)** IF images of cells expressing the indicated myc-tagged Plk-PBD constructs. Cells were treated as described in B). **D)** PBD^{WT} and PBD^{AA} stable cell lines were induced for 24 hours with tetracycline and subsequently fixed and permeabilised with PTEMF followed by staining with anti-Plk1 N-terminal antibody (red), anti- α -tubulin antibody (green) and DAPI (DNA, blue). Scale bars indicate 10 μ m.

To corroborate these results and confirm that the Plk1 PBD could displace endogenous Plk1 from its intracellular binding partners, the localisation of endogenous Plk1 was examined by using an antibody directed against the N-terminus of Plk1. After expression of PBD^{AA} for 24 hours, endogenous Plk1 could readily be detected on centrosomes and KTs (Figure 24D, upper panels), but after expression of PBD^{WT}, this localisation was clearly lost and only diffuse staining could be observed (Figure 24D, lower panels). Because cells expressing PBD^{WT} became arrested in a prometaphase-like state (see below), we were unable to demonstrate the displacement of endogenous Plk1 from the central spindle and midbody. However, considering that Plk1 localisation to these structures depends on PBD-mediated binding to phosphorylated kinesin-6,

RESULTS I

MKlp2 (Neef *et al.*, 2003), it seems legitimate to assume that PBD^{WT} overexpression would most likely displace endogenous Plk1 also from the central spindle and midbody.

Taken together, the above results suggest that PBD^{WT} overexpression causes cells to arrest in mitosis because excess PBD displaces endogenous Plk1 from PBD-docking proteins and hence from its sites of action.

3.3 PBD^{WT} expression allows bipolar spindle formation but causes chromosome congression defects

To better understand the physiological importance of Plk1 localisation, the phenotype of the mitotically arrested cells produced by PBD^{WT} overexpression was compared to that observed upon siRNA-mediated depletion of Plk1. This comparison revealed striking differences (Figure 25). In response to Plk1 depletion, about 87% of the mitotic cells exhibited spindles with monopolar or abnormally small bipolar MT arrays, centrosomes near each other, and chromosomes in a rosette-like arrangement (Figure 25A). Occasionally, Plk1-depleted cells showed bipolar spindles of apparently normal sizes, but these most often had unfocused spindle poles and, moreover, they lacked a centrosome at one pole and instead contained the unseparated centrosome pair on the opposing pole (Figure 25A, bottom row). In contrast to Plk1-depleted cells, about 82% of the mitotic cells induced to express PBD^{WT} showed bipolar spindle formation with properly separated centrosomes (Figure 25B). However, although spindles appeared to be near-normal in these cells, a clear metaphase plate was rarely observed and instead, variable numbers of chromosomes failed to congress (Figure 25B). In summary, whereas Plk1-depleted cells mostly displayed unseparated centrosomes, monoastral spindles and chromosomes in a rosette-like arrangement, PBD^{WT} expressing cells formed bipolar spindles but arrested with chromosome congression defects.

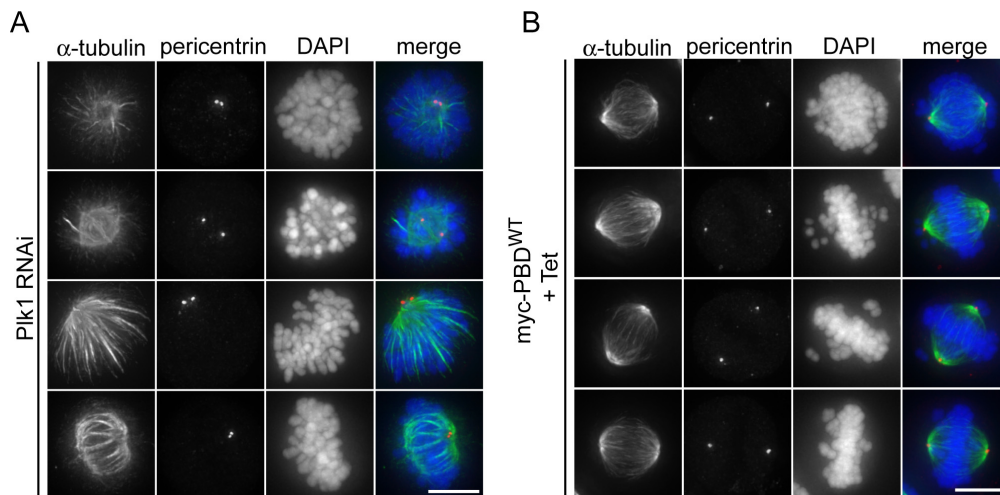


Figure 25 The mitotic phenotype of PBD^{WT} expressing cells is distinct from the phenotype of Plk1-depleted cells. A) HeLa S3 cells were treated with Plk1 siRNA duplexes for 36 hours. After fixation and permeabilisation with PTEMF cells were stained with anti-pericentrin (red), anti- α -tubulin (green) antibodies and DAPI (DNA, blue) staining. B) The PBD^{WT} stable cell line was induced for 24 hours with tetracycline. Cells were fixed, stained and analysed as described in A. Scale bars indicate 10 μ m.

To further analyse the chromosome congression defect produced by PBD^{WT} overexpression, we next examined the KT-MT attachments in these cells. In cells arrested by PBD^{WT} overexpression, the congressed chromosomes were clearly attached to KT-MT bundles, termed K-fibres (K-fibres), whereas the uncongressed chromosomes did not show obvious K-fibre attachment (Figure 26A). The KT-attached MTs in PBD^{WT} expressing cells were cold stable (Figure 26B), suggesting that proper KT-MT attachments had occurred (Rieder, 1981). In contrast, KT MTs of cells depleted of the KT protein Nuf2 were cold sensitive (Figure 26B), in agreement with previous results (DeLuca *et al.*, 2002).

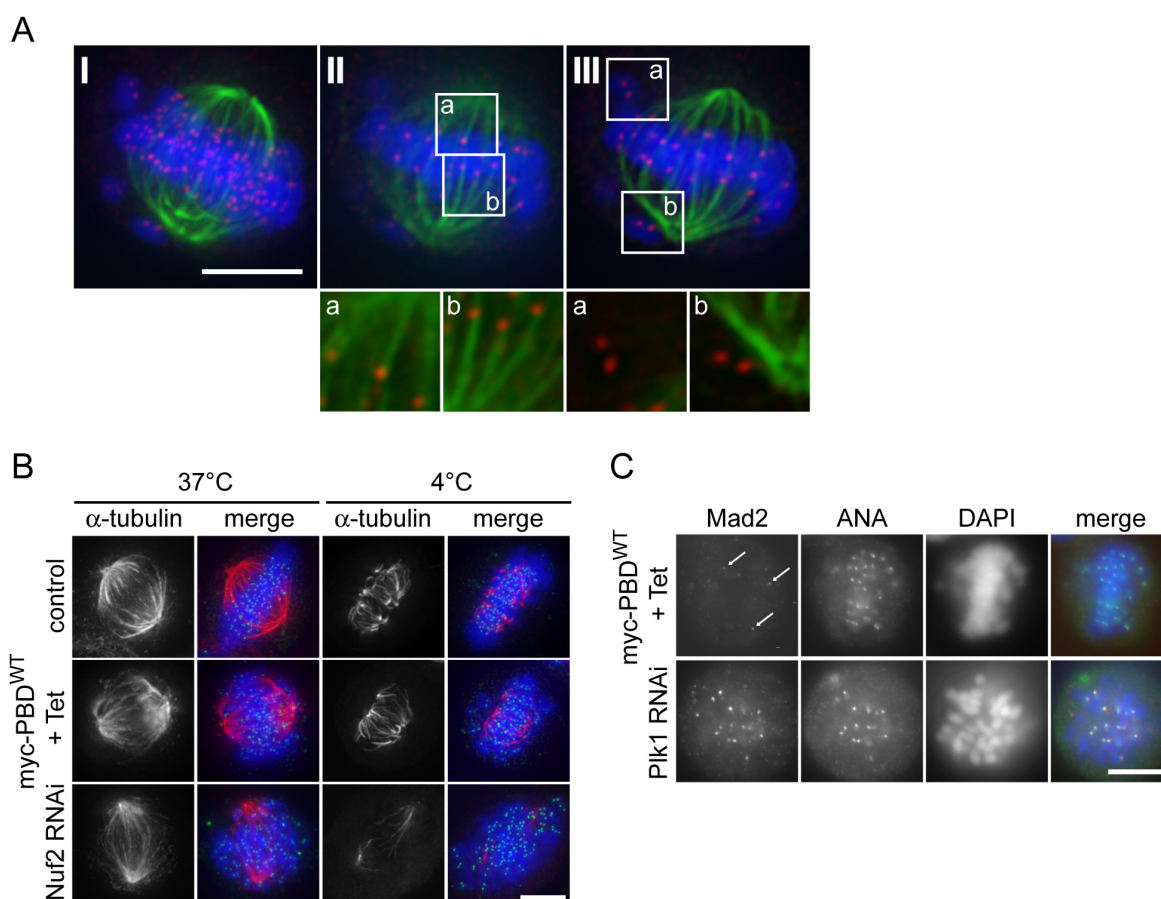


Figure 26 Lack of proper KT-MT attachments on unaligned chromosomes in PBD^{WT} expressing cells. **A)** PBD^{WT} induced cells were fixed and permeabilised with PTEMF and then stained with anti- α -tubulin (green), Hec1 (red) and DAPI (DNA, blue). A series of Z stack images was taken from a mitotic cell and subsequently deconvolved. The left panel (I) shows a projection of the total Z-stack, whereas the middle (II) and right panels (III) show single Z-stacks of the same cell (scale bar 10 μ m). Higher magnifications of the boxes indicated in panels II and III are presented below (scale bar 5 μ m). **B)** The PBD^{WT} stable cell line (middle row) was induced for 24 hours with tetracycline (+Tet) and HeLa S3 cells (bottom row) were treated with Nuf2 siRNA duplexes for 48 hours. These cells, as well as control GL2 treated cells (top row), were then incubated for 10 min on ice followed by fixation and permeabilisation with PTEMF. Cells were analysed by indirect IF microscopy using anti- α -tubulin antibody (red), CREST autoimmune serum (green) and DAPI (DNA, blue). **C)** The PBD^{WT} stable cell line (top row) was induced for 24 hours with tetracycline (+Tet) and HeLa S3 cells (bottom row) were treated with *Plk1* siRNA duplexes for 36 hours. After PTEMF fixation, cells were analysed by indirect IF microscopy using anti-Mad2 antibody (red), ANA autoimmune serum (green) and DAPI (DNA, blue) staining. Arrows indicate Mad2 positive KTs at uncongressed chromosomes. Scale bars indicate 10 μ m.

RESULTS I

In addition, in PBD^{WT} expressing cells the attached KT's were under tension, as indicated by measurements of the inter-KT distance, which was found to be $1.35 \pm 0.27 \mu\text{m}$, as compared to $1.58 \pm 0.44 \mu\text{m}$ in control cells. In contrast, KT's of uncongressed chromosomes showed inter-KT distances of only $0.73 \pm 0.14 \mu\text{m}$, which is similar to the values for nocodazole treated cells ($0.72 \pm 0.14 \mu\text{m}$). This indicates that MT-dependent pulling forces could be generated in PBD^{WT} expressing cells. In agreement with this conclusion, the SAC protein Mad2, which is known to localise to KT's that lack proper MT attachment (Waters *et al.*, 1998), could only be detected, at variable levels, at KT's of uncongressed chromosomes (Figure 26C). This is in striking contrast to Plk1-depleted cells in which most, if not all, KT's were strongly Mad2 positive, in agreement with previous results (Figure 26C) (Sumara *et al.*, 2004). In both cases, though, the presence of Mad2 on at least some KT's points to SAC activation (Howell *et al.*, 2000; Shah and Cleveland, 2000). Indeed, the arrests induced by either Plk1 depletion or PBD^{WT} overexpression were SAC-dependent, as in both cases Mad2 depletion reduced the mitotic index by about 15 fold (data not shown), confirming and extending previous results (Seong *et al.*, 2002; van Vugt *et al.*, 2004).

3.4 PBD overexpression does not interfere with centrosome maturation

One of the first demonstrated roles for Plk1 in mammalian cells relates to centrosome maturation during the G2 to M phase transition (Lane *et al.*, 1996). A hallmark of centrosome maturation is the recruitment of γ -tubulin ring complexes (γ TuRC) to the centrosomes, which is required for increased MT nucleation at the onset of mitosis (Khodjakov and Rieder, 1999; Palazzo *et al.*, 2000). We therefore analysed and compared γ -tubulin recruitment in Plk1-depleted and PBD overexpressing cells, using antibodies against centrin as a centriolar marker (Paoletti *et al.*, 1996). In agreement with previous results, γ -tubulin recruitment was impaired in the absence of Plk1 but, interestingly, it was not significantly affected in cells expressing PBD^{WT} (Figure 27A). To further characterise this centrosome maturation defect, we also analysed two other proteins, pericentrin and Aurora-A, which normally become enriched at mitotic centrosomes. Pericentrin was recruited to almost normal levels in both Plk1-depleted cells and PBD^{WT} expressing cells, arguing that Plk1 depletion does not cause a general recruitment defect (Figure 27B). Moreover, as pericentrin is one of the proteins implicated in anchoring γ TuRCs to mitotic centrosomes (Zimmerman *et al.*, 2004), this also indicates that the loss of γ -tubulin is not caused by the absence of this anchoring protein.

As Aurora-A kinase has also been implicated in centrosome maturation (Hannak *et al.*, 2001; Berdnik *et al.*, 2002), we examined the fate of this protein, too. Remarkably, in Plk1-depleted cells Aurora-A no longer localised to centrosomes, as visualised by co-staining with pericentrin, although it still localised to spindle MTs surrounding the centrosomes (Figure 27C). In PBD expressing cells, on the other hand, Aurora-A localisation to spindle poles was not affected (Figure 27C). Thus, Plk1 depletion impaired both the recruitment of γ -tubulin and Aurora-A to the

centrosome, whereas PBD^{WT} overexpression did not detectably interfere with centrosome maturation. Taken together, these results show that both centrosome maturation and separation are defective in Plk1-depleted cells but not in PBD^{WT} overexpressing cells (Table 2).

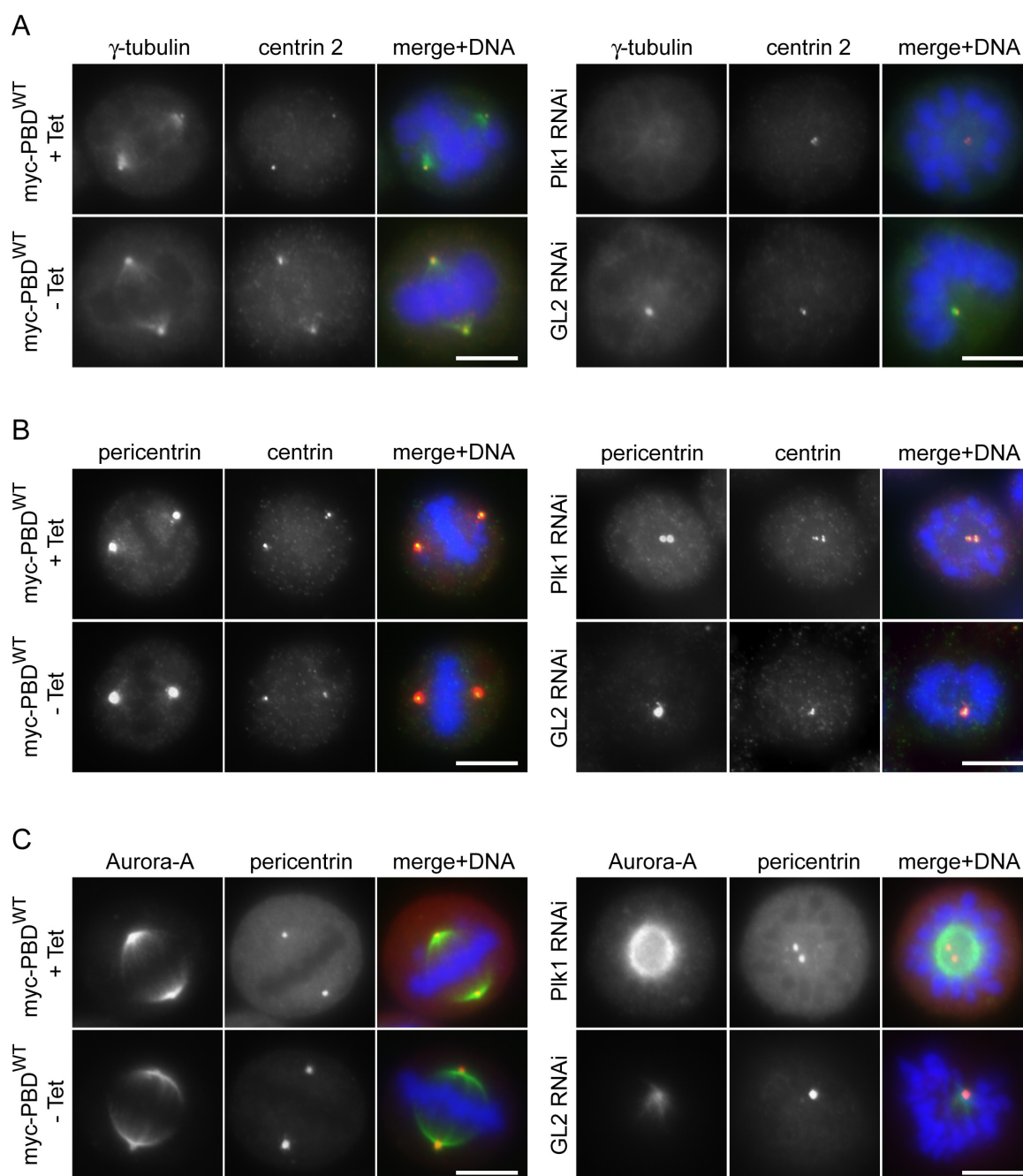


Figure 27 Centrosome maturation defects in Plk1-depleted but not PBD^{WT} induced cells. A) The PBD^{WT} stable cell line (left panels) was induced (+Tet) for 24 hours with tetracycline or left untreated (-Tet). HeLa S3 cells (right panels) were either treated with Plk1 or control (GL2) siRNA duplexes for 36 hours. After -20°C methanol fixation, cells were analysed by indirect IF microscopy using anti- γ -tubulin (green), anti-centrin antibodies (red) and DAPI (DNA, blue). B) Same as in A, but cells were analysed after staining with anti-pericentrin antibody (red), anti-centrin antibody (green) and DAPI (DNA, blue). C) Same as in A, but cells were fixed and permeabilised with PTEMF and analysed after staining with anti-Aurora-A antibody (green) and anti-pericentrin antibody (red) and DAPI (DNA, blue). Scale bars indicate 10 μ m.

RESULTS I

3.5 Chromatid arm separation occurs in PBD expressing cells but not in Plk1-depleted cells

In vertebrate cells Plk1 is required to remove the cohesin complex from sister chromatid arms during early mitosis (Sumara *et al.*, 2002; Gimenez-Abian *et al.*, 2004; Hauf *et al.*, 2005). In agreement with this conclusion, the analysis of chromosome spreads showed that sister chromatid arms remained closely paired in Plk1-depleted cells but not in nocodazole arrested control cells (Figure 28). Interestingly, sister chromatid arms were also separated in cells expressing PBD^{WT} (Figure 28). This indicates that PBD overexpression, in contrast to Plk1 depletion, did not significantly interfere with the removal of the cohesin complex from chromosome arms (Table 2).

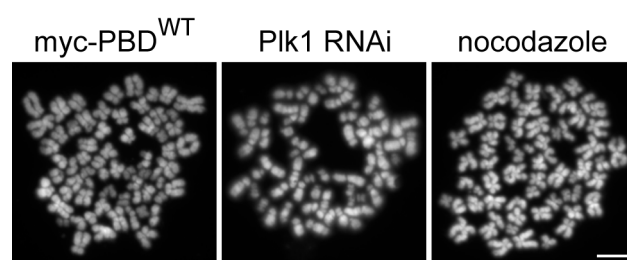


Figure 28 Chromosome spreads display dissociated chromosome arms in PBD^{WT} induced but not Plk1-depleted cells. Mitotic PBD^{WT} cells were obtained by tetracycline induction of the stable cell line for 24 hours (left). HeLa S3 cells were either arrested in mitosis by siRNA-mediated Plk1 depletion for 36 hours (middle) or by nocodazole treatment for 14 hours (right). Mitotic chromosome spreads of all cells were stained with DAPI. Scale bar indicates 10 μ m.

3.6 The PBD is essential for mitotic progression

As shown above, the PBD-induced mitotic arrest phenotype most likely results from the displacement of endogenous Plk1 from its docking partners and sites of action (Figure 24D). The observation that, overall, the mitotic arrest phenotype produced by PBD overexpression was less severe than the Plk1 depletion phenotype suggested that not all Plk1 functions were dependent to similar extent on the correct localisation of Plk1 activity. To test the hypothesis that some Plk1 functions strictly required correct localisation of Plk1 whereas others could be performed even if Plk1 was displaced, we attempted to rescue the Plk1 depletion phenotype by different Plk1 constructs. These rescue experiments involved co-transfection of a RNAi-vector targeting Plk1 with an RNAi-resistant expression plasmid coding for wild-type or mutant myc-tagged Plk1 proteins. Co-transfection of the Plk1 RNAi vector with a plasmid coding for a myc-tagged marker protein showed that about 34 % of all transfected cells accumulated in mitosis (Figure 29A). Although less pronounced, this phenotype is similar to that observed after transfection of siRNA oligonucleotides (compare Figure 29A with Figure 24A). Concomitant expression of myc-tagged Plk1^{WT} with the Plk1 specific RNAi-vector drastically reduced the mitotic index, whereas a catalytically inactive form of Plk1 (Plk1^{K82R}) failed to rescue (Figure 29A). These results confirm that Plk1 activity is required for progression through mitosis. Most importantly, expression of the Plk1 catalytic domain (Plk1^{cat})

was not sufficient to override the mitotic arrest produced by the Plk1 specific RNAi-vector (Figure 29A). Since all myc-tagged Plk1 proteins were expressed to similar levels (Figure 29B), these differences can not be attributed to different expression levels. These results therefore clearly show that PBD-dependent targeting of Plk1 is critical for mitotic progression.

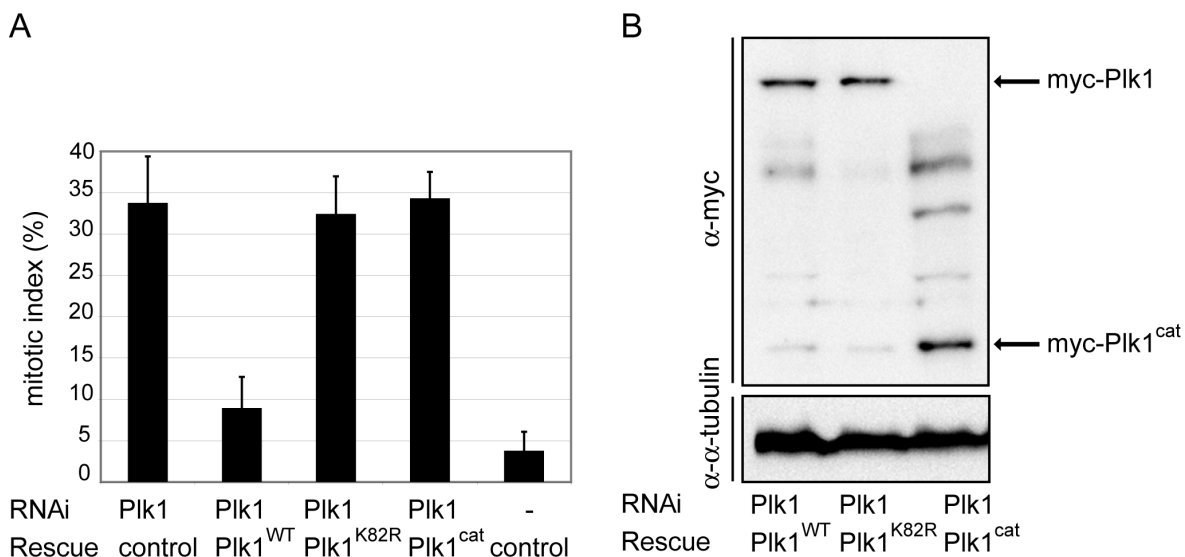


Figure 29 Expression of only the Plk1 catalytic domain in a Plk1-depleted background is not sufficient to overcome mitotic arrest. **A)** HeLa S3 cells were co-transfected for 40 hours with an empty RNAi vector (-) or an insert targeting Plk1, together with protein expression vectors (Rescue) coding for different myc-tagged Plk1 constructs or a myc-tagged control protein, as indicated. Cells were fixed and permeabilised with PTEMF and were stained with anti-pericentrin antibody, anti-myc 9E10 antibody and DAPI (DNA). The mitotic indexes were determined as in Figure 24B. Histogram shows the results of three independent experiments (300-500 cells each) and bars indicate standard deviations (left panel). **B)** Expression levels of the different myc-tagged Plk1 proteins (Rescue) were analysed by Western blotting using the anti-myc 9E10 antibody and detection of α -tubulin was used as a loading control.

3.7 The PBD is dispensable for centrosome maturation and separation but not for chromosome congression

To determine which, if any, of the defects apparent in the Plk1-depleted cells could be rescued by expression of delocalised Plk1^{cat}, we investigated the corresponding arrest phenotype in more detail. This analysis revealed that Plk1^{cat} could indeed restore several of the Plk1-dependent processes that were defective in Plk1-depleted cells. Whereas proper centrosome separation and bipolar spindle formation were impaired in Plk1-depleted cells (Figure 30A), in agreement with the data shown above (Figure 25A), these defects were no longer observed in depleted cells expressing the Plk1^{cat} domain (Figure 30A). Moreover, both γ -tubulin and Aurora-A recruitment were clearly impaired in Plk1-depleted cells, but these defects could also be rescued by expressing the Plk1^{cat} domain (Figure 30B). These experiments also confirmed that the catalytic domain alone is not able to localise to centrosomes and KTs, although some spindle-like staining could be observed (Figure 30A and 30B). This is similar to the endogenous Plk1 localisation in PBD^{WT} expressing cells (Figure 24D) and suggests that Plk1 could interact in a PBD independent manner

RESULTS I

with MTs. The most straightforward interpretation of these data is that the PBD is essential for mitotic progression but not strictly required for centrosomal functions of Plk1 (Table 2).

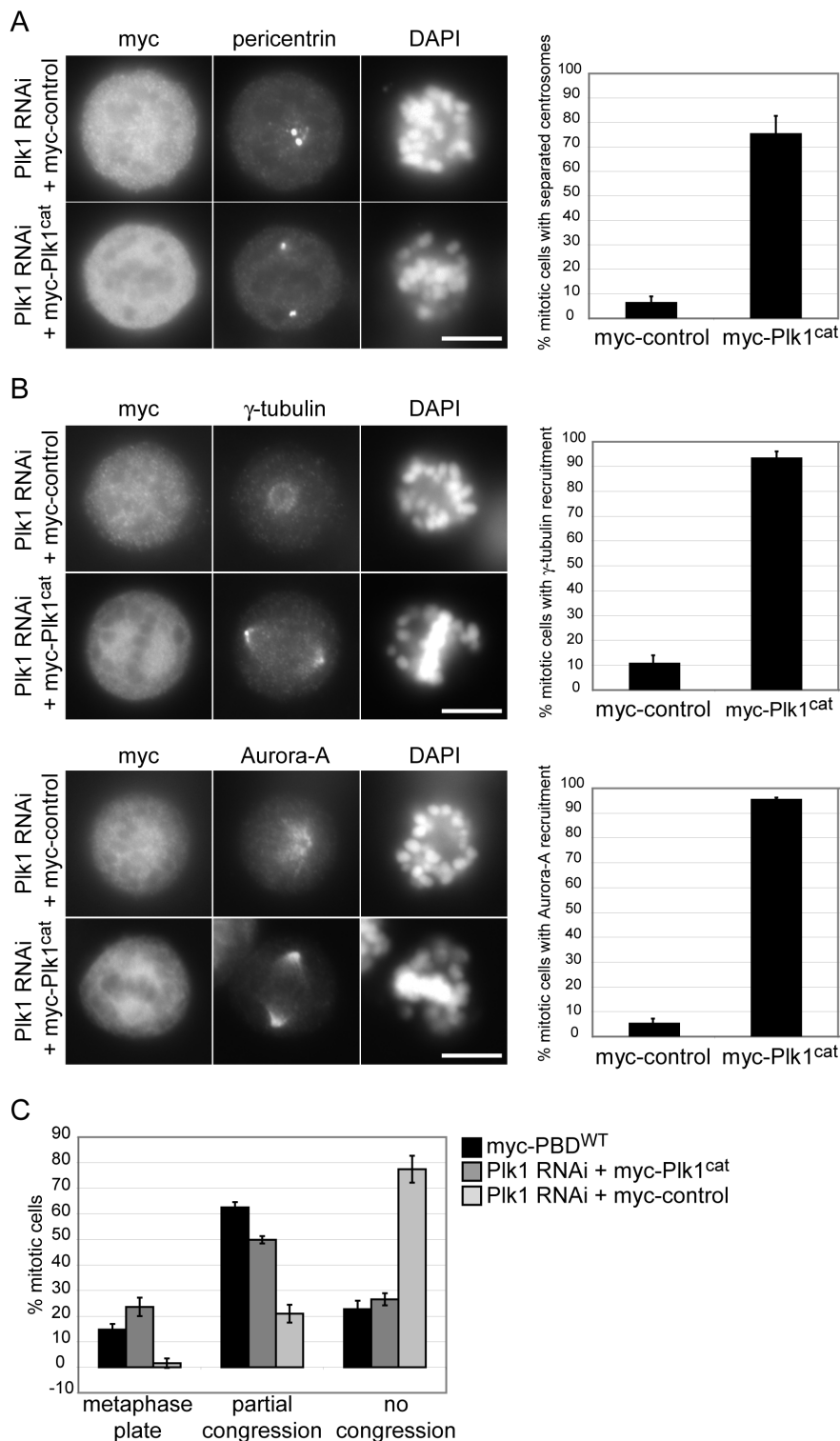


Figure 30 The PBD is dispensable for centrosome maturation and separation but required for chromosome congression. A) HeLa S3 cells were co-transfected for 40 hours with a Plk1 targeting RNAi vector and plasmids coding for either a myc-control protein or the myc-Plk1 catalytic domain. Cells were fixed and permeabilised with PTEMF and then stained with anti-myc 9E10 antibody, DAPI (DNA) and anti-pericentrin antibody to visualise centrosome separation. Histogram shows the quantification of cells with separated

centrosomes. Centrosomes were regarded as separated if they were positioned at opposite sites of the chromosome masses. Results are of three independent experiments (more than 100 cells each) and bars indicate standard deviations. B) Same as in A, but cells were either fixed and permeabilised with -20°C methanol and stained with anti-myc 9E10 antibody, anti- γ -tubulin antibody and DAPI (upper panels) or fixed and permeabilised with PTEMF and stained with anti-myc 9E10 antibody, anti-Aurora-A antibody and DAPI (lower panels). Histograms show the quantification of the recruitment of γ -tubulin and Aurora-A, respectively. Results are of three independent experiments (more than 100 cells each) and bars indicate standard deviations. C) Histogram shows quantification of the different degrees of chromosome congression to the metaphase plate in PBD^{WT} expressing cells (black bars), in cells expressing the *Plk1* catalytic domain in a *Plk1*-depleted background (dark grey bars) and in *Plk1*-depleted cells (light grey bars). The term 'partial congression' is used to describe cells, in which a metaphase-like plate is present together with variable numbers of uncongressed chromosomes, whereas 'no congression' describes cells that do not show an obvious metaphase plate. Results are of three independent experiments (100 cells each) and bars indicate standard deviations. Scale bars indicate 10 μm .

Despite recovery from the centrosome and spindle formation defects, cells expressing the catalytic domain still arrested in mitosis, most likely because of chromosome congression defects (Figure 30A and 30B). Quantitative analysis of the extent of chromosome congression revealed that in *Plk1*-depleted cells most chromosomes were not congressed, as expected for cells with monopolar spindles (Figure 30C, light grey bars). In depleted cells expressing the *Plk1* catalytic domain, however, most cells showed partially congressed chromosomes, very similar to the phenotype seen with cells overexpressing the PBD (Figure 30C, dark grey and black bars, respectively, Table 2). These results therefore indicate that proper chromosome alignment requires PBD-dependent targeting of *Plk1* activity.

	Control	PBD^{WT}	<i>Plk1</i> depletion	<i>Plk1</i> depletion + catalytic domain
Centrosome maturation:				
γ -tubulin recruitment	+	+	-	+
Aurora-A recruitment	+	+	-	+
Centrosome separation	+	+	-	+
Spindle formation	+	+	-	+
Chromosome congression	+	-	-	-
Loss of arm cohesion	+	+	-	Nd*

Table 2 Comparison of the different *Plk1* associated mitotic defects

* Due to technical limitations this could not be determined in these transiently transfected cells.

DISCUSSION I

1 Plk1 PBD pull downs and immunoprecipitations revealed many PBD interacting proteins

Plk1 is involved in many processes during mitotic progression and consistently localises in a very dynamic manner to all important mitosis specific subcellular structures like centrosomes, spindle poles, KTs, midzone and midbody (Barr *et al.*, 2004). It seems therefore self-evident that precise targeting of Plk1 is crucial for its function. The Yaffe group has revealed that the C-terminal targeting domain of Plk1, the PBD, is a phosphopeptide binding domain. Together with the identification of the optimal binding motif of the PBD, these findings opened the way for a deeper understanding of the mechanisms of Plk1 recruitment to the different mitotic structures. A priming kinase, like e. g. Cdk1/Cyclin B, phosphorylates the Plk1 docking protein at a serine/threonine residue within the PBD binding motif thereby enabling the PBD to subsequently bind to it. PBD binding releases concurrently the N-terminal kinase domain, which in turn is now active to phosphorylate its downstream target proteins (Elia *et al.*, 2003a; Elia *et al.*, 2003b). Despite this rather precise model of Plk1 targeting, the proteins to which Plk1 eventually binds and possibly further phosphorylates are largely unknown. This holds especially true for Plk1 action at the spindle poles and even more at the KTs. Our aim was therefore to elucidate the molecular mechanisms of Plk1 functions by identifying mitotic, phosphorylated Plk1 interaction partners. Unbound Plk1 is supposed to be in an inactive, folded back conformation due to intramolecular inhibitory interaction of its kinase domain and with the PBD (Jang *et al.*, 2002a; Elia *et al.*, 2003b). Since for this reason the PBD alone has a higher affinity for phosphopeptides than full length Plk1 (Elia *et al.*, 2003a), and moreover, since we were especially interested in proteins whose interaction with Plk1 was phosphorylation dependent, we searched for interacting proteins by using the PBD alone as a “bait”, not the full length protein.

For this purpose pull downs with recombinant GST-PBD were performed. In order to increase the specificity and to bias the search for mitotically phosphorylated Plk1 interaction partners, we used pure mitotic extracts, precleared the extracts with GST-PBD^{AA}, the PBD phosphopeptide binding mutant, and additionally narrowed down the potential interactors by only analysing proteins, which could be eluted from the PBD^{WT} by competition with the optimal PBD binding phosphopeptide, the PBDtide. Two thirds of the PBD eluted potential interactors, that is more than 200 proteins, were specific for the PBD^{WT} (Table 6) but this large number raised the possibility that the GST-PBD alone may engage in many interactions if exposed to the whole pool of cytoplasmic proteins. Although we can not exclude that some of these PBD^{WT} eluted proteins might indeed represent specific interaction partners, most of the different protein groups like metabolic enzymes, proteins binding to DNA and assisting DNA synthesis, chaperons and proteins involved in membrane trafficking seemed not obviously relevant for our aim to gain insights into

how Plk1 functions in spindle formation and chromosome segregation. For other groups of proteins mitotic functions could be conceivable like for proteins with an ubiquitin ligase activity and for nucleoporins, the proteins of the nuclear pore complexes (NPCs). In fact, Nup133, the Nup107 subcomplex (Nup107, Nup160, Nup37 and Nup43, Seh1) and Nup358 (RanBP2) are known to associate with KT's during mitosis (Belgareh *et al.*, 2001; Salina *et al.*, 2003; Loiodice *et al.*, 2004; Orjalo *et al.*, 2006) and in yeast, yet another subcomplex of nucleoporins has been demonstrated to interact with the SAC component Mad2 at the NPCs during interphase (Iouk *et al.*, 2002). Furthermore, a complex of Rae1 and Nup98 has recently been implicated in inhibiting securin degradation by an inhibitory interaction with APC/C-Cdh1 (Jeganathan *et al.*, 2005). Interestingly, Nup133, Nup160, Nup43 and Nup98 were found in our pull down experiment. However, due to the high overall amount of detected proteins we did not feel confident in choosing a candidate among these groups of proteins for more detailed analysis of a potential Plk1 interaction.

The few obviously interesting candidates, like NuMA, Condensin subunit, Hurler, Mad2 and Bub3, had low scores in the MS analysis (Table 6). Remarkably, the few established PBD interacting partners, e. g. Cdc25C (Elia *et al.*, 2003a; Elia *et al.*, 2003b) and Mklp2 (Neef *et al.*, 2003), were not found in this pull down (Table 6). They might have escaped detection by MS due to a relatively low abundance of their tryptic peptides compared to the otherwise complex mixture of the digested samples. Furthermore, in the case of Mklp2, the state in which the cells were harvested for subsequent lysis (prometaphase, metaphase) was not yet the one during which the interaction normally occurs in the cell (anaphase, telophase) (Neef *et al.*, 2003).

Taken together, the *in vitro* pull down approach, which involves large amounts of recombinant GST-PBD incubated in a whole cell extract, turned out to be not specific enough for reliably identifying novel interesting and mitotically relevant Plk1 PBD interaction partners.

We sought to further increase the specificity of PBD binding by expressing the PBD *in vivo* and by allowing potential interactions to take place within the intact cell at the physiological sites of Plk1 action, namely the spindle poles and KT's. Stable inducible HeLa S3 cell lines were therefore generated, which expressed myc-tagged PBD^{WT} and PBD^{AA}, respectively, upon addition of tetracycline (Figure 14A). In accordance with the results from transient overexpressions of the PBD (Elia *et al.*, 2003b), also the myc-PBD^{WT} induction in the stable cell line led to a mitotic arrest, whereas the PBD^{AA} expression did not obviously impair mitotic progression (Figure 14A and 24A). Moreover, the PBD^{WT} of the stable cell line localised to the same structures as described for endogenous Plk1 attesting to proper functioning of the PBD generated within the stable cell lines (Figure 23A). IPs performed with the myc-PBDs resulted in only few distinct PBD^{WT} specific bands but neither a KT, centrosome or spindle associated nor otherwise interesting candidate with respect to mitotic functions of Plk1 was obtained (Table 1).

Commonly found in both PBD interaction approaches were lamins, proteins of the replication licensing minichromosomal maintenance complex (MCM2-7) and vimentin, all of them highly abundant proteins and therefore easily detectable by MS (Table 6 and Table 1). Recently, the PBD as well as full length Plk1 have also been shown by another group to interact with MCM2

DISCUSSION I

and MCM7. From this mere interaction a function of Plk1 in coordinating DNA replication and mitosis was suggested (Tsvetkov *et al.*, 2005). Also Plk1 interaction with vimentin had been confirmed later by the Inagaki group (Yamaguchi *et al.*, 2005). They could show that in line with the Yaffe model of Plk1 action, Cdk1 phosphorylation of vimentin was required for Plk1 binding to and further phosphorylation of vimentin in mitosis. The phosphorylation of vimentins by Plk1 seemed important for proper segregation of this intermediate filaments to the daughter cells during cytokinesis (Yamaguchi *et al.*, 2005).

2 The significance of the specific Cdc20-Plk1 and MST2-Plk1 interactions remains to be elucidated

Since PBD pull downs and IPs failed to result in either a reasonable number of distinct proteins whose Plk1 interaction could have been further established by additional experiments or in apparently interesting and relevant interaction partners in the context of mitotic events, we decided to bias our search of PBD interactors for known KT and centrosome proteins. Among the proteins, which co-IPed specifically with the PBD^{WT} and not the PBD^{AA}, both expressed in inducible stable HeLa S3 cell lines, we concentrated on Cdc20 (Figure 16B). Cdc20 seemed particularly interesting as a Plk1 interacting candidate not only because it localises to the outer KT, just as Plk1 does, and has been shown to be phosphorylated during mitosis but also because it is the APC/C activator and the downstream target of the SAC. Plk1 activity seems not to be essential for the SAC but might assist its activation by phosphorylating components, e. g. Cdc20. Bub1, a KT associated SAC kinase, which also specifically co-IPed with the PBD^{WT} in our experiment, had been shown to phosphorylate Cdc20 and the presence of these phosphorylations was required to inhibit the APC/C (Tang *et al.*, 2004). One of the Bub1 phosphorylation sites was a conserved potential PBD docking site (pS161). Therefore, we envisioned a scenario in which Bub1 acts as a priming kinase for subsequent Plk1 binding to Cdc20. Moreover, the Plk1-Bub1 interaction might be advantageous for maintaining Bub1 in the proximity to Cdc20, thus facilitating the additional phosphorylations of Cdc20 that support the APC/C inhibition. Recently, Bub1 has indeed been shown to interact with the PBD and to be required for Plk1 KT localisation (Qi *et al.*, 2006). In support of the Plk1 PBD-Cdc20 interaction, we could show binding of endogenous Cdc20 to full length overexpressed Plk1, which was particularly strong in mitotic cells, (Figure 18A) and furthermore, could demonstrate the specificity of this interaction for Plk1, as all the other Plk family members despite their strong sequence similarities failed to co-IP endogenous Cdc20 (Figure 18C). However, it was not possible to analyse the effect of the Cdc20 S161A phosphomutation on the Plk1 PBD interaction because both N-terminally and C-terminally FLAG-tagged versions of Cdc20 turned out to be generally unable to bind Plk1 (Figure 19A). Untagged versions of Cdc20 could have overcome these limitations in a background depleted of the endogenous protein.

In parallel, another mitosis and phosphorylation specific interaction partner of both full length Plk1 and the PBD alone emerged: MST2, a member of the Ste20 kinase family (Figure 20A, B, D).

Although MST2 had neither been implicated in any mitotic events (Lee *et al.*, 2001; Harvey *et al.*, 2003) nor apparently localised to any mitotic structures (Eunice Chan, unpublished data), the interaction was very specific for the only mitotically crucial Plk1 family member, Plk1. Moreover, MST1, the closest paralogue of MST2, did not bind (Figure 20A, B). Interestingly, another member of the Ste20 kinase family, Ste20-like kinase (SLK) had been proposed to be an upstream regulatory kinase for Plk1 during the G2/M transition (Ellinger-Ziegelbauer *et al.*, 2000). However, SLK as the activating kinase of Plk1 was never confirmed thereafter. Although all our experiments on characterising the Plk1-MST2 interactions were very clear and reproducible, we eventually failed to assign a physiological role to this interaction, in particular as we had to learn that these strong kinases did not even phosphorylate each other *in vitro* (Figure 21C).

3 PBD expression shows distinct requirements of different Plk1 functions for PBD-mediated targeting and reveals a novel role of Plk1 in chromosome congression

With the stable inducible PBD cell lines we had generated a suitable tool to study not only the consequences of PBD^{WT} versus PBD mutant overexpression on mitotic progression but also a tool to examine the importance of PBD-mediated localisation for different mitotic functions of Plk1.

Upon prolonged expression of the PBD^{WT} in the HeLa S3 stable cell line, we observed a robust mitotic arrest, almost certainly due to the displacement of endogenous Plk1 from PBD-docking proteins and hence its sites of action (Figure 24). Most interestingly, this arrest phenotype was clearly distinct from that seen in Plk1-depleted cells (Table 2). This suggests that proper Plk1 localisation is critical for some, but not all, mitotic functions of Plk1. In support of this conclusion, we could demonstrate that overexpression of the Plk1 catalytic domain in a Plk1-depleted background resulted in a phenotype very similar to that seen in PBD overexpressing cells (Table 2). This rescue experiment confirms that sufficient amounts of delocalised Plk1 activity can perform centrosome maturation, separation and spindle formation but not proper chromosome congression. From the perspective of therapeutic approaches aimed at inhibiting Plk1 activity, this observation opens the interesting possibility that drugs targeting the PBD could be tailored such as to interfere only with a subset of Plk1 functions.

Moderate expression of the PBD^{WT} and the PBD^{AA} in the stable cell lines allowed the analysis of their respective localisations. The PBD^{WT} localised to the same structures as endogenous Plk1 confirming its targeting ability (Figure 23A). Additionally, we revealed that Plk1 recruitment to centrosomes, KTs, central spindle and to a lesser extent to the midbody required the PBD phosphopeptide binding ability *in vivo*, since the PBD^{AA} failed to properly localise to these structures (Figure 23B). This demonstrates a requirement of phosphorylation of the Plk1 docking proteins.

DISCUSSION I

PBD^{WT} expression resulted in a SAC-dependent mitotic arrest, whereas expression of neither PBD1^{AA} nor the PBDs of Plk2 and Plk3 interfered with mitotic progression (Figure 24B). PBD2 and PBD3 were demonstrated to have the same preferences concerning the optimal phosphopeptide ligand as Plk1 PBD (Elia *et al.*, 2003b). It is therefore important to note that the respective PBDs alone possess a structural specificity beyond the phosphopeptide binding cleft. The former is obviously sufficient to prevent a Plk1 PBD-like localisation pattern even when their expressions were untimely and exogenously induced as in our experiment. This implicates that also Plk1 residues apart from its PBD docking consensus play a crucial role in specific targeting.

Not only expression of the PBD^{WT} in an otherwise endogenous background but also depleting endogenous Plk1 by RNAi arrested cells in mitosis in a SAC-dependent manner but interestingly the phenotypes of the arrested cells were strikingly different (Figure 25). In contrast to Plk1 depletion, PBD expression did not significantly impair centrosome maturation and separation, loss of sister chromatid arm cohesion and bipolar spindle formation. Instead, PBD expression affected a later process in the sequence of mitotic events, which occurs only after bipolar spindle assembly: the congression of the chromosomes to the metaphase plate (Table 2). At first sight, one could argue that this defect might reflect direct inhibition of endogenous Plk1 by PBD. However, this interpretation is unlikely, for the following reasons. First, PBD expression was previously shown not to affect the bulk activity of endogenous Plk1 (Seong *et al.*, 2002). Second, the critical chromosome congression defect was observed only in cells expressing PBD^{WT} but not in cells expressing a PBD^{AA} mutant. Considering that both wild type and mutant PBDs are able to interact with the catalytic domain of Plk1 (Elia *et al.*, 2003b), a direct inhibitory interaction of the PBD^{WT} with endogenous Plk1 appears unlikely. Thus, the most straightforward interpretation of our results is that PBD^{WT}, but not PBD^{AA}, competes in a dominant-negative manner with endogenous Plk1 for the binding to phosphorylated docking proteins. This conclusion is strongly supported by our observation that endogenous Plk1 could be displaced from centrosomes and KTs by PBD^{WT} but not by PBD^{AA} (Figure 24D). Furthermore, our rescue experiments showed that Plk1-depleted cells expressing only the catalytic domain of Plk1 displayed a mitotic phenotype very similar to that seen in PBD^{WT} expressing cells (Figure 30). Thus, although delocalised Plk1 activity appears to be sufficient for some Plk1 functions, it cannot provide all functions required for mitotic progression (Figure 31).

In agreement with previous results (Lane *et al.*, 1996; Sumara *et al.*, 2004; van Vugt *et al.*, 2004), our study confirms that Plk1 is required for γ -tubulin recruitment during centrosome maturation. In addition, we discovered that the centrosomal recruitment of Aurora-A, a kinase also implicated in centrosome maturation and bipolar spindle formation (Nigg, 2001), was abolished in the absence of Plk1. In contrast, Aurora-A localisation to spindle MTs was not affected (Figure 27). These results clearly demonstrate that Plk1 regulates Aurora-A recruitment to the centrosome. Regardless of whether this Plk1 requirement reflects a direct or indirect mechanism, this observation suggests that Plk1 acts upstream of Aurora-A in centrosome maturation and spindle formation.

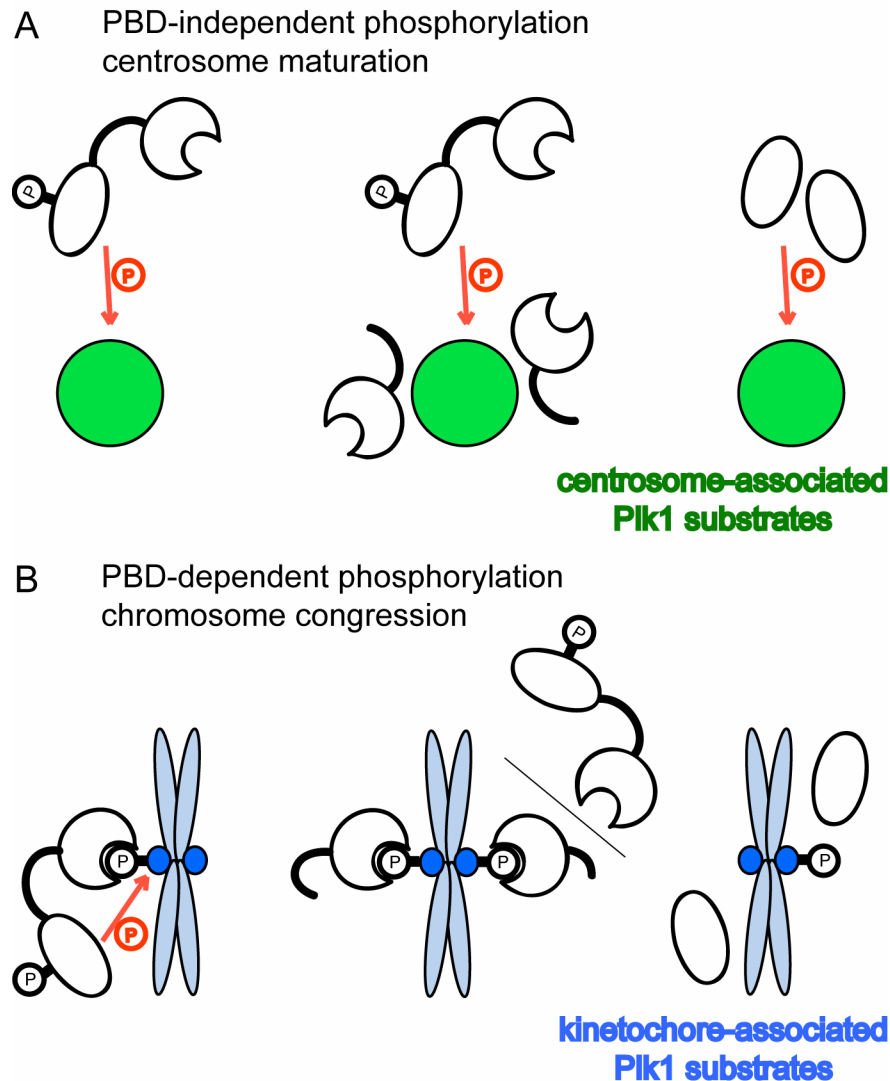


Figure 31 Distinct Plk1 functions have different requirements for PBD-mediated targeting. A) Plk1 functions in centrosome maturation and separation do not strictly require PBD-mediated targeting of Plk1 to the centrosomes. B) Plk1 function in chromosome congression requires PBD-mediated targeting to the KTs. The simplified models summarise the different situations in unperturbed cells (A, B left panels), in PBD expressing cells (A, B middle panels) and in Plk1-depleted cells rescued with the catalytic domain of Plk1 (A, B right panels). Red arrows indicate phosphorylation events, P stands for phosphorylation.

Since endogenous Plk1 prominently localises to centrosomes it may appear surprising that PBD-mediated displacement of Plk1 did not interfere with centrosome maturation and separation. It is difficult to rigorously exclude that very low levels of Plk1 might have remained at centrosomes in PBD^{WT} expressing cells, and although undetectable by IF microscopy, might have been sufficient to carry out the analysed centrosome functions. However, the fact that overexpression of the catalytic domain in Plk1-depleted cells was sufficient to restore centrosome maturation and spindle assembly would argue that localised Plk1 activity is not absolutely required for the analysed centrosome functions. Furthermore, it implies that Plk1 function in centrosome maturation and separation is mainly enzymatic, i. e. phosphorylating specific centrosomal targets, and not structural such as forming a docking site at the centrosome for the recruitment of additional centrosomal components e. g. maturation factors. Consequently, two described centrosomal Plk1

DISCUSSION I

substrates, Nlp and Asp, would still receive their respective functionally essential phosphorylations at the onset of mitosis even without targeted Plk1 activity (do Carmo *et al.*, 2001; Casenghi *et al.*, 2003). In contrast, the catalytic domain alone was unable to restore sufficient chromosome congression to satisfy the SAC so that Plk1-depleted cells expressing only delocalised activity arrested with a phenotype closely resembling that seen in PBD expressing cells (Figure 30). Taken together, these results indicate that the investigated centrosomal functions of Plk1 are less dependent on localised Plk1 activity than the chromosome congression function (Figure 31).

The stable PBD expressing cell lines provide a useful tool to specifically study Plk1 function in chromosome alignment without severely interfering with its chronologically earlier functions in mitosis, while disrupting Plk1 function by other common means like RNAi or antibody microinjection arrests cells already at earlier stages with monopolar spindles. Although suggested previously (Seong *et al.*, 2002), a role of Plk1 in chromosome congression has not attracted attention so far, most likely because of the apparent limitations to study Plk1 function without impairing bipolar spindle assembly.

The exact nature of the chromosome congression defect in cells harbouring only delocalised Plk1 activity remains to be determined but our observation that unaligned chromosomes were not attached to K-fibres in PBD expressing cells suggests that MT capture or maintenance of KT-MT attachments depend on localised Plk1 activity most apparently at the KTs. Plk1 has long been known to localise to KTs (Arnaud *et al.*, 1998), and with the identification of a PBD-dependent role of Plk1 in chromosome congression this strongly points to a critical function at this site. Remarkably, the time frames of Plk1 KT localisation and chromosome alignment coincide in prometaphase and metaphase, both ceasing upon anaphase onset.

Tension across sister KTs has to be sensed and further translated into a signal, which is finally transduced to the SAC machinery. Since the 3F3/2 phosphoepitopes are only present at unattached or unaligned KTs and vanish as soon as tension is exerted across the sister KTs, they might play a role in the system that transmits mechanical changes into chemical modifications (Gorbsky *et al.*, 1993; Nicklas *et al.*, 1995). Plk1 turned out to be the kinase that creates the 3F3/2 phosphoepitopes (Ahonen *et al.*, 2005). Accordingly, Plk1 localised preferably to unaligned KTs that lack tension. Thus, both Plk1 localisation and its kinase activity generating 3F3/2 epitopes are increased upon reduction of tension (Ahonen *et al.*, 2005). The function of the 3F3/2 epitopes is not known but it seems apparent that their phosphorylation must signal downstream components to maintain the SAC in an active state or/and to facilitate recruitment of proteins to the unaligned KTs that promote proper attachment. Since disruption of Plk1 function has so far never been shown to impair SAC signalling, the latter option seems more likely (van Vugt *et al.*, 2004; Gimenez-Abian *et al.*, 2004). In such a scenario unlocalised Plk1 activity, as present in PBD expressing cells or in the cells rescued with the catalytic domain only, failed to mark the unattached KTs with a “phosphorylation-tag” and as a consequence, factors at the KTs required for capturing MTs or maintaining KT-MT attachments were inefficiently recruited, resulting in defective chromosome alignment and mitotic arrest. The dynein-motor associated factor NudC, which had previously been implicated in cytokinesis (Zhou *et al.*, 2003), was recently shown to be phosphorylated by Plk1 *in*

vivo and was suggested to be subsequently required to recruit Plk1 to the KTs. Upon depletion of NudC, Plk1 was no longer detected at the KTs and, confirming our results, also these cells exhibited congression defects (Nishino *et al.*, 2006).

To entirely understand the exact mechanism of Plk1 action at the KTs, two aspects will be important to explore: first, to find out how the PBD congression phenotype arises. Live-cell imaging of chromosome movements of PBD expressing cells will help to distinguish between failures in initial MT capture or in the maintenance of KT-MT attachments. Secondly, it will be crucial to identify Plk1 PBD interacting proteins amongst KT components and to examine how they are involved in chromosome congression. Of special interest are PBD interacting proteins, which are dispersed from the KTs upon PBD expression and show a congression phenotype similar to the PBD expressing cells upon disruption of their function.

SUMMARY I

Plk1 has multiple important functions during M phase progression. In addition to a catalytic domain, Plk1 possesses a phosphopeptide-binding motif, the PBD, which is required for proper localisation.

In order to gain insight into how Plk1 exerts its different mitotic functions we aimed to find Plk1 interacting proteins whose binding was mediated by the PBD. The unbiased search for mitotic Plk1 PBD interacting proteins by both *in vitro* PBD pull downs and *in vivo* myc-PBD IPs revealed the PBD as a protein domain, which is able to bind a range of different proteins. Consequently, it was very difficult to discriminate between unspecific and physiologically relevant interaction partners. The employment of myc-PBD stable inducible HeLa S3 cell lines for IPs strongly reduced the amount of potential Plk1 interactors but still did not result in candidates, which were obviously interesting with respect to mitotic processes. When we tested PBD-IPs of the stable cell lines by Western blotting with a set of antibodies directed against proteins of mainly the KTs and centrosomes, sites to which also endogenous Plk1 localises, Cdc27, Bub1, Ect2, Cdc20 and MST2 were shown to specifically bind the PBD^{WT}. The latter two, Cdc20 and MST2, also interacted with full length endogenous Plk1 but the physiological relevance of the established interactions remains to be unravelled.

Next we explored the importance of correct Plk1 subcellular targeting for its mitotic functions. We either displaced endogenous Plk1 through overexpression of the PBD or introduced the catalytic domain of Plk1, lacking the PBD, into Plk1-depleted cells. Both treatments resulted in remarkably similar phenotypes, which were distinct from the Plk1 depletion phenotype. Cells depleted of Plk1 mostly arrested with monoastral spindles, due to inhibition of centrosome maturation and separation. In contrast, these functions were not impaired in cells with mislocalised Plk1. Instead, these latter cells showed a SAC-dependent mitotic arrest characterised by impaired chromosome congression. Thus, whereas chromosome congression requires localised Plk1 activity, other investigated Plk1 functions are less dependent on correct PBD-mediated targeting.

PART II

**Characterisation of two novel
spindle and kinetochore associated proteins,
termed Ska1 and Ska2**

RESULTS II

1 Localisation analysis of uncharacterised proteins from a proteomic spindle inventory

Our department was interested in the composition of the human mitotic spindle and in finding novel spindle components. Therefore, a spindle inventory was performed on isolated taxol stabilised, mitotic spindles from HeLa S3 cells. The spindle associated proteins were separated on a NuPAGE gradient gel, followed by tryptic in-gel digestion of the obtained protein bands and analysis by MS-MS (Sauer *et al.*, 2005). 19% of the identified proteins of the spindle preparation were known spindle proteins, 62% of the proteins could not be assigned to any obviously mitosis-relevant function and for 19% of the proteins no function had ever been described. Out of these 154 uncharacterised candidates 17 genes were cloned as 3xmyc-tagged constructs and 6 out of these turned out to associate to spindle structures when transfected into HeLa S3 cells.

I participated in the cloning and sequencing of 6 candidates and tested the localisation of their encoded proteins by transiently expressing myc-tagged versions in HeLa S3 followed by IF analysis. Whereas 4 out of these constructs coded for proteins, which did not show any mitosis-specific staining when probed with the anti-myc 9E10 antibody (data not shown), two proteins, encoded by the cDNA clones KIAA0007 and IMAGp958K072621Q2, localised to mitotic structures (Figure 32).

The protein encoded by the cDNA clone IMAGp958K072621Q2 clearly localised to the KTs from prometaphase to anaphase, as confirmed by co-staining with the KT marker Hec1, and to the spindle pole from metaphase on (Figure 32A). While the work was in progress a paper was published identifying the IMAGp958K072621Q2 protein as a novel subunit of the Ndc80 KT complex, called hSpc24 (McClelland *et al.*, 2004; Bharadwaj *et al.*, 2004), confirming our localisation data.

The KIAA1187 protein, instead, entirely co-localised with spindle MTs throughout mitosis as shown by co-staining with anti- α -tubulin antibody (Figure 32B). Interestingly, the KIAA1187 protein induced MT bundling when overexpressed in interphase cells (Figure 32B, bottom row). This is in line with a predicted MT binding motif within the KIAA1187 sequence, which can also be found in other MT associated proteins (MAPs) like EMAP115 or MAP7. Depletion of KIAA1187 by two different RNAi oligos, however, did not result in any obvious phenotypes (data not shown) but it has to be noted that we were not able to test the depletion efficiency of this protein as no anti-KIAA1187 antibody was available.

Altogether, 2 out of 6 proteins from the proteomic spindle screen, whose expression vectors I cloned, were indeed spindle proteins. But since IMAGp958K072621Q2 (hSpc24) was meanwhile characterised by other groups and RNAi of KIAA1187 did not show any obvious phenotype, I continued working on a different novel spindle protein found in the spindle inventory.

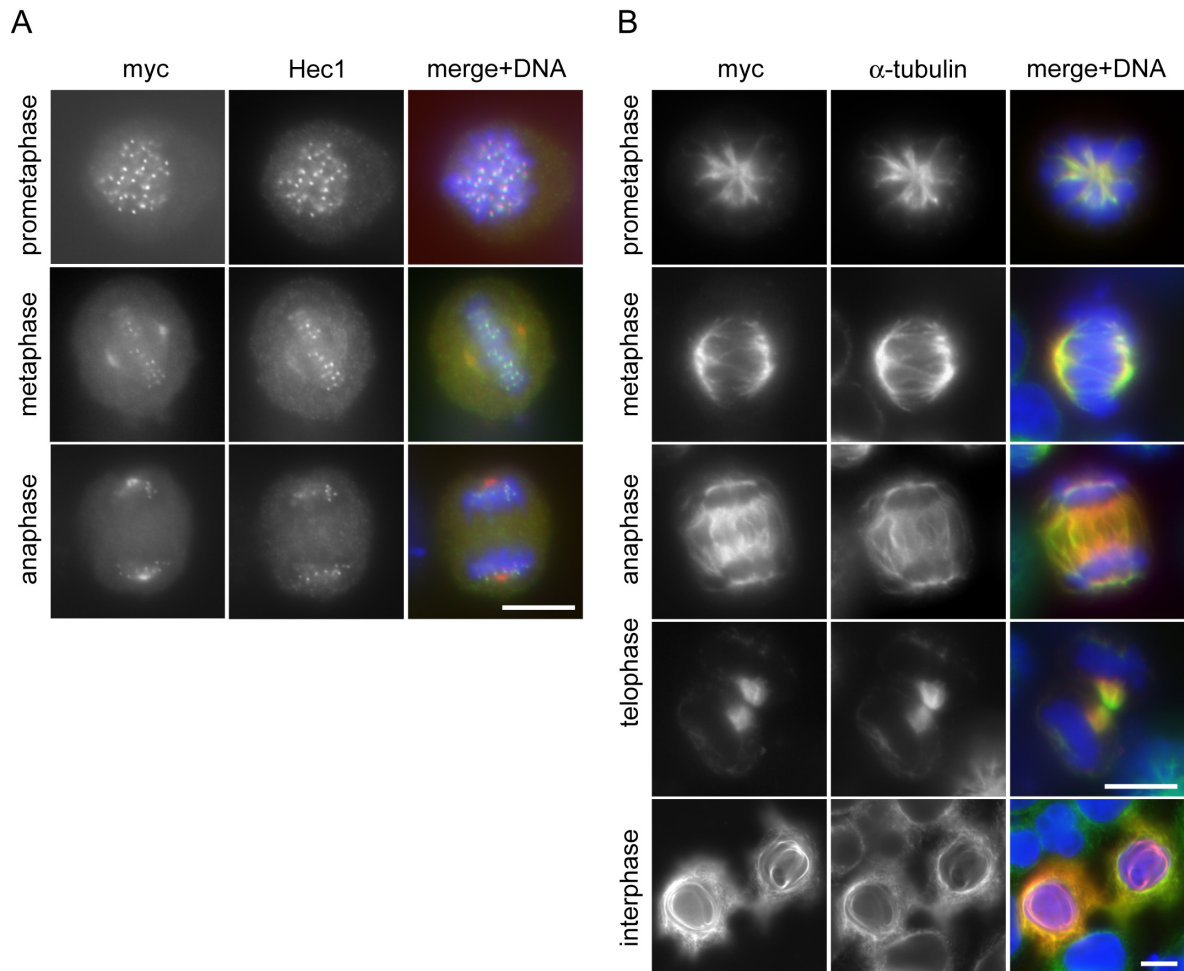


Figure 32 IMAGp958K072621Q2 and KIAA1187, identified in the spindle inventory, localise to mitotic structures. A) HeLa S3 cells were transfected with a myc-tagged IMAGp958K072621Q2 construct for 24 hours. Cells were fixed with paraformaldehyde, permeabilised with Triton-X100 and stained with anti-myc antibody (9E10-TRITC, red), anti-Hec1 antibody (green) and DAPI (DNA, blue). B) Same as in A) but cells were transfected with myc-tagged KIAA1187 and co-stained with anti- α -tubulin antibody (green) instead of anti-Hec1. Scale bars indicate 10 μ m.

2 Ska1, identified in the spindle inventory, in complex with Ska2 is required for timely anaphase onset

2.1 Identification of Ska1 at spindle MTs and outer KTs

C18Orf24 was identified as a putative spindle component in the MS based spindle inventory (Sauer *et al.*, 2005). Inspection of the primary sequence of this 30 kDa protein revealed no known structural motifs, except for a predicted N-terminal coiled coil domain. To determine if C18Orf24 constitutes a genuine spindle component, we transiently expressed the myc-tagged protein in HeLa S3 cells and analysed its localisation by indirect IF microscopy. Co-staining with α -tubulin showed that the myc-tagged protein partly co-localised with spindle MTs in mitotic cells (Figure 34A). In addition, it localised to bright dots on chromosomes that were identified as KTs/centromeres by co-staining with CREST serum (Figure 34A). This localisation prompted us to designate C18Orf24 as Ska1 (Spindle and Kinetochores Associated 1). Database searches indicated the existence of putative Ska1 homologues in other vertebrates, as well as in *Caenorhabditis elegans* (NP_492739), *Anopheles gambiae* (mosquito) (EAL39257), *Arabidopsis thaliana* (NP_191625) and *Oryza sativa* (rice) (XP_478114). In contrast, no obvious homologues could be detected in yeast.

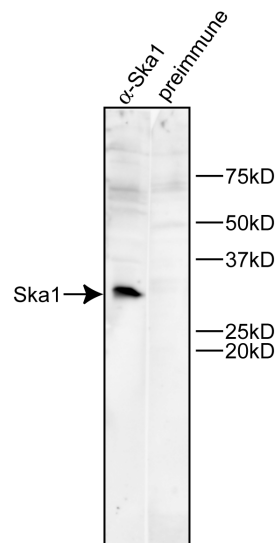


Figure 33 Ska1 antibody specificity. Equal amount of asynchronous HeLa S3 extracts were separated on a SDS-PAGE gel and probed after Western blotting with affinity-purified anti-Ska1 antibody and the corresponding preimmune serum.

To investigate the localisation of endogenous Ska1 a polyclonal rabbit antibody was raised. This antibody detected a prominent band of the expected size in Western blots performed on whole HeLa S3 cell lysates (Figure 33). It also stained both spindle and KT structures in mitotic cells (Figure 34B), confirming the localisation of the myc-Ska1 protein (Figure 34A). Weak spindle staining, particularly in the region of the forming poles, could already be observed in early prophase and persisted until mid-anaphase. Upon furrow ingression in late anaphase, Ska1 then localised

diffusely to the central spindle and later to midbody structures. KT staining appeared during prometaphase, was most prominent from late prometaphase through mid-anaphase, and then vanished in telophase. Co-staining of mitotic cells with anti-Ska1 antibodies and reagents detecting either the centromeres (CREST serum) or the outer KTs (anti-CENP-E) revealed that Ska1 partly co-localised with CENP-E, adjacent to the CREST staining (Figure 34C). Ska1 also co-localised with the outer KT protein Hec1 (data not shown), confirming that this protein is concentrated at the outer KTs. During interphase, anti-Ska1 antibodies produced a diffuse staining of both the cytoplasm and the nucleus but no association with either MTs or centromeres could be observed (Figure 34D). Taken together, these results show that Ska1 is a novel mitotic spindle and KT associated protein.

2.2 Requirements for Ska1 localisation to KTs

Since Ska1 staining at KTs increased during prometaphase (Figure 34B), we asked whether this localisation might depend on KT-MT interactions. When cells were treated with the MT depolymerising drugs nocodazole or colchicine, Ska1 failed to accumulate at KTs (Figure 35A). Similarly, addition of nocodazole to cells already arrested in mitosis (by noscapine treatment (Zhou *et al.*, 2002)) resulted in the loss of Ska1 from KTs, concomitant with the loss of MTs (Figure 35B). Conversely, when cells were released from a nocodazole arrest, the KT localisation of Ska1 was restored in parallel with reformation of the spindle (Figure 35B). Addition of the MT-stabilising drug taxol did not impair Ska1 localisation to KTs (Figure 35A), suggesting that the presence of MTs, rather than their dynamic properties, was important for Ska1 localisation.

Taken together, the above data suggested that KT-MT interactions regulate the accumulation and maintenance of Ska1 at KTs. In analogy to other proteins whose KT association had previously been shown to depend on MTs (Joseph *et al.*, 2004), it was tempting to conclude that MTs are required for transporting Ska1 to KTs. Surprisingly, however, cold-induced depolymerisation of MTs did not result in the loss of Ska1 from KTs (Figure 36A), in striking contrast to the drug-induced effects described above. To rule out the persistence of short MTs in these experiments, cells were pre-treated with nocodazole and then incubated on ice in the continued presence of nocodazole. Under these conditions, Ska1 was initially lost from KTs in response to nocodazole, consistent with the data shown above, but KT staining was subsequently recovered upon incubation in the cold, even in the continued presence of nocodazole (Figure 36B, C). Interestingly, cold treatment of nocodazole-exposed cells did not restore KT localisation to RanGAP1 and RanBP2 (Figure 36D and data not shown), two proteins that are known to depend on MTs for transport to the KT (Joseph *et al.*, 2004). These data indicate that the dependency of Ska1 localisation on MT attachment does not simply reflect a requirement for MT-mediated transport. Instead, we conclude that the attachment of MTs to KTs either generates docking sites for the recruitment of Ska proteins or prevents their release, and that MT attachment can be mimicked by exposure to low temperature.

RESULTS II

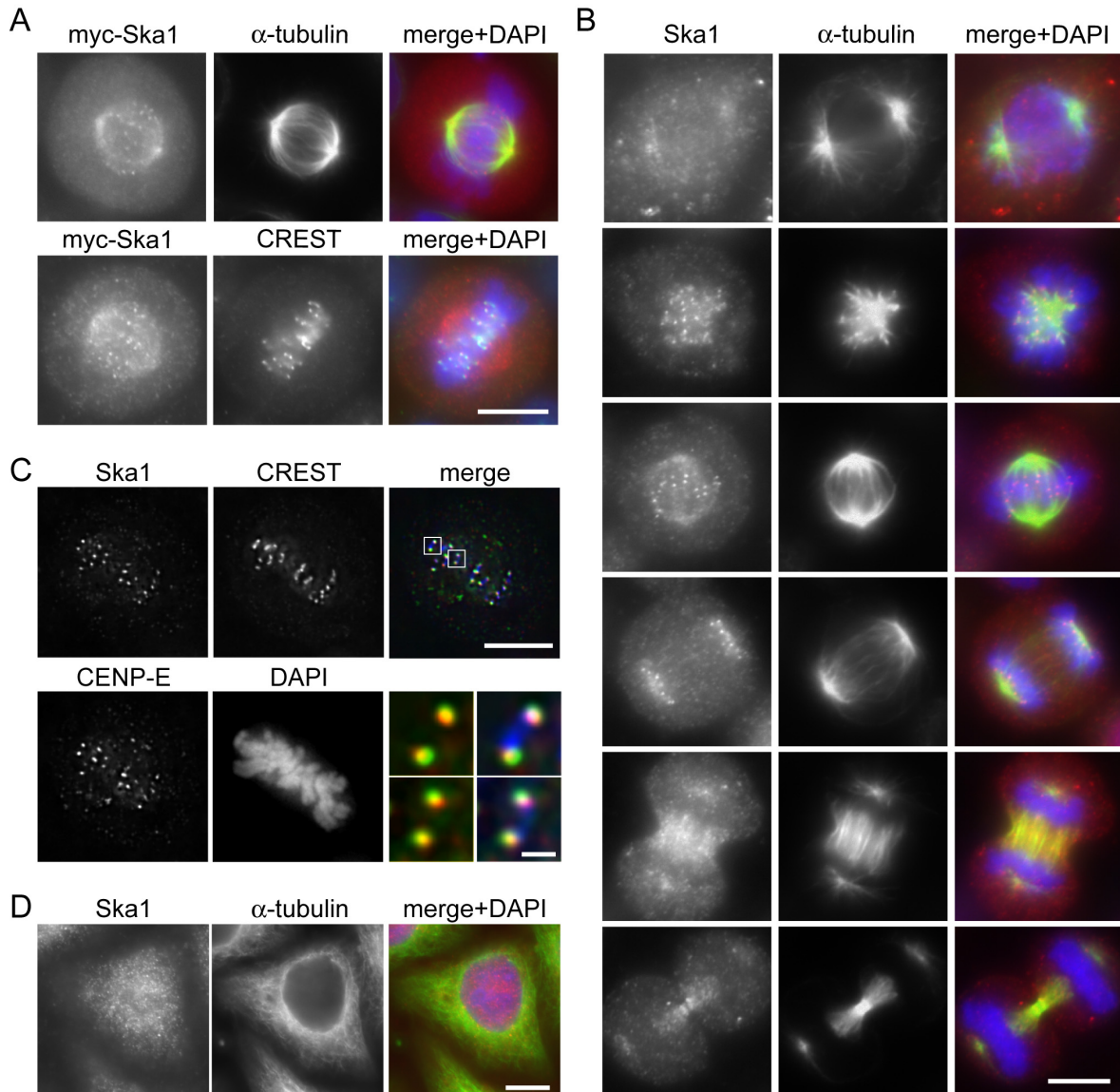


Figure 34 Mitotic spindle and outer KT localisation of Ska1. **A)** HeLa S3 cells were transfected with a myc-tagged Ska1 construct and then fixed with PTEMF. Cells were stained with anti-myc 9E10 antibody (red), DAPI (DNA, blue) and with either anti- α -tubulin antibody (green) (upper panel) or CREST serum (green) (bottom panel). **B)** HeLa S3 cells were fixed with PTEMF and then stained with anti-Ska1 antibody (red), anti- α -tubulin antibody (green) and DAPI (DNA, blue). **C)** Same as in **B** except that cells were stained with anti-Ska1 antibody, anti-CENP-E antibody, CREST serum and DAPI followed by imaging with a Deltavision microscope. Merged pictures are single, deconvolved focal planes and show CREST (blue), CENP-E (green) and Ska1 (red). Right panels in the bottom row are magnifications of the above marked areas with scale bar indicating 1 μ m. **D)** An interphase cell is shown, which was fixed with paraformaldehyde, permeabilised with Triton-X100 and stained as in **B**. Scale bars indicate 10 μ m.

In contrast to Ska1, the KT localisation of the SAC protein Mad2 is lost upon MT attachment (Waters *et al.*, 1998) but can readily be restored by nocodazole treatment (Figure 36E). Remarkably, however, the association of Mad2 with KTs was strongly reduced when nocodazole treated cells were incubated in the cold (Figure 36E). Thus, the KT localisation of Mad2 appears to depend on conditions that are exactly opposite to those required for Ska1 recruitment (compare Figures 36B and 36E).

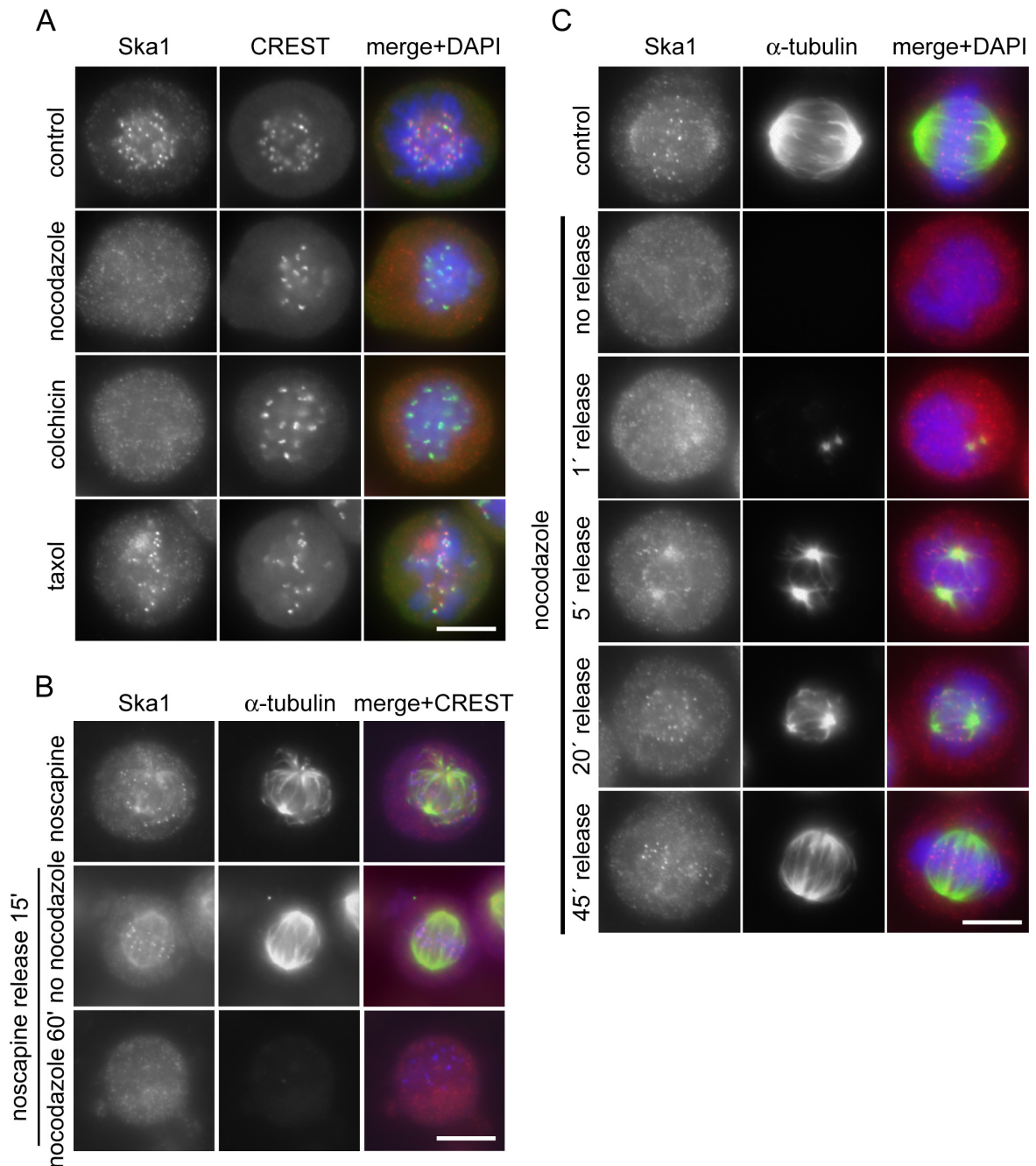


Figure 35 Ska1 KT localisation requires KT-MT attachment at physiological temperatures. A) HeLa S3 cells were either left untreated as a control or treated for 14 hours with nocodazole, colchicin and taxol, respectively. After PTEMF fixation cells were stained with anti-Ska1 antibody (red), CREST serum (green) and DAPI (DNA, blue). B) HeLa S3 cells were arrested with noscapine for 14 hours and either directly fixed with PTEMF (top row) or released for 15 min and then fixed (middle row) or treated with nocodazole for another hour (lower row). Cells were stained with anti-Ska1 (red), anti- α -tubulin (green) and CREST serum (blue). C) HeLa S3 cells were treated for 14 hours with nocodazole and subsequently released for the indicated times from this nocodazole block. As a control an untreated cell is shown at the top row. After PTEMF fixation cells were stained with anti-Ska1 antibody (red), anti- α -tubulin (green) and DAPI (DNA, blue). Scale bars indicate 10 μ m.

In order to exclude a direct role of Mad2 in preventing Ska1 KT localisation as long as MTs are not properly attached we depleted Mad2 by RNAi (control GL2 RNAi) and checked Ska1 localisation in cells treated without and with nocodazole (Figure 36F). Also in cells depleted of

RESULTS II

Mad2 (for Mad2 depletion efficiency see Figure 36G) Ska1 KT localisation could not be restored in the absence of MTs (Figure 36F).

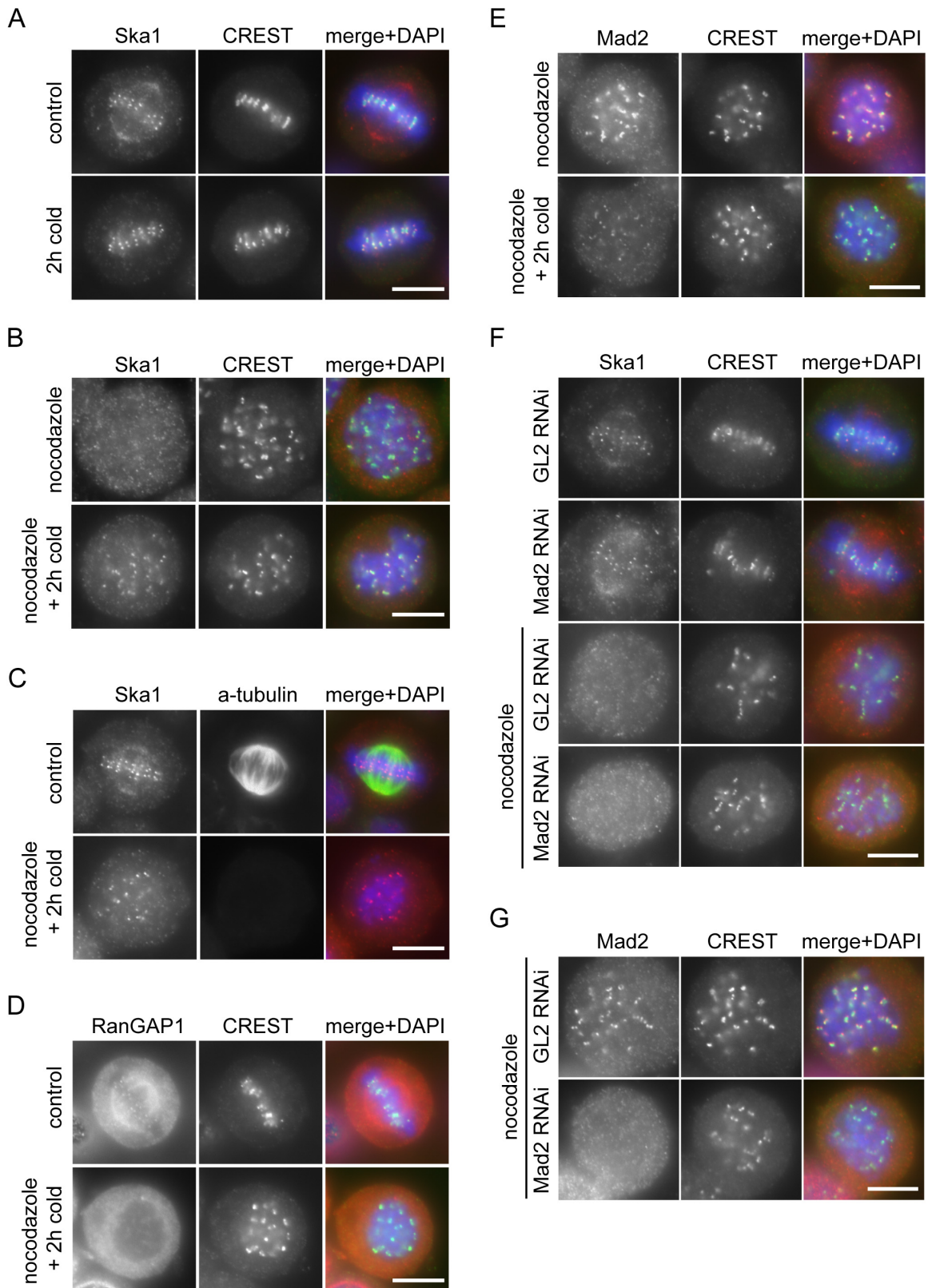


Figure 36 Cold treatment of nocodazole treated HeLa S3 cells can rescue Ska1 but not RanGAP1 KT localisation and has effects on Mad2 localisation opposite to those on Ska1 A) HeLa S3 cells were fixed with PTEMF either directly (control) or after incubation in ice-cold medium. Cells were stained with anti-Ska1

antibody (red), CREST serum (green) and DAPI (DNA, blue). B) HeLa S3 cells were treated with nocodazole for 14 hours and then either fixed directly or incubated in ice-cold medium for another 2 hours in the presence of nocodazole. Cells were fixed and stained as in B. C) HeLa S3 cells were either left untreated (control) or arrested in mitosis with nocodazole for 14 hours followed by 2 hours incubation in ice-cold medium in the continued presence of nocodazole. Cells were permeabilised with PTEMF and stained with anti-Ska1 antibody (red), DAPI (DNA, blue) and anti- α -tubulin (green) in order to check for complete MT depolymerisation in these cells. D) HeLa S3 cells were treated as in C, but stained with anti-RanGAP1 antibody (red), CREST serum (green) or DAPI (DNA, blue). E) HeLa S3 cells were treated as in B but stained with anti-Mad2 antibody (red), CREST serum (green) and DAPI (DNA, blue). F) HeLa S3 cells were treated for 48 hours with control (GL2) and Mad2 specific siRNAs, respectively, and released from an aphidicolin block for 11 hours. During the last 3 hours the releasing cells were either incubated with nocodazole or left untreated before PTEMF fixation and staining with anti-Ska1 (red), CREST serum (green) and DAPI (DNA, blue). G) HeLa S3 cells were treated as in F, but stained with anti-Mad2 (red), CREST serum (green) and DAPI (DNA, blue). Only the nocodazole treated cells are shown. Scale bars indicate 10 μ m.

Cold treatment could influence the enzymatic activities of kinases or phosphatases at the KTs, respectively. Concomitantly, the phosphorylation status of potential KT proteins involved in Ska1 targeting could be altered in a way that makes their interaction and therefore the Ska1 recruitment to KTs less favourable. If that was the case inhibition of one of these enzymatic activities should change Ska1 KT localisation. In order to decrease the overall phosphatase activity both nocodazole arrested and cold treated cells were incubated with high concentrations of NaF. However, Ska1 KT localisation was neither restored in nocodazole treated cells nor reduced in cold treated cells (Figure 37A). In order to test whether inactivation of kinases was the cause of Ska1 recruitment in cold treated cells, HeLa S3 cells were treated as above but instead of NaF the broad-specificity kinase inhibitor staurosporine was used (Figure 37B). Similarly, nocodazole arrested cells were also treated with an inhibitor of Aurora-B (ZM447439) (Ditchfield *et al.*, 2003), a centromere associated kinase involved in destabilising improper KT-MT attachments (Figure 37C). Concentration and incubation times for ZM447438 had been tested before by Anna Santamaria. Neither staurosporine nor ZM447439 had any effect on Ska1 localisation (Figure 37B, C). Although we did not prove whether the chosen concentrations and incubation times of the respective inhibitors were sufficient to switch off the activities of their targets, it seems rather unlikely that changes in a kinase-phosphatase equilibrium directly regulate Ska1 KT recruitment.

RESULTS II

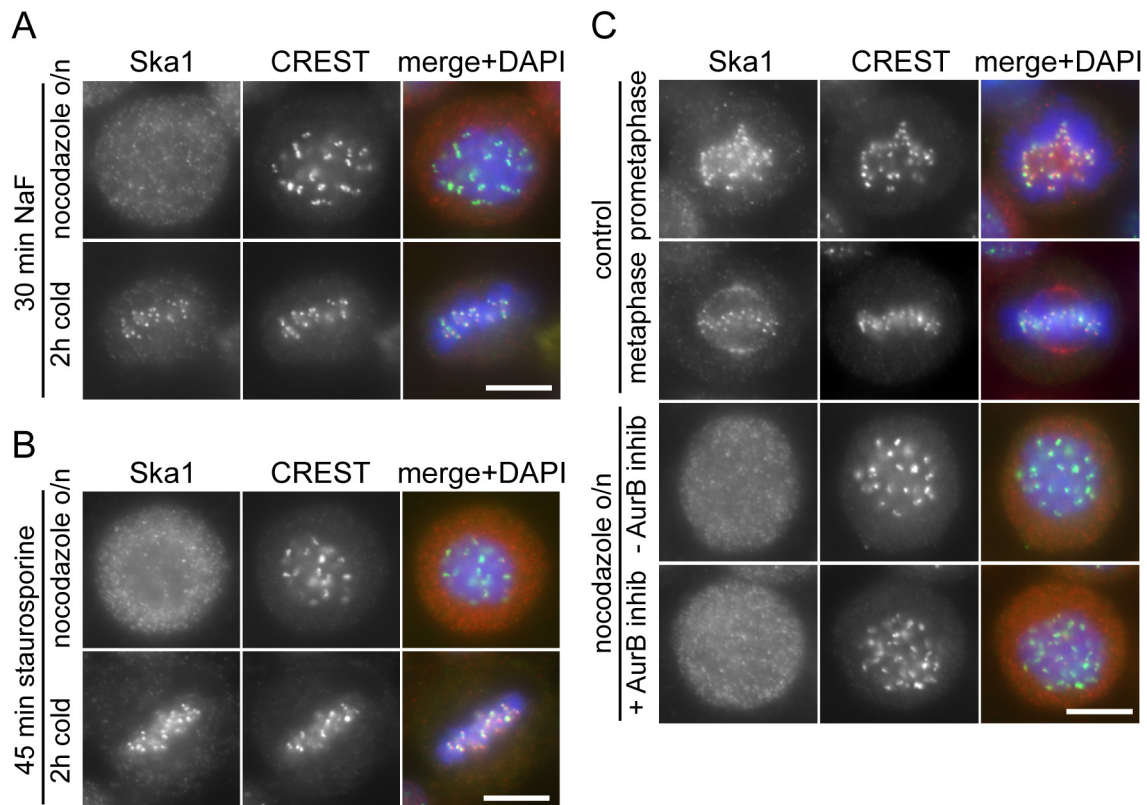


Figure 37 Changes in the kinase-phosphatase equilibrium at KTs of cold treated cells seem not to be the cause for Ska1 KT recruitment in the absence of MTs. **A)** HeLa S3 cells were either arrested with nocodazole for 14 hours or cold treated for 2 hours. For the last 30 min high concentrations of NaF were added, followed by PTEMF fixation and staining of the cells with anti-Ska1 (red), CREST serum (green) and DAPI (DNA, blue). **B)** Same as in A except that cells were treated for the last 45 min with staurosporine instead of NaF. **C)** HeLa S3 cells were treated with nocodazole for 14 hours or left untreated. Cells were then either fixed directly (- AurB inhib) or treated with the Aurora-B inhibitor (+ AurB inhib) for 1 hour, before PTEMF fixation and staining of the cells with anti-Ska1 (red), CREST serum (green) and DAPI (DNA, blue).

To determine which proteins might be required for KT localisation of Ska1, several KT associated proteins were depleted by RNAi. Of all proteins tested, only depletion of the outer KT protein Hec1 clearly reduced the concentration of Ska1 at KTs (Figure 38A). In contrast, depletion of Bub1, Aurora-B, CENP-E, CENP-F, RanBP2, RanGAP1, CLIP170 and EB1 did not significantly affect Ska1 localisation to KTs (Figure 38F and data not shown). Cold treatment of Hec1-depleted cells did not restore Ska1 to the KT, although it did so in control treated cells (Figure 38B), arguing for a structural effect of Hec1 depletion on the Ska1 docking site(s) rather than an indirect effect through impaired KT-MT interaction (Ciferri *et al.*, 2005; DeLuca *et al.*, 2005). We have explored the possibility that Hec1 might recruit Ska1 to the KT via a direct interaction but failed to detect Hec1 in Ska1 IPs (Figure 38C). Similarly, none of several KT and centromere proteins analysed could be found in Ska1 IPs (Figure 38C). Furthermore, depletion of Ska1 did not affect Hec1 KT localisation (Figure 38D) nor did it displace any of the tested KT and centromere components (Figure 38E and data not shown) arguing that Ska1 is not required for overall KT structure.

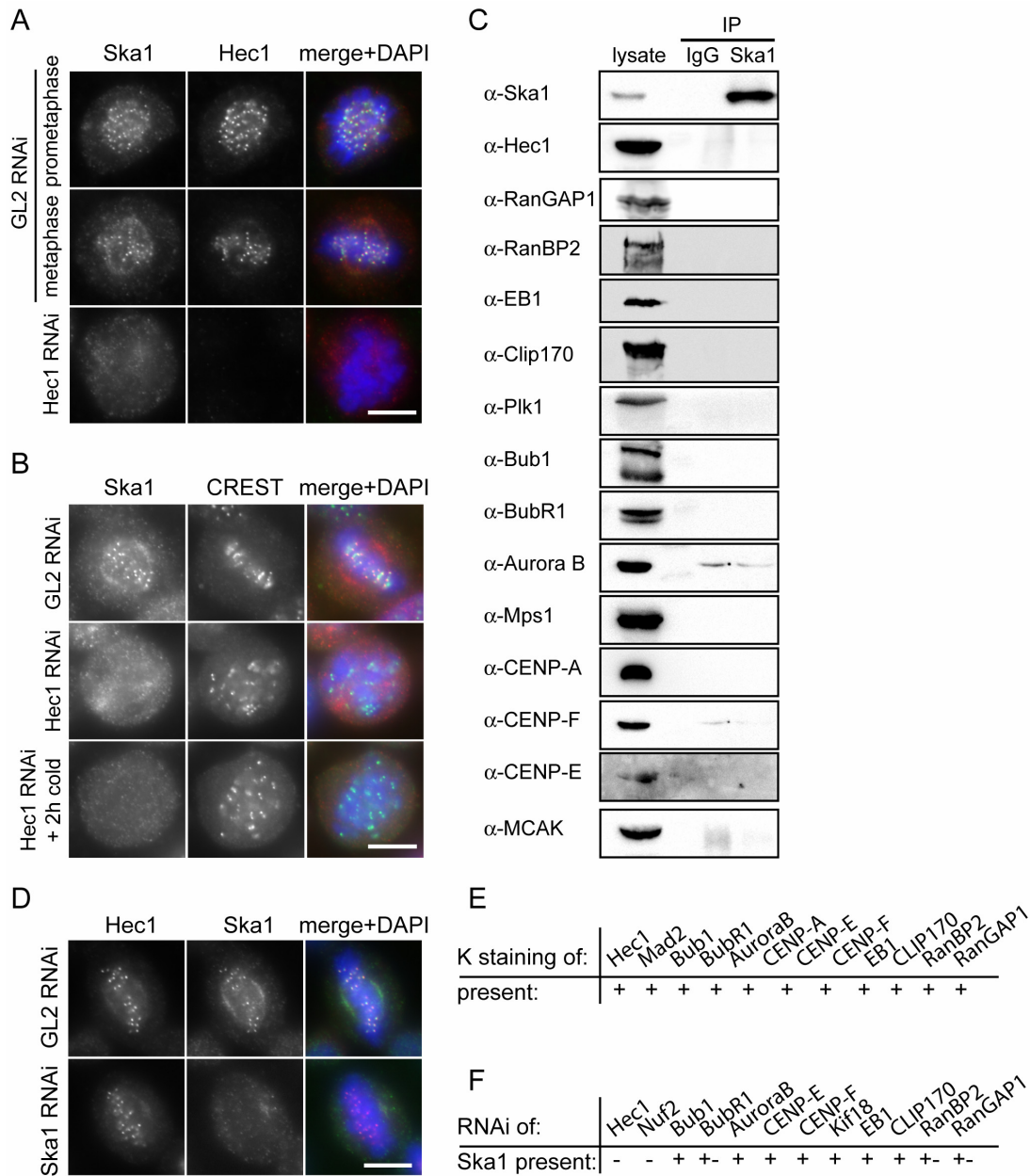


Figure 38 Ska1 KT localisation requires the presence of Hec1 even in cold treated cells but Ska1 presence at the KTs is dispensable for all tested major KT components. A) HeLa S3 cells were treated for 48 hours with control (GL2) and Hec1 specific siRNAs, respectively, then fixed with PTEMF and stained with anti-Ska1 (red), anti-Hec1 (green) and DAPI (DNA, blue). B) HeLa S3 cells were treated for 48 hours with control (GL2) and Hec1 specific siRNAs, respectively, before half the samples were incubated for 2 hours in ice-cold medium. Cells were fixed as in A but stained with anti-Ska1 antibody (red), CREST serum (green) and DAPI (DNA, blue). C) Investigation of potential Ska1 interacting proteins by co-IPs. Mitotic HeLa S3 cell lysates were used for IPs with anti-Ska1 antibody and rabbit IgGs, respectively. The isolated protein complexes were separated by SDS-PAGE, followed by transfer onto nitrocellulose membranes. Membranes were subsequently probed with the indicated antibodies to reveal interactions with Ska1. D) HeLa S3 cells were treated for 48 hours with control (GL2) and Ska1 specific siRNAs, respectively, then fixed with PTEMF and stained with anti-Hec1 (red), anti-Ska1 (green) and DAPI (DNA, blue). Scale bars indicate 10 μm. E) HeLa S3 cells were treated as in D and localisation of key KT components was analysed by IF. Table summarises the observed effects on their respective KT localisation in the absence of Ska1. F) HeLa S3 cell were treated between 48 and 72 hours with specific siRNAs against the indicated KT components and KT localisation of Ska1 was analysed by IF. Table summarises the effects of their respective depletion on Ska1 KT recruitment. +/- indicates reduced but still detectable KT staining of Ska1.

RESULTS II

2.3 Ska1 interacts with Ska2 (FAM33A)

As the above experiments had failed to reveal any binding partners of Ska1, a yeast two-hybrid screen with full length Ska1 as a bait was performed by Anja Wehner. This screen did not yield known KT proteins but resulted in the repeated isolation of cDNAs coding for a 14 kDa protein (Figure 39A), which we now refer to as Ska2 (formerly this hypothetical protein had been designated FAM33A). Database searches revealed the existence of Ska2 homologues in several other vertebrate but not invertebrate species. Considering that Ska1 genes are present in both invertebrates and plants, we assume that the difficulty to detect Ska2 homologues outside of vertebrates most likely reflects small size and absence of known diagnostic motifs.

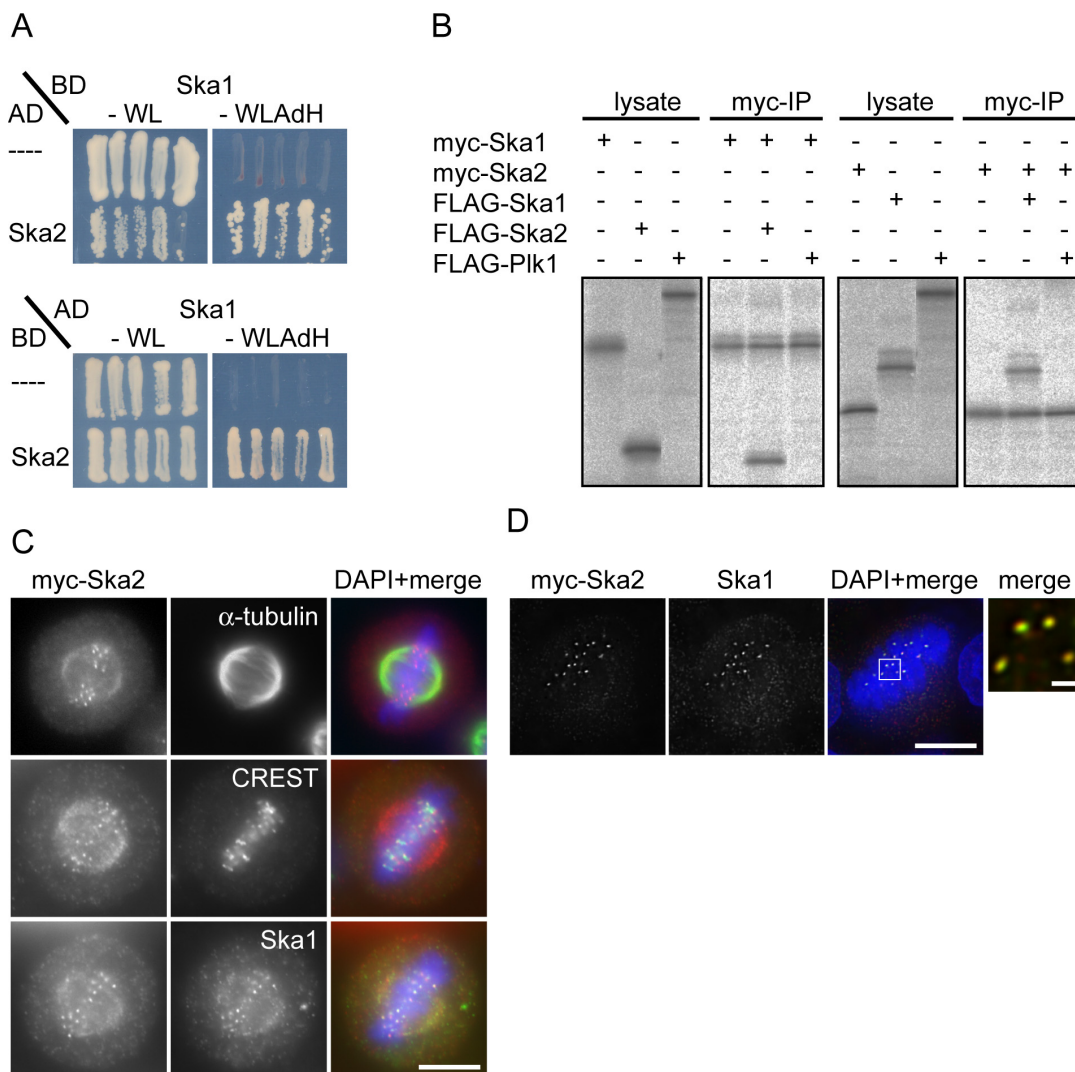


Figure 39 Ska1 interacts with another novel protein termed Ska2 (FAM33A) *in vitro* and both Ska1 and Ska2 co-localise *in vivo*. **A)** Yeast two-hybrid interaction between Ska1 expressed as a binding domain (BD) fusion and Ska2 expressed as an activation domain (AD) fusion (top panel). In the bottom panel Ska1 is expressed from the AD vector and Ska2 from the BD vector. As negative controls, the empty AD or BD (-) vectors were used. Interactions were reflected by growth on selective medium (-WLAdH, right panels). For control, growth on non-selective plates is also shown (-WL, left panels). **B)** Myc- and FLAG-tagged versions of Ska1, Ska2 and Plk1 (negative control) were produced in different combinations by IVT in the presence of ^{35}S -labelled

methionine. Myc-tagged Ska1 (left panels) or Ska2 (right panels) were subsequently IPed and IVT input and myc-IPs were analysed by SDS-PAGE followed by autoradiography. C) Myc-tagged Ska2 was transiently expressed in HeLa S3 cells for 48 hours. After PTEMF fixation cells were stained with anti-myc 9E10 antibody (red), DAPI (DNA, blue) and with either anti- α -tubulin antibody (upper panel), CREST serum (middle panel) or anti-Ska1 antibody (bottom panel) (all in green). D) As in C. After staining with anti-myc 9E10 antibody (red), anti-Ska1 antibody (green) and DAPI (DNA, blue), cells were imaged with a Deltavision microscope. Pictures are single, deconvolved focal planes. Right panel is a magnification of the marked area in the merged picture with scale bar indicating 1 μ m. Other scale bars indicate 10 μ m.

To confirm the interaction between Ska1 and Ska2, tagged versions of the two proteins were produced *in vitro* by coupled transcription-translation (IVT), in the presence of 35 S-methionine, and IPs were performed. Myc-tagged Ska1 and Ska2 readily IPed FLAG-Ska2 and FLAG-Ska1, respectively. In contrast, FLAG-tagged Plk1, used as a negative control, was not co-IPed, attesting to the specificity of the observed interactions (Figure 39B).

Next we analysed the localisation of transiently expressed myc-tagged Ska2 in HeLa S3 cells (Figure 39C). Similar to Ska1, Ska2 showed faint spindle localisation as well as prominent KT localisation. Moreover, myc-Ska2 co-localised exactly with Ska1 (Figure 39C), as confirmed by high-resolution analysis of a single deconvolved Z-stack (Figure 39D). Together these experiments identify Ska2 as a second novel spindle and KT associated protein and as an *in vitro* binding partner of Ska1.

2.4 Ska1 and Ska2 levels are constant throughout the cell cycle

To investigate the properties of endogenous Ska2 a polyclonal antibody was raised in rabbits. Western blot analysis was then used to explore the cell cycle expression of Ska1 and Ska2. As shown in Figure 40A, both Ska1 and Ska2 were present at similar levels in asynchronous, G1/S phase (aphidicolin treated) and mitotic (nocodazole/taxol treated) cells. However, an additional Ska2 band with a slower electrophoretic mobility could be observed in lysates prepared from mitotically arrested cells. As shown below (Figure 41B), this band disappeared upon siRNA-mediated depletion of Ska2, suggesting that it represents a variant or modified form of the protein. Since a retarded electrophoretic mobility often reflects phosphorylation, we examined the sensitivity of the upshifted Ska2 band to phosphatase treatment. No change in Ska2 migration could be observed in response to alkaline phosphatase, type 1 phosphatase or lambda phosphatase, although BubR1 and Cdc27, two mitotic phosphoproteins known to undergo phosphorylation-induced mobility changes (Li *et al.*, 1999; Kraft *et al.*, 2003), readily responded to these treatments (Figure 40B and data not shown). Thus, Ska2 is either phosphorylated on a site that is particularly resistant to phosphatase or, alternatively, subject to another type of modification. Whatever its molecular identity, the variant Ska2 persisted for more than 2 hours after release of nocodazole arrested cells, long after Cyclin B was degraded (Figure 40C). These results show that both Ska1 and Ska2 proteins are expressed at near constant levels throughout the cell cycle but that an as yet unidentified variant of Ska2 is present throughout mitosis.

RESULTS II

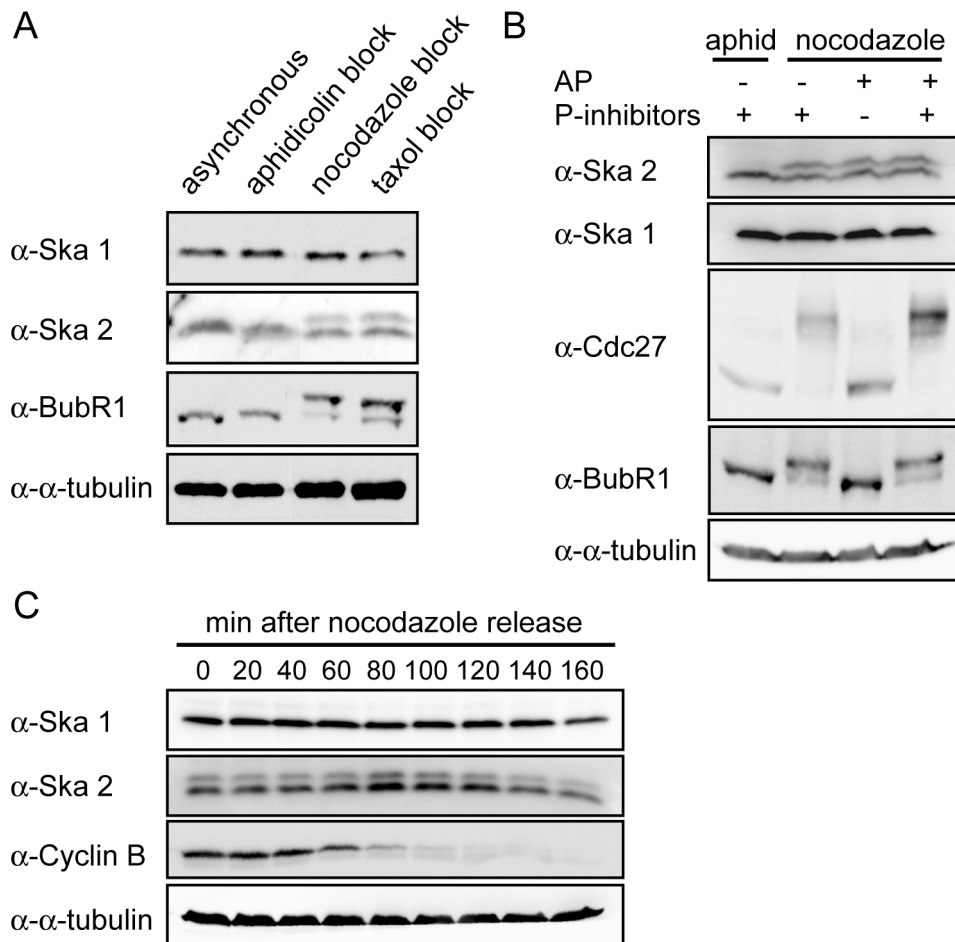


Figure 40 Constant expression of Ska1 and Ska2 throughout the cell cycle and identification of a mitotic Ska2 variant A) Lysates were prepared from asynchronously growing, aphidicolin arrested (G1/S phase), nocodazole arrested shake off (M phase) and taxol arrested shake off (M phase) HeLa S3 cells, respectively. Equal amounts of cell lysates were separated by SDS-PAGE and probed by Western blotting with the indicated antibodies. B) The upshifted Ska2 form is not sensitive to alkaline phosphatase treatment. HeLa S3 lysates from aphidicolin and nocodazole arrested cells, respectively, were either incubated with alkaline phosphatase (AP) or with phosphatase inhibitors (P-inhibitors) for 1 hour at 30°C. Equal amounts of cell lysates were separated by SDS-PAGE and probed after Western blotting with the indicated antibodies. C) HeLa S3 cells were synchronised by a sequential aphidicolin/nocodazole block release protocol. After nocodazole release samples were taken every 20 min. Equal amounts of cell extracts were separated by SDS-PAGE and probed by Western blotting with the indicated antibodies.

2.5 Influence of Ska complex formation on protein stability and localisation

To investigate the interaction of Ska1 and Ska2 *in vivo*, co-IP experiments were performed on lysates prepared from HeLa S3 cells that had been synchronised in M phase by nocodazole treatment, followed by a 40 min release to allow for spindle re-formation (Figure 41A). While neither Ska1 nor Ska2 were precipitated by control IgGs, both forms of Ska2 could readily be detected in anti-Ska1 precipitates and, conversely, anti-Ska2 antibodies brought down Ska1 (Figure 41A), demonstrating the existence of a specific complex *in vivo*. To analyse whether the stability and localisation of Ska1 and/or Ska2 depends on complex formation, we depleted each protein

individually, using specific siRNA oligonucleotides. As shown by Western blotting, Ska1 was efficiently depleted within 48 hours of siRNA treatment (Figure 41B). Interestingly, this resulted in the concomitant disappearance of both forms of Ska2, indicating that Ska2 proteins require Ska1 for stability. Ska2 could also be depleted efficiently, but in this case, the level of Ska1 was not significantly affected (Figure 41B). We also examined the influence of complex formation on the localisation of Ska proteins. When either Ska1 or Ska2 were depleted by siRNA, Ska1 was lost from the spindle and KTs (Figure 41C), indicating that complex formation between the two proteins is required for correct localisation of Ska1. The converse experiment could not be carried out, because the available anti-Ska2 antibody does not perform well in IF experiments. However, since the bulk of Ska2 is degraded upon Ska1 depletion (Figure 41B), one would predict that Ska2 is lost from spindle and KT structures when Ska1 is absent. Taken together, these results establish that Ska2 requires Ska1 for stability while Ska1 requires Ska2 for correct localisation.

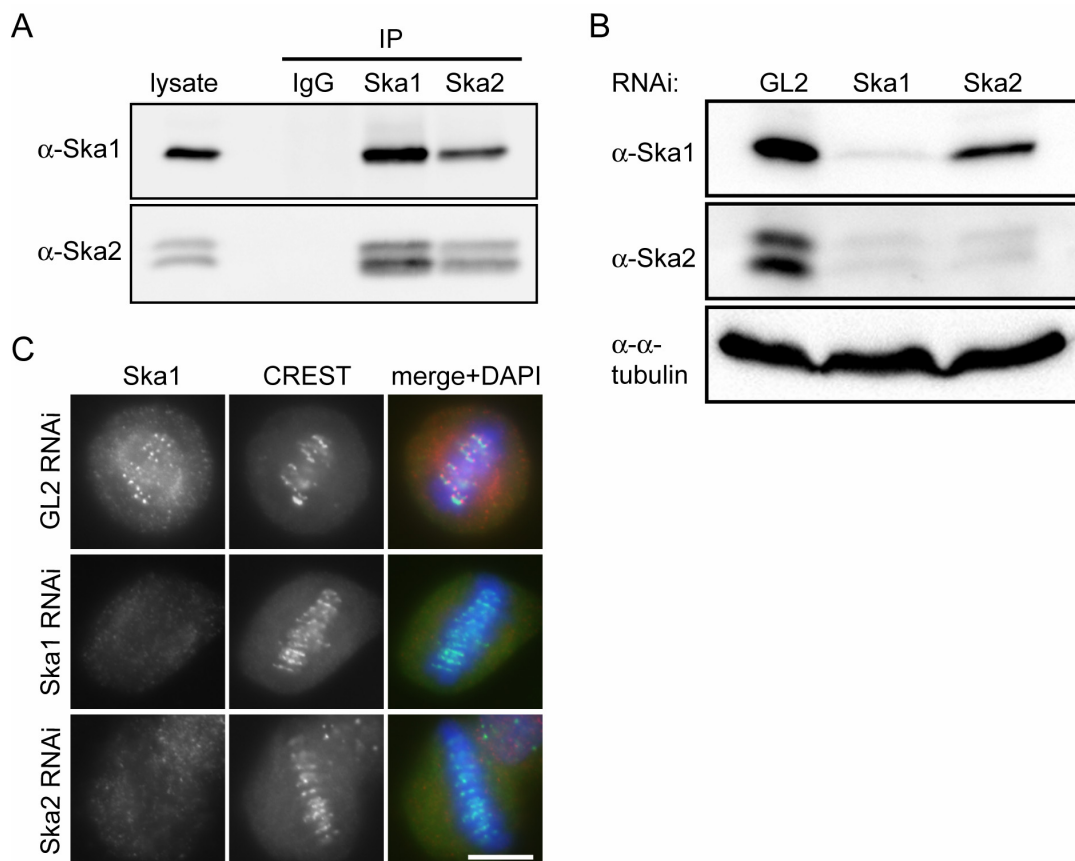


Figure 41 Ska1 and Ska2 in vivo interactions and interdependencies. **A)** Lysates were prepared from mitotic HeLa S3 cells. They were then used for IPs with anti-Ska1 antibody, anti-Ska2 antibody and rabbit IgGs (negative control), respectively. Lysate and immune complexes were separated by SDS-PAGE and probed by Western blotting with anti-Ska1 and anti-Ska2 antibodies, as indicated. **B)** HeLa S3 cells were treated for 48 hours with control (GL2) and Ska1 and Ska2 specific siRNAs, respectively. Equal amounts of cell extracts were separated by SDS-PAGE and probed by Western blotting with anti-Ska1 and anti-Ska2 antibodies. Detection of α -tubulin was used as a loading control. **C)** HeLa S3 cells were treated for 48 hours with control (GL2), Ska1 and Ska2 specific siRNAs, respectively, then fixed with PTEMF and stained with anti-Ska1 antibody (red), CREST serum (green) and DAPI (DNA, blue). Scale bar indicates 10 μ m.

2.6 Ska1 and Ska2 are required for proper mitotic progression

To examine the functional consequence of depleting the Ska complex, HeLa S3 cells were depleted of Ska proteins and then examined by IF microscopy. As described above (Figure 38E), Ska complex is not required for overall KT structure. However, when cells were examined 48 hours after siRNA-mediated depletion of either Ska1 or Ska2, a strong increase in mitotic index could be observed (Figure 42A). Analysis of the resulting mitotic cells by DAPI staining revealed that most of them showed a metaphase-like appearance (Figure 42B), with apparently normal mitotic spindles (Figure 43A, left column). While many disturbances of mitotic progression result primarily in an increased prometaphase population (Biggins *et al.*, 2003), we were surprised to find that 60 % of all pre-anaphase cells showed chromosomes aligned in a near-perfect metaphase plate. This strongly indicates that depletion of the Ska complex did not primarily impair chromosome congression but instead caused cells to arrest or delay in a metaphase-like state. To investigate this unusual mitotic phenotype in more detail, time-lapse video microscopy was performed on HeLa S3 cells that stably express a histone H2B-GFP fusion protein (Figure 42C). These experiments confirmed that mitotic progression was strongly delayed in Ska-depleted cells and that most of the delay occurred in a metaphase-like state. Eventually, however, cells were able to progress through mitosis (Figure 42C).

Quantification of the above data showed that control (GL2) depleted cells proceeded from prophase to anaphase onset in 47 ± 9.7 minutes. In Ska1- and Ska2-depleted cells this period was highly variable but, on average, took about four times longer (179 ± 141 and 174 ± 120 minutes, respectively). Most remarkably, most Ska1- and Ska2-depleted cells (57% and 67%, respectively), as well as all (GL2 treated) controls, completed alignment of chromosomes in a metaphase plate within 60 min after onset of chromosome condensation (Figure 42D, left histogram). This indicates that although a defect in chromosome congression contributed to the lengthening of mitotic progression, it did not constitute the primary reason for the strong delay seen in most Ska-depleted cells. Instead, the clearest difference between control cells and Ska-depleted cells was that almost all control cells initiated anaphase within 20 min of metaphase plate formation (average of 14 min), whereas Ska1- and Ska2-depleted cells spent highly variable amounts of time at this metaphase-like state, requiring an average of 76 min and 100 min, respectively, for progressing to anaphase onset (Figure 42D, right histogram). Moreover, about 60 % of the delayed Ska-depleted cells were unable to keep all chromosomes fully aligned in a metaphase plate, so that, occasionally, individual chromosomes moved out of the plate and back in (Figure 42C).

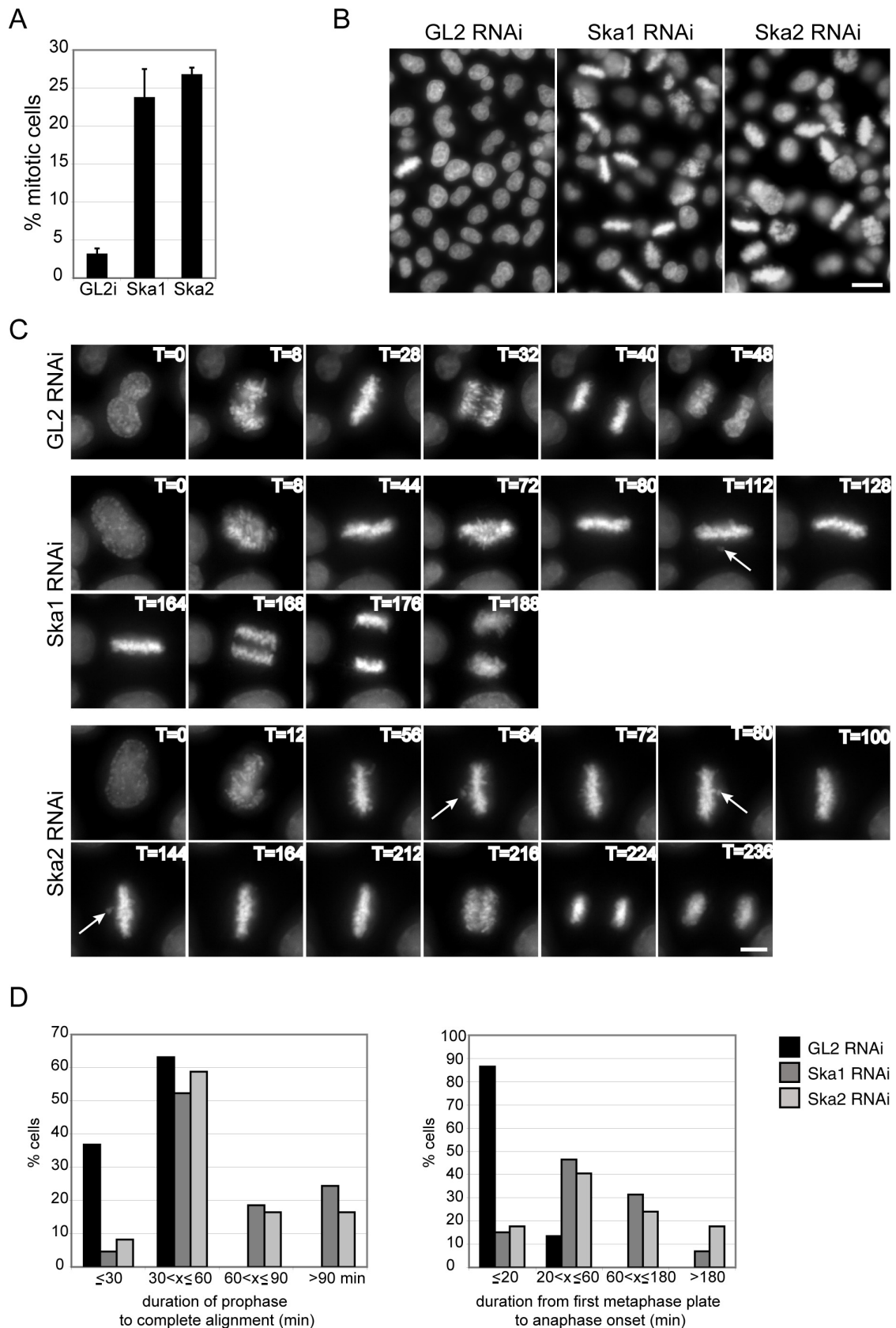


Figure 42 Depletion of Ska1 and Ska2 results in a metaphase delay. A) HeLa S3 cells were treated for 48 hours with control (GL2), or Ska1 and Ska2 specific siRNAs, respectively. The mitotic indexes were determined by light microscopy. B) The same cells as in A were fixed and stained with DAPI (DNA). Scale bar indicates 20 μ m. C) Live-cell imaging of H2B-GFP expressing HeLa S3 cells. Selected images show H2B-

RESULTS II

GFP stained chromosomes of HeLa S3 cells progressing through mitosis. Cells were treated with GL2 (control), or Ska1 and Ska2 specific siRNAs, respectively, for 30 hours before filming. T = 0 was defined as the time point at which chromosome condensation became evident (prophase). Time points are indicated in minutes. Arrows point to chromosomes that have transiently moved out of the metaphase plate. Scale bar indicates 10 μm . D) The durations of different periods from prophase to anaphase onset were calculated from time-lapse movies (C) of at least 37 control (GL2), and at least 76 Ska1 and Ska2 siRNA treated cells. T=0 was defined as in C. Complete alignment was defined as the duration from T=0 to the first time point at which a perfect metaphase plate was observed and anaphase onset was calculated from the first frame at which chromosome segregation was visible. Histograms show the percentages of mitotic cells that had progressed within the indicated time frames from prophase to the first complete metaphase plate (left panel) and from first metaphase plate to anaphase onset (right panel).

2.7 Role of Ska complex in stabilisation of KT-MT interaction and SAC silencing

To further characterise the molecular mechanism underlying the Ska depletion phenotype, Ska-depleted cells were challenged by short exposure to low temperature in order to test the stability of K-fibres (Rieder, 1981). When compared to control cells and Nuf2-depleted cells - which are known to be impaired in KT-MT attachment (DeLuca *et al.*, 2002) - the K-fibres of Ska-depleted cells showed an intermediate cold-sensitivity (Figure 43A). This result suggests that K-fibres, although functional, were weakened, in keeping with the observation that a majority of Ska-depleted cells was able to accomplish near-normal chromosome congression (Figure 42D, left histogram), but then failed to maintain a metaphase plate (Figure 42C). One straightforward interpretation of these results is that a transient impairment of K-fibre stability caused the occasional loss of KT-MT interaction, allowing individual chromosomes to escape from the metaphase plate. Consistent with this view, most of the metaphase plates present in Ska-depleted cells contained at least one or two Mad2-positive KTs (85% for Ska1-depleted, 87% for Ska2-depleted metaphase cells, s.d. ≤ 2) (Figure 43B). As the KT association of Mad2 usually (albeit not invariably; (Martin-Lluesma *et al.*, 2002)) correlates with an active SAC, this observation indicates that Ska-depleted cells failed to turn off the SAC. Indeed, the mitotic delay induced by Ska depletion could readily be overcome by co-depletion of Mad2, demonstrating its dependency on the SAC (Figure 43C). Furthermore, although inter-KT distances were normal amongst the aligned chromosomes in Ska1- and Ska2-depleted cells ($1,60 \pm 0,3 \mu\text{m}$ and $1,63 \pm 0,3 \mu\text{m}$, respectively, $n = 19$ cells/total 189 KTs, as compared to $1,59 \pm 0,3 \mu\text{m}$ in control cells, $n = 20$ cells/total 235 KTs), the rare 'escaper' chromosomes showed inter-KT distances similar to those seen in nocodazole arrested cells ($0,83 \pm 0,2 \mu\text{m}$, $n = 16$ cells/total 189 KTs), suggesting a reduction in tension only at the rare chromosomes that had been lost from the metaphase plate.

Taken together, these results lead us to propose that the Ska complex is required primarily for the maintenance (rather than the establishment) of a metaphase plate and/or the silencing of the SAC.

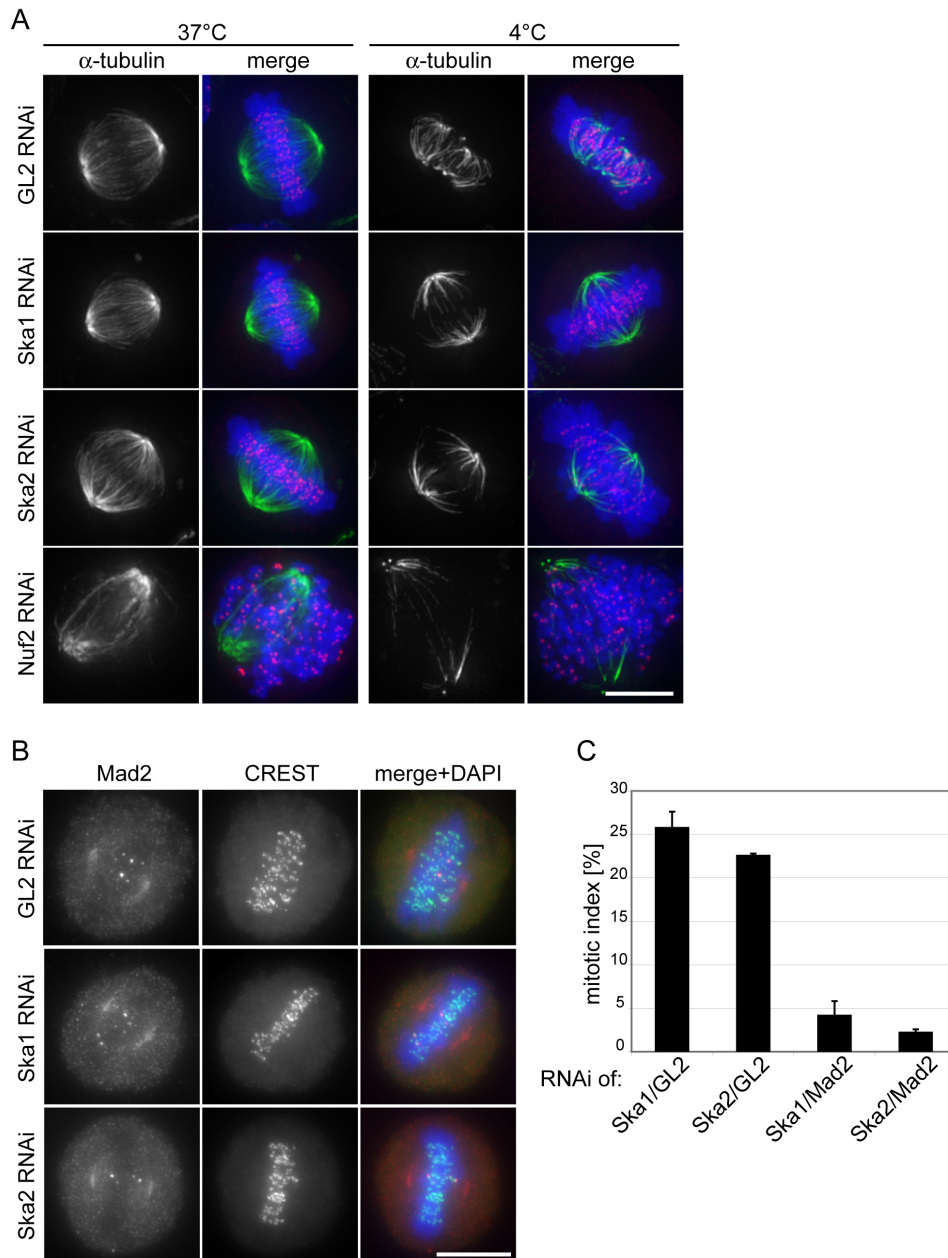


Figure 43 Characterisation of Ska depletion phenotype. **A)** HeLa S3 cells were treated for 48 hours with control (GL2), Ska1, Ska2 and Nuf2 specific siRNAs, respectively. They were fixed directly (left column, 37°C) or after incubation for 10 min at 4°C (right column, 4°C) before staining with anti- α -tubulin antibody (green), CREST serum (red) and DAPI (DNA, blue). **B)** HeLa S3 cells were treated for 48 hours with control (GL2), or Ska1 and Ska2 specific siRNAs, respectively, then fixed with PTEMF and stained with anti-Mad2 antibody (red), CREST serum (green) and DAPI (DNA, blue). Scale bars indicate 10 μ m. **C)** Quantification of the mitotic indices (300 cells each) after 48 hours of Ska1 and Ska2 RNAi together with control GL2 RNAi or after simultaneous depletion of Mad2.

DISCUSSION II

The mitotic spindle is a highly organised complex structure. Knowing its composition is crucial for understanding the dynamics of assembly and chromosome movements. Therefore a MS based inventory of the human mitotic spindle, isolated from HeLa S3 cells, was conducted. Several so far uncharacterised genes were cloned and their spindle localisation examined by transient transfections and IF microscopy (Sauer *et al.*, 2005) (Figure 32). In the course of our examination and validation process some of the newly identified spindle proteins, e. g. Spc24, have soon thereafter been published by other groups (McClelland *et al.*, 2004; Bharadwaj *et al.*, 2004), whereas the initial description of HURP was accomplished in our department (Sillje *et al.*, 2006).

Herein, the characterisation of Ska1, a novel spindle and KT associated protein, is described, which was originally identified as a candidate spindle component in the spindle inventory screen (Sauer *et al.*, 2005). Furthermore, we identified a second novel protein, termed Ska2 that interacts with Ska1 both *in vitro* and *in vivo*. Complex formation between the two proteins is required for Ska2 stability as well as Ska protein localisation to spindle MTs and KTs. During prometaphase, the Ska complex associates with KTs only after MT attachment, suggesting that this complex is not required for KT-MT interactions *per se*. Depletion studies by siRNA showed that the absence of the Ska complex did not overtly affect general KT structure. Furthermore, although increased cold-sensitivity suggests a weakening of K-fibres, initial chromosome congression was only modestly impaired. Instead, depletion of the Ska complex caused cells to spend prolonged periods of time in a metaphase-like state characterised by occasional loss of individual chromosomes and a persistent activation of the SAC. Taken together, our data indicate that the Ska complex is required for the maintenance of chromosomes in a fully aligned metaphase plate and for SAC silencing.

At physiological temperature, Ska1 localisation to KTs requires KT-MT attachments since it accumulates at the KTs during prometaphase (Figure 34B) and is lost from the KTs as soon as MTs are depolymerised by drug treatment (Figure 35A). Therefore one could argue that Ska1 might rather constitute a MT (+) TIP protein than a *bona fide* KT component. EB1 and APC are (+) TIPs whose KT localisation depends on the presence of MTs. But compared to the comet-like EB1 staining of all growing MT plus-ends of the spindle array, Ska1 was detected only at dot-like structures adjacent to chromosomes (data not shown and Figure 34B, C). Furthermore, no specific staining of MTs by the Ska1 antibody was observed in interphase cells in contrast to the strong EB1 MT plus-end staining (Figure 34D and data not shown). In addition to their apparently distinct staining patterns, Ska1 recruitment to the dot-like structures failed if cells were defective in KT-MT attachments caused by Hec1 depletion, whereas EB1 staining of the plus-ends was unaffected (Figure 38A and data not shown). Thus, we conclude that instead of localising to the MT plus-ends, Ska1 is a KT component whose localisation requires MT attachment.

When Ska1 localisation was followed in cells released from nocodazole, it was first seen at the poles and subsequently, as the spindle reformed, it became more and more evident at the KTs

(Figure 35C). This redistribution could be the consequence of an active motor-dependent transport from the poles to the KTs along MTs. Obvious candidates were plus-end directed motors like CENP-E, Kif18, Eg5 and MCAK. But RNAi of none of these proteins impaired Ska1 KT localisation. Moreover, we found to our surprise that Ska1 strongly concentrated on KTs in cells whose MTs were depolymerised by cold treatment and that Ska1 KT localisation could even be rescued in these cells by low temperature in the continued presence of nocodazole (Figure 36A, B). Importantly, RanGAP1 and RanBP2 KT localisation, which was shown to be MT-dependent (Joseph *et al.*, 2004), was not restored by cold-treatment in the absence of MTs (Figure 36D). Apart from this observation being the final proof that Ska1 is indeed a *bona fide* KT protein, it further revealed that Ska1 KT localisation does not require motor-mediated transport along MTs. Together these data suggest that Ska1 binding to KTs depends on docking sites that, at physiological temperature, are created by MT attachment but that can also be generated when cells are incubated in the cold, in the absence of MTs.

One explanation for the unexpected Ska1 KT localisation in the cold is that docking sites are generated by a shift in the balance of opposing enzymatic activities e. g. a disturbance of kinase/phosphatase equilibria. Depending on which of the opposing activities was more sensitive to low temperature, cold treatment would generate a hypo- or hyperphosphorylated docking protein that is eventually more potent in recruiting Ska proteins. If this hypothesis was correct, Ska1 KT localisation in cold and nocodazole treated cells, respectively, should change in one of these conditions upon inhibition of kinases or phosphatases. But neither NaF (phosphatase inhibitor) nor staurosporine (kinase inhibitor) treatment turned out to alter Ska1 localisation under these circumstances (Figure 37A, B).

Alternatively, it is possible that Ska proteins turn over constitutively at KTs and that their release requires an energy-dependent enzymatic activity, which is blocked by MT attachment (at physiological temperature) or cold treatment. In this context the specific inhibition of the centromere associated kinase Aurora-B, which is known to resolve improper attachment, appeared most attractive. But again Ska1 KT localisation could not be rescued in nocodazole treated cells when Aurora-B activity was inhibited (Figure 37C). Although established concentrations and incubation times for the different inhibitors were applied, we can not rule out that inhibition of the respective targets was not efficient enough. Still these results render the idea less likely that cold induced imbalances of the kinase/phosphatase equilibrium could cause Ska1 KT targeting.

Regardless of the molecular nature of the Ska docking sites, it is striking that Ska proteins and Mad2 display opposite requirements for KT localisation under all conditions examined. At physiological temperature, Ska docking sites are generated in response to MT attachment, while, concomitantly, Mad2 is lost from KTs. Conversely, nocodazole treatment abolishes Ska localisation to KTs but causes the recruitment of Mad2, and finally, cold treatment restores Ska docking sites even in the absence of MTs, while inducing the loss of Mad2 (Figure 36B, E). Considering the striking correlation between the creation of Ska binding sites and the loss of Mad2 from KTs, the question arises of whether the recruitment of the Ska complex directly contributes to the release of Mad2 from KTs or *vice-versa*, by either directly competing for the same binding site at the KT-MT

DISCUSSION II

attachment spot or by sterically preventing each other's further localisation. However, the observation that Mad2 was absent from the KTs of most aligned chromosomes in Ska-depleted cells argues against a direct, active role of the Ska complex in Mad2 displacement (Figure 43B). Conversely, when cells were depleted of Mad2, Ska1 was still detected at the KTs, and the absence of Mad2 did not enable Ska1 KT recruitment in the absence of MTs (Figure 36F). Instead, a particular structural change produced at KTs upon MT attachment (or cold treatment in the absence of MTs) may cause both Ska recruitment and Mad2 displacement. However, Ska1 might become an interesting marker for the presence of KT-MT attachments in the future, similar to Mad2 whose staining reveals insufficiently unattached KTs.

As indicated by comparative sequence analyses, homologues of Ska1 are present in the genomes of vertebrates and invertebrates as well as plants. Ska2 genes could be identified with confidence only in vertebrates, but considering the functional interaction between Ska1 and Ska2, we presume that Ska2 genes are also present in invertebrates and plants, although they are impossible to detect by current search algorithms. Neither Ska1 nor Ska2 homologues could be identified in yeast but, again, this does not necessarily imply that functional homologues are truly absent. In recent years, it has become increasingly apparent that yeast and vertebrate KTs share many more components than had previously been appreciated (Meraldi *et al.*, 2006). One notable exception to this conclusion concerns the yeast Dash/Dam1 complex, comprising 10 different small subunits, for which no counterpart has yet been identified in mammals (Cheeseman *et al.*, 2001; Miranda *et al.*, 2005; Westermann *et al.*, 2005). It is intriguing, therefore, that several of the properties of the Ska complex described here are reminiscent of results described for the yeast Dash/Dam1 complex. Specifically, the Dash/Dam1 complex of *Saccharomyces cerevisiae* has been shown to localise to spindle MTs and KTs (Hofmann *et al.*, 1998; Cheeseman *et al.*, 2001) and to require both an intact Ndc80 complex (the yeast homologue of the human Hec1 complex) and MTs for KT localisation (Janke *et al.*, 2002). Moreover, this budding yeast complex is known to contribute to the stabilisation of KT-MT interactions (Cheeseman *et al.*, 2001; Miranda *et al.*, 2005). Interestingly, the Dash/Dam1 complex is essential for viability in *S. cerevisiae* (Hofmann *et al.*, 1998) but not in *Schizosaccharomyces pombe* (Sanchez-Perez *et al.*, 2005). Instead, mutations in *S. pombe* Dash/Dam1 proteins result in a delayed anaphase onset and persistent SAC activation (Sanchez-Perez *et al.*, 2005), similar to the Ska1 and Ska2 depletion phenotype described here. Thus, in spite of the absence of obvious sequence similarity between Ska1, Ska2 and any of the Dash/Dam1 complex components, it is possible that the human Ska complex and the yeast Dash/Dam1 complex perform at least partially similar roles. One interesting question for the future is whether Ska proteins are able to form ring structures around MTs, as described for the Dash/Dam1 complex (Miranda *et al.*, 2005; Westermann *et al.*, 2005).

Depletion of human Ska proteins did not affect the localisation of any other KT protein examined so far, arguing that the Ska complex is not required for overall KT structure. Moreover, the mitotic spindle appeared to form normally in Ska-depleted cells and although K-fibres were weakened (Figure 43A), chromosome congression was not fundamentally impaired in a majority of cells (Figure 42C, D). However, it would be premature to exclude that a complete (genetic) knock-

out of Ska1 and Ska2 might reveal a more severe phenotype. The most striking consequence of siRNA-mediated depletion of Ska proteins was a delayed anaphase onset preceded by a prolonged metaphase-like state. This unusual phenotype was characterised by individual chromosomes occasionally moving out of (and back into) the metaphase plate (Figure 42C), rare KTMs staining positive for Mad2 and persistent SAC activation (Figure 43B, C). On the basis of these results we propose that the Ska complex is required for stabilising KT-MT attachments and/or SAC silencing.

In line with this a model is conceivable in which the Ska complex is recruited to KTMs as soon as they are attached to MTs, probably enabled by certain favourable structural changes of the KT surface, and then clamps down on these MTs to stabilise and maintain the attachments (Figure 44).

In principle, the failure of Ska-depleted cells to silence the SAC could be a consequence of an occasional destabilisation of KT-MT interactions at individual chromosomes. Alternatively, Ska-depleted cells could primarily be impaired in switching off the SAC, in which case the occasional loss of individual chromosomes from the metaphase plate could be a consequence of the extended metaphase delay. In particular, it is tempting to speculate that the Ska complex could contribute to functionally down-regulate some of the KT associated proteins that are responsible for relaying the inhibitory SAC signal (e. g. one or several of the SAC kinases). Thus, we anticipate that the discovery of the vertebrate Ska complex will prompt new lines of enquiry into the coupling of MT attachment to the KT and SAC silencing.

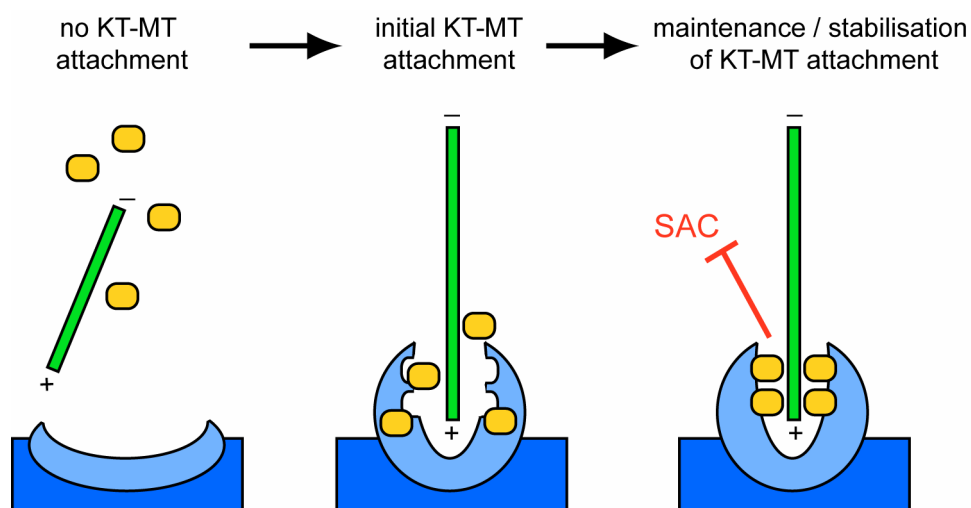


Figure 44 Model of Ska complex targeting and action at the KT. A) As long as the MT (green bar) is not attached to the MT binding site (light blue) at the KT (dark blue), Ska complexes (yellow boxes) localise to the spindle poles. B) MT attachment to its binding site at the KT induces a structural change of the KT surface creating Ska docking sites at the KT. C) Ska complexes maintain KT-MT attachments by clamping down to the MT and anchoring it. Furthermore, they promote SAC silencing.

SUMMARY II

Chromosome segregation during mitosis requires that each chromosome undergoes bipolar attachment on spindle MTs and subsequent silencing of the SAC.

Originally identified in a spindle inventory, we characterised of a novel spindle and KT associated complex that is required for timely anaphase onset. The complex comprises at least two proteins, termed Ska1 and Ska2. Ska1 associates with KTs following MT attachment during prometaphase. Ska1 and Ska2 interact with each other and Ska1 is required for Ska2 stability *in vivo*. Depletion, by siRNA, of either Ska1 or Ska2 results in the loss of both proteins from the KT. The absence of Ska proteins does not disrupt overall KT structure but K-fibres show an increased cold-sensitivity. Most strikingly, Ska-depleted cells undergo a prolonged SAC-dependent delay in a metaphase-like state. This delay is characterised by the recruitment of Mad2 protein to a few KTs and the occasional loss of individual chromosomes from the metaphase plate. These data suggest that the Ska1/2 complex plays a critical role in the maintenance of the metaphase plate and/or SAC silencing.

MATERIALS AND METHODS

1 Cloning procedures

All cloning procedures were performed according to standard techniques as described in Molecular Cloning, A Laboratory Manual, 2nd edition, Sambrook, J., Fritsch, E.F., Maniatis, T., Cold Spring Harbor Laboratory Press, 1989 and Current Protocols in Molecular Biology, Wiley, 1999. Restriction enzyme reactions were carried out as specified by the suppliers (NEB, Ipswich, MA) and ligation reactions were done using T4 DNA Ligase (Roche Diagnostics, Indianapolis, IN) or a Rapid Ligation Kit (Roche). Extraction of DNA from agarose gels and preparation of plasmid DNA were performed using kits from Qiagen according to the manufacturer's instructions. For PCR reactions, Pfu DNA polymerase was used as recommended by the manufacturer (Stratagene) and reactions were carried out in a RoboCycler Gradient 96 (Stratagene, La Jolla, CA). PCR products were checked by sequencing at Medigenomix (Martinsried, Germany) or by an inhouse sequencing service.

Plk1 PBD^{WT} (aa 326-603) was cloned in-frame by PCR into either a pGEX-6P-3 vector encoding an N-terminal GST-tag (Amersham Biosciences, Buckinghamshire, UK) or in a pcDNA3.1 vector encoding a N-terminal 3xmyc-tag (Invitrogen, Carlsbad, CA) using primers 5'-CCG GAA TTC CAG ATC TTC GAT TGC TCC CAG CAG CCT GG-3' and 5'-CCG CTC GAG TTA GGA GGC CTT GAG ACG GTT GC-3'. The myc-tagged Plk2-PBD (aa 355-685) and Plk3-PBD (aa 336-646) constructs were PCR cloned in the same vector with the primers 5'-GGC GGA TCC CAC TTA TCA AGC CCA GCT AAG-3' and 5'-GGC CTC GAG TCA GTT ACA TCT TTG TAA GAG C-3' for PBD 2 and 5'-GGC GGA TCC CCC CCC AAC CCA GCT AGG AGT C-3' and 5'-GGC CTC GAG CTA GGC TGG GCT GCG GTC CCG G-3' for PBD3. The Plk1 PBD^{AA} mutant (H538A, K540A) was made by site-directed mutagenesis using the following primers: 5'-CAA CTT CTT CCA GGA TGC CAC CGC CCT CAT CTT GTG CCC-3' and 5'-GGG CAC AAG ATG AGG GCG GTG GCA TCC TGG AAG AAG TTG-3'. For generating stable inducible cell lines, myc-tagged Plk1 PBD^{WT} and Plk1 PBD^{AA} gene fragments were cloned into a pcDNA4/TO vector (Invitrogen), in which the neomycin resistance marker had been replaced by a puromycin resistance cassette. Full length Plk1 constructs carrying different mutations were generated by PCR on existing plasmids encoding Plk1^{WT}, Plk1^{K82R} (catalytically inactive), Plk1^{T210D} (hyperactive kinase) using the primers 5'-CCC GAA TTC ATG AGT GCT GCA GTG ACT GCA GGG AAG C-3' and 5'-GAG GCG GCC GCT TAG GAG GCC TTG AGA CGG TTG CTG GCC-3' (generating EcoRI-NotI cloning sites) and cloned into the pcDNA3.1/3xmyc-C vector. For the generation of full length myc-Plk1^{AA} the above mentioned site-directed mutagenesis primers were used. The plasmid encoding the Plk1 catalytic domain (aa 1-352) was generated by inserting the EcoRI-SmaI fragment of full length Plk1 in an EcoRI-EcoRV digested pcDNA3.1/3xmyc-C vector. For rescue experiments an established Plk1 RNAi targeting sequence (Kraft *et al.*, 2003) was cloned into the pTER+ vector (Brummelkamp *et al.*, 2002;van de

MATERIALS AND METHODS

et al., 2003). RNAi resistant myc-tagged Plk1 constructs in the pcDNA3.1/3xmyc-C vector were generated by introducing 6 silent point mutations in the RNAi targeting sequence using primers 5'-CCC GAA TTC ATG AGT GCT GCA GTG ACT GCA GGG AAG C-3' and 5'-GAG GC GGC CGC TTA GGA GGC CTT GAG ACG GTT GCT GGC C-3'.

The cDNA clone IRALp962P1315Q (obtained from "Deutsches Ressourcenzentrum für Genomforschung", RZPD) was used as a template to PCR-clone Cdc20 using the primers 5'-GGC GGA TCC ATG GCA CAG TTC GCG TTC GAG AGT G-3' and 5'-GCC CTC GAG TCA GCG GAT GCC TTG GTG GAT GAG G-3' (generating BamHI-XhoI cloning sites). The PCR product was cloned into a pcDNA3.1 vector encoding a N-terminal FLAG tag or in pcDNA4/TO/myc-HisC for a C-terminal FLAG-tag. Site-directed mutagenesis primers used to introduce a S161A amino acid change in the protein sequence were 5'-GGC CAC TCC TGG CTC CGC CCG GAA GAC CTG CCG-3' and 5'-CGG CAG GTC TTC CGG GCG GAG CCA GGA GTG GCC-3'.

CDNA clones encoding for the potential spindle proteins KIAA1187, FLJ90806 (IMAGp958K072621Q2, now Spc24) and C18Orf24 (IMAGp998H169724Q, now Ska1) were obtained from the RZPD. PCR was performed on the KIAA1187 cDNA clone with primers 5'-GCC GGA TCC ATG GAG AGC GGC CCG CGT GCG GAG C-3' and 5'-GCC TCT AGA TTA AAG GAC TTC TGT GAC CTG CGG GGA C-3' (generating BamHI-XbaI cloning sites), on the FLJ90806 cDNA clone with primers 5'-GCC GGA TCC ATG GCC GCC TTC CGC GAC ATA GAG G-3' and 5'-GCC CTC GAG CTA CCA CTC GGT GTC CAC CAG ACT C-3' (generating BamHI-XhoI cloning sites) and on the C18Orf24 cDNA clone with primers 5'-CCG GGA TCC GCC ATG GCC TCG TCA GAT CTG GAA C-3' and 5'-GCC CTC GAG TCA GGT TAT AAC ATA ACG AGT AAG-3' (generating BamHI-XhoI cloning sites). These products were cloned in-frame into a pcDNA3.1 vector encoding either an N-terminal 3xmyc-tag or a FLAG tag.

The FAM33a pAct2 yeast two hybrid clone was used as a template for PCR based cloning of Ska2 using the primers 5'-GGC GGA TCC GCC ATG GAG GCG GAG GTC GAT AAG C-3' and 5'-GGC CTC GAG TCA TAA ATC TGG CAT GTG AAA TTT GAA TTG-3'. The PCR product was digested with BamHI-XhoI and inserted into either the 3xmyc-tag or FLAG tag pcDNA3.1 vector.

2 Expression and purification of recombinant protein

For production of recombinant GST-tagged PBD^{WT} and PBD^{AA} (aa 326-603) the respective plasmids were transformed into *Escherichia coli* XL1-blue, grown over night under ampicillin selection and diluted 1:5 with fresh medium the next morning. The culture was grown further until an OD₆₀₀ of 0,5-0,8 (late log-phase), when expression of the recombinant protein was induced with 0,4 mM IPTG at 37°C for 3,5 hours. Cells were then pelleted by centrifugation and lysed in buffer (10 mM Tris, pH 8,0, 150 mM NaCl, 1 mM EDTA, 0,05 % NP40, 1 mM DTT, 1 mg/ml lysozyme and protease inhibitors). GST-PBD proteins were isolated using glutathione sepharose 4B beads (Amersham Biosciences) and either directly used for the phosphopeptide binding assay or eluted from the beads by incubation in elution buffer (1 mM glutathione, 20 mM Tris-HCl, pH 7,4, 10 %

glycerol, 1 mM DTT) for Far Western analysis and if used for GST-PBD pull downs, covalently recoupled to Affi-Gel 15 beads with 3 µg protein/µl beads (Bio Rad, Hercules, CA).

3 Antibody Production

In order to produce Ska1 and Ska2 specific antibodies, the polyhistidine-tagged proteins were separately expressed in *E. coli* from pET-28 vectors (EMD Biosciences, Madison, WI) and purified under denaturing conditions over a Ni²⁺-NTA column (Qiagen). Following further purification on a preparative 15 % SDS-PAGE gel, 250 µg of the Ska1 and the Ska2 protein, respectively, were injected several times into New Zealand white rabbits (Charles River Laboratories, Romans, France). The obtained sera were affinity purified using the AminoLink Plus Immobilization Kit (Pierce Biotechnology, Rockford, IL), which were coated with the respective antigens according to the manufacturer's protocol.

4 Cell culture, synchronisation, drug concentrations and cold treatment on living cells

HeLa S3, HEK293 and HEK293T cells were grown at 37°C under 5 % CO₂ in DMEM (Invitrogen), supplemented with 10 % FCS and penicillin-streptomycin (100 IU/ml and 100 µg/ml, respectively). To prepare HeLa S3 cells for a nocodazole release experiment, exponentially growing cells were first pre-synchronised at the G1/S phase boundary by treatment with 1.6 µg/ml aphidicolin for 14 hours. Subsequently these cells were released for 6 hours in fresh prewarmed medium, before 50 ng/ml nocodazole was added and culturing was continued for additional 6 hours. Mitotic cells were collected by mitotic shake off, washed twice with PBS and incubated in fresh prewarmed medium. Cell samples were taken after release for various time intervals. In order to block HeLa S3 cells efficiently in mitosis without subsequent release final concentrations of 150-500 ng/ml nocodazole (250 ng/ml for HEK293 or HEK293T), 10 µM colchicin (MT depolymerisation drug), 10 µM taxol (MT stabilisation drug), 200 µM monastrol and 25 µM noscaphine were added to the medium for 14 hours, respectively. In order to block enzymatic activities, cells were incubated for 30 min with 1 mM NaF (phosphatase inhibitor), 45 min with 250 nM staurosporine (kinase inhibitor) and 1 hour with 10 µM ZM44743 (Aurora-B kinase inhibitor), respectively.

In order to depolymerise preferably unattached MTs in mitotic HeLa S3 cells, medium was replaced by ice-cold medium, followed by additionally placing the dishes in a closed box filled with ice. Cells were incubated therein at 4°C for 10 min before fixation. For complete depolymerisation of virtually all mitotic MTs HeLa S3 cells were incubated under the same conditions for 2 hours.

5 Generation of myc-PBD stable inducible HeLa S3 cell lines

For the generation of tetracycline-inducible cell lines the pcDNA/4TO plasmids encoding myc-tagged Plk1 PBD^{WT} and Plk1 PBD^{AA}, respectively, were transfected into a HeLa S3 cell line, which stably expressed a tet repressor gene under control of the CMV promoter (HeLa S3-TREx), together with a blasticidine resistance marker (pcDNA6/TR, Invitrogen). Stably transfected cell lines were established by selection with 5 µg/ml blasticidin and 1 µg/ml puromycin starting 24 hours after transfection and continuing for 10 days after which colonies were picked and tested for the expression of myc-PBD^{WT} and myc-PBD^{AA} by IF and Western blot analysis. Expression was induced by addition of 0.1 µg/ml tetracycline for 8 hours or 24 hours, respectively.

6 Transient transfections and RNAi

Plasmid transfections in HeLa S3 cells were performed using Fugene6 reagent (Roche). For cells covered with 2 ml medium 100 µl OptiMEM I (Invitrogen), 4 µl Fugene6 and 1,5 µg plasmid DNA were used. Transfection of HEK293(T) cells was accomplished by the calcium phosphate precipitates as described elsewhere (Seelos, 1997). Cells expressing the myc-Ska1 and myc-Ska2 constructs, respectively, were fixed 48 hours after transfection, whereas for all other transfections cells were usually treated for only 24 hours.

SiRNA duplexes were transfected using Oligofectamine (Invitrogen) (Elbashir *et al.*, 2001). For cells covered with 2 ml medium 3 µl Oligofectamine and 3 µl 20µM annealed siRNA duplexes were used. The sequences of the siRNA duplexes used in this study are listed in Table 3 (Dharmacon RNA Technologies, Lafayette, CO and Qiagen, Hilden, Germany).

For rescue experiments the Plk1-RNAi plasmid (or the empty pTER+ vector as a control) was transfected simultaneously with the respective myc-tagged Plk1 constructs (or myc-hWW45 as a control) and cells were fixed and analysed 40 hours later.

Targeted gene	siRNA oligo sense sequence	Reference
GL2 (negative control)	CGU ACG CGG AAU ACU UCG AdTdT	(Elbashir <i>et al.</i> , 2001)
Plk1	CGA GCU GCU UAA UGA CGA GdTdT	(Kraft <i>et al.</i> , 2003)
Cdc20	CAU CAG AAA GCC UGG GCU UdTdT	
Hec1	GUU CAA AAG CUG GAU GAU CdTdT	(Stucke <i>et al.</i> , 2004)
Nuf2	GCA UGC CGU GAA ACG UAU AdTdT	
Mad2	GAG UCG GGA CCA CAG UUU AdTdT	(Stucke <i>et al.</i> , 2004)
Bub1	UAG GCU AAU UGU ACU GCU CdTdT	(Stucke <i>et al.</i> , 2004)
BubR1	GGA GAU CCU CUA CAA AGG GdTdT	(Stucke <i>et al.</i> , 2004)
Aurora-B	GGU GAU GGA GAA UAG CAG UdTdT	
CENP-E	ACU CUU ACU GCU CUC CAG UdTdT	(Stucke <i>et al.</i> , 2004)
CENP-F	AAG AGA UGC UAA UAG CAG UdTdT	(Stucke <i>et al.</i> , 2004)
Kif18	CCA ACA ACA GUG CCA UAA AdTdT	
MCAK	GCU AUC UGC UGG CUC UAA AdTdT	
Eg5	CUG GAU CGU AAG AAG GCA GdTdT	
EB1	UUG CCU UGA AGA AAG UGA AdTdT	
CLIP-170	UGA AGA UGU CAG GAG AUA AdTdT	
RanGAP1	GGA AGA UUC UGG ACC CUA AdTdT	
RanBP2	GGA CAG UGG GAU UGU AGU GdTdT	(Joseph <i>et al.</i> , 2004)
Ska1	CGC UUA ACC UAU AAU CAA AdTdT GAU UGG CAA UAU UAA GAA AdTdT	
Ska2	UCA CAU GCC AGA UUU AUG AdTdT GAA AUC AAG ACU AAU CAU CdTdT	

Table 3 List of siRNA oligos used in this study, together with the respective references of the published sequences.

7 Immunofluorescence microscopy

Cells were grown on coverslips and either fixed with paraformaldehyde for 10 min at RT followed by a 5 min permeabilisation with 0.5 % Triton-X100 at 4°C or simultaneously fixed and permeabilised for 10 min at RT in PTEMF buffer (20 mM PIPES, pH 6.8, 4 % formaldehyde, 0.2 % Triton X-100, 10 mM EGTA, 1 mM MgCl₂, in particular for KT proteins), or in -20°C methanol (in particular for centrosomal proteins). Afterwards cells were incubated for 30 min at RT in blocking solution (PBS, 1 % BSA). All antibody incubations were carried out for 1 hour at RT in a humidified chamber, followed by three washes in PBS.

Primary antibodies used in this study are listed in Table 4 with the respective dilutions for IF indicated and were detected with Alexa-Fluor-488-(green) and Alexa-Fluor-555-(red) conjugated

MATERIALS AND METHODS

donkey anti-mouse, anti-rabbit or anti-sheep IgGs, respectively, Alexa-Fluor-647-(far red) conjugated anti-rabbit IgGs (1:1000, Molecular Probes, Eugene, OR) or Cy2- and Cy3-conjugated donkey anti-human IgGs (1:1000, Jackson ImmunoResearch, West Grove, PA). DNA was stained with 2 µg/ml DAPI. Cover slips were mounted in phenylenediamine in 90% glycerol.

IF microscopy was performed using a Zeiss Axioplan II microscope (Zeiss, Jena, Germany) with Apochromat 40x and 63x oil immersion objectives, respectively. Photographs were taken using a Micromax CCD camera (model CCD-1300-Y, Princeton Instruments, Trenton, NJ) and Metaview software (Visitron Systems GmbH, Puchheim, Germany). For high resolution images a microscope (Deltavision; Applied Precision, Issaquah, WA) on a base (Olympus IX71; Applied Precision) that was equipped with PlanApo 60X/1.40 oil immersion objective (Olympus) and a camera (CoolSNAP HQ;Photometrics) was used for collecting 0,15 µm-distanced optical sections in the z-axis. Images at single focal planes were processed with a deconvolution algorithm, and optical sections were projected into one picture using Softworx software (Applied Precision). The same software was used to measure inter-KT distances in images at single focal planes. Images were cropped in Adobe Photoshop 6.0 and then sized and placed in figures using Adobe Illustrator 10 (Adobe Systems, San Jose, CA).

8 Live-cell imaging

For live-cell imaging, a HeLa S3 cell line stably expressing histone H2B-GFP was used. Cells were treated with siRNAs for 30 hours, before the medium was changed into CO₂ independent medium and the culture dish was subsequently placed onto a heated sample stage within a heated chamber (37°C). Live-cell imaging was performed using the Plan Apo 40x/0.95 objective on the above described Deltavision microscope and Softworx software was used to collect and process data. Images were captured with 10 % neutral density and 200 milliseconds exposure times in 4 minutes intervals for 18 hours with three stacks per field spaced 3 µm each.

9 Cell extracts, Immunoprecipitation, Western Blot and Far Western analysis

For cell extracts HeLa S3 and HEK293(T) cells were washed once with ice-cold PBS containing 1 mM PMSF, scraped or shaken off the plate and resuspended in ice-cold RIPA lysis buffer (50 mM Tris, pH 7.4, 150 mM NaCl, 1% NP-40, 0,5 %Na-Desoxycholate) containing 1 mM DTT, 30 µg/ml RNase A, 30 µg/ml DNase, protease and phosphatase inhibitors. If cell extracts were prepared for a subsequent IP or pulldown, HEPES lysis buffer (50 mM HEPES, pH7.4, 150 mM NaCl, 0.5 % Triton X-100) was used instead. After 15 min on ice, lysed cells were centrifuged at 13000 rpm for 15 min at 4°C. Protein concentrations in the cleared lysates were determined using the Dc protein assay (Bio-Rad Laboratories, Hercules, CA).

For IP experiments, antibodies and corresponding IgGs as control were either coupled to Affi-Prep Protein A Support beads (Bio-Rad Laboratories) if antibodies were raised in rabbits, or to Protein G beads (Pierce Biotechnology, Rockford, IL) if antibodies were of mouse origin. For FLAG-IPs anti-FLAG[®]M2 Affinity gel (Sigma) was used. Respective beads were incubated with the HEPES cleared lysate for at least 4 hours at 4°C on a rotating wheel. Immune complexes were spun down, washed 4 times in the same lysis buffer and then boiled in SDS sample buffer. For all experiments equal protein amounts of each, the lysates and the IPs, were loaded on SDS-PAGE gels. Separated proteins were transferred to nitrocellulose membranes (Schleicher & Schuell, Keene, NH). Primary antibodies used in this study for Western blot analysis are listed in Table 4 with the respective dilutions indicated and were detected by HRP-conjugated goat anti-mouse and anti-rabbit (1:3000, Pierce Biotechnology, Rockford, IL) and donkey anti-sheep IgGs (1:3000, Jackson Immunoresearch). Bound antibodies were detected by ECL Supersignal (Pierce Biotechnology) using a digital Fujifilm LAS-1000 camera attached to an Intelligent Darkbox II (Raytest GmbH, Straubenhardt, Germany). For quantification of the signals the Advanced Data Image Analyser (AIDA) imaging software was used (Raytest).

Far Western ligand blots were performed in TBST (50 mM Tris-HCl, pH 7.4, 137 mM NaCl, 0.1 % Tween 20, and 5 % skim milk powder) and probed with 1 µg/ml GST-PBD^{WT} and GST-PBD^{AA}, respectively, for 6 hours at 4°C. Bound protein was detected using affinity-purified rabbit antibodies against GST.

10 Mitotic chromosome spreads

HeLa S3 cells were either treated with Plk1 siRNA oligos for 36 hours or with nocodazole (100 ng/ml) over night. The myc-PBD^{WT} stable cell line was induced for 24 hours. Mitotic cells were collected by mitotic shake off, centrifuged for 4 min at 1000 rpm and resuspended in diluted DMEM culture medium (40 % DMEM without antibiotics and 60 % deionised H₂O). The cells were allowed to swell at RT for 5 min before spinning and resuspending them in fixation solution (3:1 methanol:acetic acid). The fixed cells were incubated at 4°C for at least 20 min, washed three more times with the fixation solution and, finally, 10 µl of each cell solution were dropped on a -20°C HCl-treated cover slip, which had been moistened before by breathing on to it. After drying of the cover slip on a wet Kleenex tissue over a 60°C heating block, spreads were stained for 5 min with 0,4 µg/ml DAPI and mounted.

MATERIALS AND METHODS

Antigen	MW (kDa)	Species	IF dilution	WB dilution	Company
ANA		h	1:1000		Europa Bioproducts Ltd
Aurora-A	45	m	1:1000	1:1000	BD Biosciences Pharmingen
Aurora-B	41	m	1:500	1:250	BD Transduction Laboratories
Bub1	130	m	1:5 (62-406-3)	Undiluted (61-22-2)	homemade
Bub3	40	m		1:500	BD Transduction Laboratories
BubR1	120	m	undiluted (68-3-9)	1:10 (68-3-9)	homemade
CENP-A	17	m	1:1000	1:1000	MBL
CENP-E	310	m	1:500	-	Abcam
		g		1:200	Santa-Cruz
CENP-F	400	m	1:1000	1:1000	BD Transduction Laboratories
Centrin	20	r	1:600	1:400	homemade
Centrin-3		m	(R67) 1:5000 (20H5)	(R67)	gift from J.L.Salisbury
Cdc20	55	r	1:200	1:200	Santa-Cruz
Cdc27	97	m		1:250	BD Transduction Laboratories
CLIP-170	153	m	1:100	1:100	gift from F. Perez
Cyclin B1	60	m		1:1000	Upstate
CREST		h	1:5000		Immunovision
EB1	30	m	1:200	1:500	BD Transduction Laboratories
Ect2	100	r	1:1000 (R138)	1:1000 (R138)	homemade
Eg5	97	r	1:1000	1:1000	homemade
Emi1	44	r		1:100	Zymed
FLAG	8aa	r	1:1000	1:1000	Sigma
GST	30	r		1µg/ml	Gift from U. Grüneberg
		m		undiluted (268-44-6)	homemade
Hec1	75	m	1:1000	1:1000	Abcam
HURP	110	r	2µg/ml (R139)	2µg/ml (R140)	homemade
INCENP	120	r	1:1000 (RB55)	1:500 (RB56)	homemade
Kif18	90	r	-	1:500	homemade Stefan Hümmer
Mad2	27	r	1:500	-	Covance
		r	1:1000	-	Bethyl
MCAK	75	r	1:500	1:100	Cytoskeleton
Mps1	90	m	undiluted (3-472-1)	undiluted (3-472-1)	homemade

Antigen	MW (kDa)	Species	IF dilution	WB dilution	Company
Myc/9E10		m	1:10	1:10	homemade
Myc/9E10-TRITC		m	1:1000	-	Santa-Cruz
MST1		r	1:1000	1:1000	Cell Signalling
MST2		r	1:1000	1:1000	gift from Ch. Jonathan
CG-NAP1		r		1:1000	gift from M.Takahashi
c-Nap1	280	r		1:1000 (R63)	homemade
Nuf2	52	r		1:500 (J95, 370-03)	homemade
NuMA	200	m		1:10	gift from J. Harborth
Pericentrin	220	r	1:1000		Abcam
Plk1 (linker)	66	m	1:20 (35-206)	1:10 (PL2)	homemade
Plk1 (N-term)	66	g	1:100		Santa Cruz
RanBP2		g	1:500	1:6000	gift from F. Melchior
RanGAP1		g	1:1000	1:750	gift from F. Melchior
Ska1	30	r	1:5000 serum (452-680)	2,5µg/ml AP (452-680)	homemade
Ska2	14	r	-	5 µg/ml AP (716-724)	homemade
Tpx2	100	m	1:10		gift from O. Gruss
α-Tubulin	55	m	1:1000	1:2000	Sigma
α-Tubulin-FITC		m	1:1000	-	Santa-Cruz
γ-Tubulin	50	m	1:1000 (GTU-88)	1:1000	Sigma
		r	1:2000 (R60)		homemade

Table 4 List of antibodies used for IF or Western blot analysis in this study. First column indicates against which protein the antibody is directed (Antigen) and the second column shows the approximate molecular weight (MW) of the antigen. The species in which the antibodies were raised (m=mouse, r=rabbit, g=goat), dilutions for IF and Western blot and the source of the antibodies are indicated in the following columns. For antibodies raised in our department (homemade) the respective numbers are given. For empty boxes the dilutions were not determined while a "-" marks this antibody as non-functional for that purpose.

11 *In vitro* phosphopeptide binding

Recombinant GST, GST-PBD^{WT} and GST-PBD^{AA} were purified from *E. coli* using glutathione-Sepharose 4B beads (Amersham Biosciences). These immobilised recombinant proteins were incubated in HEPES binding buffer (25 mM HEPES, pH 7.4, 2 mM EGTA, 2 mM MgCl₂, 1 mM DTT, 100 ng/ml okadaic acid) containing 75 µM of the optimal PBD binding phosphopeptide (Elia *et al.*, 2003a). After over night incubation at 4°C the beads were washed 3 times with binding buffer and bound peptides were subsequently eluted with 30 % formic acid at RT. The presence of phosphopeptides in these eluates was then determined by MALDI mass spectrometry.

12 *In vitro* kinase assays

To obtain FLAG-MST kinases HEK293T were transfected with plasmids coding for FLAG-MST2, MST1, WT and KD versions, respectively, in the absence of nocodazole (to obtain moderately active kinases) before lysis in HEPES lysis buffer. Overexpressed FLAG-tagged proteins were isolated by anti-FLAG®M2 Affinity gel (Sigma) and eluted from the beads after two times washing with buffer D (20 mM HEPES, pH 7.8, 250 mM KCl, 0.2 mM EDTA and 0.1 % NP40) by incubation in the same buffer including 100 µg/ml FLAG-peptide (Sigma) for 30 min at RT. For the production of GST-Plk1, WT and KD versions, Sf9 insect cells were infected with the respective P3 baculovirus supernatants for 48 hours in the absence of an 3 hours incubation step with 100 nM okadaic acid (to obtain moderately active kinases) before lysis (10 mM HEPES, pH 7.7, 5 mM EGTA, 5 mM β-mercaptoethanol, 20 mM β-glycerophosphate, 0,1 mM NaVanadate, 5 mM NaF, protease inhibitors). For *in vitro* kinase assays, FLAG-MST proteins were either combined with Cdk1/Cyclin B (kind gift from Rüdiger Neef) in BRB80 buffer (80 mM Pipes, pH 6.8, 1 mM MgCl₂, 1 mM EGTA) (Neef *et al.*, 2003) or with GST-Plk1 in Plk1 kinase buffer (20 mM HEPES, pH 7.7, 10 mM MgCl₂, 1 mM EGTA, 1 mM DTT, phosphatase and kinase inhibitors). Kinase reactions were carried out at 30°C for 30-60 min in these buffers supplemented with 10 µM ATP and 2 µCi [γ -³²P] ATP (Amersham Corp.). Reactions were stopped by the addition of SDS sample buffer and heating at 95°C for 5 min. Reaction products were visualised by SDS-PAGE followed by autoradiography.

13 Phosphatase assays

HeLa S3 cells were arrested with either 1,6 µg/ml aphidicolin (G1/S phase) or with 150 ng/ml nocodazole (M phase) for 14 hours. The aphidicolin treated cells were scraped off the plate, whereas the nocodazole treated mitotic cells were obtained by shake off, and then washed in PBS with 1 mM PMSF and lysed in NP40 buffer (50 mM Tris, pH 7.4, 150 mM NaCl, 1 % NP40, 0,5 % Na-Desoxycholate) containing protease inhibitors, RNase, DNase and DTT as described above, either in the presence or in the absence of phosphatase inhibitors. After 15 minutes on ice cells were pelleted and the supernatants of the lysates were either treated with Alkaline Phosphatase (AP, 1:50 final concentration in lysate, Roche) or left untreated for 1 hour at 30°C. The phosphatase reaction was stopped by addition of sample buffer followed by boiling. Equal protein amounts were loaded and separated on a SDS-PAGE gel followed by Western blot analysis.

14 Yeast-two hybrid analysis

Yeast two hybrid screen was performed by Anja Wehner using a system described previously (James *et al.*, 1996). The full length Ska1 cDNA was cloned into a pFBT9 Gal4 DNA binding domain vector. A human HEK293 two-hybrid library (BD Clontech, Mountain View, CA) was

screened, and clones able to activate both the Ade2 and His3 selection markers, specifically in the presence of the bait, were selected.

15 *In vitro* coupled transcription translation

The respective 3xmyc- and FLAG-tagged proteins were produced by *in vitro* coupled transcription translation (IVT) in the presence of ³⁵S-methionine using the TNT T7 Quick Coupled Transcription/Translation System (Promega, Madison, WI). For IP these reactions were diluted in LS buffer (50 mM Tris, pH 8.0, 100 mM NaCl, 0,1 % NP40 and protease inhibitors) and incubated with anti-myc antibody (9E10) coated Protein G beads (Pierce Biotechnology) for 90 minutes at 4°C on a rotating wheel. After washing, samples were boiled in sample buffer and equal protein amounts of input and myc-precipitates were separated by SDS-PAGE and visualised by autoradiography.

APPENDIX

1 List of abbreviations

All units are abbreviated according to the International Unit System.

aa:	amino acid
ATP:	adenosine 5'-triphosphate
BSA:	bovine serum albumin
CDK:	cyclin-dependent kinase
CPC:	chromosomal passenger complex
C-terminus;	carboxy-terminus
DAPI:	4',6-diamidino-2-phenylindole
DTT:	dithiothreitol
ECL:	enhanced chemiluminescence
EDTA:	ethylene-dinitrilo-tetraacetic acid
EGTA:	ethylene-glycol-tetraacetic acid
FCS:	Fetal calf serum
GFP:	green fluorescent protein
HCl:	hydrochloric acid
HEPES:	N-2-Hydroxyethylpiperazine-N'-2-ethane sulfonic acid
IF:	immunofluorescence
IgG:	Immunoglobulin G
IP:	immunoprecipitation
IPTG:	isopropyl-beta-D-thiogalactopyranoside
KD:	kinase dead
KT:	kinetochore
mAb:	monoclonal antibody
MALDI:	Matrix assisted laser desorption ionisation
min	minute(s)
MS:	mass spectrometry
MT:	MT
N-terminus:	amino-terminus
PBD:	Polo-box domain
PBS:	Phosphate-buffered saline
PCR:	Polymerase chain reaction
PIPES:	1,4-Piperazinediethanesulfonic acid
Plk:	Polo-like kinase

PMSF: phenylmethylsulfonyl fluoride
RNA: Ribonucleic Acid
RT: room temperature
SAC: spindle assembly checkpoint
SDS-PAGE: Sodium dodecylsulfate polyacrylamid gelelectrophoresis
siRNA: small interference ribonucleic acid
WT: wildtype

2 Table of created plasmids

Plasmid	Tag	Gene	Insert	Vector
AH1	GST	Plk1	PBD WT, aa 326-603	pGEX-6P-3
AH2	GST	Plk1	PBD, aa 410-437 deleted	pGEX-6P-3
AH3	GST	Plk1	PBD YQL425-427AAA	pGEX-6P-3
AH4	GST	Plk1	PBD HK530/540AA	pGEX-6P-3
AH5	Strep			pQE-30
AH6	Strep	Plk1	PBD WT	pQE-30
AH7	Strep	Plk1	PBD HK530/540AA	pQE-30
AH8	Strep	Pin1	FI, WT	pQE-30
AH9	Strep	Pin1	FI, W34A, RR68/69AA	pQE-30
AH10	EGFP	Plk1	PBD WT	pEGFP-T7/C1
AH11	EGFP	Plk1	PBD HK530/540AA	pQE-30
AH12	myc	Plk1	PBD WT	pcDNA3.1/3xmyc-C
AH13	myc	Plk1	PBD HK530/540AA	pcDNA3.1/3xmyc-C
AH14	myc	Plk1	Catalytic domain WT, aa 1-330	pcDNA3.1/3xmyc-C
AH15	myc	Plk1	Catalytic domain K82R, aa 1-330	pcDNA3.1/3xmyc-C
AH16	myc	Plk1	PBD WT	pcDNA/TOPuromycin
AH17	myc	Plk1	PBD HK530/540AA	pcDNA/TOPuromycin
AH18	myc	Plk1	FI, HK538/540AA	pRcCMV
AH19	myc	Cdc27	FI WT	pcDNA3.1/3xmyc-C
AH20	myc	Cdc20	FI WT	pcDNA3.1/3xmyc-C
AH21	FLAG	Cdc20	FI WT	pcDNA3.1/FLAG-C
AH22	myc	BubR1	FI WT	pcDNA3.1/3xmyc-C
AH23	FLAG	BubR1	FI WT	pcDNA3.1/FLAG-C
AH24	myc	Mis12	FI WT	pcDNA3.1/3xmyc-C
AH25	FLAG	Cdc27	FI WT	pcDNA3.1/FLAG-C
AH26	myc	SLK	FI WT	pcDNA3.1/3xmyc-C
AH27	FLAG	SLK	FI WT	pcDNA3.1/FLAG-C
A28H	myc	Bub1	FI WT	pcDNA3.1/3xmyc-C
AH29	FLAG	Bub1	FI WT	pcDNA3.1/FLAG-C
AH30	FLAG	Plk1	FI WT	pcDNA3.1/FLAG-C
AH31	FLAG	Plk1	FI HK538/540AA	pcDNA3.1/FLAG-C
AH32	FLAG	Plk1	FI K82R	pcDNA3.1/FLAG-C
AH33	FLAG	Plk1	FI T210D	pcDNA3.1/FLAG-C
AH34	FLAG	Bub1	FI D946A	pcDNA3.1/FLAG-C
AH35	FLAG	Mps1	FI WT	pcDNA3.1/FLAG-A
AH36	myc	Plk1	Catalytic domain, aa 1-352 RNAi mut	pcDNA3.1/3xmyc-C
AH37	myc	Plk1	FI WT, RNAi mut	pcDNA3.1/3xmyc-C
AH38	FLAG	Plk1	FI WT, RNAi mut	pcDNA3.1/FLAG-C
AH39	FLAG	Plk1	FI K82R, RNAi mut	pcDNA3.1/FLAG-C
AH40	FLAG	Plk1	FI HK538/540AA, aa 1-152 RNAi mut	pcDNA3.1/FLAG-C
AH41		CENP-A	cDNA clone	

AH42	FLAG	Cdc20	FI WT	pcDNA3.1/FLAG-C
AH43	FLAG	Cdc20	FI S161A	pcDNA3.1/FLAG-C
AH44	myc	Plk1	FI K82R, RNAi mut	pcDNA3.1/3xmyc-C
AH45	myc	Plk1	FI HK538/540AA, RNAi mut	pcDNA3.1/3xmyc-C
AH46	FLAG	Emi1	FI WT	pcDNA3.1/FLAG-C
AH47	myc	Nup155	FI WT	pcDNA3.1/3xmyc-C
AH48		Nup155	cDNA clone KIAA0791	
AH49	myc	Plk3	PBD aa 336-646	pcDNA3.1/3xmyc-C
AH50	myc	Plk2	PBD aa 355-685	pcDNA3.1/3xmyc-C
AH51	FLAG	BubR1	FI D911A	pcDNA3.1/FLAG-C
AH52	C-myc	Ska1/C18Orf24	FI WT	
AH53		C21Orf45	cDNA clone	
AH54		OIP5	cDNA clone	
AH55	myc	Snapin	FI WT	pcDNA3.1/3xmyc-C
AH56	myc	Ska2/Fam33a	FI WT	pcDNA3.1/3xmyc-C
AH57	myc	C21Orf45	FI WT	pcDNA3.1/3xmyc-C
AH58	myc	OIP5	FI WT	pcDNA3.1/3xmyc-C
AH59	AD	Ska1/C18Orf24	FI WT	pGAD-C1
AH60	AD	Snapin	FI WT	pGAD-C1
AH61	AD	Ska2/Fam33a	FI WT	pGAD-C1
AH62	AD	C21Orf45	FI WT	pGAD-C1
AH63	AD	OIP5	FI WT	pGAD-C1
AH64	BD	Snapin	FI WT	pFBT9'
AH 65	BD	Ska2/Fam33a	FI WT	pFBT9'
AH66	BD	C21Orf45	FI WT	pFBT9'
AH67	BD	OIP5	FI WT	pFBT9'
AH68	GST	Ska2/Fam33a	FI WT	pGEX-6P-3
AH69	His	Ska2/Fam33a	FI WT	pET-28b
AH70	FLAG	Ska2/Fam33a	FI WT	pcDNA3.1/FLAG-C
AH71		MGC88047	FI WT	
AH72	myc	MGC88047	FI WT	pcDNA3.1/3xmyc-C
AH73	His	MGC88047	FI WT	pET-28b
AH74	FLAG	MGC88047	FI WT	pcDNA3.1/FLAG-C
AH75	HA	MGC88047	FI WT	pcDNA3.1/HA-C
AH76	EGFP	Ska2/Fam33a	FI WT	pEGFP-T7/C1
AH77		BubR1	cDNA clone	
AH78		Bub1	cDNA clone	
AH79		Cdc20	cDNA clone	
AH80		Cdc27	cDNA clone	
AH81		Mis12	cDNA clone	
AH82	myc	KIAA0007	cDNA clone	pcDNA3.1/3xmyc-C
AH83	myc	KIAA0539	cDNA clone	pcDNA3.1/3xmyc-C
AH84	myc	KIAA0663	cDNA clone	pcDNA3.1/3xmyc-C
AH85	myc	KIAA1187	cDNA clone	pcDNA3.1/3xmyc-C
AH86	myc	Cirhin		pcDNA3.1/3xmyc-C
AH87	myc	DKFZp686J1577	cDNA clone	pcDNA3.1/3xmyc-C
AH88	myc	KIAA1988	cDNA clone	pcDNA3.1/3xmyc-C
AH89	myc	Spc24	FLJ90806, cDNA clone	pcDNA3.1/3xmyc-C

APPENDIX

AH90	myc	IRAKp961L1148Q2	FLJ35834, cDNA clone	pcDNA3.1/3xmyc-C
AH91		KIAA0007	cDNA clone	
AH92		KIAA0539	cDNA clone	
AH93		KIAA0663	cDNA clone	
AH94		KIAA1187	cDNA clone	
AH95		DKFZp686J1577	cDNA clone	
AH96		KIAA1988	cDNA clone	
AH97		Spc24	FLJ90806, cDNA clone	
AH98		IRAKp961L1148Q2	FLJ35834, cDNA clone	

Table 5 Table of all plasmids created in the course of the PhD work. FI indicates full length genes, RNAi mut indicates silent mutations in the Plk1 sequence, which render the plasmid derived RNA insensitive to the Plk1 specific siRNA duplexes.

3 Table of proteins identified by mass spectrometry in GST-PBD pull down

The following table has been generated by Roman Körner.

Name of protein identified in PBD pulldown

Dynein Heavy Chain

Desmoplaktin

Echinoderm MT-associated protein-like 4

Tpr

ALG-2 interacting protein 1

Lamin A

DNA replication licensing factor MCM6

Kinesin heavy chain

dnaK-type molecular chaperone

Transitional endoplasmic reticulum ATPase

DNA replication licensing factor MCM7

Keratin, type II cytoskeletal 8

KIAA1521

DNA replication licensing factor MCM3

dnaK-type molecular chaperone HSP70-1

Similar to tubulin, beta, 2

Ubiquitin-conjugating enzyme E2

DNA replication licensing factor MCM2

HECT domain protein LASU1

Vimentin

Hsp90-beta

Hypothetical ubiquitin-associated domain containing protein

Retinoblastoma-associated factor 600

tubulin alpha-1 chain

S-adenosylhomocysteine hydrolase-like protein

Similar to Werner helicase interacting protein

keratin 7

MCM5_HUMAN

ATP citrate synthase

Adapter-related protein complex 3 delta 1 subunit

Rho-kinase

14-3-3 protein zeta/delta

BiP protein

Keratin, type I cytoskeletal 18 (Cytokeratin 18) (K18)

replication licensing factor MCM4

Hsp90-alpha

Casein kinase II, alpha chain

alpha-complex protein 1

Adapter-related protein complex 3 beta 2 subunit

Kinesin light chain 2

APPENDIX

SH3-containing GRB2-like protein 1
DNA primase chain p58
Transcription intermediary factor 1-beta
14-3-3 protein beta/alpha
TBP-interacting protein TIP120
Heterogeneous nuclear ribonucleoprotein K
14-3-3 protein eta
MOP-3
Adapter-related protein complex 3 mu 1 subunit
ORTHOLOG of mouse P47
Importin beta-1 subunit
Protein tyrosine phosphatase TD14
E3 ligase for inhibin receptor
ribosomal protein S3
Treacher Collins Syndrom Protein
KIAA0992
D-3-phosphoglycerate dehydrogenase
Polymerase (DNA directed), alpha.
heat shock protein 27
ABP130
casein kinase II (EC 2.7.1.-) alpha' chain
Poly(RC)-binding protein 2, isoform b
HPV16 E1 protein binding protein
14-3-3 protein theta
lamin B1
Nucleophosmin
F-actin capping protein alpha-1 subunit
SEC13-related protein
RuvB-like 2
Retinoblastoma-binding protein 4
Ribonucleoside-diphosphate reductase M2 chain
Importin alpha-2 subunit
Transcription intermediary factor 1-gamma
hepatoma-derived growth factor
Transducin-like enhancer protein 3 (ESG3).-
Insulin receptor tyrosine kinase substrate.

5'-AMP-activated protein kinase, gamma-1 subunit
F-actin capping protein beta subunit
Sorting nexin 2
Eukaryotic initiation factor 4A-I (eIF4A-I
TRIP protein
14-3-3 protein gamma
Hypothetical protein Q96HC3
casein kinase II (EC 2.7.1.-) beta chain
U2 small nuclear ribonucleoprotein A'
T-complex protein 1, gamma subunit
Adenosine monophosphate deaminase 2 (Isoform L).-
Goodpasture antigen-binding protein (kinase)

40S ribosomal protein S9

gamma-actin

Golgi-specific brefeldin A-resistance guanine nucleotide exchange factor 1

Ras-related protein Rab-1B

Hypothetical protein Q96F86

NGFI-A binding protein 1

Hypothetical protein FLJ12470

flightless-1 homolog - human

Importin 7 (RanBP7)

Adapter-related protein complex 3 sigma 1 subunit

Nck-associated protein 1

Nucleoporin Nup43

SH3-containing GRB2-like protein 2

Histone deacetylase 2

RanBP3-a

Tumor protein D54

STAM

Hypothetical protein FLJ21190 (CDA03)

EF11 translation elongation factor eEF-1 alpha-1 chain

CGI-74 protein

Nuclear pore complex protein Nup160

translation initiation factor eIF-4B**ribosomal protein S18**

Metastasis associated protein MTA2

protein kinase (EC 2.7.1.-) PRK2

Hypothetical protein FLJ22276

Uridine-cytidine kinase 2

eukaryotic initiation factor 4AII**Nucleosome assembly protein 1-like 4**

Nucleosome assembly protein 1-like 1

Elongation factor 2 (EF-2).-**FLJ00147 protein (Fragment).-**

Adaptor protein APPL

Nup98

ribose-phosphate diphosphokinase (EC 2.7.6.1) catalytic chain I

40S ribosomal protein S16.-

Nup133

Histone deacetylase 1

Alpha-centractin**ribosomal protein S25**

CoREST protein

DNA damage binding protein 1

Probable ATP-dependent RNA helicase p54 (Oncogene RCK) (DEAD-box protein 6).-

Myristoylated alanine-rich C-kinase substrate (MARCKS)

Dynein, cytoplasmic, light intermediate polypeptide 2

Inhibitor of nuclear factor kappa-B kinase alpha subunit

KIAA1167

Serine/threonine protein kinase MASK (Serine/threonine protein kinase MST4)

APPENDIX

WD-repeat protein 5

40S ribosomal protein S8

Cell division protein kinase 9

Sporulation-induced transcript 4-associated protein SAPLb

Similar to RIKEN cDNA 0610034P02 gene

BAG-family molecular chaperone regulator-3

Neural Wiskott-Aldrich syndrome protein (N-WASP)

BAG-family molecular chaperone regulator-2

Cullin homolog 4B

KIAA1600

Casein kinase I

Rb-associated protein

Ribonuclease P protein subunit p30

kinesin light chain

Hypothetical Combined RanBP1/wasp domain

Serine/threonine protein phosphatase 6

Transforming acidic coiled-coiled containing protein 3 (TAC3)

40S ribosomal protein S19

DNA polymerase alpha 70 kDa subunit

Sequence 326 from Patent WO0222660

GTP-binding protein beta chain

Beta-centractin

Hypothetical protein FLJ30656

Dynein light chain-A.-

Sorting nexin 24

Cyclic GMP inhibited phosphodiesterase A

Gene trap ankyrin repeat containing protein

TRK-fused gene/anaplastic large cell lymphoma kinase extra long form

Nup75

Serine/threonine protein phosphatase 2A, 65 KDA regulatory subunit A, alpha isoform

SH3 adapter protein SPIN90

Peroxiredoxin 1

40S ribosomal protein S13

Myocyte-specific enhancer factor 2D

60S ribosomal protein L13

Hypothetical protein (Calcyclin binding protein) (Siah-interacting protein).-

Programmed cell death 10.-

p53 inducible protein

Cofilin, non-muscle isoform

Nuclear receptor co-repressor/HDAC3 complex subunit TBLR1

KIAA1598

40S ribosomal protein S10

40S ribosomal protein S14

40S ribosomal protein S5

40S ribosomal protein S23

Keratin, type I cytoskeletal 14 (Cytokeratin 14)

Colon carcinoma laminin-binding protein

T-complex protein 1, theta subunit

Cdc42 effector protein 4 mRNA
 Vinexin
 Hypothetical protein Q9BPU7
 Dynactin 1
 40S ribosomal protein S6
 LIPOMA PREFERRED partner (LPP)
 similar to 40S ribosomal protein S7 (S8)
 40S ribosomal protein S11
 AP-3 complex beta3A chain
 Neuroblast differentiation associated protein AHNAK
 LIM protein
 Dynactin subunit
 TAK1-binding protein 1
 Adapter-related protein complex 3 sigma 2 subunit
 Ribonucleases P/MRP protein subunit POP1
 ribosomal protein L11
 60S acidic ribosomal protein P0
 Caldesmon
 Kinesin-like protein Kif2
 Calmodulin 2
 hypothetical protein DKFZp434C212.1
 Hypothetical protein FLJ13081
 FLJ20302
 Homo sapiens ZIS2 mRNA
 Similar to chromodomain helicase DNA binding protein 4
 GTP-binding protein SAR1a
 MT-vesicle linker CLIP-170
 Hypothetical protein (Fragment).-
 Hypothetical protein FLJ14632 (kinase)
 Hypothetical RabGAP/TBC domain containing protein
 NuMa
 40S ribosomal protein S4
 Ubiquitin carboxyl-terminal hydrolase 24
 Ran GTPase
 Serine/threonine protein phosphatase 2A, catalytic subunit, alpha isoform
 Zyxin
 60S ribosomal protein L23a
 ELKS gamma
 Transcription initiation factor IIF, beta subunit
 Nucleolar phosphoprotein p130.-
 Ubiquitin carboxyl-terminal hydrolase FAF-X
 nuclear matrix protein NMP 238
 kinase complex-associated protein
 COP9 subunit 4
 14-3-3 protein sigma
 Condensin subunit 2
 Protein involved in sexual development.-
 60S ribosomal protein L24

APPENDIX

Coatmer zeta-1 subunit
Hypothetical protein (fragment)
Protein C20orf11
5'-AMP-activated protein kinase, catalytic alpha-1 chain
Ataxin-2 related domain protein
receptor-associated coactivator 3 (RAC3)
transcription coactivator CREB-binding protein
5'-AMP-activated protein kinase, beta-1 subunit
60S ribosomal protein L7
WD-repeat protein An11 homolog
60S ribosomal protein L35
Mob1 protein
Hypothetical protein FLJ13910
Hypothetical protein KIAA0585 (Fragment).-
Gamma-actin
Dynactin complex 50 kDa subunit
MOV34 ISOLOG (COP9 subunit 6)
NGFI-A binding protein 2
HURP
Gamma adducin
Eukaryotic translation initiation factor 4 gamma
L-lactate dehydrogenase A chain
Thymopoietin, isoform delta
60S ribosomal protein L12
KIAA0035
hypothetical 109.6K protein
Human full-length cDNA clone CS0DK007YN03 of HeLa cells of Homo sapiens
RalBP1 associated Eps domain containing protein 1
Similar to spectrin SH3 domain binding protein 1
polyadenylate binding protein II
Serine/threonine protein phosphatase PP1-beta catalytic subunit
RNA-binding region containing protein 2
Splicing factor 3A subunit 3
Oxysterol binding protein-related protein 10
53 kDa BRG1-associated factor A
WD-repeat protein 13
HRS protein (Hepatocyte growth factor-regulated tyrosine kinase substrate).-
Similar to myosin phosphatase, target subunit 1
Ribonuclease P protein subunit p38
Methyl-CpG binding protein MBD3
Alpha adducin
heat shock protein Hsp47 precursor
Clathrin coat assembly protein AP180
Polynucleotide adenylyltransferase alpha
Similar to evidence:NAS hypothetical protein putative
KIAA0144
Ubiquilin
GRG protein

RanBP1
 CD2-associated protein
 SET protein
 ralA-binding protein 1
PLK-1
 Dystrophin
 ARF GTPase-activating protein GIT1
 Proteasome zeta chain
 Eukaryotic translation initiation factor 4E
 Hypothetical protein FLJ21613
hypothetical protein FLJ23316
 Transforming protein N-Ras
Mitotic spindle assembly checkpoint protein MAD2A
 Poly(rC)-binding protein 3
 cDNA DKFZp686H1588 (from clone DKFZp686H1588);
 Similar to CamKI-like protein kinase
 Poly(A) polymerase gamma
Nup107
P150 target of rapamycin (TOR)-scaffold protein containing WD-repeats
 Pre-mRNA cleavage complex II protein Clp1
small nuclear ribonucleoprotein associated protein b sm motif, chain L
 KIAA0540
 Striatin
Hypothetical protein
 MG81 protein
 UV-damaged DNA binding factor
 mRNA-associated protein mrnp 41
 Diaphanous protein homolog 1
 DNA-damage inducible protein 2
 DNA mismatch repair protein Mlh1
 Meiotic recombination protein REC14
 Transcription initiation factor IIE
 Ataxin-2
 NGFI-A binding protein 1
 T-complex protein 1, zeta subunit
 mitogen-activated protein kinase kinase (EC 2.7.1.-) 6
 Factor VIII intron 22 protein
 Oxysterol binding protein-related protein 9
Adrenal gland protein AD-005 homolog
 H3 histone family, member T
ribosomal protein L27
 Proteasome subunit beta type 3
 Oxysterol binding protein-related protein 11
 Retinoic acid receptor RXR-beta
60S ribosomal protein L26-like 1
 Ribonuclease P protein subunit p20
 C330027G06Rik protein (Fragment).-
 MOB3

APPENDIX

ubiquitin
Epithelial protein lost in neoplasm
My004 protein
ribosomal protein L27a
Sirtuin type 1
Similar to wiskott-aldrich syndrome protein interacting protein
myosin regulatory light chain MRCL3
Likely ortholog of mouse ubiquitin-conjugating enzyme E2-230K
vasodilator-stimulated phosphoprotein (VASP)
Hypothetical protein Q86UY4
Lysosomal trafficking regulator 2
Synaptojanin
Histone RNA hairpin-binding protein
Mitotic checkpoint protein BUB3
Septin 7
ribosomal protein L4
Nuclear respiratory factor-1
H4 protein
FHOS
Heat shock factor protein 1
Neuronal tropomodulin
28 kDa heat- and acid-stable phosphoprotein
Sorting nexin 5
Hypothetical protein FLJ90489
Hypothetical protein KIAA1543 (Fragment)
Rho-GTPase activating protein 5
Peroxiredoxin 4
Ribonuclease P protein subunit p29
Arginyl-tRNA--protein transferase 1
U2 small nuclear ribonucleoprotein B"
40S ribosomal protein S2
Hypothetical protein
Trafficking protein particle complex subunit 3
Ubiquitin-like protein SUMO-1 conjugating enzyme
Phosphatidylinositol-3 phosphate 3-phosphatase adaptor subunit
protein-tyrosine kinase (EC 2.7.1.112) ABL2
chloride channel protein I-Cl_n
Calpain inhibitor
ribosomal protein S17
Ras and Rab interactor 1
5'-AMP-activated protein kinase, catalytic alpha-2 chain
Hyaluronan mediated motility receptor
DEAH-box protein 8
G1 to S phase transition protein 1 homolog
Clathrin heavy chain
Peptidyl-prolyl cis-trans isomerase A
MLL septin-like fusion protein

Table 6 Table of the 375 different proteins identified in the PBD pull down by LC-MS/MS. Proteins are listed according to their Mascot score starting with the highest score. Proteins written in red colour have been found in both GST-PBD^{WT} and GST-PBD^{AA} (negative control) eluates, whereas proteins written in black were specific for the GST-PBD^{WT} eluate.

ACKNOWLEDGEMENTS

I like to thank Prof. Dr. Erich Nigg for giving me the opportunity to work in this very well organised and equipped cell biology department, for his support and his excellent feeling of choosing again and again people who with respect to their characters fit well in the lab thereby creating a very relaxed and friendly atmosphere.

Furthermore, I'm grateful to Prof. Dr. Georg Krohne for continuously accompanying and advising me from the early semesters of my studies on, in practical courses, during the diploma exams, until finally the end of my PhD. I deeply appreciate that he agreed on being my "Doktorvater" at the University.

My special thanks go to my supervisor Herman Silljé. He was the one who taught me patiently the different techniques and introduced me into the field of mitosis, always open to discuss, explain and help, thereby greatly influencing my current way of performing experiments and approaching problems. With his ongoing optimism, interest in everything and good mood he created a wonderful atmosphere in the lab with respect to both working and personal relationships.

For further technical help I especially like to thank Anja Wehner and Elena Nigg. I like to thank Roman Körner, Francis Barr, Thomas Mayer and Ulli Grüneberg for helpful discussions and my gorgeous sweet labmates, all the other PhD students and postdocs for their scientific support and helpfulness. I'm also grateful to Albert Ries for patiently answering my tons of computer related questions.

I enjoyed the fruitful discussions, the harmless gossip and helpful advice beyond scientific issues during the coffee breaks and lunch times with Eunice, Ravi, Anna, Susanna, Anja, Robert and Xiumin on regular base and the spontaneous time-outs with Evelyn, Kerstin, Christoph and many more people. Outside our department, the meetings in the "ZdB" with Angelika Kuhl and Anna LeBris were especially energising. They are the ones who made me entering the lab happily every morning again even during frustrating and hard times and they are responsible for rendering my PhD time so enjoyable and unforgettable.

I will deeply miss you all.

REFERENCES

1. Abrieu A, Brassac T, Galas S, Fisher D, Labbe JC, and Doree M (1998) The Polo-like kinase Plx1 is a component of the MPF amplification loop at the G2/M-phase transition of the cell cycle in *Xenopus* eggs. *J Cell Sci*, **111** (Pt 12), 1751-1757.
2. Adams RR, Maiato H, Earnshaw WC, and Carmena M (2001) Essential roles of *Drosophila* inner centromere protein (INCENP) and aurora B in histone H3 phosphorylation, metaphase chromosome alignment, kinetochore disjunction, and chromosome segregation. *J Cell Biol*, **153**, 865-880.
3. Ahonen LJ, Kallio MJ, Daum JR, Bolton M, Manke IA, Yaffe MB, Stukenberg PT, and Gorbsky GJ (2005) Polo-like kinase 1 creates the tension-sensing 3F3/2 phosphoepitope and modulates the association of spindle-checkpoint proteins at kinetochores. *Curr Biol*, **15**, 1078-1089.
4. Alexandru G, Uhlmann F, Mechtler K, Poupart MA, and Nasmyth K (2001) Phosphorylation of the cohesin subunit Scc1 by Polo/Cdc5 kinase regulates sister chromatid separation in yeast. *Cell*, **105**, 459-472.
5. Andrews PD, Ovechkina Y, Morrice N, Wagenbach M, Duncan K, Wordeman L, and Swedlow JR (2004) Aurora B regulates MCAK at the mitotic centromere. *Dev Cell*, **6**, 253-268.
6. Arnaoutov A, Azuma Y, Ribbeck K, Joseph J, Boyarchuk Y, Karpova T, McNally J, and Dasso M (2005) Crm1 is a mitotic effector of Ran-GTP in somatic cells. *Nat Cell Biol*, **7**, 626-632.
7. Arnaoutov A and Dasso M (2005) Ran-GTP regulates kinetochore attachment in somatic cells. *Cell Cycle*, **4**, 1161-1165.
8. Arnaud L, Pines J, and Nigg EA (1998) GFP tagging reveals human Polo-like kinase 1 at the kinetochore/centromere region of mitotic chromosomes. *Chromosoma*, **107**, 424-429.
9. Barr FA, Sillje HH, and Nigg EA (2004) Polo-like kinases and the orchestration of cell division. *Nat Rev Mol Cell Biol*, **5**, 429-440.
10. Belgareh N, Rabut G, Bai SW, Van OM, Beaudouin J, Daigle N, Zatssepina OV, Pasteau F, Labas V, Fromont-Racine M, Ellenberg J, and Doye V (2001) An evolutionarily conserved NPC subcomplex, which redistributes in part to kinetochores in mammalian cells. *J Cell Biol*, **154**, 1147-1160.
11. Berdnik D and Knoblich JA (2002) *Drosophila* Aurora-A is required for centrosome maturation and actin-dependent asymmetric protein localization during mitosis. *Curr Biol*, **12**, 640-647.
12. Bharadwaj R, Qi W, and Yu H (2004) Identification of two novel components of the human NDC80 kinetochore complex. *J Biol Chem*, **279**, 13076-13085.
13. Biggins S and Murray AW (2001) The budding yeast protein kinase Ipl1/Aurora allows the absence of tension to activate the spindle checkpoint. *Genes Dev*, **15**, 3118-3129.
14. Biggins S and Walczak CE (2003) Captivating capture: how microtubules attach to kinetochores. *Curr Biol*, **13**, R449-R460.

REFERENCES

15. Blangy A, Lane HA, d'Herin P, Harper M, Kress M, and Nigg EA (1995) Phosphorylation by p34cdc2 regulates spindle association of human Eg5, a kinesin-related motor essential for bipolar spindle formation in vivo. *Cell*, **83**, 1159-1169.
16. Blow JJ and Dutta A (2005) Preventing re-replication of chromosomal DNA. *Nat Rev Mol Cell Biol*, **6**, 476-486.
17. Brassac T, Castro A, Lorca T, Le PC, Doree M, Labbe JC, and Galas S (2000) The polo-like kinase Plx1 prevents premature inactivation of the APC(Fizzy)-dependent pathway in the early *Xenopus* cell cycle. *Oncogene*, **19**, 3782-3790.
18. Brummelkamp TR, Bernards R, and Agami R (2002) A system for stable expression of short interfering RNAs in mammalian cells. *Science*, **296**, 550-553.
19. Carazo-Salas RE, Guarguaglini G, Gruss OJ, Segref A, Karsenti E, and Mattaj IW (1999) Generation of GTP-bound Ran by RCC1 is required for chromatin-induced mitotic spindle formation. *Nature*, **400**, 178-181.
20. Carroll CW and Straight AF (2006) Centromere formation: from epigenetics to self-assembly. *Trends Cell Biol*, **16**, 70-78.
21. Carvalho A, Carmena M, Sambade C, Earnshaw WC, and Wheatley SP (2003) Survivin is required for stable checkpoint activation in taxol-treated HeLa cells. *J Cell Sci*, **116**, 2987-2998.
22. Casenghi M, Meraldi P, Weinhart U, Duncan PI, Korner R, and Nigg EA (2003) Polo-like kinase 1 regulates Nlp, a centrosome protein involved in microtubule nucleation. *Dev Cell*, **5**, 113-125.
23. Chalamalasetty RB, Hummer S, Nigg EA, and Sillje HH (2006) Influence of human Ect2 depletion and overexpression on cleavage furrow formation and abscission. *J Cell Sci*, **119**, 3008-3019.
24. Chan EH, Nousiainen M, Chalamalasetty RB, Schafer A, Nigg EA, and Sillje HH (2005a) The Ste20-like kinase Mst2 activates the human large tumor suppressor kinase Lats1. *Oncogene*, **24**, 2076-2086.
25. Chan GK, Jablonski SA, Sudakin V, Hittle JC, and Yen TJ (1999) Human BUBR1 is a mitotic checkpoint kinase that monitors CENP-E functions at kinetochores and binds the cyclosome/APC. *J Cell Biol*, **146**, 941-954.
26. Chan GK, Liu ST, and Yen TJ (2005b) Kinetochores structure and function. *Trends Cell Biol*, **15**, 589-598.
27. Chan GK and Yen TJ (2003) The mitotic checkpoint: a signaling pathway that allows a single unattached kinetochore to inhibit mitotic exit. *Prog Cell Cycle Res*, **5**, 431-439.
28. Cheeseman IM, Brew C, Wolyniak M, Desai A, Anderson S, Muster N, Yates JR, Huffaker TC, Drubin DG, and Barnes G (2001) Implication of a novel multiprotein Dam1p complex in outer kinetochore function. *J Cell Biol*, **155**, 1137-1145.
29. Chen RH, Shevchenko A, Mann M, and Murray AW (1998) Spindle checkpoint protein Xmad1 recruits Xmad2 to unattached kinetochores. *J Cell Biol*, **143**, 283-295.
30. Chen RH, Waters JC, Salmon ED, and Murray AW (1996) Association of spindle assembly checkpoint component XMAD2 with unattached kinetochores. *Science*, **274**, 242-246.

31. Cheng KY, Lowe ED, Sinclair J, Nigg EA, and Johnson LN (2003) The crystal structure of the human polo-like kinase-1 polo box domain and its phospho-peptide complex. *EMBO J*, **22**, 5757-5768.
32. Ciferri C, De LJ, Monzani S, Ferrari KJ, Ristic D, Wyman C, Stark H, Kilmartin J, Salmon ED, and Musacchio A (2005) Architecture of the human ndc80-hec1 complex, a critical constituent of the outer kinetochore. *J Biol Chem*, **280**, 29088-29095.
33. Cimini D, Wan X, Hirel CB, and Salmon ED (2006) Aurora kinase promotes turnover of kinetochore microtubules to reduce chromosome segregation errors. *Curr Biol*, **16**, 1711-1718.
34. Clarke AS, Tang TT, Ooi DL, and Orr-Weaver TL (2005) POLO kinase regulates the Drosophila centromere cohesion protein MEI-S332. *Dev Cell*, **8**, 53-64.
35. Cleveland DW, Mao Y, and Sullivan KF (2003) Centromeres and kinetochores: from epigenetics to mitotic checkpoint signaling. *Cell*, **112**, 407-421.
36. De AA, Pearson CG, Cimini D, Canman JC, Sala V, Nezi L, Mapelli M, Sironi L, Faretta M, Salmon ED, and Musacchio A (2005) The Mad1/Mad2 complex as a template for Mad2 activation in the spindle assembly checkpoint. *Curr Biol*, **15**, 214-225.
37. DeAntoni A, Sala V, and Musacchio A (2005) Explaining the oligomerization properties of the spindle assembly checkpoint protein Mad2. *Philos Trans R Soc Lond B Biol Sci*, **360**, 637-47, discussion.
38. Debec A, Detraves C, Montmory C, Geraud G, and Wright M (1995) Polar organization of gamma-tubulin in acentriolar mitotic spindles of Drosophila melanogaster cells. *J Cell Sci*, **108 (Pt 7)**, 2645-2653.
39. DeLuca JG, Dong Y, Hergert P, Strauss J, Hickey JM, Salmon ED, and McEwen BF (2005) Hec1 and nuf2 are core components of the kinetochore outer plate essential for organizing microtubule attachment sites. *Mol Biol Cell*, **16**, 519-531.
40. DeLuca JG, Moree B, Hickey JM, Kilmartin JV, and Salmon ED (2002) hNuf2 inhibition blocks stable kinetochore-microtubule attachment and induces mitotic cell death in HeLa cells. *J Cell Biol*, **159**, 549-555.
41. Descombes P and Nigg EA (1998) The polo-like kinase Plx1 is required for M phase exit and destruction of mitotic regulators in Xenopus egg extracts. *EMBO J*, **17**, 1328-1335.
42. Dewar H, Tanaka K, Nasmyth K, and Tanaka TU (2004) Tension between two kinetochores suffices for their bi-orientation on the mitotic spindle. *Nature*, **428**, 93-97.
43. Ditchfield C, Johnson VL, Tighe A, Ellston R, Haworth C, Johnson T, Mortlock A, Keen N, and Taylor SS (2003) Aurora B couples chromosome alignment with anaphase by targeting BubR1, Mad2, and Cenp-E to kinetochores. *J Cell Biol*, **161**, 267-280.
44. do Carmo AM, Tavares A, and Glover DM (2001) Polo kinase and Asp are needed to promote the mitotic organizing activity of centrosomes. *Nat Cell Biol*, **3**, 421-424.
45. Dujardin D, Wacker UI, Moreau A, Schroer TA, Rickard JE, and De M, Jr. (1998) Evidence for a role of CLIP-170 in the establishment of metaphase chromosome alignment. *J Cell Biol*, **141**, 849-862.
46. Elbashir SM, Harborth J, Lendeckel W, Yalcin A, Weber K, and Tuschl T (2001) Duplexes of 21-nucleotide RNAs mediate RNA interference in cultured mammalian cells. *Nature*, **411**, 494-498.

REFERENCES

47. Elia AE, Cantley LC, and Yaffe MB (2003a) Proteomic screen finds pSer/pThr-binding domain localizing Plk1 to mitotic substrates. *Science*, **299**, 1228-1231.
48. Elia AE, Rellos P, Haire LF, Chao JW, Ivins FJ, Hoepker K, Mohammad D, Cantley LC, Smerdon SJ, and Yaffe MB (2003b) The molecular basis for phosphodependent substrate targeting and regulation of Plks by the Polo-box domain. *Cell*, **115**, 83-95.
49. Ellinger-Ziegelbauer H, Karasuyama H, Yamada E, Tsujikawa K, Todokoro K, and Nishida E (2000) Ste20-like kinase (SLK), a regulatory kinase for polo-like kinase (Plk) during the G2/M transition in somatic cells. *Genes Cells*, **5**, 491-498.
50. Fang G (2002) Checkpoint protein BubR1 acts synergistically with Mad2 to inhibit anaphase-promoting complex. *Mol Biol Cell*, **13**, 755-766.
51. Fang G, Yu H, and Kirschner MW (1998) The checkpoint protein MAD2 and the mitotic regulator CDC20 form a ternary complex with the anaphase-promoting complex to control anaphase initiation. *Genes Dev*, **12**, 1871-1883.
52. Ferrari S (2006) Protein kinases controlling the onset of mitosis. *Cell Mol Life Sci*, **63**, 781-795.
53. Gadde S and Heald R (2004) Mechanisms and molecules of the mitotic spindle. *Curr Biol*, **14**, R797-R805.
54. Gaglio T, Saredi A, Bingham JB, Hasbani MJ, Gill SR, Schroer TA, and Compton DA (1996) Opposing motor activities are required for the organization of the mammalian mitotic spindle pole. *J Cell Biol*, **135**, 399-414.
55. Gimenez-Abian JF, Sumara I, Hirota T, Hauf S, Gerlich D, de la TC, Ellenberg J, and Peters JM (2004) Regulation of sister chromatid cohesion between chromosome arms. *Curr Biol*, **14**, 1187-1193.
56. Golan A, Yudkovsky Y, and Hershko A (2002) The cyclin-ubiquitin ligase activity of cyclosome/APC is jointly activated by protein kinases Cdk1-cyclin B and Plk. *J Biol Chem*, **277**, 15552-15557.
57. Golsteyn RM, Mundt KE, Fry AM, and Nigg EA (1995) Cell cycle regulation of the activity and subcellular localization of Plk1, a human protein kinase implicated in mitotic spindle function. *J Cell Biol*, **129**, 1617-1628.
58. Gorbsky GJ and Ricketts WA (1993) Differential expression of a phosphoepitope at the kinetochores of moving chromosomes. *J Cell Biol*, **122**, 1311-1321.
59. Green RA, Wollman R, and Kaplan KB (2005) APC and EB1 function together in mitosis to regulate spindle dynamics and chromosome alignment. *Mol Biol Cell*, **16**, 4609-4622.
60. Gruss OJ and Vernos I (2004) The mechanism of spindle assembly: functions of Ran and its target TPX2. *J Cell Biol*, **166**, 949-955.
61. Habu T, Kim SH, Weinstein J, and Matsumoto T (2002) Identification of a MAD2-binding protein, CMT2, and its role in mitosis. *EMBO J*, **21**, 6419-6428.
62. Hannak E, Kirkham M, Hyman AA, and Oegema K (2001) Aurora-A kinase is required for centrosome maturation in *Caenorhabditis elegans*. *J Cell Biol*, **155**, 1109-1116.
63. Harvey KF, Pflieger CM, and Hariharan IK (2003) The *Drosophila* Mst ortholog, hippo, restricts growth and cell proliferation and promotes apoptosis. *Cell*, **114**, 457-467.

REFERENCES

64. Hauf S, Roitinger E, Koch B, Dittrich CM, Mechtler K, and Peters JM (2005) Dissociation of cohesin from chromosome arms and loss of arm cohesion during early mitosis depends on phosphorylation of SA2. *PLoS Biol*, **3**, e69.
65. Hayden JH, Bowser SS, and Rieder CL (1990) Kinetochores capture astral microtubules during chromosome attachment to the mitotic spindle: direct visualization in live newt lung cells. *J Cell Biol*, **111**, 1039-1045.
66. Heald R, Tournebise R, Blank T, Sandaltzopoulos R, Becker P, Hyman A, and Karsenti E (1996) Self-organization of microtubules into bipolar spindles around artificial chromosomes in *Xenopus* egg extracts. *Nature*, **382**, 420-425.
67. Hoffmann I, Clarke PR, Marcote MJ, Karsenti E, and Draetta G (1993) Phosphorylation and activation of human cdc25-C by cdc2--cyclin B and its involvement in the self-amplification of MPF at mitosis. *EMBO J*, **12**, 53-63.
68. Hofmann C, Cheeseman IM, Goode BL, McDonald KL, Barnes G, and Drubin DG (1998) *Saccharomyces cerevisiae* Duo1p and Dam1p, novel proteins involved in mitotic spindle function. *J Cell Biol*, **143**, 1029-1040.
69. Hori T, Haraguchi T, Hiraoka Y, Kimura H, and Fukagawa T (2003) Dynamic behavior of Nuf2-Hec1 complex that localizes to the centrosome and centromere and is essential for mitotic progression in vertebrate cells. *J Cell Sci*, **116**, 3347-3362.
70. Howell BJ, Hoffman DB, Fang G, Murray AW, and Salmon ED (2000) Visualization of Mad2 dynamics at kinetochores, along spindle fibers, and at spindle poles in living cells. *J Cell Biol*, **150**, 1233-1250.
71. Howell BJ, McEwen BF, Canman JC, Hoffman DB, Farrar EM, Rieder CL, and Salmon ED (2001) Cytoplasmic dynein/dynactin drives kinetochore protein transport to the spindle poles and has a role in mitotic spindle checkpoint inactivation. *J Cell Biol*, **155**, 1159-1172.
72. Hoyt MA (2001) A new view of the spindle checkpoint. *J Cell Biol*, **154**, 909-911.
73. Hoyt MA, Totis L, and Roberts BT (1991) *S. cerevisiae* genes required for cell cycle arrest in response to loss of microtubule function. *Cell*, **66**, 507-517.
74. Hwang LH, Lau LF, Smith DL, Mistrot CA, Hardwick KG, Hwang ES, Amon A, and Murray AW (1998) Budding yeast Cdc20: a target of the spindle checkpoint. *Science*, **279**, 1041-1044.
75. Iouk T, Kerscher O, Scott RJ, Basrai MA, and Wozniak RW (2002) The yeast nuclear pore complex functionally interacts with components of the spindle assembly checkpoint. *J Cell Biol*, **159**, 807-819.
76. James P, Halladay J, and Craig EA (1996) Genomic libraries and a host strain designed for highly efficient two-hybrid selection in yeast. *Genetics*, **144**, 1425-1436.
77. Jang YJ, Lin CY, Ma S, and Erikson RL (2002a) Functional studies on the role of the C-terminal domain of mammalian polo-like kinase. *Proc Natl Acad Sci U S A*, **99**, 1984-1989.
78. Jang YJ, Ma S, Terada Y, and Erikson RL (2002b) Phosphorylation of threonine 210 and the role of serine 137 in the regulation of mammalian polo-like kinase. *J Biol Chem*, **277**, 44115-44120.
79. Janke C, Ortiz J, Tanaka TU, Lechner J, and Schiebel E (2002) Four new subunits of the Dam1-Duo1 complex reveal novel functions in sister kinetochore biorientation. *EMBO J*, **21**, 181-193.

REFERENCES

80. Jeganathan KB, Malureanu L, and van Deursen JM (2005) The Rae1-Nup98 complex prevents aneuploidy by inhibiting securin degradation. *Nature*, **438**, 1036-1039.
81. Joseph J, Liu ST, Jablonski SA, Yen TJ, and Dasso M (2004) The RanGAP1-RanBP2 complex is essential for microtubule-kinetochore interactions in vivo. *Curr Biol*, **14**, 611-617.
82. Joseph J, Tan SH, Karpova TS, McNally JG, and Dasso M (2002) SUMO-1 targets RanGAP1 to kinetochores and mitotic spindles. *J Cell Biol*, **156**, 595-602.
83. Kallio MJ, McClelland ML, Stukenberg PT, and Gorbsky GJ (2002) Inhibition of aurora B kinase blocks chromosome segregation, overrides the spindle checkpoint, and perturbs microtubule dynamics in mitosis. *Curr Biol*, **12**, 900-905.
84. Kapoor TM and Compton DA (2002) Searching for the middle ground: mechanisms of chromosome alignment during mitosis. *J Cell Biol*, **157**, 551-556.
85. Kapoor TM, Lampson MA, Hergert P, Cameron L, Cimini D, Salmon ED, McEwen BF, and Khodjakov A (2006) Chromosomes can congress to the metaphase plate before biorientation. *Science*, **311**, 388-391.
86. Kapoor TM, Mayer TU, Coughlin ML, and Mitchison TJ (2000) Probing spindle assembly mechanisms with monastrol, a small molecule inhibitor of the mitotic kinesin, Eg5. *J Cell Biol*, **150**, 975-988.
87. Karsenti E, Newport J, and Kirschner M (1984) Respective roles of centrosomes and chromatin in the conversion of microtubule arrays from interphase to metaphase. *J Cell Biol*, **99**, 47s-54s.
88. Khodjakov A, Cole RW, Oakley BR, and Rieder CL (2000) Centrosome-independent mitotic spindle formation in vertebrates. *Curr Biol*, **10**, 59-67.
89. Khodjakov A, Copenagle L, Gordon MB, Compton DA, and Kapoor TM (2003) Minus-end capture of preformed kinetochore fibers contributes to spindle morphogenesis. *J Cell Biol*, **160**, 671-683.
90. Khodjakov A and Rieder CL (1999) The sudden recruitment of gamma-tubulin to the centrosome at the onset of mitosis and its dynamic exchange throughout the cell cycle, do not require microtubules. *J Cell Biol*, **146**, 585-596.
91. Kim SH, Lin DP, Matsumoto S, Kitazono A, and Matsumoto T (1998) Fission yeast Slp1: an effector of the Mad2-dependent spindle checkpoint. *Science*, **279**, 1045-1047.
92. Kimura K, Hirano M, Kobayashi R, and Hirano T (1998) Phosphorylation and activation of 13S condensin by Cdc2 in vitro. *Science*, **282**, 487-490.
93. King JM and Nicklas RB (2000) Tension on chromosomes increases the number of kinetochore microtubules but only within limits. *J Cell Sci*, **113 Pt 21**, 3815-3823.
94. Kirschner M and Mitchison T (1986) Beyond self-assembly: from microtubules to morphogenesis. *Cell*, **45**, 329-342.
95. Kline-Smith SL, Khodjakov A, Hergert P, and Walczak CE (2004) Depletion of centromeric MCAK leads to chromosome congression and segregation defects due to improper kinetochore attachments. *Mol Biol Cell*, **15**, 1146-1159.
96. Knowlton AL, Lan W, and Stukenberg PT (2006) Aurora B is enriched at merotelic attachment sites, where it regulates MCAK. *Curr Biol*, **16**, 1705-1710.

REFERENCES

97. Kotani S, Tanaka H, Yasuda H, and Todokoro K (1999) Regulation of APC activity by phosphorylation and regulatory factors. *J Cell Biol*, **146**, 791-800.
98. Kotani S, Tugendreich S, Fujii M, Jorgensen PM, Watanabe N, Hoog C, Hieter P, and Todokoro K (1998) PKA and MPF-activated polo-like kinase regulate anaphase-promoting complex activity and mitosis progression. *Mol Cell*, **1**, 371-380.
99. Kraft C, Herzog F, Gieffers C, Mechtler K, Hagting A, Pines J, and Peters JM (2003) Mitotic regulation of the human anaphase-promoting complex by phosphorylation. *EMBO J*, **22**, 6598-6609.
100. Kufer TA, Nigg EA, and Sillje HH (2003) Regulation of Aurora-A kinase on the mitotic spindle. *Chromosoma*, **112**, 159-163.
101. Kumagai A and Dunphy WG (1996) Purification and molecular cloning of Plx1, a Cdc25-regulatory kinase from *Xenopus* egg extracts. *Science*, **273**, 1377-1380.
102. Lampson MA and Kapoor TM (2005) The human mitotic checkpoint protein BubR1 regulates chromosome-spindle attachments. *Nat Cell Biol*, **7**, 93-98.
103. Lampson MA, Renduchitala K, Khodjakov A, and Kapoor TM (2004) Correcting improper chromosome-spindle attachments during cell division. *Nat Cell Biol*, **6**, 232-237.
104. Lan W, Zhang X, Kline-Smith SL, Rosasco SE, Barrett-Wilt GA, Shabanowitz J, Hunt DF, Walczak CE, and Stukenberg PT (2004) Aurora B phosphorylates centromeric MCAK and regulates its localization and microtubule depolymerization activity. *Curr Biol*, **14**, 273-286.
105. Lane HA and Nigg EA (1996) Antibody microinjection reveals an essential role for human polo-like kinase 1 (Plk1) in the functional maturation of mitotic centrosomes. *J Cell Biol*, **135**, 1701-1713.
106. Lee KK, Ohyama T, Yajima N, Tsubuki S, and Yonehara S (2001) MST, a physiological caspase substrate, highly sensitizes apoptosis both upstream and downstream of caspase activation. *J Biol Chem*, **276**, 19276-19285.
107. Lee KS, Grenfell TZ, Yarm FR, and Erikson RL (1998) Mutation of the polo-box disrupts localization and mitotic functions of the mammalian polo kinase Plk. *Proc Natl Acad Sci U S A*, **95**, 9301-9306.
108. Lee KS, Song S, and Erikson RL (1999) The polo-box-dependent induction of ectopic septal structures by a mammalian polo kinase, plk, in *Saccharomyces cerevisiae*. *Proc Natl Acad Sci U S A*, **96**, 14360-14365.
109. Lee KS, Yuan YL, Kuriyama R, and Erikson RL (1995) Plk is an M-phase-specific protein kinase and interacts with a kinesin-like protein, CHO1/MKLP-1. *Mol Cell Biol*, **15**, 7143-7151.
110. Li R and Murray AW (1991) Feedback control of mitosis in budding yeast. *Cell*, **66**, 519-531.
111. Li W, Lan Z, Wu H, Wu S, Meadows J, Chen J, Zhu V, and Dai W (1999) BUBR1 phosphorylation is regulated during mitotic checkpoint activation. *Cell Growth Differ*, **10**, 769-775.
112. Li X and Nicklas RB (1997) Tension-sensitive kinetochore phosphorylation and the chromosome distribution checkpoint in praying mantid spermatocytes. *J Cell Sci*, **110 (Pt 5)**, 537-545.

REFERENCES

113. Li Y and Benezra R (1996) Identification of a human mitotic checkpoint gene: hsMAD2. *Science*, **274**, 246-248.
114. Lindon C and Pines J (2004) Ordered proteolysis in anaphase inactivates Plk1 to contribute to proper mitotic exit in human cells. *J Cell Biol*, **164**, 233-241.
115. Liodice I, Alves A, Rabut G, Van OM, Ellenberg J, Sibarita JB, and Doye V (2004) The entire Nup107-160 complex, including three new members, is targeted as one entity to kinetochores in mitosis. *Mol Biol Cell*, **15**, 3333-3344.
116. Lowe M, Rabouille C, Nakamura N, Watson R, Jackman M, Jamsa E, Rahman D, Pappin DJ, and Warren G (1998) Cdc2 kinase directly phosphorylates the cis-Golgi matrix protein GM130 and is required for Golgi fragmentation in mitosis. *Cell*, **94**, 783-793.
117. Lowery DM, Lim D, and Yaffe MB (2005) Structure and function of Polo-like kinases. *Oncogene*, **24**, 248-259.
118. Luo X, Tang Z, Rizo J, and Yu H (2002) The Mad2 spindle checkpoint protein undergoes similar major conformational changes upon binding to either Mad1 or Cdc20. *Mol Cell*, **9**, 59-71.
119. Luo X, Tang Z, Xia G, Wassmann K, Matsumoto T, Rizo J, and Yu H (2004) The Mad2 spindle checkpoint protein has two distinct natively folded states. *Nat Struct Mol Biol*, **11**, 338-345.
120. Maddox P, Straight A, Coughlin P, Mitchison TJ, and Salmon ED (2003) Direct observation of microtubule dynamics at kinetochores in *Xenopus* extract spindles: implications for spindle mechanics. *J Cell Biol*, **162**, 377-382.
121. Maiato H, Fairley EA, Rieder CL, Swedlow JR, Sunkel CE, and Earnshaw WC (2003) Human CLASP1 is an outer kinetochore component that regulates spindle microtubule dynamics. *Cell*, **113**, 891-904.
122. Maiato H, Khodjakov A, and Rieder CL (2005) *Drosophila* CLASP is required for the incorporation of microtubule subunits into fluxing kinetochore fibres. *Nat Cell Biol*, **7**, 42-47.
123. Maiato H, Rieder CL, and Khodjakov A (2004) Kinetochore-driven formation of kinetochore fibers contributes to spindle assembly during animal mitosis. *J Cell Biol*, **167**, 831-840.
124. Maiato H and Sunkel CE (2004) Kinetochore-microtubule interactions during cell division. *Chromosome Res*, **12**, 585-597.
125. Maiorano D, Lutzmann M, and Mechali M (2006) MCM proteins and DNA replication. *Curr Opin Cell Biol*, **18**, 130-136.
126. Martin-Lluesma S, Stucke VM, and Nigg EA (2002) Role of Hec1 in spindle checkpoint signaling and kinetochore recruitment of Mad1/Mad2. *Science*, **297**, 2267-2270.
127. Marumoto T, Zhang D, and Saya H (2005) Aurora-A - a guardian of poles. *Nat Rev Cancer*, **5**, 42-50.
128. Mayer TU, Kapoor TM, Haggarty SJ, King RW, Schreiber SL, and Mitchison TJ (1999) Small molecule inhibitor of mitotic spindle bipolarity identified in a phenotype-based screen. *Science*, **286**, 971-974.
129. Mazumdar M and Misteli T (2005) Chromokinesins: multitasking players in mitosis. *Trends Cell Biol*, **15**, 349-355.

REFERENCES

130. McClelland ML, Gardner RD, Kallio MJ, Daum JR, Gorbsky GJ, Burke DJ, and Stukenberg PT (2003) The highly conserved Ndc80 complex is required for kinetochore assembly, chromosome congression, and spindle checkpoint activity. *Genes Dev*, **17**, 101-114.
131. McClelland ML, Kallio MJ, Barrett-Wilt GA, Kestner CA, Shabanowitz J, Hunt DF, Gorbsky GJ, and Stukenberg PT (2004) The vertebrate Ndc80 complex contains Spc24 and Spc25 homologs, which are required to establish and maintain kinetochore-microtubule attachment. *Curr Biol*, **14**, 131-137.
132. McEwen BF, Chan GK, Zubrowski B, Savoian MS, Sauer MT, and Yen TJ (2001) CENP-E is essential for reliable bioriented spindle attachment, but chromosome alignment can be achieved via redundant mechanisms in mammalian cells. *Mol Biol Cell*, **12**, 2776-2789.
133. McEwen BF, Hsieh CE, Mattheyses AL, and Rieder CL (1998) A new look at kinetochore structure in vertebrate somatic cells using high-pressure freezing and freeze substitution. *Chromosoma*, **107**, 366-375.
134. McGuinness BE, Hirota T, Kudo NR, Peters JM, and Nasmyth K (2005) Shugoshin prevents dissociation of cohesin from centromeres during mitosis in vertebrate cells. *PLoS Biol*, **3**, e86.
135. Meraldi P, McAinsh AD, Rheinbay E, and Sorger PK (2006) Phylogenetic and structural analysis of centromeric DNA and kinetochore proteins. *Genome Biol*, **7**, R23.
136. Miranda JJ, De WP, Sorger PK, and Harrison SC (2005) The yeast DASH complex forms closed rings on microtubules. *Nat Struct Mol Biol*, **12**, 138-143.
137. Mitchison T, Evans L, Schulze E, and Kirschner M (1986) Sites of microtubule assembly and disassembly in the mitotic spindle. *Cell*, **45**, 515-527.
138. Mitchison T and Kirschner M (1984) Dynamic instability of microtubule growth. *Nature*, **312**, 237-242.
139. Mitchison TJ (1989) Polewards microtubule flux in the mitotic spindle: evidence from photoactivation of fluorescence. *J Cell Biol*, **109**, 637-652.
140. Moshe Y, Boulaire J, Pagano M, and Hershko A (2004) Role of Polo-like kinase in the degradation of early mitotic inhibitor 1, a regulator of the anaphase promoting complex/cyclosome. *Proc Natl Acad Sci U S A*, **101**, 7937-7942.
141. Mundt KE, Golsteyn RM, Lane HA, and Nigg EA (1997) On the regulation and function of human polo-like kinase 1 (PLK1): effects of overexpression on cell cycle progression. *Biochem Biophys Res Commun*, **239**, 377-385.
142. Murray AW (2004) Recycling the cell cycle: cyclins revisited. *Cell*, **116**, 221-234.
143. Musacchio A and Hardwick KG (2002) The spindle checkpoint: structural insights into dynamic signalling. *Nat Rev Mol Cell Biol*, **3**, 731-741.
144. Nakajima H, Toyoshima-Morimoto F, Taniguchi E, and Nishida E (2003) Identification of a consensus motif for Plk (Polo-like kinase) phosphorylation reveals Myt1 as a Plk1 substrate. *J Biol Chem*, **278**, 25277-25280.
145. Nakamura M, Zhou XZ, and Lu KP (2001) Critical role for the EB1 and APC interaction in the regulation of microtubule polymerization. *Curr Biol*, **11**, 1062-1067.
146. Neef R, Preisinger C, Sutcliffe J, Kopajtich R, Nigg EA, Mayer TU, and Barr FA (2003) Phosphorylation of mitotic kinesin-like protein 2 by polo-like kinase 1 is required for cytokinesis. *J Cell Biol*, **162**, 863-875.

REFERENCES

147. Nicklas RB, Campbell MS, Ward SC, and Gorbsky GJ (1998) Tension-sensitive kinetochore phosphorylation in vitro. *J Cell Sci*, **111 (Pt 21)**, 3189-3196.
148. Nicklas RB and Ward SC (1994) Elements of error correction in mitosis: microtubule capture, release, and tension. *J Cell Biol*, **126**, 1241-1253.
149. Nicklas RB, Ward SC, and Gorbsky GJ (1995) Kinetochore chemistry is sensitive to tension and may link mitotic forces to a cell cycle checkpoint. *J Cell Biol*, **130**, 929-939.
150. Nigg EA (2001) Mitotic kinases as regulators of cell division and its checkpoints. *Nat Rev Mol Cell Biol*, **2**, 21-32.
151. Nishino M, Kurasawa Y, Evans R, Lin SH, Brinkley BR, and Yu-Lee LY (2006) NudC is required for Plk1 targeting to the kinetochore and chromosome congression. *Curr Biol*, **16**, 1414-1421.
152. Orjalo AV, Arnautov A, Shen Z, Boyarchuk Y, Zeitlin SG, Fontoura B, Briggs S, Dasso M, and Forbes DJ (2006) The Nup107-160 nucleoporin complex is required for correct bipolar spindle assembly. *Mol Biol Cell*, **17**, 3806-3818.
153. Palazzo RE, Vogel JM, Schnackenberg BJ, Hull DR, and Wu X (2000) Centrosome maturation. *Curr Top Dev Biol*, **49:449-70.**, 449-470.
154. Palmer DK, O'Day K, Trong HL, Charbonneau H, and Margolis RL (1991) Purification of the centromere-specific protein CENP-A and demonstration that it is a distinctive histone. *Proc Natl Acad Sci U S A*, **88**, 3734-3738.
155. Paoletti A, Moudjou M, Paintrand M, Salisbury JL, and Bornens M (1996) Most of centrin in animal cells is not centrosome-associated and centrosomal centrin is confined to the distal lumen of centrioles. *J Cell Sci*, **109**, 3089-3102.
156. Patra D and Dunphy WG (1998) Xe-p9, a Xenopus Suc1/Cks protein, is essential for the Cdc2-dependent phosphorylation of the anaphase-promoting complex at mitosis. *Genes Dev*, **12**, 2549-2559.
157. Perez F, Diamantopoulos GS, Stalder R, and Kreis TE (1999) CLIP-170 highlights growing microtubule ends in vivo. *Cell*, **96**, 517-527.
158. Peter M, Heitlinger E, Haner M, Aebi U, and Nigg EA (1991) Disassembly of in vitro formed lamin head-to-tail polymers by CDC2 kinase. *EMBO J*, **10**, 1535-1544.
159. Pfarr CM, Coue M, Grissom PM, Hays TS, Porter ME, and McIntosh JR (1990) Cytoplasmic dynein is localized to kinetochores during mitosis. *Nature*, **345**, 263-265.
160. Pinsky BA and Biggins S (2005) The spindle checkpoint: tension versus attachment. *Trends Cell Biol*, **15**, 486-493.
161. Qi W, Tang Z, and Yu H (2006) Phosphorylation- and Polo-Box-dependent Binding of Plk1 to Bub1 Is Required for the Kinetochore Localization of Plk1. *Mol Biol Cell*, ..
162. Qian YW, Erikson E, and Maller JL (1998) Purification and cloning of a protein kinase that phosphorylates and activates the polo-like kinase Plx1. *Science*, **282**, 1701-1704.
163. Rattner JB, Rao A, Fritzler MJ, Valencia DW, and Yen TJ (1993) CENP-F is a .ca 400 kDa kinetochore protein that exhibits a cell-cycle dependent localization. *Cell Motil Cytoskeleton*, **26**, 214-226.

164. Reynolds N and Ohkura H (2003) Polo boxes form a single functional domain that mediates interactions with multiple proteins in fission yeast polo kinase. *J Cell Sci*, **116**, 1377-1387.
165. Rieder CL (1982) The formation, structure, and composition of the mammalian kinetochore and kinetochore fiber. *Int Rev Cytol*, **79**, 1-58.
166. Rieder CL (1981) The structure of the cold-stable kinetochore fiber in metaphase PtK1 cells. *Chromosoma*, **84**, 145-158.
167. Rieder CL (2005) Kinetochore fiber formation in animal somatic cells: dueling mechanisms come to a draw. *Chromosoma*, **114**, 310-318.
168. Rieder CL and Alexander SP (1990) Kinetochores are transported poleward along a single astral microtubule during chromosome attachment to the spindle in newt lung cells. *J Cell Biol*, **110**, 81-95.
169. Rieder CL, Cole RW, Khodjakov A, and Sluder G (1995) The checkpoint delaying anaphase in response to chromosome monoorientation is mediated by an inhibitory signal produced by unattached kinetochores. *J Cell Biol*, **130**, 941-948.
170. Rieder CL, Schultz A, Cole R, and Sluder G (1994) Anaphase onset in vertebrate somatic cells is controlled by a checkpoint that monitors sister kinetochore attachment to the spindle. *J Cell Biol*, **127**, 1301-1310.
171. Rogers SL, Rogers GC, Sharp DJ, and Vale RD (2002) Drosophila EB1 is important for proper assembly, dynamics, and positioning of the mitotic spindle. *J Cell Biol*, **158**, 873-884.
172. Salina D, Enarson P, Rattner JB, and Burke B (2003) Nup358 integrates nuclear envelope breakdown with kinetochore assembly. *J Cell Biol*, **162**, 991-1001.
173. Sanchez-Perez I, Renwick SJ, Crawley K, Karig I, Buck V, Meadows JC, Franco-Sanchez A, Fleig U, Toda T, and Millar JB (2005) The DASH complex and Klp5/Klp6 kinesin coordinate bipolar chromosome attachment in fission yeast. *EMBO J*, **24**, 2931-2943.
174. Sauer G, Korner R, Hanisch A, Ries A, Nigg EA, and Sillje HH (2005) Proteome analysis of the human mitotic spindle. *Mol Cell Proteomics*, **4**, 35-43.
175. Schaar BT, Chan GK, Maddox P, Salmon ED, and Yen TJ (1997) CENP-E function at kinetochores is essential for chromosome alignment. *J Cell Biol*, **139**, 1373-1382.
176. Schmidt A, Duncan PI, Rauh NR, Sauer G, Fry AM, Nigg EA, and Mayer TU (2005) Xenopus polo-like kinase Plx1 regulates XErp1, a novel inhibitor of APC/C activity. *Genes Dev*, **19**, 502-513.
177. Seelos C (1997) A critical parameter determining the aging of DNA-calcium-phosphate precipitates. *Anal Biochem*, **245**, 109-111.
178. Seong YS, Kamijo K, Lee JS, Fernandez E, Kuriyama R, Miki T, and Lee KS (2002) A spindle checkpoint arrest and a cytokinesis failure by the dominant-negative polo-box domain of Plk1 in U-2 OS cells. *J Biol Chem*, **277**, 32282-32293.
179. Shah JV and Cleveland DW (2000) Waiting for anaphase: Mad2 and the spindle assembly checkpoint. *Cell*, **103**, 997-1000.
180. Sharp DJ, Rogers GC, and Scholey JM (2000) Cytoplasmic dynein is required for poleward chromosome movement during mitosis in Drosophila embryos. *Nat Cell Biol*, **2**, 922-930.

REFERENCES

181. Shirayama M, Zachariae W, Ciosk R, and Nasmyth K (1998) The Polo-like kinase Cdc5p and the WD-repeat protein Cdc20p/fizzy are regulators and substrates of the anaphase promoting complex in *Saccharomyces cerevisiae*. *EMBO J*, **17**, 1336-1349.
182. Shonn MA, McCarroll R, and Murray AW (2000) Requirement of the spindle checkpoint for proper chromosome segregation in budding yeast meiosis. *Science*, **289**, 300-303.
183. Sillje HH, Nagel S, Korner R, and Nigg EA (2006) HURP is a Ran-importin beta-regulated protein that stabilizes kinetochore microtubules in the vicinity of chromosomes. *Curr Biol*, **16**, 731-742.
184. Skibbens RV, Skeen VP, and Salmon ED (1993) Directional instability of kinetochore motility during chromosome congression and segregation in mitotic newt lung cells: a push-pull mechanism. *J Cell Biol*, **122**, 859-875.
185. Skoufias DA, Andreassen PR, Lacroix FB, Wilson L, and Margolis RL (2001) Mammalian mad2 and bub1/bubR1 recognize distinct spindle-attachment and kinetochore-tension checkpoints. *Proc Natl Acad Sci U S A*, **98**, 4492-4497.
186. Stern BM and Murray AW (2001) Lack of tension at kinetochores activates the spindle checkpoint in budding yeast. *Curr Biol*, **11**, 1462-1467.
187. Steuer ER, Wordeman L, Schroer TA, and Sheetz MP (1990) Localization of cytoplasmic dynein to mitotic spindles and kinetochores. *Nature*, **345**, 266-268.
188. Stucke VM, Baumann C, and Nigg EA (2004) Kinetochore localization and microtubule interaction of the human spindle checkpoint kinase Mps1. *Chromosoma*, **113**, 1-15.
189. Sudakin V, Chan GK, and Yen TJ (2001) Checkpoint inhibition of the APC/C in HeLa cells is mediated by a complex of BUBR1, BUB3, CDC20, and MAD2. *J Cell Biol*, **154**, 925-936.
190. Sullivan KF, Hechenberger M, and Masri K (1994) Human CENP-A contains a histone H3 related histone fold domain that is required for targeting to the centromere. *J Cell Biol*, **127**, 581-592.
191. Sumara I, Gimenez-Abian JF, Gerlich D, Hirota T, Kraft C, de la TC, Ellenberg J, and Peters JM (2004) Roles of polo-like kinase 1 in the assembly of functional mitotic spindles. *Curr Biol*, **14**, 1712-1722.
192. Sumara I, Vorlaufer E, Stukenberg PT, Kelm O, Redemann N, Nigg EA, and Peters JM (2002) The dissociation of cohesin from chromosomes in prophase is regulated by Polo-like kinase. *Mol Cell*, **9**, 515-525.
193. Sunkel CE and Glover DM (1988) polo, a mitotic mutant of *Drosophila* displaying abnormal spindle poles. *J Cell Sci*, **89 (Pt 1)**, 25-38.
194. Szollosi D, Calarco P, and Donahue RP (1972) Absence of centrioles in the first and second meiotic spindles of mouse oocytes. *J Cell Sci*, **11**, 521-541.
195. Tanaka TU, Rachidi N, Janke C, Pereira G, Galova M, Schiebel E, Stark MJ, and Nasmyth K (2002) Evidence that the Ipl1-Sli15 (Aurora kinase-INCENP) complex promotes chromosome bi-orientation by altering kinetochore-spindle pole connections. *Cell*, **108**, 317-329.
196. Tanenbaum ME, Galjart N, van Vugt MA, and Medema RH (2006) CLIP-170 facilitates the formation of kinetochore-microtubule attachments. *EMBO J*, **25**, 45-57.
197. Tang Z, Bharadwaj R, Li B, and Yu H (2001) Mad2-Independent inhibition of APCCdc20 by the mitotic checkpoint protein BubR1. *Dev Cell*, **1**, 227-237.

198. Tang Z, Shu H, Oncel D, Chen S, and Yu H (2004) Phosphorylation of Cdc20 by Bub1 provides a catalytic mechanism for APC/C inhibition by the spindle checkpoint. *Mol Cell*, **16**, 387-397.
199. Tanudji M, Shoemaker J, L'Italien L, Russell L, Chin G, and Schebye XM (2004) Gene silencing of CENP-E by small interfering RNA in HeLa cells leads to missegregation of chromosomes after a mitotic delay. *Mol Biol Cell*, **15**, 3771-3781.
200. Taylor SS, Ha E, and McKeon F (1998) The human homologue of Bub3 is required for kinetochore localization of Bub1 and a Mad3/Bub1-related protein kinase. *J Cell Biol*, **142**, 1-11.
201. Taylor SS, Hussein D, Wang Y, Elderkin S, and Morrow CJ (2001) Kinetochore localisation and phosphorylation of the mitotic checkpoint components Bub1 and BubR1 are differentially regulated by spindle events in human cells. *J Cell Sci*, **114**, 4385-4395.
202. Taylor SS and McKeon F (1997) Kinetochore localization of murine Bub1 is required for normal mitotic timing and checkpoint response to spindle damage. *Cell*, **89**, 727-735.
203. Tirnauer JS, Canman JC, Salmon ED, and Mitchison TJ (2002a) EB1 targets to kinetochores with attached, polymerizing microtubules. *Mol Biol Cell*, **13**, 4308-4316.
204. Tirnauer JS, Grego S, Salmon ED, and Mitchison TJ (2002b) EB1-microtubule interactions in *Xenopus* egg extracts: role of EB1 in microtubule stabilization and mechanisms of targeting to microtubules. *Mol Biol Cell*, **13**, 3614-3626.
205. Topper LM, Campbell MS, Tugendreich S, Daum JR, Burke DJ, Hieter P, and Gorbsky GJ (2002) The dephosphorylated form of the anaphase-promoting complex protein Cdc27/Apc3 concentrates on kinetochores and chromosome arms in mitosis. *Cell Cycle*, **1**, 282-292.
206. Toyoshima-Morimoto F, Taniguchi E, and Nishida E (2002) Plk1 promotes nuclear translocation of human Cdc25C during prophase. *EMBO Rep*, **3**, 341-348.
207. Tsvetkov L and Stern DF (2005) Interaction of chromatin-associated Plk1 and Mcm7. *J Biol Chem*, **280**, 11943-11947.
208. Vagnarelli P and Earnshaw WC (2004) Chromosomal passengers: the four-dimensional regulation of mitotic events. *Chromosoma*, **113**, 211-222.
209. van de WM, Oving I, Muncan V, Pon Fong MT, Brantjes H, van Leenen D, Holstege FC, Brummelkamp TR, Agami R, and Clevers H (2003) Specific inhibition of gene expression using a stably integrated, inducible small-interfering-RNA vector. *EMBO Rep*, **4**, 609-615.
210. van Vugt MA, van de Weerd BC, Vader G, Janssen H, Calafat J, Klompmaker R, Wolthuis RM, and Medema RH (2004) Polo-like kinase-1 is required for bipolar spindle formation but is dispensable for anaphase promoting complex/Cdc20 activation and initiation of cytokinesis. *J Biol Chem*, **279**, 36841-36854.
211. VandenBeldt KJ, Barnard RM, Hergert PJ, Meng X, Maiato H, and McEwen BF (2006) Kinetochores use a novel mechanism for coordinating the dynamics of individual microtubules. *Curr Biol*, **16**, 1217-1223.
212. Visintin R, Prinz S, and Amon A (1997) CDC20 and CDH1: a family of substrate-specific activators of APC-dependent proteolysis. *Science*, **278**, 460-463.
213. Walczak CE, Vernos I, Mitchison TJ, Karsenti E, and Heald R (1998) A model for the proposed roles of different microtubule-based motor proteins in establishing spindle bipolarity. *Curr Biol*, **8**, 903-913.

PUBLICATIONS

214. Watanabe N, Arai H, Nishihara Y, Taniguchi M, Watanabe N, Hunter T, and Osada H (2004) M-phase kinases induce phospho-dependent ubiquitination of somatic Wee1 by SCFbeta-TrCP. *Proc Natl Acad Sci U S A*, **101**, 4419-4424.
215. Waters JC, Chen RH, Murray AW, and Salmon ED (1998) Localization of Mad2 to kinetochores depends on microtubule attachment, not tension. *J Cell Biol*, **141**, 1181-1191.
216. Weaver BA, Bonday ZQ, Putkey FR, Kops GJ, Silk AD, and Cleveland DW (2003) Centromere-associated protein-E is essential for the mammalian mitotic checkpoint to prevent aneuploidy due to single chromosome loss. *J Cell Biol*, **162**, 551-563.
217. Weinstein J (1997) Cell cycle-regulated expression, phosphorylation, and degradation of p55Cdc. A mammalian homolog of CDC20/Fizzy/slp1. *J Biol Chem*, **272**, 28501-28511.
218. Westermann S, Vila-Sakar A, Wang HW, Niederstrasser H, Wong J, Drubin DG, Nogales E, and Barnes G (2005) Formation of a dynamic kinetochore- microtubule interface through assembly of the Dam1 ring complex. *Mol Cell*, **17**, 277-290.
219. Wollman R, Cytrynbaum EN, Jones JT, Meyer T, Scholey JM, and Mogilner A (2005) Efficient chromosome capture requires a bias in the 'search-and-capture' process during mitotic-spindle assembly. *Curr Biol*, **15**, 828-832.
220. Wong OK and Fang G (2005) Plx1 is the 3F3/2 kinase responsible for targeting spindle checkpoint proteins to kinetochores. *J Cell Biol*, **170**, 709-719.
221. Xia G, Luo X, Habu T, Rizo J, Matsumoto T, and Yu H (2004) Conformation-specific binding of p31(comet) antagonizes the function of Mad2 in the spindle checkpoint. *EMBO J*, **23**, 3133-3143.
222. Yamaguchi T, Goto H, Yokoyama T, Sillje H, Hanisch A, Uldschmid A, Takai Y, Oguri T, Nigg EA, and Inagaki M (2005) Phosphorylation by Cdk1 induces Plk1-mediated vimentin phosphorylation during mitosis. *J Cell Biol*, **171**, 431-436.
223. Yao X, Abrieu A, Zheng Y, Sullivan KF, and Cleveland DW (2000) CENP-E forms a link between attachment of spindle microtubules to kinetochores and the mitotic checkpoint. *Nat Cell Biol*, **2**, 484-491.
224. Yao X, Anderson KL, and Cleveland DW (1997) The microtubule-dependent motor centromere-associated protein E (CENP-E) is an integral component of kinetochore corona fibers that link centromeres to spindle microtubules. *J Cell Biol*, **139**, 435-447.
225. Yen TJ, Compton DA, Wise D, Zinkowski RP, Brinkley BR, Earnshaw WC, and Cleveland DW (1991) CENP-E, a novel human centromere-associated protein required for progression from metaphase to anaphase. *EMBO J*, **10**, 1245-1254.
226. Yu H (2006) Structural activation of Mad2 in the mitotic spindle checkpoint: the two-state Mad2 model versus the Mad2 template model. *J Cell Biol*, **173**, 153-157.
227. Zhou J, Panda D, Landen JW, Wilson L, and Joshi HC (2002) Minor alteration of microtubule dynamics causes loss of tension across kinetochore pairs and activates the spindle checkpoint. *J Biol Chem*, **277**, 17200-17208.
228. Zhou T, Aumais JP, Liu X, Yu-Lee LY, and Erikson RL (2003) A role for Plk1 phosphorylation of NudC in cytokinesis. *Dev Cell*, **5**, 127-138.
229. Zimmerman WC, Sillibourne J, Rosa J, and Doxsey SJ (2004) Mitosis-specific anchoring of gamma tubulin complexes by pericentrin controls spindle organization and mitotic entry. *Mol Biol Cell*, **15**, 3642-3657.

PUBLICATIONS

Parts of this work are published in:

Hanisch A., Silljé HH. and Nigg EA., Timely anaphase onset requires a novel spindle and KT associated complex comprising the proteins Ska1 and Ska2, *in press, EMBO Journal*, 2006

Hanisch A., Wehner A., Nigg EA., Silljé HH., Different Plk1 functions show distinct dependencies on Polo-Box domain-mediated targeting, *Mol Biol Cell*, 2006

Yamaguchi T., Goto H., Yokoyama T., Silljé H., Hanisch A., Uldschmid A., Takai Y., Oguri T., Nigg EA., Inagaki M., Phosphorylation by Cdk1 induces Plk1-mediated vimentin phosphorylation during mitosis, *J Cell Biol.*, 2005

Sauer G., Körner R., Hanisch A., Ries A., Nigg EA., Silljé HH., Proteome analysis of the human mitotic spindle, *Mol Cell Proteomics*, 2005

LEBENS LAUF

Anja Hanisch

Max-Planck Institut für Biochemie
Abteilung Zellbiologie
Am Klopferspitz 18
82152 Martinsried
Deutschland

Email: hanisch@biochem.mpg.de
Tel: +49 0179 8121534

Geburtstag: 10th Dezember, 1977
Geburtsort: Flensburg, Deutschland
Familienstand: ledig

Schule und Studium

- | | |
|-----------|---|
| 1984-1997 | Grundschule und humanistisches Gymnasium, Nürnberg, Deutschland
Abschluß: Allgemeine Hochschulreife (Note: 1,0) |
| 1998-2003 | Julius-Maximilians-Universität, Würzburg, Deutschland
Biologiestudium <ul style="list-style-type: none">• Hauptfach: Zell- und Entwicklungsbiologie• Nebenfächer: Biochemie, Immunologie/Virologie• Abschluß: Diplom (Note: 1,0 mit Auszeichnung)• Stipendium "Bayrische Begabtenförderung" |

Forschungserfahrung

- | | |
|---------------------|--|
| 03/2003-
10/2006 | Doktorarbeit
Max-Planck Institut für Biochemie Martinsried, Deutschland
Abteilung Zellbiologie, Prof. Dr. Erich .A. Nigg,
Arbeitsgruppe Dr. Herman Silljé |
|---------------------|--|

Themen:

- Funktionelle Analyse der Plk1-Polo-box Domäne im Hinblick auf das korrekte Fortschreiten der Mitose
- Charakterisierung von zwei neuen Spindel- und Kinetochor-assoziierten Proteinen, Ska1 und Ska2

03/2002-
01/2003 Diplomarbeit
Julius-Maximilians-Universität, Würzburg, Deutschland
Physiologische Chemie I, Prof. Dr. Manfred Scharl,
Arbeitsgruppe Dr. Burkhard Kneitz

In Kollaboration mit Albert-Einstein-College of Medicine, New York
City, USA, Abteilung Biology, Prof. Dr. Winfried Edelmann

Thema:

- Funktionelle Analyse pathogener Mutationen innerhalb des
"Mismatch Repair" Genes *mMlh1* in murinen embryonalen
Stammzellen

Kurse und Workshops

2006 Bioinformatik Kurs "NCBI resources"
Max-Planck Institut für Biochemie, Martinsried, Deutschland

2005 EMBO Workshop am EMBL, Heidelberg, Deutschland
"Methods in Cell Biology"

2002 Exkursion nach Wales im Rahmen des Biologiestudiums,
„Gezeitenzone“,
Prof. Dr. Georg Krohne

Auslandserfahrung

10-12/2003 Albert-Einstein-College of Medicine, New York City, USA
im Rahmen der Diplomarbeit

01-03/1998 Tutor der Deutschklasse des "Widnes Sixth Form College", Widnes,
UK

07-09/1997 Sprachschule Cavilam, Vichy, France

Sprachen Deutsch muttersprachlich
Englisch fließend
Französisch mäßig fließend